Intraspecific variation and thermal acclimation effects on mitochondrial function in a eurythermal teleost (*Fundulus heteroclitus*)

by

Dillon James Chung-Chun-Lam

HB.Sc., The University of Western Ontario, 2010
M.Sc., The University of Western Ontario, 2012

A THESIS SUBMITTED IN PARTIAL FULFILLMENT OF
THE REQUIREMENTS FOR THE DEGREE OF

Doctor of Philosophy

in

THE FACULTY OF GRADUATE AND POSTDOCTORAL STUDIES
(Zoology)

THE UNIVERSITY OF BRITISH COLUMBIA
(Vancouver)

February 2018

Abstract

Ambient temperature is a pervasive environmental stressor for ectotherms, with effects from individual atoms to the population level. Indeed, the effects of temperature on organismal performance are suggested to constrain species' geographic distributions. Aerobic metabolism is proposed to underlie the thermal limits of organisms, with thermal constraints occurring at the level of the mitochondrion due to its position at the terminus of the O_2 transport cascade and as the primary site of cellular ATP production. Despite this theoretical link, there is limited understanding of the relationship between mitochondrial function and thermal tolerance, particularly for interacting responses among multiple biological timescales.

I used two subspecies of Atlantic killifish (*Fundulus heteroclitus*) to characterize mitochondrial responses to acute thermal shifts following thermal acclimation to 5, 15, and 33 °C, and putative local adaptation. Northern killifish exhibited higher liver mitochondrial respiratory capacity and lower mitochondrial O_2 binding affinity when compared to the southern subspecies. Subspecies variation in mitochondrial function was associated with differences in electron transport system (ETS) complex IV capacity. Decreasing acclimation temperature increased liver mitochondrial respiratory capacity and decreased mitochondrial O_2 binding affinity in both subspecies. Thermal acclimation effects on liver mitochondrial respiratory capacity were associated with ETS complex I. In contrast, heart and brain mitochondrial respiratory capacity decreased following acclimation to both high and low thermal extremes and did not differ between subspecies. Thermal acclimation effects on liver mitochondrial performance were not associated with increased reactive oxygen species production or a loss of mitochondrial proton motive force at high assay temperatures. Liver mitochondrial membrane composition varied in response to thermal acclimation and differed between subspecies, with thermal acclimation effects being largely consistent between subspecies. Mitochondrial lipid remodeling was primarily associated with changes in specific phospholipid species, suggesting a role for targeted membrane remodeling as a mechanism underlying variation in mitochondrial function.

My data provide evidence for variation in mitochondrial function as a mechanism that differentiates aerobic and thermal performance between *F. heteroclitus* subspecies and that is involved in thermal acclimation responses. These mitochondrial responses likely underlie the

aerobic performance limits of ectotherms and influence species' fitness and geographic distributions.

Lay Summary

Environmental temperature shapes organisms' performance in natural environments, and this relationship influences species' geographic distributions. Organisms' responses to temperature are thought to be due to effects on the mitochondrion which is the primary source of cellular ATP. I investigated the effects of prolonged high and low-temperature exposure on mitochondrial function in two genetically distinct populations of the Atlantic killifish. I found that prolonged exposure to decreasing temperature increases mitochondrial performance and that fish from northern latitudes also maintained higher mitochondrial function. These fish remodeled their mitochondrial membranes, which might underlie observed differences in mitochondrial function. Mitochondrial responses to prolonged temperature exposure and population differences varied among the heart, brain, and liver. Finally, prolonged temperature exposure did not result in trade-offs in mitochondrial function. Mitochondrial function likely underlies organisms' responses to changes in environmental temperature. These data thus provide insight into the mechanisms organisms use in response to changing temperature.

Preface

A version of Chapter 2 has been submitted for publication as Patterns of mitochondrial membrane remodeling parallel functional adaptations to thermal stress. This chapter is part of a collaborative project with Drs. G. C. Sparagna, A. J. Chicco, and P. M. Schulte. I designed the experiments, collected all of the mitochondrial respiration data, collected all of the HPLC-UV data, collected all of the GC-FID data, analyzed all of the data, and wrote the manuscript under the supervision of Dr. P. M. Schulte. Dr. G. C. Sparagna collected the HPLC-ESI-MS data. All collaborators read the manuscript and provided editorial feedback.

A version of Chapter 3 has been published as Chung, D. J.; Morrison, P. R.; Bryant, H. J.; Jung, E; Brauner, C. J.; Schulte, P. M. (2017) Intraspecific variation and plasticity in mitochondrial oxygen binding affinity as a response to environmental temperature. *Scientific Reports*. 7, 16328. I designed the experiments, collected all of the samples, collected all of the mitochondrial oxygen binding affinity data, analyzed all of the data, and wrote the manuscript under the supervision of Dr. P. M. Schulte. P. R. Morrison and E. Jung collected the hemoglobin oxygen binding affinity data. H. J. Bryant collected the time to loss of equilibrium in hypoxia data. All collaborators read the manuscript and provided editorial feedback.

A version of Chapter 4 has been published as Chung, D. J. and Schulte, P. M. (2015). Mechanisms and costs of mitochondrial thermal acclimation in a eurythermal killifish (*Fundulus heteroclitus*). *Journal of Experimental Biology*. 218, 1621-1631. I designed the experiment, collected and analyzed all of the data, and wrote the manuscript under the supervision of Dr. P. M. Schulte.

A version of Chapter 5 has been published as Chung, D. J.; Bryant, H. J.; Schulte, P. M. (2017). Thermal acclimation and subspecies-specific effects on heart and brain mitochondrial performance in a eurythermal teleost (*Fundulus heteroclitus*). *Journal of Experimental Biology*. 220: 1459-1471. I designed the experiment, collected all of the data with the assistance of H. J. Bryant, I analyzed all of the data and wrote the manuscript under the supervision of Dr. P. M. Schulte. All collaborators read the manuscript and provided editorial feedback.

The experiments in this thesis followed the protocol approved by the UBC Animal Care Committee: # A11-0372.

Table of Contents

List of Tables

List of Figures

List of Abbreviations

ANT	adenine nucleotide transferase
ATP	adenosine triphosphate
BMR	basal metabolic rate
BSA	bovine serum albumin
CCO	cytochrome c oxidase
CL	cardiolipin
CS	citrate synthase
CT_{max}	critical thermal maximum
CT_{min}	critical thermal minimum
CTR	percent contribution of individual variables to the principal component
Cyt c	cytochrome c
D6D	Δ6-desaturase
DBI	double bond index
deoxyHb	deoxygenated Hb
ETS	electron transport system
FA	fatty acid
FCCP	carbonyl cyanide-*p*-trifluoro-methoxyphenylhydrazone
FRL	free radical leak
Hb-P_{50}	the partial pressure at which Hb is 50% saturated
HVA	homeoviscous adaptation
IMM	inner mitochondrial membrane
IMS	inter-membrane space
LDH	lactate dehydrogenase
LOE_{hyp}	time to loss of equilibrium in hypoxia
m/z	mass/charge ratio
Mito-P_{50}	O_2 partial pressure where mitochondrial O_2 consumption is 50% of maximum flux
MLCL	monolyso-cardiolipin
MTE	metabolic theory of ecology
n	sample size
OCLTT	oxygen and capacity limited thermal tolerance hypothesis
OD	optical density
OEC	oxygen equilibrium curve
OM	outer membrane
OXP	oxidative phosphorylation
oxyHb	oxygenated Hb
PC	phosphatidylcholine
PCA	principal component analysis
PE	phosphatidylethanolamine
PL	phospholipid
PO_2	O_2 partial pressure
PUFA	polyunsaturated fatty acid
Q_{10}	temperature coefficient
RBC	red blood cell
RCR	respiratory control ratio

ROS	reactive O_2 species
SCD	stearoyl-CoA destaturase
SUIT	substrate uncoupler inhibitor titration
T_a	ambient temperature
T_b	body temperature
TCA cycle	tricarboxylic acid cycle
TMPD	N,N,N',N'-tetramethyl-p-phenylenediamine
TPC	thermal performance curve
TPP^+	tetraphenylphosphonium
UCP	uncoupling proteins
UQ	ubiquinone
$\Delta H°$	van't Hoff isochore
Δp	proton motive force
Ψ_m	membrane potential

Acknowledgements

I would like to take a moment to acknowledge the many people whose patience, help and kindness have allowed me to achieve what has been one of the most challenging yet rewarding experiences of my life thus far. The following people may not realize the magnitude of their contributions; be it their time, friendship, insights, or the often-necessary Friday beer. Your efforts are reflected in following pages, all of which would not be possible without you.

I would like first to thank and acknowledge my Ph.D. supervisor, Trish Schulte. As a supervisor, Trish sets the highest standard. When it comes to the quality of my work I will always wonder if it's 'good enough for Trish'. Trish has always been my greatest advocate; she makes sure that I see the value of those datasets that seem most hopeless, and ensured that I have every opportunity to succeed. If there is anything that I have learned from my time working with Trish, it is that you have to make time to see the forest for the trees and that I need to stop being so wordy.

To my committee members: Jeff Richards, Colin Brauner, and Bill Milsom. You have each provided much-needed mentorship throughout my Ph.D. I have always appreciated that your approach never left me feeling like my opinions were somehow beneath yours. Hopefully, my science is better for it.

To members of the Schulte lab, past, and present. You have all been unbelievably supportive, particularly when it comes to my affinity for the so-called 'powerhouse of the cell.' Thank you again; Tim Healy, Taylor Gibbons, Kyle Crowther, Tara McBryan, Sara Northrup, Sarah Gignac, Marina Giacomin, Dave Metzger, Shawn Lin, Heather Bryant, and Michelle Chow.

To other members of the UBC Zoology department (in no particular order), Derek Somo, Till Harter, Gigi Lau, Yvonne Dzal, Cris Gomez, Jo Theriault, Pat Tamkee, Phil Morrison, Ryan Shartau, Mike Sackville, Matt Reagan. There isn't a better group of people that I could have hoped to go through my Ph. D. with, thank you for being there for me.

I would like to acknowledge my family, Mom, Dad, Lianne, and Evan, without whom I would probably still be poking around in the dirt. You have always been there in the background cheering me on. For that I am grateful. To my now growing family, Jeanne, Gillian, Jim, and Mark, your support over the last few years means so much to me. Thanks for always making me feel so welcome. To my animal companions, Celery and Siri, thanks for making sure that I always get out of bed in the morning.

Perhaps most importantly, Alex. I don't think that anyone else has had a closer look at the ups and downs of this Ph.D. Your patience and support have made this process so much easier, and for that, I will always be in your debt. Oh, and thanks for the schematic of the mitochondrion.

For my family
(especially Alex)

.

Chapter 1 General introduction

Ambient temperature is a critically important abiotic environmental stressor as it exerts an influence from individual atoms up to the level of the biosphere (Hochachka and Somero, 2002). Temperature is also thought to be an important determinant of species' geographic distributions (Angilletta, 2009; Deutsch et al., 2015; Sunday et al., 2011). Given the recent rapid increase in average global temperature (IPCC, 2014), species' distributions and abundances are proposed to change in ways that can be predicted based on their thermal tolerance limits and capacity to adjust to these novel environmental conditions (Deutsch et al., 2015; Pörtner, 2001). As a result, a great deal of research has been performed to help improve our understanding of how animals cope with changes in environmental temperature. By elucidating the physiological and biochemical mechanisms that underlie thermal tolerance limits, and the mechanisms that allow organisms to adjust these limits, we can improve our ability to predict if and how organisms will respond to changing climactic conditions.

Ambient temperature changes at a variety of temporal scales, which is important because organisms' responses to thermal stress vary depending on the duration and intensity of exposure to the stressor (Angilletta, 2009; Hochachka and Somero, 2002; Sørensen et al., 2016). In addition, responses to temperature variation at one timescale have the potential to affect responses at other timescales. For example, thermal adaptation could act to alter thermal acclimation responses. Nevertheless, it is common for comparative physiologists to investigate physiological and biochemical responses to temperature change at only a single biological timescale. Investigating the effects of environmental stressors across biological timescales is necessary as the physiological mechanisms organisms employ, and the potential interactions among timescales will better reflect how these processes occur in natural environments.

Thus, the objective of my thesis was to investigate the effects of thermal variation on physiological responses across multiple biological timescales. To do this, I utilized subspecies of the Atlantic killifish (*Fundulus heteroclitus*) acclimated to a range of temperatures that are reflective of their thermal tolerance limits. In this chapter, I provide a conceptual background for my thesis followed by the objectives and rationale for the questions that I addressed.

1.1 Timescales of responses to abiotic stressors

Environments vary across multiple time scales (e.g., minute-to-minute variation, daily variation, variation across tidal cycles, seasonal variation, and variation across glacial cycles), and animal responses vary depending on the duration of the change in environment. Active acute responses are rapid (on the order of minutes to hours) and are often reversible; these changes are usually dependent on an animal's current physiology (e.g., increasing heart rate), through changes in the activity of existing biochemical mechanisms (e.g., opening of ion channels, phosphorylation or de-phosphorylation of existing proteins). The expression of different phenotypes within the same individual (i.e., one genotype) is known as phenotypic plasticity, a class of responses that includes: acclimation or acclimatization (sometimes called phenotypic flexibility), developmental plasticity, and transgenerational epigenetic plasticity. Acclimation or acclimatization responses (occurring in the lab and field respectively) take place following prolonged exposure to an environmental stressor resulting in the modification of an organisms' biochemistry and anatomy, and these responses are typically thought of as being reversible. Plastic responses can also be irreversible; such is the case for developmental plasticity, which arises when organisms express alternative traits as a result of exposure to an altered environment during development (Nettle and Bateson, 2015). Transgenerational epigenetic inheritance is the transfer of information between generations (typically parent to offspring) that does not involve alteration of an organism's genetic sequence (Heard and Martienssen, 2014). These epigenetic modifications occur through multiple mechanisms including histone modification, DNA methylation, and RNA interference and can alter organism's physiology. In environments with sustained differences in abiotic conditions, local populations may undergo adaptation, resulting in improved physiological performance as a result of changes in allele frequencies (Hochachka and Somero, 2002). Variation in performance as a consequence of adaptation results in improved fitness and increases genetic contribution to subsequent generations. The sum of physiological responses across biological timescales ultimately shapes species' fitness within their local environment. In my thesis, I addressed physiological responses across acute, acclimation and adaptation timescales.

1.2 Temperature

Temperature is a measure of the average kinetic energy of molecules within a system. Kinetic energy influences the rate at which biological processes (e.g., enzyme function, aerobic metabolism) occur; and as such, large changes in temperature have direct and profound effects on organisms. The influence of temperature on organisms is particularly apparent for aquatic ectotherms whose body temperature (T_b) closely matches that of the environment. These temperature effects are reflected in the relationship between species' distributions and geographic patterns of ambient temperature (T_a; Deutsch et al., 2015; Hochachka and Somero, 2002; Sunday et al., 2011). Given the constraints temperature imposes on all organisms, understanding the underlying mechanisms of these limitations continues to be an intensely studied question in comparative physiology. Elucidating these mechanisms will improve understanding of how species respond to changes in environmental temperature.

The relationship between temperature and reaction rate can be quantified with a temperature coefficient (i.e., Q_{10} effect; Eqn. 1).

$$Q_{10} = \left(\frac{k_1}{k_2}\right)^{\left(10/t_1 - t_2\right)} \qquad \text{Equation 1.}$$

Where k_1 and k_2 are rate constants determined at temperatures, t_1 and t_2 respectively.

Within the range of a species' 'physiological' body temperatures, a 10 °C increase typically results in a two to three-fold increase in reaction rate (Eqn. 1; Hochachka and Somero, 2002; Van 't Hoff, 1899). Q_{10} effects are typically attributed to temperature effects on the thermodynamics of enzyme activity (Schulte et al., 2011). Indeed, increases in a system's total kinetic energy (and consequently temperature) increases enzyme catalytic rates, as demonstrated by thermal performance curves (Fig. 1.1, TPC). In general, TPCs are divided into three distinct regions: (1) a region with increasing activity, (2) a plateau where activity is at its maximum (thermal optimum: T_{opt}) and (3) a phase with a rapid decline in activity (Dell et al., 2013). Although Q_{10} effects can account for the rising phase of TPCs (i.e., region 1), they are unable to explain decreased activity during the plateau and declining phases (i.e., regions 2 and 3). These declines in activity are often attributed to the loss of protein tertiary and quaternary structure,

which are contingent on relatively weak chemical bonds (e.g., H^+-bonds, disulfide bridges). Loss of enzyme structure and catalytic capacity have therefore been suggested to contribute to temperature-induced declines in activity across levels of biological organization (for review see: Schulte, 2015).

Despite numerous characterizations of TPCs, the mechanisms constraining whole-animal thermal tolerance remain poorly understood (Angilletta, 2009; Pörtner et al., 2006). Recent models have attempted to make these links, placing focus on the processes associated with aerobic metabolism. Testing predictions derived from these models is critical, as they can improve understanding of species' responses to variation in ambient temperature.

1.3 Temperature and aerobic metabolism

Although most biochemical pathways are sensitive to changes in temperature, those associated with aerobic metabolism have been proposed to constrain whole-animal thermal performance. This is due to the O_2 dependence that most eukaryotes exhibit at some point during their life history, as well as the role aerobic metabolism plays in supplying the energy needed to maintain homeostasis (Brown et al., 2004; Fry and Hart, 1948; Pörtner, 2001; Schulte, 2015). Given the temperature-sensitive nature of aerobic metabolism, it is predicted that species must exhibit a capacity for acclimation or adaptive responses to maintain energetic balance as temperature changes.

The Oxygen and Capacity Limited Thermal Tolerance hypothesis (OCLTT; Pörtner, 2001) posits that thermally induced declines in aerobic scope (i.e., the difference between maximum and standard metabolic rate) are responsible for reductions in whole-organism performance, which ultimately constrains species' geographic distributions. The OCLTT is based on early work by Fry and Hart (1948), who demonstrated that aerobic scope in goldfish (*Carassius auratus*) increases with T_a up to an optimum and declines rapidly thereafter. This phenomenon has been demonstrated in several marine invertebrates and fishes in fully aerated water, implicating a role of O_2 limitation at the tissue level (for review see: Pörtner, 2001).

Given its role in maintaining systemic O_2 supply, temperature-induced declines in cardiac performance are thought to underlie reduced aerobic scope (Pörtner, 2001). At high temperatures, Q_{10} effects increase basal activity and consequently O_2 consumption. As there is an

upper limit to the cardiac and respiratory systems' activity, the ability to supply O_2 to systemic tissues becomes limited inducing a systemic hypoxemia. As a result, basal O_2 demand approaches maximum aerobic capacity, and aerobic scope declines. Similar to acute high-temperature shifts; low-temperature declines in aerobic scope are thought to be a consequence of Q_{10} effects. As Q_{10} effects reduce the maximum capacity for cardiac activity, the ability to deliver O_2 to systemic tissues becomes compromised. Under these conditions both maximum aerobic capacity and aerobic scope decline. Declines in aerobic scope are thus thought to limit performance at thermal extremes.

Although not an explicit test of mechanisms underlying thermal tolerance limits, the Metabolic Theory of Ecology (MTE) identifies the relationship between temperature and aerobic metabolism as being central to organisms' responses to thermal variation (Brown et al., 2004). At its core, the MTE links temperature effects on biological reaction rates (i.e., Van't Hoff-Arrhenius relationship; Van 't Hoff, 1899) with the allometric scaling relationship between body mass and metabolic rate (i.e., ¾ power law, Kleiber, 1932; Kleiber, 1947; West et al., 1997). The combination of these phenomena and thus the basis of MTE, are described in equation 2 (Eqn. 2).

$$I = i_0 M^{3/4} e^{-E/k_B T} \qquad \text{(Equation 2)}$$

Where I is metabolic rate, i_0 is a normalization constant independent of body size and temperature, M is body mass, e is the base of the natural logarithm, E is the activation energy, k_B is Boltzmann's constant and T is the absolute temperature (Brown et al., 2004).

The MTE proposes that constraints on aerobic metabolism arise due to limitations in the ability to deliver O_2 and substrates to the tissues (West et al., 1997). This limitation in delivery is suggested to be a consequence of biological delivery networks following a fractal scaling pattern which in turn is used to explain the ¾ power scaling relationship between organisms' metabolic rate and mass (Kleiber, 1932; Kleiber, 1947).

In addition to proposing mechanisms that underlie relationships between environmental temperature and aerobic metabolism, both the MTE and OCLTT have been used to establish links across levels of biological organization, suggesting that temperature effects on aerobic

metabolism result in whole-organism fitness costs (Brown et al., 2004; Pörtner, 2001; West et al., 1997). These constraints, therefore, ought to account for the relationship between geographic thermal gradients and species distributions. Indeed, relationships between species' maximum thermal performance and environmental temperatures have been demonstrated in some species (Eliason et al., 2011; Pörtner and Farrell, 2008; Sunday et al., 2011; White et al., 2012). In addition, the MTE has been used to predict ecological consequences of environmental thermal variation (e.g., Dillon et al., 2010). Given the fitness costs that thermal shifts are suggested to impose on organisms, species are predicted to respond to thermal stressors following prolonged exposures to maintain aerobic performance.

Perhaps because of their far-reaching theoretical implications, both the OCLTT and MTE have been subject to high levels of scrutiny. Indeed, the OCLTT has been criticized as its predictions have not been supported in certain taxa (e.g., absence of temperature induced cardiac compromise in air-breathing insects, maintenance of fitness measures at thermal extremes in aquatic eurytherms; Clark et al., 2011; Ern et al., 2014; Fobian et al., 2014; Healy and Schulte, 2012; Klok et al., 2004). Meanwhile, the MTE has been criticized based on its assumption that metabolic rates are set according to rates of substrate supply (e.g., Darveau et al., 2002). Whether the OCLTT and MTE are internally consistent and universally applicable is beyond the scope of this discussion. At a broad level, these theories retain considerable utility as they identify the importance of aerobic metabolism in shaping organisms' responses to environmental temperature. Indeed, there is strong evidence that temperature applies selective pressure on aerobic metabolism, forcing species to respond in order to maintain fitness. This is reflected in multiple observations that aerobic function across levels of biological organization correlates with fitness and performance measures in many taxa (Eliason et al., 2011; Hosler et al., 2000; Hulbert, 2003; Iftikar and Hickey, 2013; Miller and Stillman, 2012).

Declines in neural function have been suggested as an alternative mechanism underlying whole-organism thermal tolerance, perhaps accounting for the inconsistencies of the OCLTT. Indeed, there are significant correlations between whole-organism thermal tolerance limits and neural performance in ectothermic invertebrates such as Porcelain Crabs (Genus: *Petrolisthes*; Miller and Stillman 2012) and the European crayfish (*Astacus astacus*; Ern et al., 2015). It should be noted that neural processes and aerobic metabolism may nevertheless both be involved

in the setting of thermal tolerance limits. But the relative importance of each organ system in setting thermal tolerance limits may be species dependent (Ern et al. 2015).

The above discussion highlights aerobic metabolism's putative role in shaping organisms' response to temperature. Limitations on aerobic metabolism brought on by environmental stress can be thought of as inducing an imbalance between energetic supply and demand (i.e., balanced ATP turnover). Thus, aerobic limitations on performance may occur across multiple tissues due to effects on the mitochondrion (Fangue et al., 2009; Iftikar and Hickey, 2013; O'Brien et al., 1991). Given the energetic requirements of maintaining homeostasis in thermally stressful environments, it is expected that mitochondrial performance must be adjusted to meet changing demand.

1.4 Temperature and mitochondria

The mitochondrion holds a critical position as the terminus of the O_2 transport cascade and as the primary site of energy supply for most eukaryotes. For this reason, declines in mitochondrional function associated with thermal variation have been suggested as a mechanism that constrains whole-organism thermal tolerance as a component of the OCLTT (Pörtner, 2001). This organelle is characterized by a double-membrane structure which is a hallmark of its endosymbiont origin (Fig. 1.2., Sagan, 1967). The inner mitochondrial membrane (IMM) separates the matrix and inter-membrane space (IMS) which are all bound within the outer membrane. In addition to its structural function, the IMM houses key oxidative phosphorylation enzymes (i.e., electron transport system) which are critical for ATP synthesis. Although typically portrayed as having a 'bean-like' structure, the mitochondrion is a highly dynamic and structured organelle often closely resembling a reticulum (Glancy et al., 2015). Mitochondria have also been identified as playing critical roles in cellular functions beyond ATP production (e.g., regulating apoptosis, cellular signaling, regulating cellular metabolism; McBride et al., 2006).

Another important feature of the mitochondrion is the presence of a mitochondrial genome (Taanman, 1999). The mitochondrial genome encodes 13 subunits of the oxidative phosphorylation system, 22 tRNAs, and two rRNAs. Mitochondrially encoded oxidative phosphorylation enzyme subunits represent a subset of all subunits contained within functional oxidative phosphorylation enzymes (approximately 74 total), with the remainder being imported

nuclear gene products. Thus, the synthesis of electron transport system enzymes is highly coordinated, with dysfunction resulting in mitochondrial pathologies (Taanman 1999).

The majority of cellular ATP is synthesized via oxidative phosphorylation, which utilizes free energy captured from substrate oxidation and electron transfer to generate a proton motive force (Fig 1.2.; Δp; comprised of an electrical: Ψ_m and chemical gradient: pH) to drive ATP synthesis through the F_1F_O-ATP synthase (see: chemiosmotic hypothesis; Mitchell, 1961; Nicholls and Ferguson, 2013). In eukaryotes, substrate oxidation is generally achieved through the tricarboxylic acid cycle and fatty-acid oxidation; substrates for these reactions are obtained from cytosolic precursors (derived from glycolysis and β-oxidation; Houten and Wanders, 2010). Substrate oxidation generates electron carriers (NADH and $FADH_2$) that are further oxidized by IMM-bound electron transport system (ETS) proteins. NADH dehydrogenase (complex I) and succinate dehydrogenase (complex II) oxidize NADH and $FADH_2$ respectively passing their electrons to ubiquinone (UQ). This electron carrier moves through the hydrophobic core of the IMM entering the Q-cycle to donate its electron to the cytochrome bc_1 complex (complex III). Complex III further oxidizes the electron and passes it on to cytochrome *c* (Cyt. *c*). Cytochrome *c* is finally oxidized by cytochrome *c* oxidase (complex IV) where the electron is donated to O_2, producing H_2O. A primary function of the ETS is harnessing free energy from these redox reactions to drive proton transport (through complexes I, III, and IV) from the matrix to the IMS. By partitioning H^+ across the IMM, Δp is generated which can be used by the F_1F_0-ATP synthase (complex V) to couple the movement of H^+ back into the matrix with ATP synthesis. ATP is subsequently shuttled out of the matrix via the adenine nucleotide transporter (ANT). A buildup of cytoplasmic ATP generates a mass-action gradient that can be used to drive energetically unfavorable biochemical reactions (Nicholls and Ferguson, 2013).

Despite the generation of Δp and ATP synthesis being highly regulated, the movement of energy from substrates to ATP is not perfect. Inefficiencies can arise due to the loss of Δp via H^+ leak through the IMM, decreasing the driving force to synthesize ATP (Fig. 1.2). Indeed, non-phosphorylating proton conductance occurs in all mitochondria and consumes a large proportion of Δp (Brand, 1997; Brand and Nicholls, 2011). Although the exact mechanisms of H^+ leak are not fully understood, controlled leak is known to occur through uncoupling proteins (UCPs; Nicholls, 2006), and leak also occurs at the interface between IMM lipids and the ANT (although leak at this junction is thought to be unregulated; Brand et al., 1994; Samartsev et al., 1997).

Although H^+ leak may reduce ATP synthesizing capacity, some level of basal leak is thought to be necessary as a large Δp is thought to maintain ETS complexes in a reduced state, which inhibits electron flow (Brand, 2010). A proposed consequence of constricted electron flow is an increased likelihood of 'electron slip', or the escape of electrons from the ETS (primarily at complex I and III; though the physiological importance of this process is equivocal, see: Brand et al., 1994; Jastroch et al., 2010), resulting in reactive O_2 species production (ROS; including: superoxide radicals, $O_2^{\cdot -}$; H_2O_2; and hydroxyl radicals, $OH^{\cdot -}$; Brand, 2010; Jastroch et al., 2010). At low levels, ROS act as intracellular signaling molecules, critical to maintaining cellular homeostasis (Finkel, 2001). But when ROS production exceeds cellular scavenging capacity (e.g., superoxide dismutase, glutathione reductase), ROS can decrease performance by damaging biomolecules (i.e., lipids, nucleic acids, proteins) and ultimately induce apoptosis (Harman, 1956).

Pathological fluctuations in Δp and increased ROS production during acute shifts in temperature are thought to constrain whole-animal thermal tolerance (Grim et al., 2010; Guderley, 2011; Johnston et al., 1994; St-Pierre et al., 1998). Indeed, an accumulation of temperature-associated mitochondrial dysfunction should decrease cellular and whole-animal energetic balance. By investigating the acute thermal responses of mitochondrial components underlying this proposed dysfunction, and the associated acclimation responses we can elucidate the mechanistic role mitochondria play in constraining whole-animal thermal tolerance. Ultimately, this investigation allows us to test the predicted role of the mitochondrion in constraining whole-organism thermal tolerance as suggested by broader theories such as the OCLTT.

Aberrant mitochondrial function resulting from acute shifts in temperature (up to and including the point of failure) is thought to occur due to thermodynamic effects on mitochondrial components (i.e., lipid bilayers and enzymes). Indeed, low-temperature effects on mitochondrial performance are thought to occur due to associated decreases in kinetic energy. Under conditions of decreasing T_a, membrane fluidity decreases as lipid bilayers enter gel-like states (Hazel, 1995). This has large consequences as proteins integral to oxidative phosphorylation (e.g., ETS components) are embedded within the IMM and the transfer of electrons between these complexes is influenced by membrane fluidity (see: fluid mosaic model, Singer and Nicolson, 1972; mitochondrial supercomplexing, Bogdanov et al., 2008; Mileykovskaya and Dowhan,

2014; homeoviscous adaptation; Hazel, 1995; Hazel and Williams, 1990). In addition, membrane fluidity also affects the transport of substrates and products associated with oxidative phosphorylation (Deuticke and Haest, 1987). Coupled with a temperature-induced reduction of protein activity, mitochondrial performance declines during acute low-temperature shifts.

In contrast to low-temperature effects, acute increases in temperature can increase IMM fluidity and enzyme activity, increasing mitochondrial performance. This increase in performance has an upper limit, however, as the increased temperature can destabilize the IMM resulting in a loss of Δp, and disrupt interactions between ETS components (Hazel, 1995). Acute increases to high temperature may also result in undesirable increases in ETS activity, causing uncontrolled O_2 consumption and perhaps ROS production (Grim et al., 2010). Like low-temperature effects, these pathologies are thought to result in a decline in performance and thus require a response to maintain homeostasis.

In order to maintain performance following prolonged thermal exposure, animals are known to alter mitochondrial properties (i.e., thermal acclimation; Guderley, 2011; Seebacher et al., 2010). Low-temperature compensation can involve increases in mitochondrial volume density and altered mitochondrial localization within a tissue (Dhillon and Schulte, 2011; Egginton and Johnston, 1984; O'Brien, 2011), alteration of mitochondrial lipid composition (see: homeoviscous adaptation, Grim et al., 2010; Guderley, 2004; Hazel, 1995; Kraffe et al., 2007), and increased enzyme activity (Dahlhoff and Somero, 1993; Fangue et al., 2009; Kraffe et al., 2007). Although less thoroughly studied, high-temperature acclimation has been shown to decrease mitochondrial respiration rate and mitochondrial phospholipid fatty-acid saturation in some species (Guderley and Johnston, 1996; Khan et al., 2014; Kraffe et al., 2007; Strobel et al., 2013). Collectively these changes are thought to maintain mitochondrial output at a level that matches cellular energetic requirements in variable thermal environments.

Positive (i.e., adaptive) selection on genes that encode mitochondrial oxidative phosphorylation proteins (both nuclear and mitochondrial) is thought to improve species fitness in variable thermal environments (Castellana et al., 2011). Some demonstrations of positive selection exist, but are subject to criticism, as supporting functional data are lacking (Ballard et al., 2007; Balloux et al., 2009; Bazin et al., 2006, Blier et al., 2014, Castellana et al., 2011). Indeed, species adapted to diverse thermal environments typically demonstrate neutral or purifying selection, which is perhaps unsurprising given the key role that mitochondria play in

energetic homeostasis (Melo-Ferreira et al., 2014; Silva et al., 2014). The synthesis of electron transport system enzymes, critical to oxidative phosphorylation, depends upon the translation of proteins encoded by both nuclear and mitochondrial genomes. The importance of coordination between these genomes has been demonstrated through hybridization and molecular experiments (Blier et al., 2014; Castellana et al., 2011). Indeed, lines of *Drosophila simulans* with two different mitochondrial genomes and a common nuclear genetic background exhibit unique thermal sensitivities of mitochondrial respiratory capacity (Pichaud et al., 2012). This variation in thermal sensitivity of respiratory capacity between these mitochondrial haplotypes is thought to be due to variation in cytochrome *c* oxidase activity or divergent kinetic properties of the electron transport system. Furthermore, hybridized human cell lines with primate mitochondria exhibit compromised mitochondrial function due to effects on complex I (Barrientos et al., 1998).

One important but often overlooked aspect of mitochondrial function is mitochondrial O_2 binding affinity. Variation in this property presumably alters the mitochondrion's ability to extract O_2 from the cellular environment. Thus, organisms are predicted to alter this kinetic property in response to hypoxemic stress brought on by environmental hypoxia or thermal stress, as posited by the OCLTT (Costa et al., 1997; Du et al., 2016; Lau et al., 2017; Zhang et al., 2013). There is evidence for variation in mitochondrial O_2 binding affinity among closely related sculpin species and migratory locusts in response to environmental hypoxia (Lau et al., 2017; Zhang et al., 2013). But similar effects are not observed following hypoxic acclimation in rats or *Fundulus heteroclitus* (Costa et al., 1997; Du et al., 2016). In contrast, little is known about variation in this parameter in response to thermal acclimation or thermal adaptation (St-Pierre et al., 2000b), which is perhaps surprising given the theoretical association between thermal stress and constraints on aerobic metabolism.

A potential consequence of altering mitochondrial function to maintain performance is a loss of function at temperatures that were not stressful prior to acclimation (representing a trade-off of acclimation). For example, a change in IMM lipid composition in order to increase membrane fluidity at low-temperatures could result in membrane destabilization and a loss of Δp at high-temperatures that were not previously stressful (Hazel, 1995). In contrast, acclimation to high-temperatures is thought to result in a suppression of mitochondrial function and reduced IMM fluidity in order to limit unsustainable O_2 consumption and ROS production. An acute

decrease in temperature following this suppression could result in mitochondrial dysfunction as the IMM enters a gel-like phase, thus constraining ETS complex interactions. Decreases in mitochondrial performance resulting from acclimation trade-offs could have consequences that extend to higher levels of organization, as cellular energetic requirements are not met. In this way, mitochondrial acclimation trade-offs may underlie shifts in whole-animal thermal limits.

1.5 Atlantic killifish (*Fundulus heteroclitus*)

I chose to use the Atlantic killifish (*Fundulus heteroclitus*; Class: Actinopterygii, Order: Cyprinodontiformes, Family: Fundulidae) to investigate mitochondrial responses to thermal stress across multiple biological timescales. This small topminnow is an ideal model in which to study these relationships as their biogeography (geographic range limits from Northern Florida, USA to Nova Scotia, Canada; a change of 1 °C per degree change in latitude, Powers et al., 1991) allows for the simultaneous investigation of thermal acclimation and local adaptation responses, and the interactions between these two factors. In addition, *F. heteroclitus* are highly eurythermal making them ideal for addressing questions about metabolic responses to thermal stress, as the mechanisms they employ should be readily detected. Indeed, studies of metabolic responses to thermal extremes often utilize stenothermal species, and the physiological responses that eurythermal organisms employ are likely not the same, and thus these species form a critical point of comparison.

F. heteroclitus reside in intertidal salt marshes, experiencing diel cycles in a variety of abiotic stressors, including ambient temperature (up to 15 °C shift within an hour, Sidell et al., 1983). Consistent with these rapid changes in ambient temperature, *F. heteroclitus* have a demonstrated ability to survive large acute thermal shifts (Fangue et al., 2006; Critical Thermal minimum = -1 °C and Critical Thermal maximum = 41 °C). *F. heteroclitus*' profound thermal tolerance extends to aerobic scope which can be maintained across a broad range of temperatures (5 °C to 30 °C) and declines only slightly outside that range (Healy and Schulte, 2012).

Given their northern temperate distribution, *F. heteroclitus* are subject to large seasonal fluctuations in ambient temperature, with winter temperatures being up to 20 °C lower when compared to summer temperatures (Fangue et al., 2006). This species does not exhibit migratory behaviors in response to these seasonal changes, as their home ranges are within 40-300 m^2

(Lotrich, 1975). Instead, *F. heteroclitus* have considerable acclimation capacity (acclimation temperature range: 2-35 °C) that is associated with a suite of physiological modifications (Fangue et al., 2006).

A large benefit of using killifish as a model of thermal adaptation is the existence of latitudinally distinct northern (*Fundulus heteroclitus macrolepidotus*, Walbaum 1792) and southern (*Fundulus heteroclitus heteroclitus*, Linneaus 1766) subspecies (Morin and Able, 1983). The range limits of the northern subspecies extend from Nova Scotia, Canada to New Jersey, USA, and the southern subspecies' range limits extend from Northern Florida to New Jersey, USA (Powers et al., 1986). The formation of these two subspecies is thought to be a consequence of isolation during past glaciation events with current distributions being maintained by selection (Brown and Chapman, 1991). Indeed, genetic differences between these subspecies have been demonstrated repeatedly (McKenzie et al., 2016; Powers and Schulte, 1998; Powers et al., 1986; Reid et al., 2016; Whitehead, 2009). The most extensive demonstration of temperature acting as a selective factor in *F. heteroclitus* is the existence of lactate dehydrogenase-B (LDH-B) isozymes unique to each subspecies (Place and Powers, 1979; Place and Powers, 1984; $Ldh\text{-}B^b$ and $Ldh\text{-}B^a$ for northern and southern subspecies respectively). These genetic differences result in altered performance such that isozymes encoded by $Ldh\text{-}B^b$ (i.e., northern) genotypes have higher catalytic efficiency at low temperatures when compared to $Ldh\text{-}B^a$ (i.e., southern) genotypes. In addition, the expression of *LDH-B* is greater in the northern subspecies as a consequence of greater gene transcription rates (Crawford and Powers, 1989), with this variation in transcription rate being associated with sequence variation between the subspecies in the promoter of this gene (Schulte et al., 1997). Variation between *LDH-B* genotypes has been associated with subspecies variation in hemoglobin and ATP ratios, swimming performance at low temperatures (Dimchele and Powers, 1982b), developmental rates (Dimichele and Westerman, 1997), and time to hatch (Dimichele and Powers, 1982a). Genetic differences between subspecies are also observed in mitochondrial genes, as fixed amino acid polymorphisms (primarily associated with ETS complex I) occur in northern killifish when compared with subspecies from lower latitudes (Whitehead, 2009). It has been speculated that these fixed amino acid polymorphisms can partly account for a three-fold higher complex I mitochondrial specific activity in northern killifish compared to their southern counterparts (Loftus and Crawford, 2013).

Killifish mitochondrial responses to thermal stress appear to differ between subspecies and are thought to occur due to genetic divergence. Low-temperature acclimation (5 °C) results in detectable responses in northern killifish, as complex I-linked mitochondrial respiration, enzyme activities, mitochondrial volume density, and cristae surface area increase significantly compared to southern killifish (Dhillon and Schulte, 2011; Fangue et al., 2009). This increase in capacity may come with a trade-off as apparent mitochondrial coupling (i.e., the ability to limit proton leak) decreases at high assay temperatures (Fangue et al., 2009). High-temperature acclimation (25 °C) may also result in trade-offs as mitochondrial respiration is apparently sustained at high assay temperatures (up to 37 °C), but declines when compared to lower-temperature acclimation treatments at low assay temperatures (5 °C; Fangue et al., 2009). Similar thermal acclimation effects on *F. heteroclitus* mitochondrial respiratory capacity have been demonstrated by other groups, but evidence for intraspecific variation in mitochondrial function remains mixed at best (Baris et al., 2016b). Despite the breadth of research on mitochondrial thermal acclimation responses among subspecies of killifish, much remains unknown about the sites of modifications associated with these changes (e.g., mitochondrial performance is often only assessed through ETS complex I), putative functional trade-offs that result from acclimation (loss of Δp, increased ROS) and the mechanisms underlying variation in mitochondrial performance (e.g., mitochondrial lipid remodeling).

1.6 Thesis objectives and organization

From the above discussion, it is apparent that thermal stress likely results in altered mitochondrial function across biological timescales. Despite this theoretical link, understanding about the mechanisms underlying these processes remains limited, particularly in the context of local adaptation. Thus, I used the Atlantic killifish as my model organism to investigate the mitochondrial mechanisms employed in response to acute temperature variation, thermal acclimation, and local adaptation.

Through the course of my thesis, I investigated variation in mitochondrial properties that are theoretically associated with setting thermal tolerance limits. These studies fell into four categories that are outlined below and are presented as individual thesis chapters (Chapters 2-5):

- Variation in mitochondrial respiratory capacity and mitochondrial phospholipid composition in response to acute thermal variation, thermal acclimation and local adaptation (Chapter 2)
- Variation in mitochondrial and hemoglobin O_2 binding kinetics in response to acute thermal variation, thermal acclimation and local adaptation (Chapter 3)
- Putative functional trade-offs in mitochondrial function associated with acute thermal variation, and thermal acclimation (Chapter 4)
- Tissue-specific variation in mitochondrial responses to acute thermal variation, thermal acclimation and local adaptation (Chapter 5)

Below I describe the specific objectives of each thesis chapter and provide a rationale for the associated experiments.

1.6.1 Chapter two outline

The objective of Chapter 2 was to determine if liver mitochondrial respiratory capacity and mitochondrial phospholipid composition (e.g., head groups, fatty acid chain length, and saturation) vary in response to thermal acclimation and local adaptation. I hypothesized that the thermodynamic effects of low temperature require compensatory increases in mitochondrial respiratory capacity over both acclimation and adaptation timescales and that this compensation would, at least in part, be achieved by increases in membrane fluidity at low acclimation temperatures and in the cold-adapted subspecies. To test my hypothesis, I measured mitochondrial respiratory capacity in northern and southern *F. heteroclitus* acclimated to 5, 15, and 33 °C using high-resolution respirometry. Mitochondrial phospholipid composition was characterized using high-performance liquid chromatography, gas chromatography, and mass spectrometry.

Using these techniques, I addressed the following specific predictions of my hypothesis:

- Decreasing acclimation temperature increases mitochondrial respiratory capacity
- Putatively cold-adapted northern *F. heteroclitus* exhibit greater mitochondrial respiratory capacity when compared to their warm-adapted, southern counterparts

- Thermal acclimation and intraspecific variation effects on mitochondrial respiratory capacity differs among electron transport system complexes
- Decreasing acclimation temperature is associated with mitochondrial membrane compositions that are consistent with greater membrane fluidity
- Northern *F. heteroclitus* have a mitochondrial phospholipid composition that is consistent with greater membrane fluidity
- Variation in mitochondrial phospholipid composition in response to thermal acclimation and putative local adaptation corresponds with variation in mitochondrial respiratory capacity

These predictions are supported by some evidence in the literature which I discuss below.

One of the primary predictions derived from theories linking thermal tolerance limits and aerobic metabolism is that mitochondrial capacity increases in response to low temperatures. Thus, acclimation to low temperatures is predicted to increase mitochondrial function to compensate for temperature induced declines in biochemical reaction rates. Indeed, there is strong evidence for increased mitochondrial respiratory capacity following low-temperature acclimation in aquatic ectotherms (Baris et al., 2016b; Dos Santos et al., 2013; Fangue et al., 2009; Kraffe et al., 2007). In contrast, high-temperature acclimation is predicted to decrease mitochondrial function to offset high-temperature effects on biochemical reaction rates (Abele et al., 2002). Although less thoroughly studied, there are some demonstrations of these effects (Baris et al., 2016b; Iftikar and Hickey, 2013; Khan et al., 2014; Strobel et al., 2013).

Local adaptation effects on mitochondrial respiratory capacity are not well-characterized in comparison to thermal acclimation responses. In general, adaptation to cold environments is predicted to increase mitochondrial capacity (e.g., White et al., 2012). But evidence for intraspecific variation in mitochondrial respiratory capacity remains mixed (Baris et al., 2016b; Fangue et al., 2009). Evidence at other levels of biological organization provides support for these effects in *F. heteroclitus*. Indeed, northern *F. heteroclitus* exhibit greater whole-organism metabolic rates when compared to their southern counterparts (Fangue et al., 2009) and there are significant latitudinal clines in *F. heteroclitus* mitochondrial genes indicating that selection acts on mitochondrial performance in this species (McKenzie et al., 2016).

Mitochondrial oxidative phosphorylation requires the coordinated function of several multimeric enzymes. But the relative responses of these enzymes to thermal acclimation and local adaptation is unclear. Indeed, studies investigating thermal acclimation effects on mitochondrial performance often focus on flux through electron transport system complex I (Fangue et al., 2009; Guderley and Johnston, 1996; although see: Baris et al., 2016b; Dos Santos et al., 2013; Mark et al., 2012). In instances where downstream performance is assessed, an emphasis is placed on alternative entry points into the electron transport system (e.g., complex II). For example, Dos Santos *et al.* (2013) demonstrate increased mitochondrial respiratory capacity fueled through complex II when compared with complex I in the goldfish (*Carassius auratus*) as a response to low-temperature acclimation. Investigations of intraspecific variation in electron transport system complex contribution to mitochondrial respiration are uncommon. However, attempts to demonstrate variation in electron transport system complex contribution to mitochondrial flux between *F. heteroclitus* subspecies provide limited support for these effects (Baris et al., 2016b).

As discussed previously, temperature effects on mitochondrial performance can be theoretically attenuated through modification of the relative proportion of IMM polar head groups and characteristics of fatty acid chains (e.g., chain length and unsaturation; Hazel, 1984). Overall these changes are thought to improve mitochondrial performance following thermal acclimation and adaptation.

Cold-acclimation has been associated with a decreased ratio of phosphatidylcholine/ phosphatidylethanolamine (i.e., modification of polar head groups), and increased fatty acid unsaturation in biomembranes isolated from *Oncorynchus mykiss*; presumably increasing membrane fluidity (Crockett and Hazel, 1995; Hazel and Landrey, 1988). High-temperature acclimation, in contrast, has been associated with a reversal of these cold-acclimation effects; which are thought to prevent membrane destabilization and loss of membrane potential (Hazel, 1984; Pernet et al., 2007). Less is known about local adaptation effects on mitochondrial phospholipid composition. Indeed, northern killifish have been shown to enrich skeletal mitochondrial lipids with highly unsaturated fatty acids following 5 °C acclimation (Grim et al., 2010), but this phenomenon has not been investigated in southern killifish. Some work has demonstrated that yeast (Kingdom: Fungi) species adapted to different thermal regimes exhibit unique lipid modifications (e.g., increased unsaturation in cold-adapted species, Arthur and

Watson, 1976). In contrast, both cold-adapted mussels (*Mytilus edulis*) and warmer-water oysters (*Crassostrea virginica*) alter their gill and gut membrane lipids in similar ways following thermal acclimation (Pernet et al., 2007).

Attempts to link mitochondrial lipid composition and respiratory function are rare. Kraffe et al. (2007) demonstrate that variation in mitochondrial performance following thermal acclimation correlates strongly with changes in a limited set of mitochondrial phospholipids. Similarly, thermally acclimated sister species of abalone (genus: *Haliotis*) are characterized by mitochondrial performance and membrane fluidity, that is consistent with compensation of mitochondrial performance at low temperatures (Dahlhoff and Somero, 1993). But the involvement of local adaptation in these responses remains unknown.

1.6.2 Chapter three outline

The objective of Chapter 3 was to determine if hemoglobin and liver mitochondrial O_2 binding affinity vary in response to thermal acclimation and local adaptation. I hypothesized that systemic hypoxemia proposed to occur at high temperatures would act as a strong selection pressure resulting in increased mitochondrial and hemoglobin O_2 binding affinity over both acclimation and adaptation timescales as a mechanism to maintain O_2 partial pressure gradients. To test this hypothesis, I characterized mitochondrial O_2 binding affinity using high-resolution respirometry in northern and southern *F. heteroclitus* acclimated to 5, 15, and 33 °C. Hemoglobin O_2 binding affinity was characterized in the same fish by generating O_2 binding equilibrium curves with spectrophotometry.

Using these techniques, I addressed the following specific predictions from my hypothesis:

- Increasing acclimation temperatures increases mitochondrial O_2 binding affinity
- Warm-adapted southern *F. heteroclitus* exhibit greater mitochondrial O_2 binding affinity when compared to their northern counterparts
- Increasing acclimation temperature increases hemoglobin O_2 binding affinity
- Southern *F. heteroclitus* subspecies exhibit greater hemoglobin O_2 binding affinity when compared to their northern counterparts

These predictions are supported by some evidence in the literature which I discuss below.

Mitochondrial performance is typically assessed using saturating substrate quantities and O_2 partial pressures to drive maximum O_2 consumption, and these data are often used to infer *in vivo* performance. But measurements of maximum O_2 consumption likely do not fully reflect *in vivo* performance and are instead more useful for elucidating the sites that are modified in response to thermal stress (Dalziel et al., 2009). Indeed, Fangue *et al.* (2009) demonstrate that thermal acclimation effects on mitochondrial respiratory capacity do not explain whole-animal thermal acclimation responses. One way to address this issue is to assess mitochondrial performance under non-saturating O_2 partial pressures (i.e., assess mitochondrial O_2 affinity) and substrate concentrations. Indeed, mitochondrial O_2 binding affinity has been shown to predict human basal metabolic rate (Larsen et al., 2011).

Increased mitochondrial and Hb-O_2 binding affinity are thought to improve the ability to extract O_2 from their surrounding environments (i.e., the cytosol and external environment respectively). Thus O_2 binding affinity is predicted to increase in response to high temperatures. As discussed previously, there is evidence for increases in mitochondrial O_2 binding affinity as an adaptation to environmental hypoxia (Lau et al., 2017; Zhang et al., 2013), however, these effects are not observed following hypoxia acclimation (Costa et al., 1997; Du et al., 2016). In contrast, variation in mitochondrial O_2 binding affinity in response to thermal acclimation and thermal adaptation remains uninvestigated.

Hemoglobin acts as a link between the external environment and metabolizing tissues, and is thus subject to variation in local conditions throughout the circulatory system. Indeed, Hb-O_2 binding affinity can be altered through variation in temperature, pH, and allosteric modification (Jensen, 2004). Variation in Hb-O_2 binding affinity is known to occur between hybrid (New Jersey) *F. heteroclitus* with divergent LDH-B genotypes (Powers et al., 1979). Hybrid (New Jersey, USA) *F. heteroclitus* with the southern LDH genotype (LDH-B^a) exhibit greater Hb-O_2 binding affinity when compared to hybrid individuals with the northern LDH genotype (LDH-B^b). But these effects are only observed following exhaustive swimming, indicating that allosteric modification of Hb by ATP partly underlies this response. Although variation in Hb-O_2 binding affinity is well characterized in hybrid *F. heteroclitus*, the presence of variation in Hb-O_2 binding affinity between *F. heteroclitus* subspecies remains uninvestigated.

In general, an acute increase in temperature is associated with a decrease in Hb-O_2 binding affinity, which is due to the exothermic nature of Hb oxygenation (Weber and Jensen, 1988). Thus, acclimation to high temperatures is predicted to increase Hb-O_2 binding affinity to offset these acute high temperature effects and to meet systemic O_2 demand. Weber et al. (1976) demonstrated that acclimation to a range of temperatures was not associated with altered whole-blood Hb-O_2 binding affinity in rainbow trout (*Oncorynchus mykiss*). In contrast, warm-acclimated European eel (*Anguilla anguilla*) and brown bullhead (*Ictalurus nebulosus*) both increase Hb-O_2 binding affinity (Grigg, 1969; Laursen et al., 1985). But the recruitment of thermal acclimation effects on Hb-O_2 binding affinity in a more eurythermal species remains unknown.

1.6.3 Chapter four outline

The objective of Chapter 4 was to determine if thermal acclimation is associated with functional trade-offs that are revealed when thermally acclimated animals are acutely shifted to different temperatures. For example, are there negative consequences associated with acute increases in temperature following cold acclimation? I hypothesized that mitochondrial modifications associated with thermal acclimation might result in dysfunction during acute thermal shifts, which may be a potential mechanism underlying shifts in whole-organism thermal limits. To test my hypothesis, I characterized mitochondrial membrane potential, proton leak kinetics and reactive O_2 species production following acute thermal shifts in northern *F. heteroclitus* acclimated to 5, 15, and 33 °C. This was achieved using ion-selective probes and high-resolution respirometry to quantify mitochondrial membrane potential and proton leak kinetics and spectrophotometry to assess reactive O_2 species production.

Using these techniques, I addressed the following specific predictions of my hypothesis:

- Acute increases in temperature following low-temperature acclimation are associated with a decrease in mitochondrial membrane potential and increased proton conductance, perhaps due to relatively greater mitochondrial membrane instability

- Acute decreases in temperature following high-temperature acclimation are associated with a decrease in mitochondrial membrane potential and decreased proton conductance, perhaps due to thermodynamic effects on electron transport system activity
- Acute increases in temperature following low-temperature acclimation are associated with relatively greater reactive O_2 species production, perhaps due to thermodynamic effects on electron transport system activity
- Acute decreases in temperature following high-temperature acclimation are associated with relatively lower reactive O_2 species production, perhaps due to thermodynamic effects on electron transport system activity

These predictions are supported by some evidence in the literature which I discuss below.

Among the many functions of the mitochondria, the generation and maintenance of a proton motive force are perhaps the most important as it is the source of potential energy for ATP synthesis (Nicholls and Ferguson, 2013). If acute increases or decreases in temperature following low and high-temperature acclimation respectively cause a decline in Δp, cellular and indeed whole-animal performance would be expected to decline as well representing a putative acclimation trade-off. Despite its importance, thorough assessments of thermal acclimation effects on maintenance of Δp remain lacking. Indeed, measurements of 'summer-condition' acclimation effects on Ψ_m in lugworms (*Arenicola marina*) demonstrate some changes, but these animals were in breeding condition, and so disentangling the effect of life history is difficult (Keller et al., 2004).

Maximum Ψ_m is informative for assessing potential costs of thermal acclimation, as differences among acclimation groups may become apparent when mitochondrial performance is driven to its limit. Under *in vivo* conditions, however, Ψ_m is likely maintained at non-saturating levels. Indeed, maintaining Ψ_m at high levels could prove to be energetically costly in the long-term and may itself induce damage as flux through the ETS becomes inhibited (due to an inability to pump H^+). By determining the kinetics of mitochondrial O_2 consumption over varying Ψ_m insight into potential costs of thermal acclimation can be obtained. Inefficiencies in the transfer of energy between substrates and ATP can arise due to leak. A decrease in Ψ_m,

paired with an increase in proton leak at sub-saturating levels of flux through the electron transport system could, therefore, represent a trade-off of thermal acclimation.

Excessive reactive O_2 species production represents a major form of deleterious mitochondrial function. Indeed, production of ROS has been associated with several pathologies and senescence (Harman, 1956). Thus, an increase in ROS production during acute thermal shifts, following thermal acclimation may be evidence of an acclimation-induced trade-off, which may, in turn, underlie thermal-acclimation associated shifts in thermal tolerance limits (Fangue et al., 2006). Under these conditions, an increase in ROS production would require a cellular response to eliminate free radicals and repair resulting damage. Despite the potential for this trade-off, direct assessments of thermal acclimation effects on ROS production have remained relatively sparse (however, see: Grim et al., 2010; Iftikar and Hickey, 2013, for ROS associated data).

1.6.4 Chapter five outline

The objective of Chapter 5 was to determine if thermal acclimation and local adaptation effects on mitochondrial function are consistent among metabolically active tissues. I hypothesized that the metabolic demands of the liver, heart, and brain, and their contribution to setting whole-organism thermal tolerance limits are not equal, with the demands of the heart and brain being greater than that of the liver. These effects are thus predicted to be reflected as greater thermal acclimation and intraspecific responses in the heart and brain relative to the liver. To test my hypothesis, I characterized heart and brain mitochondrial performance between northern and southern *F. heteroclitus* that were acclimated to 5, 15, and 33 °C using high-resolution respirometry and compared these effects to those observed in the liver (see Chapter 2).

Using these techniques, I addressed the following specific prediction of my hypothesis:

- Thermal acclimation and local adaptation effects on heart and brain mitochondrial function are greater than those in the liver

This prediction is supported by some evidence in the literature which I discuss below.

Although the liver is critical for maintaining whole-organism homeostasis, organs such as the brain and heart may place greater constraints on acute organismal thermal performance (Pörtner, 2001). The OCLTT predicts that O_2 supply to systemic tissues is a major determinant of whole-animal thermal performance. As such, failure of the tissues primarily responsible for O_2 delivery (i.e., heart) or coordinating organismal performance (i.e., brain) may better predict thermal tolerance limits. Indeed, declines in cardiac mitochondrial ADP phosphorylating capacity have been shown to correlate with temperatures just below those that induce cardiac failure in *Notolabrus celidotus* (Iftikar and Hickey, 2013). In their investigation of thermal acclimation responses across multiple tissues in the southern catfish (*Silurus meridionalis*), Yan and Xie (2015) observed that cold-compensation of mitochondrial function appeared to occur in the heart, liver, and kidney but not the brain or white muscle. Although not strictly a thermal acclimation response, studies in hibernating mammals have also demonstrated tissue-specific mitochondrial modification (Brown et al., 2011; Heim et al., 2017). The involvement of tissue-specific mitochondrial function in response to local adaptation is unknown.

1.7 Summary

Taken together, the experiments in my thesis provide a detailed examination of how mitochondrial function is modified in response to thermal challenges across acute, acclimation, and evolutionary timescales. I provide convincing evidence for a role of mitochondrial function in both thermal acclimation and local adaptation responses (Chapters 2 and 3) and implicate mitochondrial lipid remodeling as a mechanism underlying this variation (Chapter 2). I demonstrate that substantial changes in mitochondrial function can occur following thermal acclimation without resulting in a loss of membrane potential or increased ROS production, revealing a putative mechanism underlying eurythermal physiology (Chapter 4). However, thermal acclimation and local adaptation effects were not consistent across metabolically demanding tissues, highlighting the scope of mitochondrial function available within the same organism (Chapters 2 and 5). More broadly this thesis supports a role for mitochondrial function as a key determinant of organismal thermal performance, and distribution.

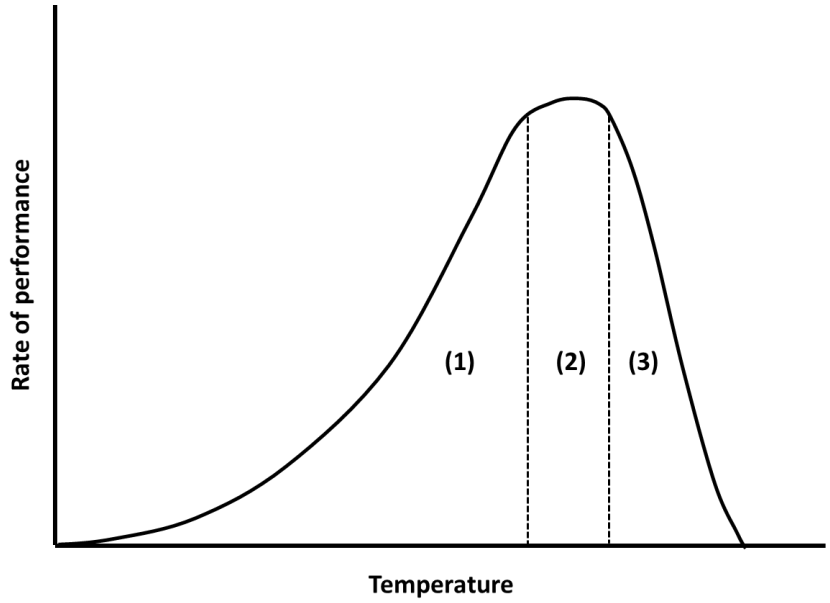

Figure 1.1. A schematic of a thermal performance curve from an ectotherm. Thermal performance curves can be conceptually divided into a region of increasing activity (1), a plateau where activity is at a maximum (2), and a region of rapidly declining activity (3).

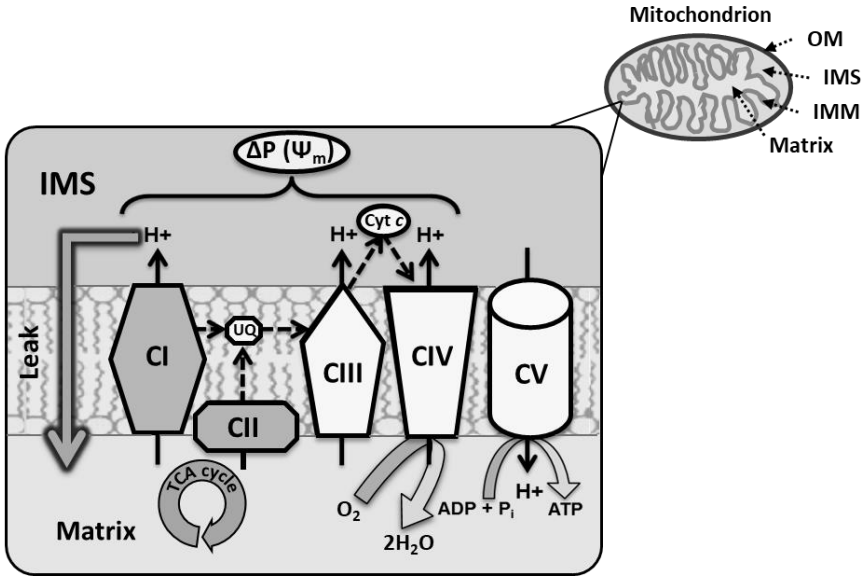

Figure 1.2. Schematic of the mitochondrion and electron transport system (Mitchell, 1961). OM: outer membrane; IMS: intermembrane space; IMM: inner-mitochondrial membrane; Δp: proton motive force; Ψ_m: mitochondrial membrane potential; Cyt. c: cytochrome c; UQ: ubiquinone; CI-V: complexes I-V; TCA cycle: tricarboxylic acid cycle.

Chapter 2 Patterns of mitochondrial membrane remodeling parallel functional adaptations to thermal stress

2.1 Summary

The effect of temperature on mitochondrial performance is thought to be due in part to its effect on mitochondrial membranes. Numerous studies have shown that thermal acclimation and adaptation can alter inner-mitochondrial membrane (IMM) amount, but little is known about the capacity of organisms to modulate mitochondrial membrane composition. Using northern and southern subspecies of Atlantic killifish (*Fundulus heteroclitus*) that are locally adapted to different environmental temperatures, we assessed whether thermal acclimation would result in changes in liver mitochondrial respiratory capacity and membrane composition and amount. We measured changes in phospholipid headgroups and headgroup-specific fatty acid (FA) remodeling, and respirometry to assess mitochondrial respiratory capacity. Acclimation to 5 and 33°C altered mitochondrial respiratory capacity in both subspecies. Northern *F. heteroclitus* exhibited greater mitochondrial respiratory capacity across acclimation temperatures, consistent with previously observed subspecies differences in whole-organism aerobic metabolism. Mitochondrial phospholipids were altered following thermal acclimation, and the direction of these changes was largely consistent between subspecies. These effects were primarily driven by remodeling of specific phospholipid classes and were associated with shifts in metabolic phenotypes. There were also differences in membrane composition between subspecies that were driven largely by differences in phospholipid classes. Changes in respiratory capacity between subspecies and with acclimation were largely but not completely accounted for by changes in IMM amount. Taken together, these results support a role for changes in liver mitochondrial function in the ectothermic response to thermal stress during both acclimation and adaptation and implicate lipid remodeling as a mechanism contributing to these changes.

2.2 Introduction

Temperature has a profound effect on the performance of ectothermic animals (Pörtner, 2001), and shapes their distribution and abundance such that the temperatures at organismal

range limits are often closely correlated with their thermal tolerance limits (Sunday et al., 2011). One key way in which temperature impacts biological processes is through its effects on phospholipid (PL) membranes. As temperature increases or decreases, the fluidity of PL membranes changes, which can affect the interactions and activities of enzymes embedded in the membrane environment. Thus, prolonged exposure to thermal stress is predicted to result in membrane remodeling to maintain fluidity as temperature changes; a process known as homeoviscous adaptation (HVA), (Hazel, 1984; Sinensky, 1974).

Remodeling of membranes can involve alterations in the distribution of PL headgroup classes (e.g., phosphatidylcholine [PC], phosphatidylethanolamine [PE]; Hazel, 1984) and their fatty acid (FA) composition. Changes in the ratio of PC/PE have been associated with thermal acclimation in ectothermic species, with increases in this ratio resulting in decreased membrane fluidity (Li et al., 2006). Membrane FA composition is thought to be altered in response to thermal challenges by changing the double-bond index or degree of unsaturation, with increased FA unsaturation being associated with more double-bonds and greater membrane fluidity (Hazel, 1984). However, the physiological contributions of membrane remodeling through either mechanism to organismal thermal acclimation and adaptation remain poorly defined (although see: Kraffe et al., 2007).

For most animals, aerobic metabolism is a critical process that provides the majority of the ATP needed for biological function. This ATP is generated through the action of proteins embedded in the inner mitochondrial membrane (IMM), including the proteins of the electron transport system and the ATP synthase. The IMM is critical not only for the proper functioning of these proteins but also for the maintenance of the proton motive force used to drive ATP synthesis. Despite the importance of the IMM, relatively little is known about the extent of homeoviscous adaptation in mitochondrial membranes compared to the numerous studies of this phenomenon for the plasma membrane. Even less is known about the role of mitochondrial function and membrane properties in local adaptation to temperature, though one study identified differences in mitochondrial membrane fluidity and function among closely related species of abalone with differing geographical distributions (Dahlhoff and Somero, 1993).

There is evidence for modifications of mitochondrial membrane composition following thermal acclimation that provides some support for HVA at the level of the mitochondrion. Low-temperature acclimation has been associated with increased mitochondrial FA unsaturation in

some studies (Caldwell and Vernberg, 1970; Grim et al., 2010; Itoi et al., 2003; Kraffe et al., 2007; Wodtke, 1981b), but not others (Crockett et al., 2001; van den Thillart and Modderkolk, 1978). Changes in mitochondrial PL class distribution in response to thermal acclimation are less clear, though effects on PL FA composition may be dependent on the PL class being investigated (Kraffe et al., 2007; Wodtke, 1981b). Importantly, mitochondria are unique in that their membranes also contain cardiolipin (CL), a dimeric PL with four FA chains that profoundly influences mitochondrial function (Chicco and Sparagna, 2007; Schlame, 2007). Cardiolipin is associated with critical mitochondrial properties including the structural stabilization of mitochondrial electron transport complexes and the formation of mitochondrial supercomplexes (Paradies et al., 2014). In *Oncorhynchus mykiss*, high-temperature acclimation is associated with CL-specific decreases in polyunsaturated FA (PUFA) content, but the functional implications of this effect are unclear (Kraffe et al., 2007).

In contrast to the dearth of studies on mitochondrial membrane remodeling, numerous studies have detected increases in cristae surface density (and thus IMM amount) with cold-acclimation and adaptation, although this pattern is not uniform across species (e.g., Archer and Johnston, 1991; Dhillon and Schulte, 2011). Thus, organisms have the potential to alter both the nature and the amount of IMM in response to thermal acclimation and adaptation.

In this study, we utilized the Atlantic killifish (*Fundulus heteroclitus*) to investigate the effects of thermal acclimation and putative local adaptation on liver mitochondrial membrane remodeling and performance to assess the potential role of HVA at both physiological and evolutionary timescales. This species is found in estuarine salt marshes along a large latitudinal thermal gradient on the east coast of North America (from northern Florida, USA to Nova Scotia, Canada) and exhibits a highly eurythermal physiology (Fangue et al., 2006; critical thermal maximum = 34 °C, critical thermal minimum = -1 °C, for 12.5 °C acclimated fish), consistent with the highly variable temperatures in its estuarine environments. In addition, this species exhibits phenotypic plasticity in response to prolonged thermal stress, recruiting a wide range of physiological mechanisms, including altered mitochondrial function (Chapters 4 and 5; Fangue et al., 2009; Healy and Schulte, 2012; McBryan et al., 2016), consistent with the strong seasonal variation in habitat temperature. There are also genetically distinct northern (*Fundulus heteroclitus macrolepidotus*) and southern (*Fundulus heteroclitus heteroclitus*) subspecies of killifish that vary in their thermal tolerance limits, consistent with the latitudes at which they are

found (Fangue et al., 2006). As such, this is an ideal species in which to address questions about temperature effects on mitochondrial properties with respect to both thermal acclimation and local adaptation.

In this study, we addressed the following questions: 1) Do *F. heteroclitus* subspecies differ in liver mitochondrial performance? 2) Do these subspecies alter mitochondrial performance following thermal acclimation (5, 15, and 33 °C) and do these responses differ between the subspecies? 3) Is *F. heteroclitus* liver mitochondrial membrane composition and amount altered following thermal acclimation, and if so, do these changes differ between the subspecies? And 4) Are variations in mitochondrial membrane composition or amount consistent with variation in mitochondrial respiratory capacity as a result of thermal acclimation and intraspecific variation? To address these questions, we employed high-resolution techniques for characterizing mitochondrial membrane composition and respiratory function between subspecies and across acclimation temperatures. Our results represent the most comprehensive investigation of these characteristics in any species to date and provide new insights into roles and potential mechanisms of mitochondrial membrane remodeling in the ectothermic response to thermal stress.

2.3 Materials and methods

2.3.1 Animals

All animal use followed The University of British Columbia approved animal care protocol A11-0372. Northern (*Fundulus heteroclitus heteroclitus*) and southern (*Fundulus heterocltius macrolepidotus*) Atlantic killifish were collected from Ogden's Pond estuary, Nova Scotia (45°71′N, 61° 90′W) and Jekyll Island, Georgia (31°02′N, 81°25′W), respectively, in September 2014. Fish were transported to the UBC Aquatics Facility and housed in 190 L recirculating tanks and were fed once daily (Tetrafin Max, Rolfe C. Hagen Inc. Montreal, QC, Canada); ambient temperature (T_a) was maintained at 15±2 °C, with 20 ppt salinity, and a 12 h: 12 h light: dark photoperiod. Following ten months of holding (July 2015), fish were transferred to 114 L tanks with T_a set at 5, 15, or 33 °C, 20 ppt salinity and a 12 h: 12 h light: dark photoperiod. Fish were acclimated to these conditions for four weeks before sampling.

2.3.2 Liver mitochondria isolation

At 09:00 AM PST seven killifish from an individual acclimation treatment were removed from their tank before daily feeding. These were the same fish used in a previous study (Chapter 5). Fish were euthanized by severing the spine with a razor blade and weighed. Liver tissue was removed, weighed individually and livers from 7 individual fish were pooled and minced (1 mm^3 pieces) in ice-cold isolation buffer (250 mM sucrose, 50 mM KCl, 0.5 mM EGTA, 25 mM KH_2PO_4, ten mM HEPES, 1.5% BSA, pH=7.4 at 20 °C). Tissue was homogenized with five passes of a loose-fitting Teflon pestle followed by filtration through one-ply cheesecloth. Crude homogenate was centrifuged at 600 *g* for 10 min at 4 °C. The fat layer was aspirated following the slow spin, and the remaining supernatant was filtered through four-ply cheesecloth. Filtered supernatant was centrifuged at 6000 *g* for 10 min at 4 °C, followed by two washes of the resulting mitochondrial pellet. The final pellet was suspended in 800 μL of BSA free isolation buffer and placed on ice until use in respirometry experiments. The protein content of the mitochondrial suspension was determined using a Bradford assay (Bradford, 1976) with BSA as a standard.

2.3.3 Mitochondrial respirometry

Mitochondrial respiratory capacity was assessed as described previously (Chapter 5) using an O2k high-resolution respirometer (Oroboros Instruments, Innsbruck, Austria). Oxygen probes were calibrated to account for background O_2 consumption and zero calibrated (using a yeast suspension) at each assay temperature (5, 15, 33 and 37 °C). Two ml of assay buffer (0.5 mM EGTA, 3 mM $MgCl_2 \cdot 6H_2O$, 60 mM lactobionic acid, 20 mM taurine, 10 mM KH_2PO_4, 20 mM HEPES, 110 mM sucrose, 1 $g \cdot l^{-1}$ fatty-acid free BSA, pH 7.1 at 25 °C) was air-equilibrated at each assay temperature followed by the addition of liver mitochondrial protein (approximately 0.5 mg). Leak respiration fueled through complex I (LEAK-I or state II) was initiated with the addition of pyruvate (10 mM) and malate (2 mM). This was followed by an addition of ADP (2.5 mM) and glutamate (10 mM) yielding complex I linked ADP phosphorylating respiration (OXPHOS-I or state III). Succinate (10 mM) was then introduced to the chamber to fuel state III respiration through complexes I and II simultaneously (OXPHOS-I, II). Carboxyatractyloside (5 μM) was then introduced to the chamber to inhibit the adenine nucleotide translocator, initiating

leak respiration through complexes I and II (LEAK-I, II). Mitochondria were then fully uncoupled with repeated injections of carbonyl cyanide p-(trifluoromethoxy) phenylhydrazone (FCCP, 0.5 μM) yielding substrate oxidation capacity (ETS-I, II). Complexes I, II and III were sequentially inhibited through the addition of rotenone (0.5 μM in ethanol, inducing ETS-II), malonate (5 mM), and antimycin A (2.5 μM). Apparent respiratory capacity through cytochrome *c* oxidase (CCO) was then initiated through the addition of ascorbate (2 mM) and N,N,N′, N′-tetramethyl-p-phenylenediamine (TMPD, 0.5 mM). We corrected for auto-oxidation of TMPD and ascorbate via chemical background corrections at each assay temperature.

We also assessed mitochondrial OXPHOS and LEAK respiration with fatty-acid substrates, as changes in fatty-acid utilization may be associated with thermal acclimation effects on whole-organism phenotypes (Chapter 4). Briefly, the respirometer and mitochondria were prepared as described above. Following air calibration and the addition of the mitochondrial sample, both palmitoyl carnitine (20 μM) and malate (2 mM) were added to the chamber yielding LEAK-Palm. C. (state II), this was followed by ADP (2.5 mM) yielding OXPHOS-Palm. C (state III).

All mitochondrial respiration rates were normalized to mitochondrial protein content. The remaining mitochondrial suspension was snap frozen in liquid N_2 and stored at -80 °C until use for phospholipid (PL) analyses. We estimated mitochondrial coupling with different substrates using the ratio of OXPHOS-I: LEAK-I (respiratory control ratio; RCR-I); OXPHOS-I, II: LEAK-I, II (RCR-I, II), and OXPHOS-Palm.C.: LEAK-Palm. C (RCR-Palm. C.).

We estimated the contribution of changes in total OXPHOS enzyme content to our observed thermal acclimation and subspecies effects on mitochondrial respiratory capacity by normalizing LEAK-I, II; OXPHOS-I, II; and ETS-I, II to apparent CCO capacity.

2.3.4 Mitochondrial phospholipid extraction for PE and PC head group analysis by LC-UV detection

Phospholipids were extracted from thawed mitochondrial isolates to determine the relative proportion of membrane phosphatidylethanolamine (PE) and phosphatidylcholine (PC) and their FA compositions as previously described (Mulligan et al., 2014). This preparation results in a combined estimate of lipid composition for both the inner and outer-mitochondrial membranes. Pelleted mitochondrial protein (0.5 mg) was suspended in 4 ml of chloroform:

methanol (2:1) with ten mM butylated hydroxytoluene (BHT) to prevent peroxidation. The solution was washed with 1 ml H_2O followed by centrifugation at 2000 *g* for 10 min at 4 °C. Phospholipids within the chloroform phase were isolated and dried under N_2 gas and resuspended in 125 µL of hexane for analysis by normal phase HPLC (Agilent 1100 series, 50 µl injection) with an Agilent Zorbax Rx-Sil column (4.6 x 250 mm, 5 µm). Mobile phases of A [hexane:isopropanol:0.3 mM potassium acetate (pH 7.0):acetic acid (424:566:10:0.1)] and B [hexane:isopropanol:5.0 mM potassium acetate (pH 7.0):acetic acid (385:515:100:1)] were used in a gradient (flow rate = 1 $ml \cdot min^{-1}$) from 100% A to 100% B over 6 min, mobile phase B was held for 5 min followed by a gradient back to phase A over 1 min. PE and PC were identified with a UV detector (λ = 206 nm) and collected based on elution times of known standards. PE and PC content were estimated using the area under the curve of the UV signal corrected to the total area under the curve for all detected PL head groups.

To determine PL class-specific FA composition, PE and PC fractions were dried under N_2 gas with 7.5 µl of internal standard (heptadecanoic acid, 17:0; 0.1 $mg \cdot ml^{-1}$) and resuspended in 600 µl of methanol. The suspension was centrifuged at 900 *g* for 5 min at 4 °C. Sodium methoxide (25 µL, 25% stock solution) was added to the supernatant and incubated for 3 min at room temperature. The reaction was stopped with the addition of methanolic HCl (75 µl, 3N). Fatty acid methyl esters were isolated with an addition of 700 µl hexane, followed by vortexing and centrifugation at 900 *g* for 1 min at 4 °C. The hexane layer was isolated and dried down under N_2 gas, followed by resuspension in 50 µl of hexane for analysis using an Agilent 6890 Series Gas Chromatograph equipped with an Agilent Technologies DB-225 column (30 m x 0.250 mm x 0.25 µm) and flame ionization detector. Flow rate, split ratio, pressure, and velocity were set at a constant 1.7 $ml \cdot min^{-1}$, 1:2, 23.59 psi and 42 $cm \cdot s^{-1}$, respectively. Oven temperature started at 120 °C, followed by an 8 min ramp at 10 $°C \cdot min^{-1}$. This was followed by a 6 min ramp at 2.5 $°C \cdot min^{-1}$ followed by 6 min at 215 °C. Individual FAs were identified based on elution time of known standards and presented as a percent of the total PL FA content.

In addition to PL class-specific analyses, we characterized the FA composition of total mitochondrial PLs (i.e., mitochondrial membrane FA composition) frequently reported in the literature. Total mitochondrial PLs were extracted and immediately processed for FA analysis as described above except that 0.1 mg of mitochondrial protein was resuspended in 600 µl methanol with BHT (10 mM) and 15 µl of internal standard, and a split ratio of 1:5 was used for GC

analysis. FA are reported as proportions of the total PL fraction. To characterize global trends in PL FA characteristics potentially relevant to membrane and organismal function, we calculated ratios of monounsaturated to polyunsaturated FA (MUFA/PUFA) and n3/n6 PUFA, the double bond index (DBI; the sum of the proportions of FA multiplied by the total number of double bonds in that FA), and chain length index (the sum of the proportions of FA multiplied by the number of carbons in that FA). To evaluate potential mechanisms of altered FA distribution, we also calculated selected FA product/precursor ratios corresponding to activities of the major endogenous FA desaturation and elongation enzymes central to long-chain fatty acid biosynthesis in the liver.

2.3.5 Cardiolipin molecular species analysis by HPLC-ESI-MS

Given the complexity of CL composition and potential importance of specific CL molecular species (FA combinations) on mitochondrial function (Schlame, 2007), we utilized HPLC-ESI-MS to evaluate CL compositional changes as previously described (Sparagna et al., 2005). Briefly, 0.1 mg of total liver mitochondria protein was mixed in a methanol (795 µl), chloroform (790 µl) and HCl (715 µl, 0.1 N with 11 mM ammonium acetate) solution with a CL reference standard (0.081 nmol, CL with four myristoyl (14:0) FA chains). Samples were centrifuged at 3000 *g* for 10 min at 4 °C, and the organic layer was isolated and dried under N_2 gas followed by resuspension in 100 µl of a hexane-isopropanol solution (30:40, v/v). Twenty-five µl of this PL extract was injected into a normal phase HPLC column (Prodigy 5 µm silica 100 Å, 1.0 x 150 mm column; Phenomenex) coupled to a mass spectrometer (API 4000). Mobile phase A [hexane:isopropanol:20 mM ammonium acetate in water, pH 5.5 (30:40:7)] and mobile phase B [hexane:isopropanol (30:40)] were used in a gradient (flow rate 50 $\mu l \cdot min^{-1}$) of 50% B for 6 min, increasing to 95% B over 10 min, and 95% B for 30 min followed by a return to 50% B at the end of the run. Electrospray ionization was run in negative ion mode at -4000 V, with declustering potential of -100 V, focusing potential of -350 V, and entrance potential of -10 V. Unit resolution was used with a step size of 0.1 amu over 4 s. Cardiolipin and monolysocardiolipin (containing 3 FAs; MLCL) molecular species were identified by mass/charge (m/z) ratio and quantified by comparison to the internal standard. Total CL and MLCL contents were estimated by the sum of CL and MLCL (total CL content) and MLCL species separately and normalized to the total mitochondrial MS signal. Thermal acclimation and

intraspecific effects on inner-mitochondrial membrane content were estimated by comparing CL content that was normalized on a per mg mitochondrial protein basis.

2.3.6 Data analysis

Data analysis was completed using R software (v 3.3.3). All data are mean ± SEM with $\alpha = .05$. Sample size (n) is indicated in relevant figure or table captions.

Effects of subspecies, acclimation and assay temperature on all mitochondrial respiration data were assessed using separate mixed linear models with individual pooled mitochondrial samples set as the random effect. The effects of subspecies and acclimation temperature on mitochondrial respiratory capacity normalized to CCO capacity (assayed at 15 °C) were analyzed by two-way ANOVA.

We assessed global changes in mitochondrial phospholipid head groups and fatty acids using a principal component analysis (PCA, see: Table 2.1 for variables included in the PCA). We identified variables that contributed most heavily to each principal component by determining both the squared cosine (Cos^2) and percent contribution factor (Ctr) of each variable within a given principal component (PC, Abdi and Williams, 2010).

A two-way ANOVA was used to assess thermal acclimation and subspecies effects on individual principal component values extracted from PC1, 2 and 3 separately. A two-way ANOVA was used to compare thermal acclimation and subspecies effects on estimates of inner-mitochondrial membrane content (i.e., CL content normalized to mg mitochondrial protein).

Two-way ANOVAs with thermal acclimation and subspecies as factors were used to assess responses of whole-animal mass, liver mass, hepatosomatic index, and all PL (fatty acid and headgroup) data. We accounted for multiple testing in the PL data by adjusting α using a Benjamini-Hochberg correction.

2.4 Results

2.4.1 Whole organism metrics

Whole organism mass differed between subspecies ($p_{subspecies} < .005$) and as a result of thermal acclimation (Fig. 2.1, $p_{acclimation} < .0001$). The northern *F. heteroclitus* used in this study

had greater whole-animal mass when compared to their southern counterparts and increasing acclimation temperature decreased whole-animal mass in both subspecies ($p_{acclimation*subspecies}$ = .195). Liver mass ($p_{subspecies}$ < .0001, $p_{acclimation}$ < .0001) and hepatosomatic index ($p_{subspecies}$ < .05, $p_{acclimation}$ < .0001) followed the same pattern as whole-organism mass, with the exception that liver mass did not differ between subspecies following 33 °C acclimation (liver mass: $p_{subspecies*acclimation}$ < .001, HSI: $p_{subspecies*acclimation}$ = .135).

2.4.2 Mitochondrial OXPHOS and LEAK

There were significant effects of subspecies and acclimation temperature on mitochondrial OXPHOS and LEAK respiration fueled by CI and CI + CII substrates (Fig. 2.2, see Table 2.2 for *p*-values). Northern *Fundulus heteroclitus* maintained higher mitochondrial respiration rates compared to the southern subspecies at all assay temperatures. Acclimation to colder temperatures tended to increase mitochondrial OXPHOS capacity in both subspecies across assay temperatures, with no significant interaction of subspecies or acclimation effects. OXPHOS and LEAK respiration rates increased with assay temperature, though OXPHOS tended to remain similar or declined from 33 °C to 37 °C. A greater thermal sensitivity of OXPHOS and LEAK respiration was observed in the northern compared to southern *F. heteroclitus*, and in 5 °C and 15 °C acclimated fish when compared to 33 °C acclimated fish (p < .05 for interactions). Similar effects of subspecies, acclimation and assay temperatures were observed for OXPHOS and LEAK respiration fueled with palmitoyl carnitine (Fig. 2.3A-D, see Table 2.2 for *p*-values), with smaller effects of thermal acclimation and assay temperature in the southern subspecies compared to the northern subspecies (p < .05 for 3-way interaction).

2.4.3 Mitochondrial maximum respiratory capacity

Subspecies and thermal acclimation effects on maximum mitochondrial respiratory capacity (ETS) fueled by CI and CI + CII substrates were similar to those described for OXPHOS and LEAK respiration (Fig. 2.4A-D, see Table 2.2 for *p*-values), suggesting changes in the mitochondrial content, membrane lipids or enzymatic capacity of the ETS machinery. Apparent cytochrome *c* oxidase (CCO) capacity was higher in northern compared to southern subspecies and increased with assay temperature (Fig. 2.4E-F, see Table 2.2 for *p*-values). However, CCO capacity greatly exceeded the integrated ETS capacity, and was unaffected by

acclimation temperature, implicating changes in upstream ETS or oxidation enzymes in the observed effects of temperature acclimation on integrated mitochondrial respiratory function in both subspecies.

2.4.4 Mitochondrial respiratory control

Mitochondrial respiratory control by ADP (an index of OXPHOS coupling) was evaluated by calculating the respiratory control ratio (OXPHOS/LEAK; RCR) for CI and CI+II substrates (Fig. 2.5) or fatty acid oxidation (Fig. 2.3E-F; see Table 2.2 for *p*-values). We detected significant effects of assay temperature on RCR supported by CI and CI+II substrates, increasing marginally between assay temperatures 5 to 15 °C then decreasing beyond 15 °C, but no other significant main or interaction effects were detected. However, significant interaction effects on fatty acid-linked RCR were observed between subspecies and with thermal acclimation. In the northern subspecies, 15 °C acclimated killifish exhibited greater RCR compared to 5 and 33 °C acclimated fish. In contrast, 33 °C acclimated southern killifish exhibited greater fatty acid-linked RCR compared to 5 and 15 °C acclimated fish. These effects were only observed at specific assay temperatures (T_{assay} = 5 and 33 °C in northern and southern *F. heteroclitus* respectively), which drove a significant interaction between assay temperature and thermal acclimation effects.

2.4.5 Mitochondrial phospholipids

To determine whether the observed variation in mitochondrial function between subspecies and acclimation temperatures was paralleled by changes in mitochondrial membrane composition, we performed a comprehensive analysis of mitochondrial phospholipid class distribution, fatty acid composition, and cardiolipin molecular species profile. Principal component analyses were initially employed to describe overall patterns of variation, which revealed acclimation temperature as the strongest modifier of mitochondrial membrane composition (Fig. 2.6A). Principal component 1 accounted for 35.5% of the total variation and fully separated thermal acclimation treatments (Fig. 2.6B, $p_{acclimation} < 1.06 \times 10^{-11}$), but did not account for subspecies variation ($p_{subspecies} = .067$) or its interaction with thermal acclimation ($p_{acclimation*subspecies} = .087$). Principal component 3 (9.1% of total PL variation) separated northern and southern *F. heteroclitus* ($p_{subspecies} < .001$) and thermally acclimated fish ($p_{acclimation} < .001$),

but there was an interaction between these factors ($p_{acclimation*subspecies} = 2.11 \times 10^{-5}$) driven by the lack of subspecies differences following 33 °C acclimation (Fig. 2.6C). Principal component 2 (16.2% of total PL variation) did not account for the effects of thermal acclimation or subspecies (Fig. 2.7; $p_{acclimation} = .687$, $p_{subspecies} = .236$, $p_{acclimation*subspecies} = .230$).

To identify the specific aspects of mitochondrial membrane composition most responsible for thermal acclimation responses and subspecies variation, we evaluated the contribution of each individual membrane feature to principal components 1 and 3 (Table 2.1). Changes in cardiolipin molecular species represented 15 of 20 strongest contributors to trends in PC1 (48% of total contribution), with PE fatty acids being the next most robust variants (30% of total contribution). Similar trends were seen in Principal component 3, with particularly strong contributions of monolyso-CL (MLCL) species and unsaturated PE fatty acids. Therefore, we next evaluated the direction of changes in PL class distribution, specific CL molecular species, and PL fatty acid characteristics (Fig. 2.8).

Acclimation temperature altered mitochondrial PL class distribution differently in northern compared to southern *F. heteroclitus* (Fig. 2.8A; Table 2.3). Acclimation from 15 °C to either 5 °C or 33 °C tended to decrease membrane PC and increase PE content in northern *F. heteroclitus*, while southern subspecies showed the opposite trend. CL content tended to increase with lower acclimation temperatures in both subspecies, with more pronounced effects in the southern subspecies. Reciprocal changes in MLCL levels at least partially implicate altered CL acyl chain hydrolysis or esterification in these CL content variations, particularly in the southern subspecies.

Acclimation temperature induced changes in the CL molecular species profile that were largely consistent between subspecies (Fig. 2.8B; Table 2.3). Lower temperatures tended to decrease CL 18:2n6 enrichment, and favored greater incorporation of 20:4n6 (arachidonic acid) and 18:1 (oleic or vaccenic acid). Similar trends were seen in the total mitochondrial PL fatty acid profile (Fig. 2.8C; Table 2.5), with particularly marked increases in 18:1n7 (vaccenic acid), but not 18:1n9 (oleic acid), following acclimation to colder temperatures. Vaccenic acid has been reported to be the predominant form of 18:1 present in CL (Wahjudi et al., 2011; Wolff et al., 2014), but its physiological role in mitochondrial membranes has remained unclear. The fatty acid composition of PC and particularly PE also varied with acclimation temperature (Fig. 2.8A, Table 2.6, Table 2.7), with class-specific changes reflecting the selectivity of PL remodeling

enzymes and perhaps an exchange of fatty acids to CL molecular species (Schlame, 2013). While PL saturated fatty acids tended to decline with colder acclimation temperatures, general membrane PL characteristics such as the fatty acid double-bond index (DBI) and chain length remained relatively stable in both subspecies (Fig. 2.8D, Table 2.8). However, consistent trends for higher n6 and n7 fatty acids were seen in both species, largely reflecting noted increases in 20:4n6 and 18:1n7.

Reciprocal changes in PL fatty acids leading to higher levels of non-essential unsaturated species suggest that fatty acid desaturase and elongase enzymes might contribute to variations in PL composition observed following acclimation to colder temperatures. Consistent with this prediction, fatty acid product/precursor ratios corresponding to n6 and n3 Δ6-desaturase (D6D), 16C stearoyl-CoA desaturase (SCD), and elongase-6 (ELOVL6) activities were all highest following acclimation to 5 °C in both northern and southern *F. heteroclitus* (Fig. 2.9A, Table 2.9). Opposite patterns of *de novo* 18:0 synthesis and desaturation (by ELOVL6 and SCD, respectively) were observed between northern and southern subspecies, but no other marked intraspecific variation in thermal acclimation responses was evident. Integration of trends observed for all fatty acids within established biosynthesis pathways indicates that a distinct pattern of long-chain fatty acids is favored in mitochondrial membranes in response to colder temperatures (Fig. 2.9B). This pattern is dominated by increases in 18:1n7, 20:4n6 and 22:6n3 in both northern and southern subspecies, despite differences between subspecies in general membrane characteristics (Fig. 2.8A and D).

2.4.6 Inner mitochondrial membrane content

We estimated thermal acclimation and subspecies effects on inner-mitochondrial membrane content by comparing cardiolipin content normalized to mg mitochondrial protein (Fig. 2.10A). In addition, we assessed thermal acclimation and subspecies effects on LEAK-I, II; OXPHOS-I, II and ETS-I, II respiratory capacity normalized to CCO capacity (Fig. 2.10B-D). Cardiolipin content was greatest following low-temperature acclimation temperature and in the northern subspecies ($p_{acclimation} < .001$, $p_{subspecies} < .005$). This subspecies effect was removed following 33°C acclimation ($p_{interaction} < .005$).

2.4.7 Respiratory capacity normalized to CCO capacity

Mitochondrial respiratory capacities (i.e., LEAK-I, II; OXPHOS-I, II and ETS-I, II) normalized to CCO capacity increased with decreasing acclimation temperature ($p_{acclimation} < .001$). Northern *F. heteroclitus* exhibited greater OXPHOS-I, II ($p_{subspecies} < .01$) and ETS-I, II ($p_{subspecies} < .05$) respiratory capacity that was normalized to CCO capacity, but the subspecies did not differ for LEAK-I, II/CCO ($p_{subspecies} = .791$). No significant interaction effects (i.e., subspecies*acclimation) were detected ($p_{LEAK} = .739$, $p_{OXPHOS} = .467$, $p_{ETS} = .141$).

2.5 Discussion

The present study provides a comprehensive analysis of mitochondrial performance and membrane composition following thermal acclimation of two locally adapted subspecies of *F. heteroclitus*. Decreasing acclimation temperature was associated with increased mitochondrial respiratory capacity. These acclimation effects were consistent for both *F. heteroclitus* subspecies. In addition, northern cold-adapted *F. heteroclitus* exhibited greater mitochondrial respiratory capacity when compared with their southern counterparts. Mitochondrial phospholipid characteristics were altered as a result of both thermal acclimation and local adaptation. As acclimation temperature decreased *F. heteroclitus* of both subspecies increased the content of specific unsaturated fatty acids (e.g., 18:1n7 and 20:4n6). Subspecies variation in mitochondrial phospholipids was largely associated with a greater relative content of PC to PE in the southern subspecies when compared with the northern subspecies. Overall, these results support a role for parallel changes in mitochondrial respiratory capacity and membrane characteristics to maintain bioenergetic homeostasis in response to thermal stress and identify novel intraspecific patterns of mitochondrial membrane remodeling under these conditions. We suggest that particular aspects of mitochondrial function and lipid metabolism are targeted by selection and contribute to the eurythermal physiology of this species.

2.5.1 Intraspecific variation in mitochondrial performance

A primary objective of this study was to determine if putatively locally adapted *F. heteroclitus* subspecies exhibit differences in liver mitochondrial performance that might underlie established differences in organismal aerobic metabolism and associated traits (e.g.,

thermal and hypoxia tolerance limits). Our results demonstrate a greater hepatic mitochondrial respiratory capacity of northern versus southern *F. heteroclitus*, which is consistent with greater aerobic metabolic rates in northern subspecies (Fig. 2.2, 2.3, 2.4; Fangue et al., 2009; Healy and Schulte, 2012). However, previous studies have produced mixed evidence for intraspecific variation in *F. heteroclitus* mitochondrial function. This may be a consequence of different tissues being utilized in different studies, as there is no evidence of increased capacity in northern killifish mitochondria in heart or brain (Chapter 5, Baris et al., 2016). Indeed, subspecies differences in *F. heteroclitus* liver mitochondrial performance are not always detected (Fangue et al., 2009). This could be due to the specific population being studied, given the genetic variation present within *F. heteroclitus* subspecies (McKenzie et al., 2016). Alternatively, differences in the substrate combinations used to assay mitochondrial function could explain the differences in findings between these studies. Our use of multiple substrates and populations from the extreme ends of the species distribution appears to provide the resolution necessary to detect subspecies variation in liver mitochondrial capacity.

Whole-organism hypoxia tolerance limits are thought to be shaped by declines in aerobic metabolism and associated mitochondrial failure (Deutsch et al., 2015; Fry and Hart, 1948; Pörtner, 2001). Our demonstration of lower mitochondrial capacity in southern *F. heteroclitus* is consistent with greater hypoxia tolerance in this subspecies (McBryan et al., 2016). Putative links between mitochondrial function and hypoxia tolerance may extend to thermal tolerance as these limits are thought to be a consequence of temperature induced systemic hypoxemia (Pörtner, 2001). Northern and southern *F. heteroclitus* exhibit thermal tolerance limits that are consistent with their northern temperate geographic distributions (Fangue et al., 2006). A lower mitochondrial capacity in the southern subspecies may reflect a lower tissue metabolic and O_2 demand, due to regulated metabolic suppression allowing for the maintenance of function at a lower absolute level at high-temperatures. Alternatively, the greater mitochondrial capacity exhibited by northern *F. heteroclitus* may help to sustain ATP production and thus maintain aerobic performance at lower temperatures.

2.5.2 Thermal acclimation effects on mitochondrial respiratory capacity

Thermal acclimation responses of ectotherms may involve changes in mitochondrial performance to maintain bioenergetic homeostasis (Guderley, 2011). Our demonstration of an

increase in mitochondrial respiratory capacity following low-temperature acclimation in both northern and southern *F. heteroclitus* is consistent with a previous report in northern subspecies (Chapter 4). Low-temperature acclimation is associated with increased mitochondrial function in other ectotherms (Dos Santos et al., 2013; Kraffe et al., 2007), perhaps reflecting a compensation for slower biochemical reaction rates in low temperatures. Although we observe a pattern of increased respiratory capacity with low-temperature acclimation, the magnitude of this effect is not large. This may indicate that the maintenance of energetic balance following thermal acclimation requires the recruitment of mechanisms such as increases in mitochondrial volume density (Dhillon and Schulte, 2011; St-Pierre et al., 1998) as well as increases in capacity.

In contrast to low-temperature effects, high-temperature acclimation decreased mitochondrial respiratory capacity. This might represent beneficial acclimation as acute increases in temperature may result in unsustainable biochemical reaction rates and reactive oxygen species generation (Abele et al., 2002). Decreased mitochondrial function with high-temperature acclimation has been previously reported in *F. heteroclitus* and other aquatic ectotherms (Chapter 4; Khan et al., 2014; Kraffe et al., 2007; Strobel et al., 2013). Although our observed decrease in mitochondrial function could be consistent with a beneficial high-temperature response, they might alternatively be a consequence of sub-lethal stress (Chapters 4 and 5). Indeed, we found that 33 °C acclimation is associated with decreased whole-organism and liver mass (Fig. 2.1). But acclimation to 33 °C is not lethal over prolonged periods (Fangue et al., 2006), suggesting that this temperature represents a sub-lethal stressor. The effect of sub-lethal temperature stress on teleost mitochondrial function is a relatively unexplored area of research with large implications for our understanding of species fitness (Iles, 2014; Lemoine and Burkepile, 2012; Salin et al., 2016).

It is important to acknowledge that our observed thermal acclimation and subspecies effects on mitochondrial respiratory capacity could be due in part to variation in whole-organism and tissue mass. Indeed, decreasing acclimation temperature and putative adaptation to northern latitudes were both associated with greater whole-organism and liver mass (Fig. 2.1). Furthermore, significant covariance of *F. heteroclitus* heart mitochondrial function and organism mass has been noted in other studies (Baris et al., 2017). It is difficult to account for mass effects on liver mitochondrial function, as we utilized a pooled liver homogenate from seven individuals. Nevertheless, a preliminary analysis of the relationship between mean whole-

organism mass within a pooled sample and mitochondrial respiratory capacity did not reveal any consistent relationships. But this crude correlation should be interpreted carefully as we utilized a limited sample size within each treatment (n = 7-8).

Changes in mitochondrial performance following thermal acclimation were not clearly associated with a single ETS component (Fig. 2.2, 2.3, 2.4). However, it should be noted that our use of substrate combinations (ETS CI and CII simultaneously) can make it difficult to disentangle the involvement of CII in the thermal acclimation response. But maximum ETS flux through CII (ETS-II; Fig. 2.4C, D) exhibited a pattern similar to both CI and CI, II-linked respiration which indicates that this is a broad-scale thermal acclimation response. In contrast, thermal acclimation did not alter apparent CCO capacity (Fig. 2.4E, F), indicating that thermal acclimation specifically alters ETS performance upstream of CCO, perhaps through CI (Chapter 4). But this effect is not universal across fishes, as increased acclimation temperature has been shown to decrease CCO activity in *Oncorynchus mykiss* (Kraffe et al., 2007). Nevertheless, thermal acclimation may alter CCO function as we have noted thermal acclimation effects on mitochondrial O_2 binding affinity in this species (Chapter 3).

Taken together, the effects of thermal acclimation on mitochondrial performance are consistent with the maintenance of biochemical reaction rates in response to temperature effects. The observed changes demonstrate the importance of maintaining mitochondrial function in the face of prolonged thermal stress and likely underlie the eurythermal physiology of this species.

2.5.3 Thermal acclimation and intraspecific effects on mitochondrial membrane composition

The present study demonstrates variation in mitochondrial membrane composition between *F. heteroclitus* subspecies that changed in parallel with respiratory function following thermal acclimation. Thermal acclimation induced the largest changes in mitochondrial membrane composition (principal component 1), primarily due to shifts in PL FAs. Subspecies effects accounted for less total variation in mitochondrial membrane composition (principal component 3) and were largely associated with variation in PL class distribution and a smaller set of unsaturated FAs. Both subspecies exhibited similar responses to thermal acclimation for the majority of mitochondrial membrane characteristics. Our findings indicate that changes in PL FA composition are the primary signature of thermal acclimation in hepatic mitochondrial membranes, while shifts in PL classes are more closely associated with putative local adaptation

responses. These responses were observed in fish held under common garden conditions in the laboratory. In nature the northern and southern subspecies may have access to different prey items and these prey items may differ among seasons. If these prey items differ in lipid composition, it is possible that natural populations may differ in lipid composition to an even greater extent than observed here. However, our data clearly show that the northern and southern populations differ in their mitochondrial membrane composition and express the ability to modify membrane composition with thermal acclimation, even when fed a common diet.

Phosphatidylcholine (PC) and phosphatidylethanolamine (PE) comprise the majority of PLs present in mitochondria, and changes in their relative proportions (i.e., PC/PE ratio) have been associated with altered membrane fluidity following thermal acclimation (Hazel and Landrey, 1988). In the present study, the PC/PE ratio was similar between *F. heteroclitus* subspecies acclimated to 15 °C but tended to increase in the southern subspecies in response to either 5 °C or 33 °C acclimation, and decrease in the northern subspecies under the same conditions. These opposing responses suggest distinct strategies between the subspecies for coping with thermal stress (rather than cold or heat, *per se*) through modulation of mitochondrial PL metabolism. Moderate (< 30%) decreases in mitochondrial PE (leading to higher PC/PE) result in a less fluid membrane environment (Li et al., 2006), and can alter cristae morphology and reduce respiratory capacity (Tasseva et al., 2013). Conversely, a 33% increase in hepatic mitochondrial PC/PE has been associated with higher respiration and ATP production (van der Veen et al., 2014). Our observed variation in PL classes is consistent with these studies as the southern subspecies, which has lower respiratory capacity, exhibited lower mitochondrial PE compared to the northern subspecies following acclimation to 5 °C or 33 °C. However, this does not explain the functional differences between the subspecies acclimated to 15 °C where PE and PC/PE were similar between subspecies. It is important to note that the global PC/PE ratio describes variation in total PL classes and does not differentiate among phospholipid subclasses (e.g., diacyl-, lyso- and plasmalogen species). Kraffe et al. (2007) demonstrate that PL classes vary following thermal acclimation in a subclass-specific manner. Although not investigated here, variation in these mitochondrial PL subclasses likely contributes to the thermal acclimation response in both subspecies and has implications for membrane properties beyond changes in fluidity. Notably, reciprocal changes in PE and PC often reflect changes in PE methyltransferase (PEMT) activity, which converts PE to PC by N-methylation and is a potent regulator of hepatic

lipoprotein assembly, choline metabolism, and gluconeogenesis (Vance et al., 2007; van der Veen et al., 2014).

In addition to PE and PC, the IMM contains mitochondrial membranes contain the unique dimeric PL cardiolipin (CL), which is known to be critical for maintaining membrane integrity and organelle function (Schlame, 2007). Consistent with previous observations in Rainbow trout (*Oncorhynchus mykiss*) acclimated to a range of temperatures (Kraffe et al., 2007), CL content expressed as a percent of total lipids did not change significantly in response to thermal acclimation or between subspecies in the present study. However, there were substantial changes in monolysocardiolipin (MLCL) with thermal acclimation in both subspecies that generally reflected reciprocal (non-significant) changes in CL content. The direction of these changes varied between subspecies, with MLCL being highest at 5 °C in the northern and at 15 °C in the southern subspecies, suggesting intraspecific variation in CL deacylation/reacylation in response to thermal stress (Taylor et al., 1999). Indeed, marked changes in CL acyl chain composition were observed across acclimation temperatures, indicating significant induction of CL remodeling pathways.

Decreasing acclimation temperature tended to decrease the proportion of CL species enriched with 18:2n6, and increase those containing 18:1, 20:4n6 and 22:6n3 in both *F. heteroclitus* subspecies. A similar pattern of CL remodeling was reported in muscle mitochondria from *Oncorhynchus mykiss* following cold acclimation (Kraffe et al., 2007), which was suggested as the potential mechanism underlying changes in respiratory capacity across acclimation temperature in this species. Compositional changes in CL generally paralleled FA shifts in the total mitochondrial PL fraction in the present study, but varied somewhat from those observed in PE and PC, suggesting a preferential enrichment of CL 18:1n7, 20:4n6 and 22:6n3 at colder temperatures. These increases in unsaturated fatty acids may help to preserve mitochondrial membrane fluidity at colder temperatures in accordance with HVA (Hazel, 1995), but were largely balanced by changes in 18:2n6 and 22:5n3 that maintained a similar membrane double-bond index across acclimation temperatures. Therefore, we postulate that shifts in the content of particular fatty acids or their PL esterification may serve more specific roles in regulating mitochondrial physiology, and perhaps reflect broader changes in cellular lipid metabolism relevant to organismal thermal adaptation. For example, changes in membrane 22:6n3 content have been associated with a wide array of metabolic phenotypes that likely

involve effects other than a contribution to membrane unsaturation (Hagve et al., 2009; Leray et al., 1984; Muriana et al., 1992; Stillwell and Wassall, 2003). Thus, our data are more consistent with a targeted mitochondrial membrane remodeling as opposed to a general shift in membrane composition to maintain fluidity (Kraffe et al. 2007, Hazel 1995).

The relative contents of selected membrane fatty acids are often used to estimate the *in vivo* activity of various desaturase and elongase enzymes involved in the biosynthesis of long-chain unsaturated fatty acids, which are predominantly esterified to membrane PLs. Thermal acclimation altered indices associated with three such enzymes, highlighting plausible mediators of the observed alterations in membrane FA composition. In particular, the accumulation of 20:4n6 and 22:6n3 following decreased acclimation temperature was associated with decreases in their FA precursors (18:2n6 and 22:5n3), suggesting an increase in both n3- and n6-PUFA delta-6 desaturase (Δ6D) activity following acclimation to low temperatures in both subspecies. Δ6D catalyzes critical rate-limiting steps in the synthesis of long-chain highly unsaturated PUFA (Fig. 2.9B), and thus has been linked to a wide range of physiological and pathological phenotypes (Tosi et al., 2014). Δ6D has also been implicated in teleost responses to low temperature and salinity, but little is known about its regulation in the context of thermal acclimation (Santigosa and Vagner, 2011).

Decreasing acclimation temperature also increased the 16:1n7/16:0 index of stearoyl-CoA desaturase (SCD) activity in both *F. heteroclitus* subspecies, which along with the conversion of 18:0 to 18:1n9, provides the major source of *de novo* synthesized monounsaturated from saturated FAs (Paton and Ntambi, 2009). This increase in the membrane content of monounsaturated/saturated FAs favors an increase in fluidity consistent with HVA to colder temperatures (Guderley, 2004). Increases in SCD activity might also regulate broader aspects of hepatic function and metabolism, including triglyceride biosynthesis, glucose utilization, inflammation and stress response (Liu et al., 2011). In addition, the SCD product 16:1n7 can be elongated by ELOVL6 to 18:1n7, which increased dramatically in response to colder temperatures along with other indices of ELOVL6 activity. In contrast to increases in FA unsaturation, longer FA chains are associated with decreased membrane fluidity (Marsh, 2010). However, average membrane FA chain length was not altered following thermal acclimation in the present study, suggesting a more specialized role of ELOVL6 toward specific substrates, or metabolism of selected products by other enzymes downstream. Interestingly, ELOVL6 activity

increases with cold exposure in mice and is essential for maintaining mitochondrial capacity and thermogenic function in brown adipose tissue (Virtue et al., 2015). Given the parallel increases in mitochondrial membrane 18:1n7 and respiratory capacity in cold-acclimated fish in the present study, the potential roles of SCD and ELOVL6 in regulating mitochondrial function in poikilotherms merit further investigation.

2.5.4 Inner mitochondrial membrane content and variation in mitochondrial respiration

Although we suggest that mitochondrial membrane composition alters the intrinsic function of the OXPHOS apparatus, thermal acclimation and intraspecific effects on mitochondrial respiratory capacity could be due to changes in total IMM content and its associated enzymes. To investigate this possibility, we compared thermal acclimation and intraspecific effects on absolute cardiolipin content normalized to total mitochondrial protein content and mitochondrial respiratory capacities normalized to CCO capacity (T_{assay} = 15 °C; Fig. 2.10). Cardiolipin content was greater in the northern subspecies and increased following cold acclimation, a pattern that was similar to variation in mitochondrial respiratory capacity (Fig. 1). This suggests that much of the difference in respiratory capacity between subspecies and with acclimation could be due to changes in the amount of IMM per mitochondrion. Consistent with this hypothesis, subspecies effects on CCO normalized mitochondrial respiratory capacity were smaller relative to those observed for respiratory capacity normalized to mitochondrial protein content. However, clear acclimation effects remained even when respiratory capacity is normalized to CCO capacity. Maximum CCO capacity did not change significantly with thermal acclimation (Fig. 2E, F) while thermal acclimation had strong effects on other components of the ETS. These data indicate that variation in IMM content partially accounts for our observed thermal acclimation and intraspecific variation effects on mitochondrial respiratory capacity, but that CCO capacity does not change in parallel. In general, CCO capacity is thought to not be limiting for ETS function (Gnaiger et al. 1998), and our data are consistent with this pattern. Taken together, a substantial component of the differences in respiratory capacity between subspecies and acclimation temperatures can be accounted for by changes in IMM amount, but we detected significant intraspecific and thermal acclimation effects on CCO normalized mitochondrial respiratory capacity which supports a role for mechanisms in addition to changes in IMM content in driving changes in mitochondrial function.

2.5.5 Conclusion

Our data provide support for mitochondrial membrane remodeling as a mechanism driving variation in mitochondrial performance following thermal acclimation and local adaptation. Respiratory capacity increased in response to decreasing acclimation temperature and was greater in the putatively cold adapted northern subspecies. This variation in mitochondrial respiration is consistent with previously observed whole-organism responses to thermal acclimation and intraspecific variation of aerobic metabolism. We demonstrate a targeted remodeling of mitochondrial phospholipids in response to acclimation and differences in membrane phospholipid composition between subspecies, indicating that *F. heteroclitus* utilizes regulated membrane remodeling as a response to thermal stress at multiple timescales. In addition, both thermal acclimation and putative local adaptation to cold temperatures were associated with greater estimates of inner mitochondrial membrane content, which partly accounts for our observed variation in mitochondrial respiratory capacity. The ability to remodel mitochondrial membrane phospholipids and alter respiratory capacity likely underlies the highly eurythermal physiology of these fish and may have been a target of natural selection.

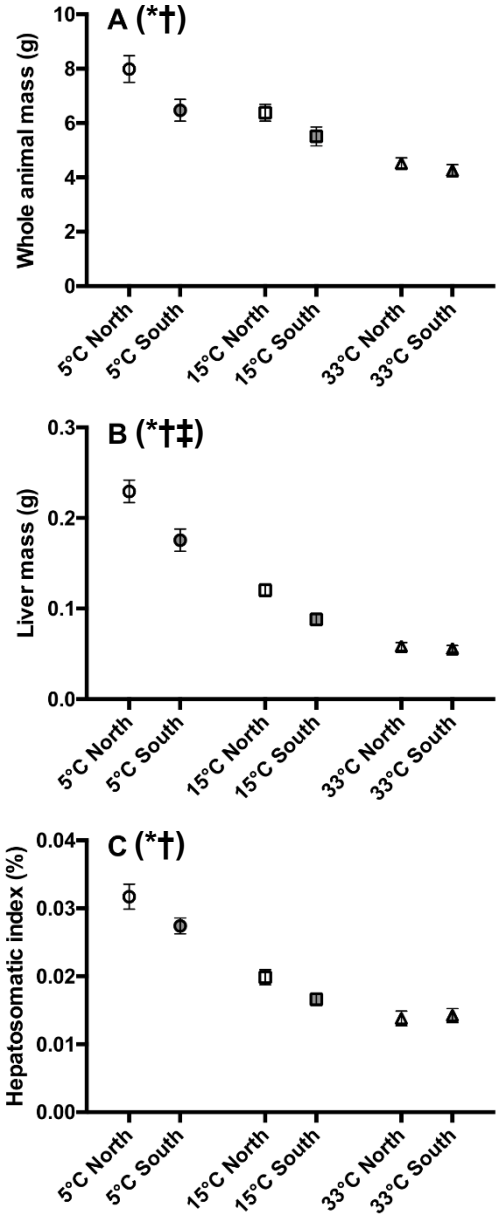

Figure 2.1. *Fundulus heteroclitus* whole-animal, liver wet mass, and somatic index. Northern and southern *F. heteroclitus* were acclimated to 5, 15, or 33 °C for four weeks. Hepatosomatic index (C) was calculated as the ratio of wet liver mass to whole-animal mass. Data are mean ± SEM; see Results for associated statistics (n = 49-56). Symbols indicate significant effects of acclimation (*), subspecies (†), and the interaction between acclimation and subspecies (‡).

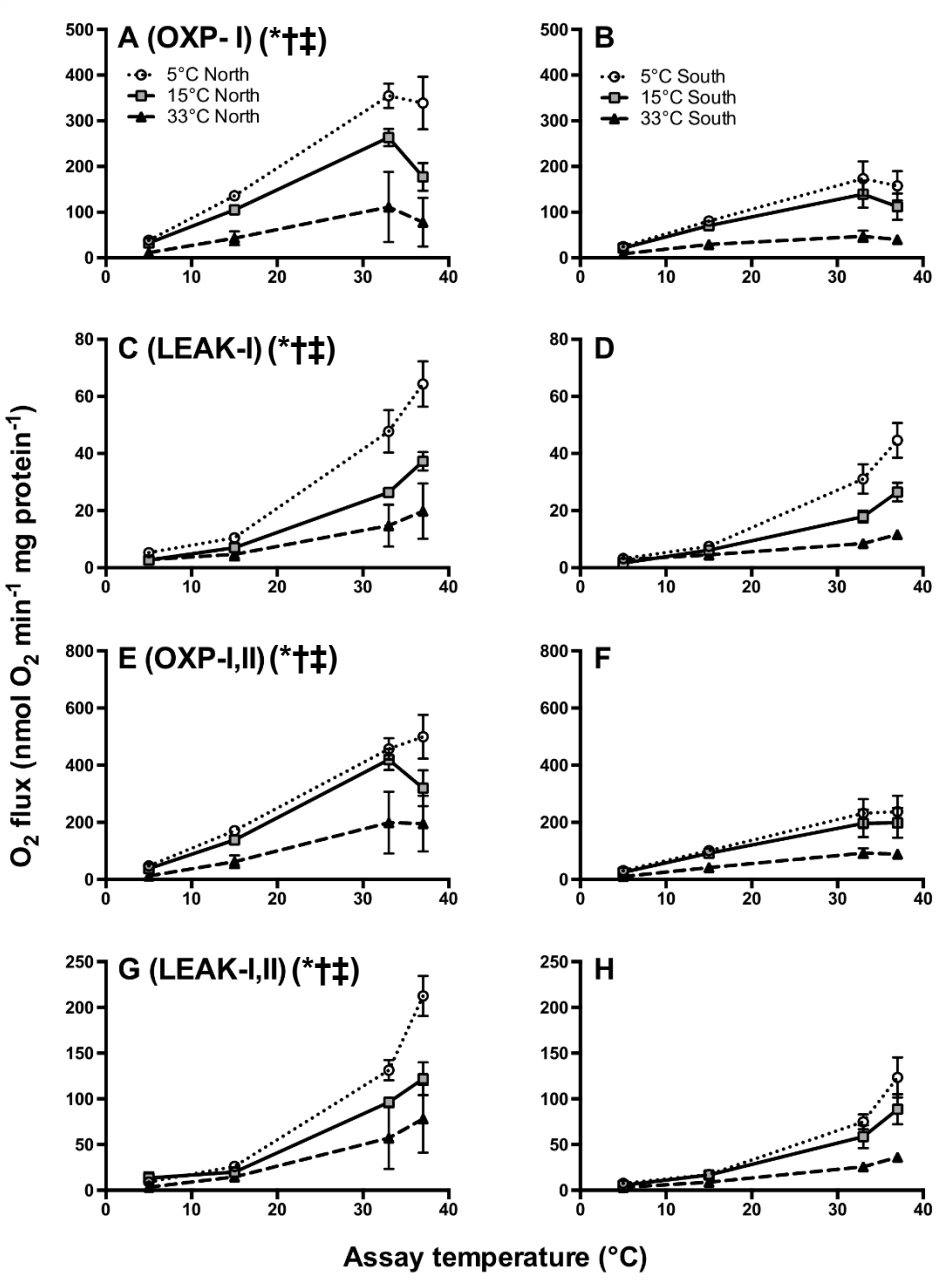

Figure 2.2. *Fundulus heteroclitus* coupled liver mitochondrial respiration. Northern (A, C, E, G) and southern (B, D, F, H) *F. heteroclitus* were acclimated to 5, 15 or 33 °C for four weeks. Oxidative phosphorylation (OXP, state 3; A, B, E, F) and LEAK (state 2 or 4; C, D, G, F) respiration rate were measured through electron transport system complex I (A-D; pyruvate, malate and glutamate as substrates) and complexes I and II simultaneously (E-H; complex I substrates and succinate). Data are mean ± SEM; see Table 2.2 for associated statistics (n = 7-8). Symbols indicate significant main effects of assay temperature (*), acclimation (†), and subspecies (‡).

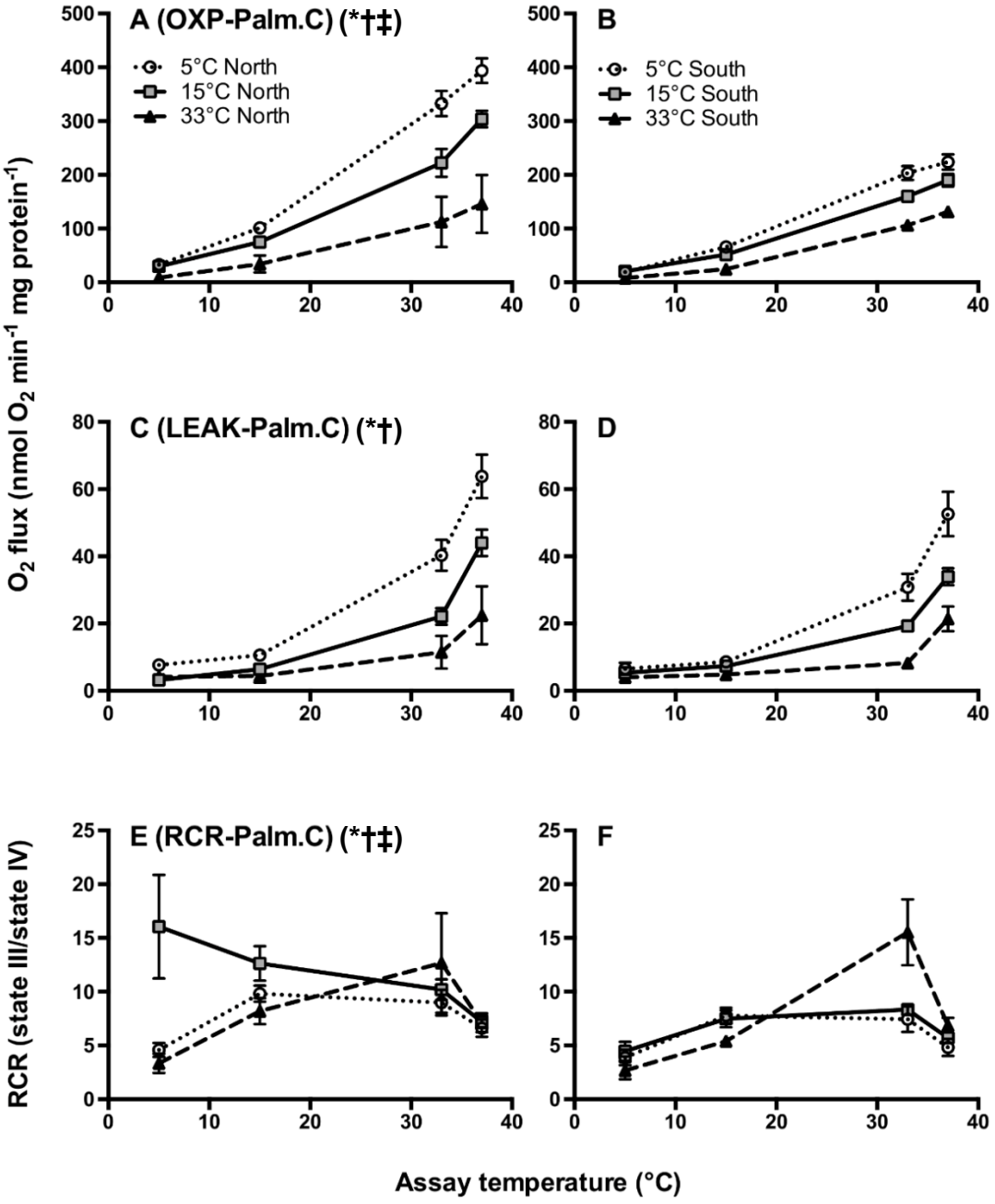

Figure 2.3. *Fundulus heteroclitus* coupled liver mitochondrial respiration and respiratory control ratio fueled with fatty-acid substrates. Northern (A, C, E) and southern (B, D, F) *F. heteroclitus* were acclimated to 5, 15 or 33 °C for four weeks. Oxidative phosphorylation (OXP, state 3; A, B) and LEAK (state 2; C, D) respiration rate were measured with fatty-acid substrates (palmitoyl carnitine and malate). Respiratory control ratio (E, F) was calculated as the ratio of OXP/LEAK. Data are mean ± SEM; see Table 2.2 for associated statistics (n = 7-8). Symbols indicate significant main effects of assay temperature (*), acclimation (†), and subspecies (‡).

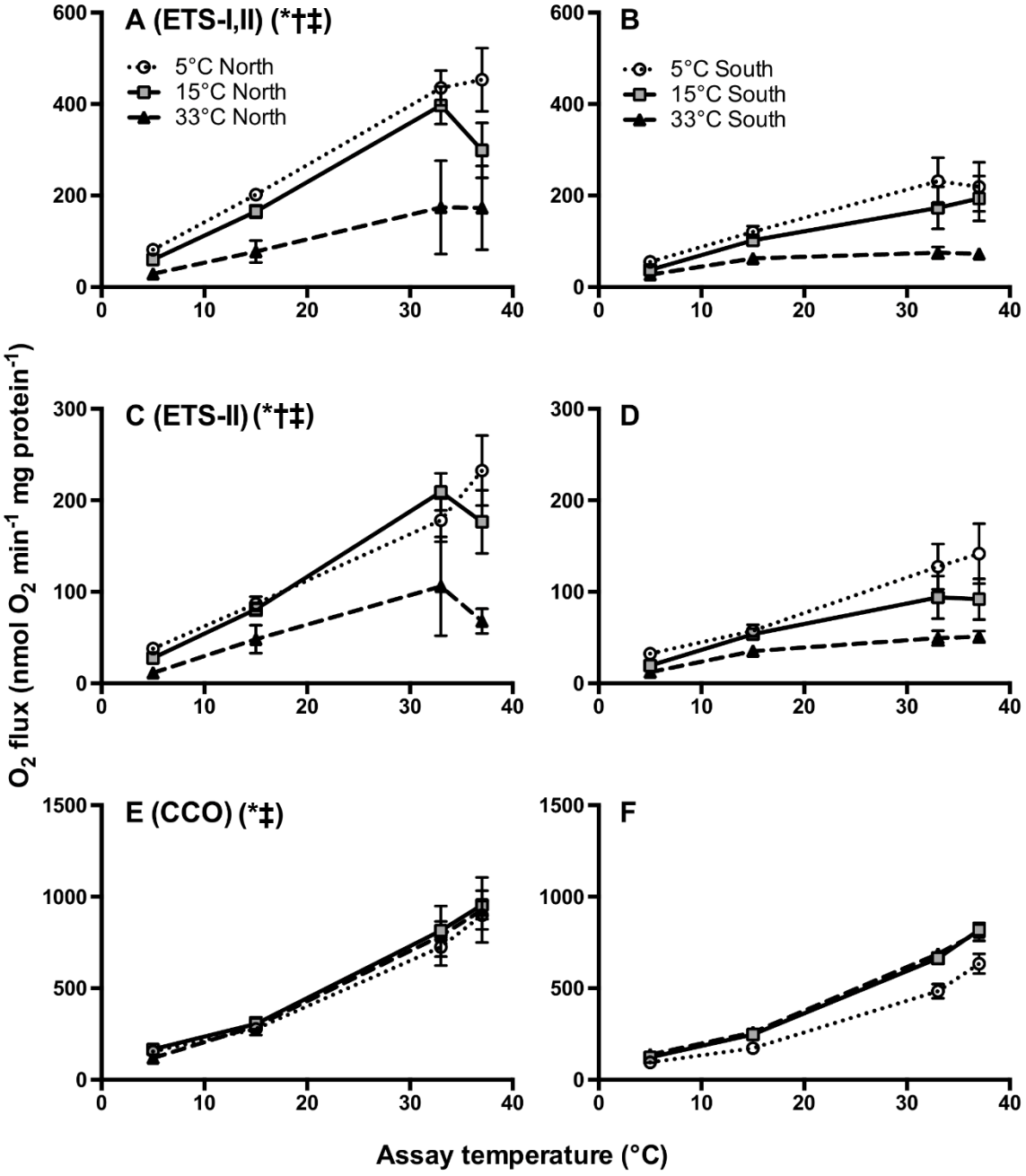

Figure 2.4. *Fundulus heteroclitus* maximum liver mitochondrial respiratory capacity. Northern (A, C, E) and southern (B, D, F) *F. heteroclitus* were acclimated to 5, 15, or 33 °C for four weeks. Substrate oxidation capacity (ETS) was fueled through electron transport system complexes I and II simultaneously (A, B; pyruvate, malate, glutamate and succinate as substrates) or complex II alone (C, D; succinate as a substrate). Apparent cytochrome c oxidase (CCO) capacity (E, F) was determined in an uncoupled state. Data are mean ± SEM, see Table 2.2 for associated statistics (n = 7-8). Symbols indicate significant main effects of assay temperature (*), acclimation (†), and subspecies (‡).

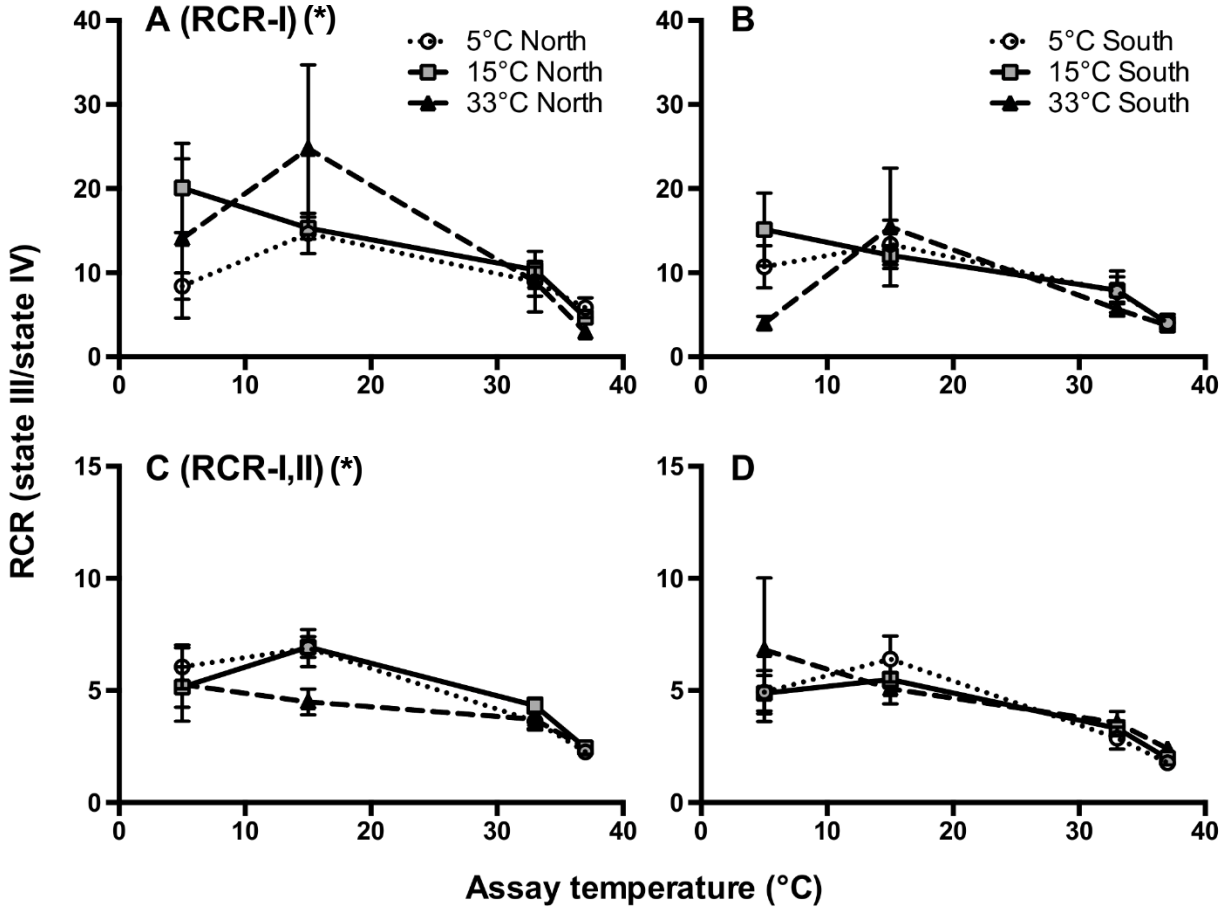

Figure 2.5. *Fundulus heteroclitus* liver mitochondrial respiratory control ratios (RCR). Northern (A, C) and southern (B, D) *F. heteroclitus* were acclimated to 5, 15, or 33 °C for four weeks. RCRs were calculated from respiratory flux fueled with electron transport system complex I (A, B; pyruvate, malate, glutamate as fuels) or complexes I and II simultaneously (C, D; complex I substrates and succinate). Data are mean ± SEM, see Table 2.2 for associated statistics. Symbols indicate significant main effects of assay temperature (*).

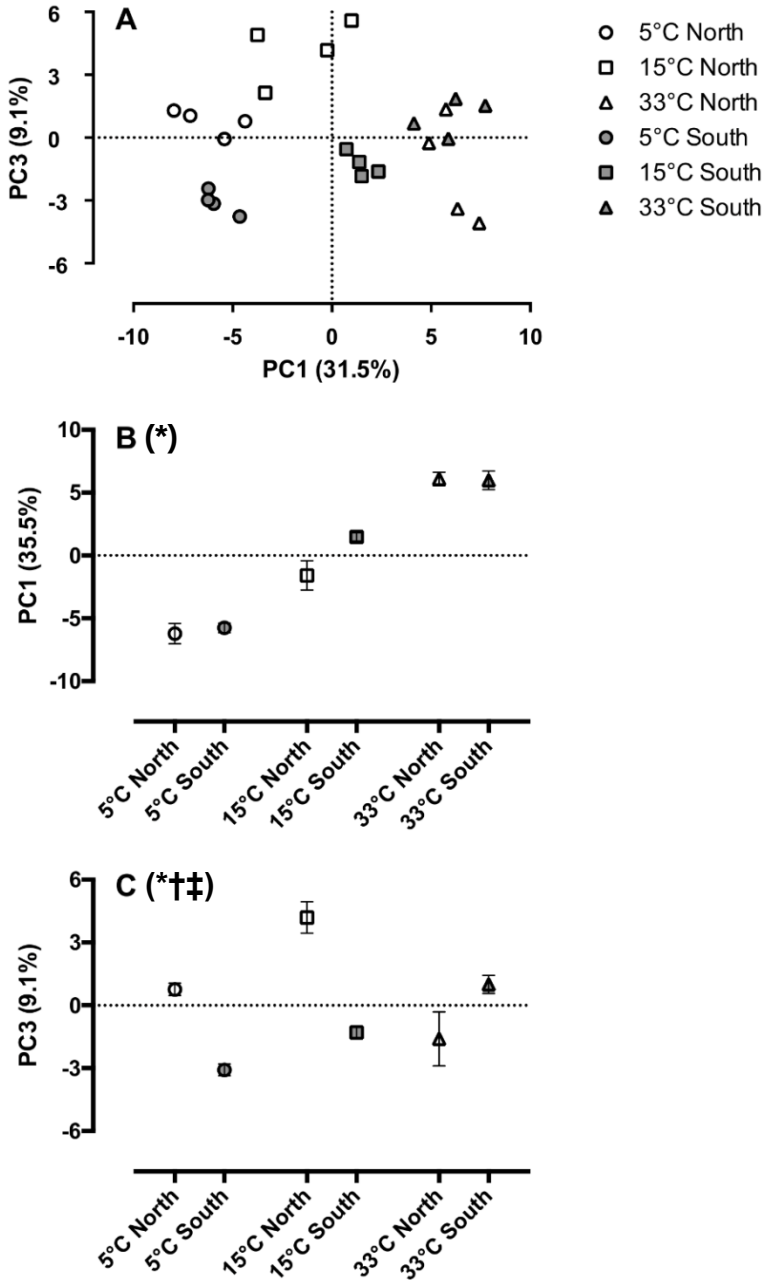

Figure 2.6. First and third principal component scores for liver mitochondrial membrane composition of thermally acclimated *Fundulus heteroclitus* subspecies. Northern (white symbols) and southern (grey symbols) *F. heteroclitus* were acclimated to 5, 15, or 33 °C for four weeks. (A) the plot of individuals along PC1 and PC3 axes. Individual values extracted from PC1 significantly separated thermal acclimation treatments (B). Individual values extracted from PC3 significantly separated both thermal acclimation and subspecies treatments (C). See the Results section for associated statistics, n = 4. Symbols indicate significant effects of acclimation (*), subspecies (†), and the interaction between acclimation and subspecies (‡).

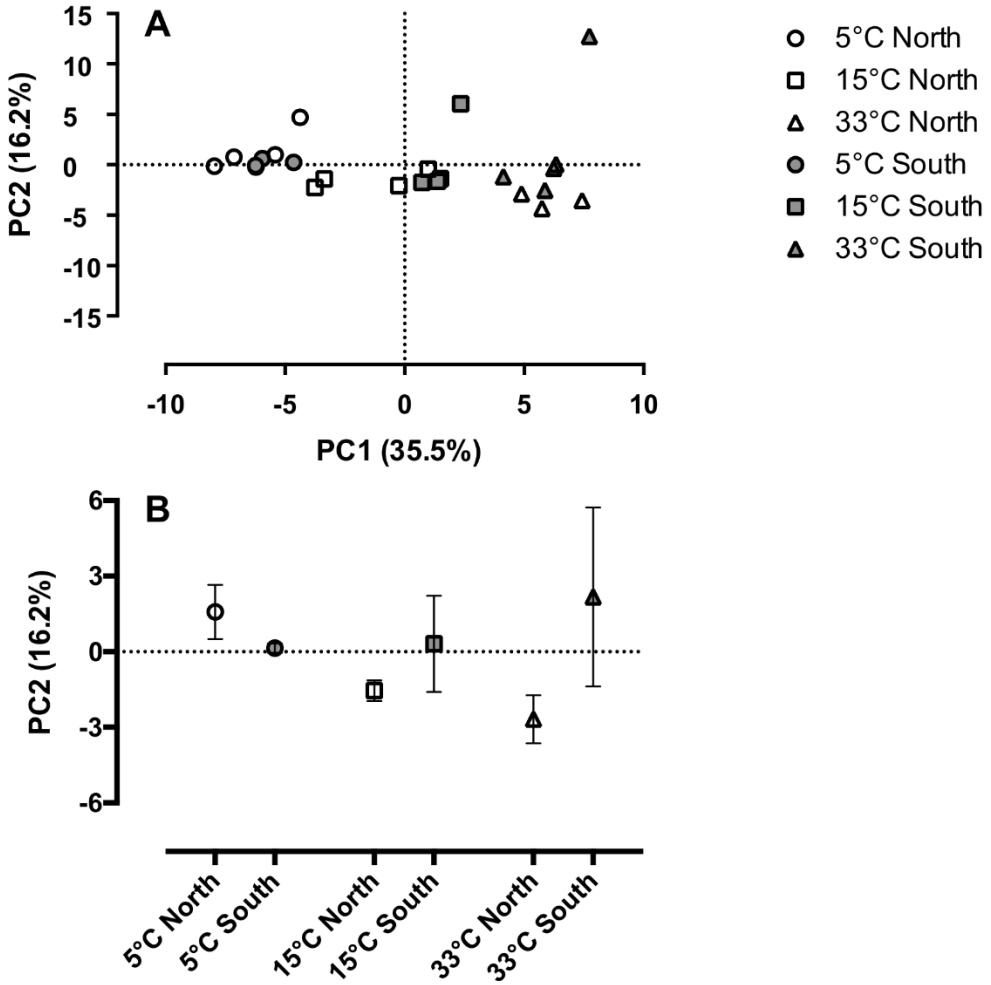

Figure 2.7. Second principal component score for liver mitochondrial membrane composition of thermally acclimated *Fundulus heteroclitus* subspecies. Northern (white symbols) and southern (grey symbols) *F. heteroclitus* were acclimated to 5, 15, or 33 °C for four weeks. (A) the plot of individuals along PC1 and PC2 axes. PC2 did not significantly separate subspecies or thermal acclimation treatment (B). See the Results section for associated statistics, $n = 4$. No significant main effects were detected.

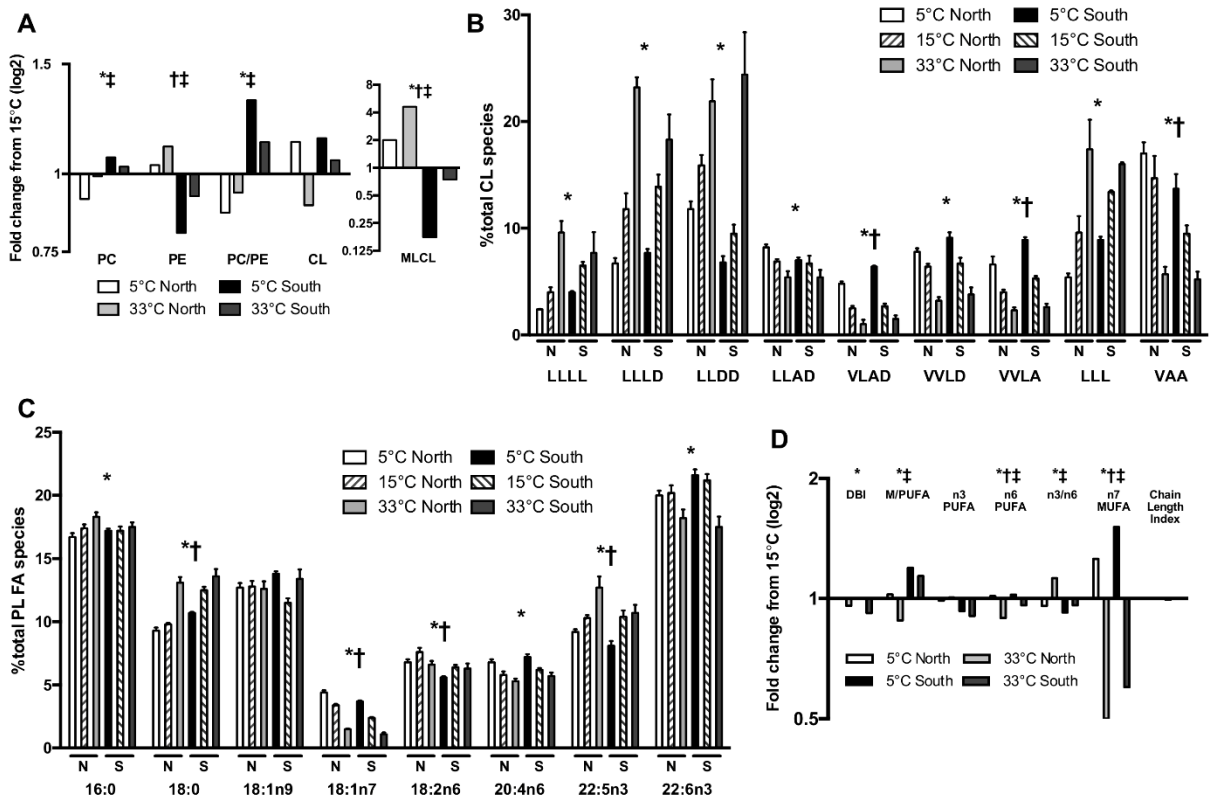

Figure 2.8. *Fundulus heteroclitus* mitochondrial membrane remodeling in response to thermal acclimation. A) Fold changes in mitochondrial phosphatidylcholine (PC), phosphatidylethanolamine (PE), the PC/PE ratio, cardiolipin (CL), and monolyso-CL (MLCL) content in response to 5 °C and 33 °C acclimation relative to 15 °C. B) Percent cardiolipin molecular species in northern (N) and southern (S) *F. heteroclitus* following acclimation to 5, 15, and 33 °C. The fatty composition of tetra-acyl (4 letters) or mono-lyso (3 letters) CL species are indicated by L (18:2n6, linoleic), D (22:6n3, docosahexaenoic), A (20:4n6, arachidonic), and V (18:1n7, vaccenic). C) Predominant fatty acids extracted from total mitochondrial phospholipids following acclimation to 5, 15, and 33 °C. D) Fold changes in general characteristics of total mitochondrial phospholipid fatty acid profile in response to 5 °C and 33 °C acclimation relative to 15 °C. DBI: double bond index, M/PUFA: the ratio of monounsaturated FA to polyunsaturated FA. Symbols indicate significant effects from a two-way ANOVA comparing associated mean values (see tables for mean values). *: acclimation; †: subspecies; ‡: acclimation and subspecies. See relevant table for sample size.

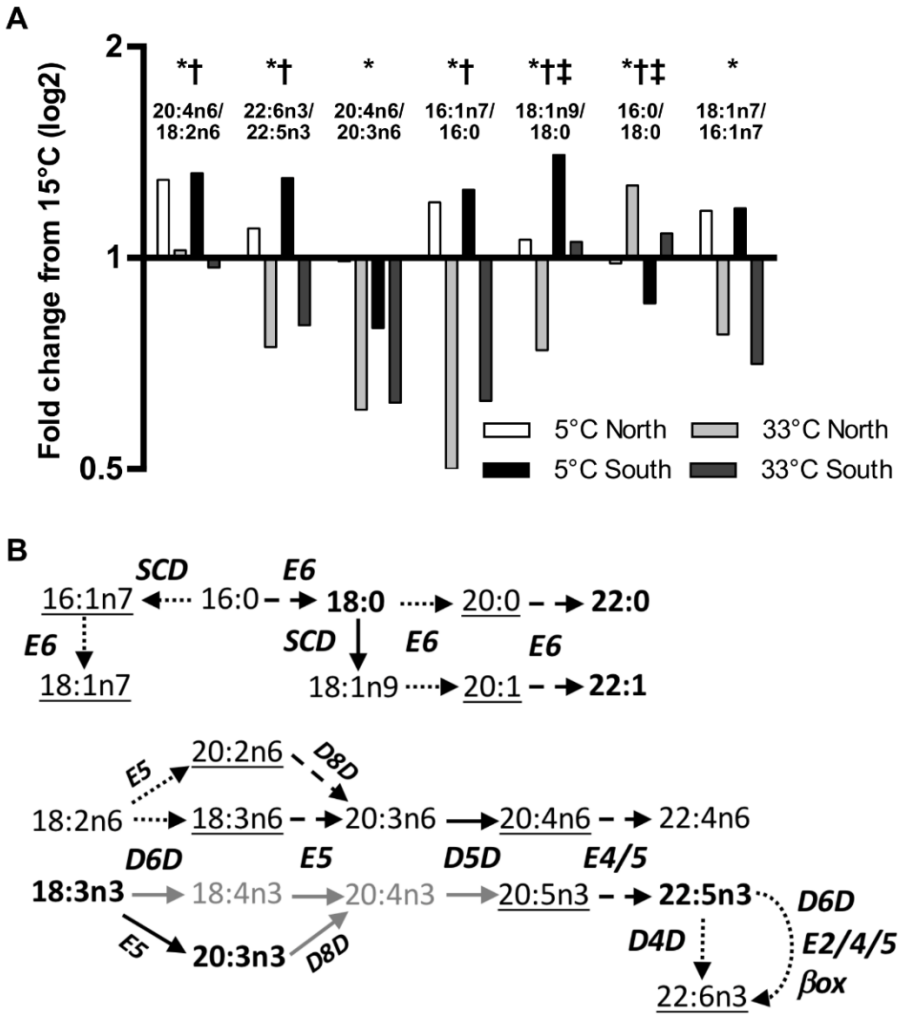

Figure 2.9. *Fundulus heteroclitus* mitochondrial membrane fatty acid desaturase and elongase product/precursor ratios following thermal acclimation A) Fold changes in selected fatty acid product/precursor ratios from total mitochondrial phospholipids in response to 5 °C and 33 °C acclimation relative to 15 °C. B) Predominant pathways of long-chain fatty acid desaturation and elongation. Fatty acids and membrane remodeling enzymes are indicated to illustrate those that tended to be highest at 5 °C (underlined FAs, black dotted arrow), highest at 33 °C (bold FAs, black dashed arrow), not uniformly respond to acclimation temperature (black unformatted FAs, solid black arrow), or were not detected (grey unformatted FAs, solid grey arrow). Enzymes are listed for each reaction include E: elongase; D6D, Δ-6 desaturase; D5D, Δ-5 desaturase; D4D, Δ-4 desaturase; D8D, Δ-8 desaturase; SCD, stearoyl-CoA desaturase, *B*ox, B-oxidation. Symbols indicate significant effects from a two-way ANOVA comparing associated mean values (see tables for mean values). *: acclimation; †: subspecies; ‡: acclimation and subspecies. *n* = 7-8.

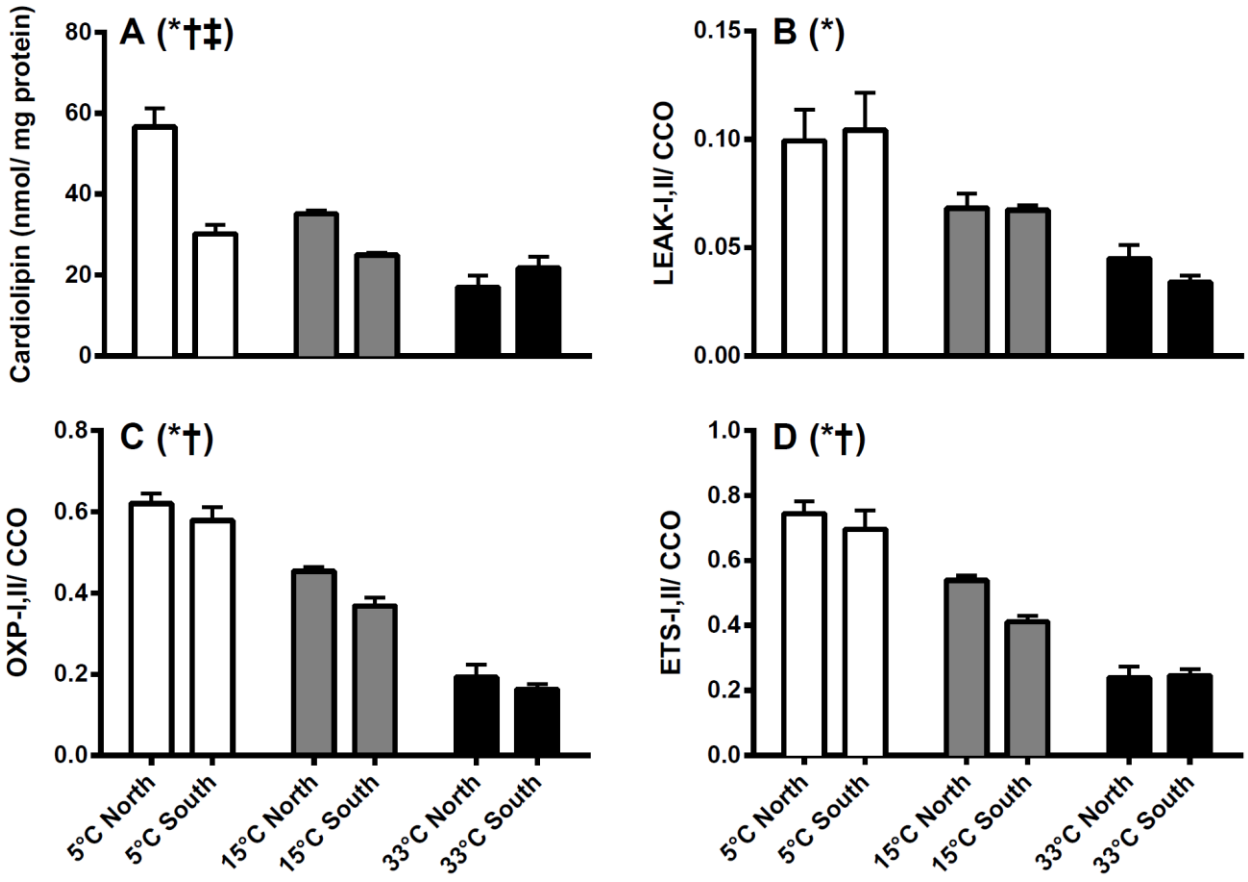

Figure 2.10. Estimates of thermal acclimation and subspecies effects on *Fundulus heteroclitus* inner mitochondrial membrane content and associated enzymes. Northern and southern *F. heteroclitus* were acclimated to 5, 15, and 33°C for four weeks. A) Whole mitochondrial cardiolipin content normalized to mg mitochondrial protein. B) LEAK respiration normalized to apparent cytochrome c oxidase (CCO) capacity. C) Oxidative phosphorylation (OXP) respiration normalized to CCO capacity. D) Substrate oxidation capacity (ETS) normalized to CCO capacity. LEAK, OXP and ETS were fueled through electron transport system complexes I and II simultaneously (I-II; pyruvate, malate, glutamate and succinate as substrates). Data are mean ± SEM, symbols indicate significant effects from a two-way ANOVA (*: acclimation; †: subspecies; ‡: acclimation and subspecies, n = 7-8).

Table 2.1. Principal component analysis factor scores, percent contribution (Ctr) of individual variables to the components, and the squared cosines of the variables on principal components 1 and 3.

	F_1	F_3	Ctr_1	Ctr_3	Cos_1^2	Cos_3^2
CL	0.42	-0.24	0.67	0.80	17.6	5.6
Monolyso-CL	0.83	-0.16	**2.63**	0.39	69.5	2.7
PE	0.59	-0.56	**1.33**	**4.49**	35.1	31.7
PC	-0.35	0.75	0.45	**7.88**	12.0	55.6
CL_1402	0.74	0.29	**2.09**	1.20	55.1	8.5
CL_1404	0.91	0.10	**3.11**	0.15	82.0	1.0
CL_1424	-0.76	0.26	**2.17**	0.98	57.2	6.9
CL_1428	0.85	-0.04	**2.76**	0.02	73.0	0.2
CL_1448	-0.77	0.20	**2.26**	0.54	59.8	3.8
CL_1450	0.59	-0.04	**1.33**	0.02	35.1	0.2
CL_1452	0.75	-0.16	**2.14**	0.38	56.5	2.7
CL_1472	-0.75	0.37	**2.13**	**1.94**	56.2	13.7
CL_1476	0.81	0.36	**2.49**	**1.83**	65.6	12.9
CL_1496	-0.89	0.03	**2.98**	0.01	78.5	0.1
CL_1498	0.06	-0.85	0.02	**10.13**	0.4	71.4
CL_1500	0.88	0.19	**2.92**	0.49	77.2	3.4
CL_1520	0.66	-0.05	**1.66**	0.04	43.8	0.3
CL_1522	0.88	0.29	**2.96**	1.19	78.2	8.4
CL_1544	-0.72	-0.26	**1.95**	0.94	51.5	6.7
CL_1546	0.72	0.00	**1.94**	0.00	51.1	0.0
CL_1566	-0.74	0.08	**2.10**	0.10	55.3	0.7
CL_1568	-0.04	0.32	0.01	**1.44**	0.2	10.2
MLCL_1164	-0.22	0.59	0.19	**4.87**	5.0	34.4
MLCL_1166	-0.36	0.34	0.49	**1.64**	13.1	11.5
MLCL_1186	-0.81	0.07	**2.50**	0.07	66.0	0.5
MLCL_1188	-0.01	-0.15	0.00	0.30	0.0	2.1
MLCL_1190	0.05	0.19	0.01	0.49	0.3	3.5
MLCL_1210	0.29	0.42	0.32	**2.51**	8.4	17.7
MLCL_1212	0.47	0.49	0.85	**3.38**	22.4	23.8
MLCL_1234	-0.50	-0.52	0.95	**3.78**	25.1	26.7
MLCL_1236	0.90	-0.18	**3.04**	0.44	80.2	3.1
MLCL_1256	-0.23	0.10	0.19	0.15	5.1	1.0
MLCL_1258	0.71	0.29	**1.89**	1.23	49.9	8.7
MLCL_1282	-0.10	-0.42	0.04	**2.53**	0.9	17.8
PC_14:0	-0.08	0.21	0.02	0.65	0.7	4.6
PC_16:0	0.46	0.28	0.80	1.12	21.2	7.9
PC_16:1	0.80	-0.19	**2.40**	0.49	63.4	3.5
PC_18:0	-0.70	0.36	**1.85**	**1.86**	48.8	13.1
PC_18:1n9	0.25	0.04	0.24	0.03	6.3	0.2

Table 2.1. Principal component analysis factor scores, percent contribution (Ctr) of individual variables to the components, and the squared cosines of the variables on principal components 1 and 3.

	F_1	F_3	Ctr_1	Ctr_3	Cos_1^2	Cos_3^2
PC_18:1n7	0.83	0.15	**2.63**	0.33	69.4	2.3
PC_18:2n6	0.09	-0.58	0.03	**4.76**	0.8	33.6
PC_18:3n6	-0.24	-0.08	0.21	0.08	5.6	0.6
PC_18:3n3	-0.26	-0.10	0.25	0.15	6.5	1.1
PC_20:0	-0.37	-0.11	0.51	0.16	13.5	1.1
PC_20:1	-0.14	-0.09	0.08	0.11	2.0	0.8
PC_20:2	-0.31	-0.16	0.36	0.35	9.5	2.5
PC_20:4n6	0.25	-0.16	0.25	0.37	6.5	2.6
PC_20:3n6	-0.51	0.00	1.00	0.00	26.4	0.0
PC_20:3n3	-0.48	-0.25	0.89	0.86	23.5	6.1
PC_20:5n3	0.22	-0.34	0.19	1.67	4.9	11.8
PC_22:0	-0.60	0.08	**1.36**	0.10	35.9	0.7
PC_22:1	-0.46	-0.07	0.82	0.07	21.5	0.5
PC_22:4	-0.31	-0.40	0.36	**2.31**	9.6	16.3
PC_22:5n3	-0.40	0.05	0.60	0.03	15.8	0.2
PC_22:6n3	0.72	0.07	**1.96**	0.08	51.7	0.5
PE_14:0	-0.81	0.06	**2.47**	0.05	65.2	0.3
PE_16:0	-0.75	-0.03	**2.13**	0.02	56.2	0.1
PE_16:1	-0.25	0.56	0.23	**4.47**	6.1	31.5
PE_18:0	-0.53	0.12	1.07	0.21	28.2	1.5
PE_18:1n9	0.73	0.34	**2.04**	**1.68**	53.8	11.9
PE_18:1n7	0.18	-0.42	0.12	**2.46**	3.1	17.4
PE_18:2n6	0.60	-0.49	**1.34**	**3.43**	35.5	24.2
PE_18:3n6	-0.35	0.31	0.46	**1.38**	12.2	9.7
PE_18:3n3	0.58	0.18	1.29	0.44	34.1	3.1
PE_20:0	0.19	-0.25	0.13	0.88	3.5	6.2
PE_20:1	0.73	0.16	**2.00**	0.35	52.8	2.5
PE_20:2	0.67	0.45	**1.71**	**2.82**	45.2	19.9
PE_20:4n6	-0.70	-0.26	**1.84**	0.99	48.5	7.0
PE_20:3n6	0.84	0.36	**2.69**	**1.84**	70.9	12.9
PE_20:3n3	-0.39	0.47	0.57	**3.16**	15.2	22.3
PE_20:5n3	0.69	0.11	**1.81**	0.17	47.8	1.2
PE_22:0	-0.82	0.21	**2.53**	0.65	66.7	4.6
PE_22:1	-0.42	-0.29	0.68	**1.16**	18.0	8.2
PE_22:4	0.72	-0.04	**1.98**	0.02	52.1	0.2
PE_22:5n3	-0.71	-0.10	**1.91**	0.14	50.3	1.0
PE_22:6n3	0.65	-0.35	**1.61**	**1.75**	42.5	12.4

The important contributions (Ctr) are in bold, indicating a greater than average variable contribution to the respective principal component (i.e., Ctr > $\frac{1}{76}$ or 1.31%). CL: cardiolipin; MLCL: monolysocardiolipin; PC: phosphatidylcholine; PE: phosphatidylethanolamine. Squared cosines have been multiplied by 100 for ease of interpretation. $n = 4$

Table 2.2. P-values for three-way ANOVAs of *Fundulus heteroclitus* liver mitochondrial parameters

	p-values						
Parameter	Subspecies	Acclimation temperature	Assay temperature	Subspecies* Acclimation	Subspecies*Assay	Acclimation*Assay	Subspecies* Acclimation*Assay
OXPHOS-I	**<.0005**	**<.0001**	**<.0001**	.157	**<.0001**	**<.0001**	.352
LEAK-I	**<.05**	**<.0001**	**<.0001**	.507	**<.005**	**<.0001**	.881
OXPHOS-I, II	**<.0005**	**<.001**	**<.0001**	.413	**<.0001**	**<.005**	.605
LEAK-I, II	**<.005**	**<.0005**	**<.0001**	.505	**<.0005**	**<.0001**	.602
OXPHOS-Palm.C.	**<.0005**	**<.0001**	**<.0001**	**<.05**	**<.0001**	**<.0001**	**<.01**
LEAK-Palm.C	.115	**<.0001**	**<.0001**	.560	**<.05**	**<.0001**	.811
ETS- I, II	**<.0005**	**<.0005**	**<.0001**	.406	**<.0005**	**<.005**	.631
ETS-II	**<.001**	**<.0005**	**<.0001**	.419	**<.001**	**<.001**	.478
CCO	**<.01**	.198	**<.0001**	.530	**<.01**	.344	.975
RCR-I	.107	.793	**<.0001**	.594	.639	.076	.795
RCR-I, II	.462	.971	**<.0001**	.475	.881	.248	.949
RCR-Palm.C.	**<.005**	**<.05**	**<.0005**	**<.05**	.114	**<.0005**	.240

Significant *p*-values are in bold. OXPHOS: oxidative phosphorylation, Palm. C: palmitoyl carnitine, ETS: maximum mitochondrial substrate oxidation capacity, CCO: apparent cytochrome *c* oxidase capacity, RCR: respiratory control ratio (OXPHOS/LEAK), I: flux fueled through ETS complex-I, II: flux fueled through ETS complex II; n = 7-8.

Table 2.3. Hepatic mitochondrial phospholipid class distribution and cardiolipin molecular species from thermally acclimated *Fundulus heteroclitus* subspecies.

Mitochondrial PL classes	5 °C		15 °C		33 °C	
	North	South	North	South	North	South
CL	27.8±1.15	24.3±2.02	24.7±.93	21.3±.60	22.0±.77	22.4±2.11
MLCL (*†‡)	3.2±.28	1.7±.26	1.6±.12	9.7±.05	7.4±.09	7.2±.02
PE (†‡)	31.0±.83	24.6±1.21	30.0±1.47	30.6±.33	33.2±.99	28.2±1.39
PC (*‡)	41.1±.89	51.0±.90	45.1±1.92	48.0±.75	44.7±.68	49.3±1.08
PC/PE (*‡)	1.3±.04	2.1±.07	1.5±.14	1.6±.04	1.4±.05	1.8±.08
CL Molecular species						
CL_1402 (*)	0.9±.11	1.1±.11	0.5±.06	0.9±.19	0.1±.05	0.05±.01
CL_1404 (*)	$1.6\pm1.1\times10^{-3}$	$1.4\pm6.7\times10^{-4}$	$0.7\pm9.2\times10^{-4}$	$0.9\pm2.2\times10^{-3}$	$0.01\pm2.3\times10^{-5}$	$0.03\pm1.3\times10^{-4}$
CL_1424 (*‡)	0.6±.05	0.9±.04	0.9±.12	1.6±.16	1.7±.13	1.4±.20
CL_1428 (*)	3.3±.17	2.2±.19	1.7±.22	2.2±.39	0.2±.05	0.2±.03
CL_1448 (*)	2.4±.04	4.0±.11	4.0±.46	6.5±.35	9.6±1.08	7.7±1.93
CL_1450 (*)	5.6±.31	6.3±.33	6.3±.34	6.2±.62	3.7±.58	3.7±.82
CL_1452 (*)	4.4±.24	3.6±.19	4.2±.55	4.2±.26	1.7±.33	1.7±.24
CL_1472 (*‡)	5.7±.38	6.6±.55	6.0±.38	9.3±1.05	9.9±.24	8.7±.27
CL_1476 (*†)	6.6±.76	8.9±.25	4.0±.24	5.3±.21	2.3±.28	2.6±.32
CL_1496 (*)	6.7±.50	7.7±.36	11.8±1.47	13.9±1.12	23.2±.94	18.3±2.37
CL_1498 (*‡)	10.9±.23	7.9±.34	14.4±.56	9.6±.97	8.2±.95	11.7±.79
CL_1500 (*)	7.8±.33	9.1±.52	6.4±.27	6.7±.53	3.2±.35	3.8±.65
CL_1520 (*)	8.2±.28	7.0±.25	6.9±.21	6.7±.71	5.4±.58	5.4±.69
CL_1522 (*†)	4.8±.21	6.4±.08	2.5±.21	2.7±.24	1.0±.41	1.5±.32
CL_1544 (*)	11.8±.72	6.8±.58	15.9±.96	9.5±.84	21.9±2.06	24.4±3.97
CL_1546 (*)	6.6±.49	6.4±.25	5.3±.35	3.8±.96	3.5±.47	4.3±1.05
CL_1566 (*)	1.0±.14	0.68±.11	1.0±.14	1.0±.13	2.6±.37	2.2±.44
CL_1568	0.7±.11	1.1±.13	0.6±.10	0.7±.12	0.8±.32	1.0±.16
MLCL_1164 (*)	4.4±.53	6.1±.52	3.4±.27	8.3±.57	5.6±.95	5.8±.95
MLCL_1166	2.8±.39	4.1±.33	2.3±.69	3.5±.45	4.2±.29	4.0±1.20
MLCL_1186 (*)	5.4±.37	8.9±.30	9.6±1.54	13.4±.14	17.4±2.78	16.0±.17
MLCL_1188 (*)	7.9±.46	8.4±.88	11.9±.97	10.7±.27	9.5±1.21	6.8±1.95
MLCL_1190	6.0±.42	7.0±.47	5.4±.71	6.4±1.51	5.8±.56	6.1±1.86
MLCL_1210	10.5±1.05	11.4±.62	8.2±.49	10.2±.53	8.8±1.36	9.7±.85
MLCL_1212 (*)	7.6±.77	9.3±.84	3.8±.66	5.7±1.15	5.4±.81	5.5±.90
MLCL_1234 (*)	14.2±.78	12.2±1.54	20.9±.99	13.5±1.17	19.8±2.83	20.8±2.79
MLCL_1236 (*†)	17.0±1.06	13.7±1.38	14.7±2.08	9.5±.77	5.7±.69	5.2±.73
MLCL_1256	4.8±1.19	3.9±.33	4.9±.85	6.2±1.33	5.7±1.00	5.2±1.45
MLCL_1258 (*)	8.0±.48	6.9±.65	3.3±1.15	5.1±1.12	2.8±1.73	1.4±.20
MLCL_1282	10.8±1.65	7.5±.75	10.8±1.33	7.0±.83	8.6±1.12	13.0±2.94

Data are mean % of total head group or fatty acid ± SEM (n = 4). Symbols indicate significant effects from a two-way ANOVA *: acclimation; †: subspecies; ‡: acclimation x subspecies. The number following CL or MLCL corresponds to the MW (see Table 2.4) of the PL species and corresponds to the FA chains as indicated below. CL: cardiolipin; MLCL: monolysocardiolipin; PC: phosphatidylcholine; PE: phosphatidylethanolamine. PC\PE: the ratio of phosphatidylcholine to phosphatidylethanolamine.

Table 2.4. Fatty acid composition of cardiolipin and monolysocardiolipin molecular species determined by HPLC-ESI-MS/MS

CL Molecular Species (m/z)	16:0	16:1	18:1	18:2	18:3	20:4	22:6
CL_1402	1	1	2				
CL_1404	2		2				
CL_1424		1	1	2			
CL_1428		1	3				
CL_1448				4			
CL_1450			1	3			
CL_1452			2	2			
CL_1472				3		1	
CL_1476			2	1		1	
CL_1496				3			1
CL_1498			1	2			1
CL_1500			2	1			1
CL_1520				2		1	1
CL_1522			1	1		1	1
CL_1544				2			2
CL_1546			1	1			2
CL_1566					1	1	2
CL_1568				1		1	2
MLCL_1164		1	2				
MLCL_1166	1		2				
MLCL_1186				3			
MLCL_1188			1	2			
MLCL_1190			2	1			
MLCL_1210				2		1	
MLCL_1212			1	1		1	
MLCL_1234				1		2	
MLCL_1236			1			2	
MLCL_1256					1	1	1
MLCL_1258				1		1	1
MLCL_1282				1			2

CL: Cardiolipin, MLCL: monolysocardiolipin, m/z: mass to charge ratio (equivalent to molecular weight). The number following CL or MLCL corresponds to the MW of the PL species and corresponds to the FA chains.

Table 2.5. Total hepatic mitochondrial phospholipid FA composition from thermally acclimated *Fundulus heteroclitus* subspecies.

	5 °C acclimated		15 °C acclimated		33 °C acclimated	
Fatty acids	North	South	North	South	North	South
14:0 (*)	0.9±.06	1.0±.05	1.0±.06	1.0±.03	1.2±.06	1.0±.06
16:0 (*)	16.7±.32	17.2±.17	17.4±.31	17.2±.34	18.3±.37	17.5±.36
16:1 (*†)	2.1±.09	1.9±.13	1.8±.09	1.4±.14	1.1±.001	0.9±.02
18:0 (*†)	9.3±.24	10.7±.09	9.8±.11	12.5±.26	13.1±.44	13.6±.58
18:1n9	12.7±.37	13.8±.19	12.8±.43	11.5±.35	12.6±.61	13.4±.75
18:1n7 (*†)	4.4±.18	3.7±.07	3.4±.11	2.4±.06	1.5±.05	1.1±.14
18:2n6 (*†)	6.8±.23	5.6±.09	7.6±.34	6.4±.19	6.6±.30	6.3±.40
18:3n6 (*)	0.21±.031	0.27±.027	0.34±.015	0.19±.037	0.18±.036	0.17±.052
18:3n3 (*)	$0.19\pm1.4\times10^{-4}$	$0.15\pm1.0\times10^{-4}$	$0.18\pm7.1\times10^{-5}$	$0.17\pm 9.1\times10^{-5}$	$0.20\pm4.5\times10^{-5}$	$0.21\pm1.5\times10^{-4}$
20:0 (*†)	0.48±.068	0.29±.014	0.39±.036	0.28±.028	0.31±.025	0.24±.041
20:1 (*)	1.3±.07	1.2±.06	1.0±.04	0.8±.04	0.6±.06	0.7±.08
20:2 (*)	1.0±.11	1.0±.07	0.9±.06	0.7±.03	0.6±.03	0.8±.12
20:4n6 (*)	6.8±.23	7.2±.24	5.8±.27	6.2±.13	5.3±.20	5.7±.28
20:3n6 (*)	0.40±.053	0.50±.040	0.35±.062	0.34±.022	0.47±.037	0.57±.105
20:3n3 (*)	0.69±.086	0.59±.041	0.72±.065	0.68±.039	0.92±.055	0.97±.149
20:5n3 (‡)	2.6±.16	1.8±.14	1.7±.12	2.0±.11	1.3±.08	1.9±.23
22:0 (*)	0.9±.07	0.8±.06	1.1±.07	1.1±.06	1.4±.12	1.4±.16
22:1 (*)	0.61±.088	0.43±.021	0.62±.046	0.57±.025	0.68±.059	0.78±.097
22:4	1.8±.09	1.6±.09	1.2±.24	1.4±.05	1.4±.20	2.1±.26
22:5n3 (*†)	9.2±.21	8.1±.38	10.3±.23	10.4±.50	12.7±.89	10.7±.64
22:6n3 (*)	20.0±.37	21.6±.46	20.2±.60	21.2±.49	18.2±.68	17.5±.82

Fatty acid data are mean % of total ± SEM (n = 7-8). Symbols indicate significant effects from a two-way ANOVA *: acclimation; †: subspecies; ‡: acclimation x subspecies.

Table 2.6. Hepatic mitochondrial phosphatidylcholine (PC) fatty composition from thermally acclimated *Fundulus heteroclitus* subspecies.

	5 °C		15 °C		33 °C	
Phosphatidylcholine (PC) fatty acids	North	South	North	South	North	South
PC_14:0	0.7±.14	0.6±.03	0.5±.16	0.7±.04	0.5±.12	0.6±.10
PC_16:0	19.7±1.99	20.4±.61	18.0±.84	17.9±1.23	18.6±.73	15.9±2.18
PC_16:1 (*)	1.8±.09	1.5±.07	1.5±.18	1.3±.14	0.7±.04	1.0±.16
PC_18:0 (†)	7.6±.77	7.5±.41	7.3±.86	10.1±.27	11.3±.64	10.1±1.26
PC_18:1n9	12.2±.41	13.2±.34	12.8±.86	11.1±.73	13.0±.74	11.3±2.51
PC_18:1n7 (*)	2.7±.20	2.9±.06	1.9±.27	1.5±.15	1.0±.06	1.5±.48
PC_18:2n6	5.7±.52	4.7±.07	6.2±.82	5.3±.31	4.9±.38	5.5±.43
PC_18:3n6	0.8±.66	0.2±.03	0.1±.04	0.8±.55	0.1±.05	1.4±.69
PC_18:3n3	0.9±.83	0.1±.003	0.1±.05	0.9±.75	0.1±.04	1.8±.93
PC_20:0	0.8±.44	0.2±.01	0.3±.15	1.3±1.12	0.3±.03	2.8±1.45
PC_20:1	1.2±.49	1.0±.07	0.7±.08	1.0±.52	0.4±.09	1.9±.63
PC_20:2	1.2±.67	0.6±.08	0.8±.24	1.1±.66	0.5±.03	2.5±1.02
PC_20:4n6	3.8±.20	3.6±.25	3.3±.32	3.6±.21	2.2±.64	3.8±.66
PC_20:3n6	0.9±.35	0.5±.02	0.7±.27	0.9±.38	1.1±.29	1.7±.58
PC_20:3n3	0.5±.20	0.2±.01	0.3±.14	0.5±.17	0.5±.22	1.2±.42
PC_20:5n3	2.1±.19	1.6±.11	2.0±.26	1.9±.28	0.9±.11	2.0±.51
PC_22:0 (*)	1.2±.19	0.8±.08	1.1±.39	1.3±.17	1.7±.30	2.1±.65
PC_22:1	0.7±.11	0.4±.05	0.6±.24	0.5±.10	0.8±.19	1.7±.83
PC_22:4	0.3±.06	0.4±.21	1.3±.51	0.8±.12	1.1±.32	0.6±.27
PC_22:5n3	11.2±1.64	9.8±0.91	12.2±3.01	11.1±1.50	18.0±1.98	11.0±0.81
PC_22:6n3 (*)	18.3±2.24	25.0±1.00	20.6±3.31	18.0±2.13	14.8±0.96	11.6±2.07

Data are mean % of total head group or fatty acid ± SEM (n = 4). Symbols indicate significant effects from a two-way ANOVA *: acclimation; †: subspecies; ‡: acclimation x subspecies.

Table 2.7. Hepatic mitochondrial phosphatidylethanolamine (PE) fatty composition from thermally acclimated *Fundulus heteroclitus* subspecies.

	5 °C		15 °C		33 °C	
Phosphatidylethanolamine (PE) fatty acids	North	South	North	South	North	South
PE_14:0 (*)	0.9± .08	0.8±.11	1.1±.11	1.6±.16	1.5±.13	1.5±.03
PE_16:0 (*)	12.7±.43	11.6±.68	13.1±.75	14.5±.35	14.9±.31	14.5±.19
PE_16:1	0.7±.10	0.6±.05	0.3±.13	0.8±.18	1.2±.41	0.6±.16
PE_18:0 (*†)	13.1±.46	15.3±0.39	13.7±1.23	16.0±0.91	15.4±0.48	17.6±0.65
PE_18:1n9 (*)	6.9±.15	6.6±.36	3.1±1.08	2.7±.14	3.3±.18	3.1±.30
PE_18:1n7	4.4±.41	3.9±.13	4.3±.63	4.3±.18	3.7±.22	4.2±.25
PE_18:2n6 (*)	2.0±.21	1.6±.11	2.2±.45	1.2±.27	1.0±.13	0.8±.05
PE_18:3n6	0.2±.04	0.1±.05	0.1±.05	0.3±.05	0.3±.02	0.3±.11
PE_18:3n3 (*)	0.4±.04	0.3±.04	0.2±.08	0.3±.06	0.2±.02	0.1±.06
PE_20:0	0.4±.01	0.3±.04	0.5±.29	0.3±.06	0.3±.07	0.1±.09
PE_20:1 (*)	1.3±.11	1.3±.10	0.7±.27	1.1±.45	0.2±.14	0.1±.10
PE_20:2 (*)	0.8±.06	1.0±.07	0.4±.16	0.4±.16	0.5±.19	0.06±.06
PE_20:4n6 (*)	0.4±.03	0.3±.03	3.4±1.08	4.7±.68	3.9±.41	3.6±.06
PE_20:3n6 (*)	6.4±.24	7.7±.44	2.1±1.21	1.4±.15	1.4±.30	0.6±.38
PE_20:3n3 (*)	1.1±.08	1.1±.06	0.4±.29	0.7±.33	1.6±.33	1.7±.27
PE_20:5n3 (*)	2.3±.26	2.3±.10	1.8±.24	1.5±.25	1.4±.37	1.2±.22
PE_22:0 (*)	1.6±.09	1.6±.16	2.0±.10	2.5±.27	2.9±.31	2.6±.19
PE_22:1 (*)	0.6±.02	0.6±.02	1.4±.41	1.0±.12	1.1±.14	0.9±.11
PE_22:4 (*)	3.2±.74	3.1±.73	2.2±1.53	1.2±.91	1.1±.46	1.6±.39
PE_22:5n3 (*)	15.2±.40	16.1±0.72	21.7±1.96	22.3±2.47	22.4±1.23	21.2±0.65
PE_22:6n3 (*)	16.7±1.54	15.8±2.51	16.2±4.38	9.2±5.43	9.9±4.08	11.5±1.35

Data are mean % of total head group or fatty acid ± SEM (n = 4). Symbols indicate significant effects from a two-way ANOVA *: acclimation; †: subspecies; ‡: acclimation x subspecies.

Table 2.8. Characteristics of hepatic mitochondrial phospholipid fatty acid composition from thermally acclimated *Fundulus heteroclitus* subspecies.

	5 °C acclimated		15 °C acclimated		33 °C acclimated	
Total Phospholipids	North	South	North	South	North	South
MUFA/PUFA (*‡)	0.43±.013	0.43±.010	0.42±.019	0.36±.011	0.37±.021	0.41±.062
DBI (*)	2.5±.028	2.5±.019	2.5±.037	2.5±.019	2.4±.056	2.3±.062
n3/n6 (*‡)	2.3±.048	2.4±.069	2.4±.035	2.6±.047	2.7±.119	2.5±.117
Total n3 PUFA	0.328±.0043	0.323±.0043	0.332±.0064	0.347±.0037	0.334±.0105	0.314±.0111
Total n6 PUFA (*†‡)	0.143±.0020	0.135±.0028	0.141±.0017	0.132±.0011	0.126±.0021	0.127±.0017
Total n7 PUFA (*†‡)	0.078±.0018	0.068±.0015	0.062±.0017	0.045±.0017	0.031±.0008	0.027±.0008
Chain length	19.18±.037	19.15±.022	19.19±.035	19.27±.035	19.19±.063	19.24±.079
Phosphatidylcholine	North	South	North	South	North	South
PC-MUFA/PUFA	0.4±.02	0.4±.01	0.3±.01	0.4±.09	0.3±.02	0.4±.04
PC-DBI	2.4±.09	2.6±.05	2.5±.07	2.2±.25	2.4±.10	2.1±.04
PC-n3/n6 (‡)	3.1±.48	4.0±.19	3.4±.29	2.7±.49	4.1±.38	2.3±.33
PC-Total n3 PUFA	0.3±.02	0.3±.01	0.3±.01	0.3±.04	0.3±.01	0.2±.01
PC-Total n6 PUFA (‡)	0.11±.015	0.09±.003	0.10±.006	0.11±.014	0.09±.005	0.13±.017
PC-Total n7 PUFA (*‡)	0.06±.007	0.05±.001	0.04±.004	0.04±.007	0.02±.001	0.04±.005
PC-Chain length	19.0±.05	19.2±.05	19.3±.06	19.3±.14	19.2±.10	19.1±.11
Phosphatidylethanolamine	North	South	North	South	North	South
PE-MUFA/PUFA (*)	0.31±.009	0.27±.008	0.20±.012	0.24±.032	0.22±.019	0.23±.004
PE-DBI (*‡)	2.7±.03	2.7±.07	2.8±.14	2.4±.06	2.4±.08	2.4±.01
PE-n3/n6 (*‡)	3.9±.19	3.6±.19	5.1±.55	4.4±.45	5.5±.64	6.6±.44
PE-Total n3 PUFA (‡)	0.38±.003	0.38±.011	0.43±.021	0.38±.002	0.39±.013	0.40±.003
PE-Total n6 PUFA (*)	0.09±.004	0.10±.004	0.08±.004	0.08±.007	0.07±.007	0.06±.003
PE-Total n7 PUFA	0.06±.005	0.06±.002	0.05±.009	0.07±.008	0.05±.002	0.05±.002
PE-Chain length (‡)	19.6±.06	19.6±.06	19.7±.12	19.4±.04	19.4±.04	19.5±.03

Symbols indicate significant effects from a two-way ANOVA *: acclimation; †: subspecies; ‡: acclimation x subspecies. MUFA/PUFA: the ratio of monounsaturated fatty-acid to polyunsaturated fatty-acid. DBI: fatty acid double-bound (unsaturation) index. n3/n6: the ratio of n3 PUFA to n6 PUFA. n = 7-8 (total PL) or 4 (PE and PC).

Table 2.9. Hepatic mitochondrial phospholipid fatty acid product/precursor ratios and their associated desaturase and elongase enzymes.

			5 °C		15 °C		33 °C	
Product	**Precursor**	**Enzyme**	North	South	North	South	North	South
18:0	16:0	Elovl6 (*†‡)	0.55±.020	0.62±.009	0.56±.011	0.72±.021	0.71±.028	0.78±.033
18:1n7	16:1n7	Elovl6 (*)	2.1±.12	2.0±.12	1.8±.05	1.7±.16	1.4±.05	1.2±.14
20:0	18:0	Elovl6 (*†)	0.05±.018	0.03±.003	0.04±.009	0.02±.005	0.02±.004	0.02±.008
20:1n9	18:1n9	Elovl6 (*)	0.10±.008	0.08±.005	0.07±.005	0.06±.002	0.04±.002	0.05±.004
22:0	20:0	Elovl6	0.02±.014	0.04±.020	0.01±.009	0.03±.015	0.01±.008	0.01±.009
22:1n9	20:1n9	Elovl6 (*)	0.45±.051	0.36±.025	0.62±.030	0.76±.071	1.28±.191	1.22±.204
20:2n6	18:2n6	Elovl5 (*)	0.15±.020	0.18±.013	0.11±.011	0.11±.005	0.10±.004	0.13±.023
20:3n3	18:3n3	Elovl5	3.72±.650	3.86±.232	3.86±.398	4.01±.471	4.56±.290	4.60±.526
20:3n6	18:3n6	Elovl5 (*)	2.19±.534	1.89±.167	1.03±.196	2.07±.315	3.31±.793	2.98±.632
22:4n6	20:4n6	Elovl4/5 (*)	0.26±.007	0.23±.014	0.22±.041	0.23±.010	0.26±.028	0.36±.037
22:5n3	20:5n3	Elovl4/5 (*†‡)	3.54±.260	4.74±.588	5.94±.388	5.18±.451	9.54±.555	6.13±.758
18:1n9	18:0	SCD (*†‡)	1.38±.044	1.29±.023	1.30±.042	0.92±.034	0.96±.024	0.97±.031
16:1n7	16:0	SCD (*†)	0.12±.003	0.10±.006	0.10±.005	0.08±.008	0.05±.002	0.05±.001
18:3n6	18:2n6	Δ6D (‡)	0.03±.003	0.04±.004	0.04±.002	0.03±.005	0.02±.004	0.02±.010
22:6n3	22:5n3	Δ6D[#] (*†)	2.17±.074	2.69±.150	1.97±.090	2.07±.141	1.47±.133	1.66±.137
20:4n6	20:3n6	Δ5D (*)	18.9±2.24	14.7±1.08	19.1±2.16	18.5±1.72	11.6±1.11	11.5±1.70
20:4n6	18:2n6	Δ6D/Elovl5/Δ5D (*†)	1.02±.072	1.28±.055	0.79±.071	0.97±.053	0.81±.068	0.94±.109
20:3n6	20:2n6	Δ8D (*†)	0.38±.035	0.49±.021	0.40±.049	0.48±.027	0.71±.032	0.68±.041

Data are mean ± SEM (n = 7-8). Symbols indicate significant effects from a two-way ANOVA. *: acclimation; †: subspecies; ‡: acclimation x subspecies. [#]: Reaction also requires Elovl2/4/5 and peroxisomal β-oxidation; or can be catalyzed by Δ4D. Elovl, elongase; Δ6D, Δ-6 desaturase; Δ5D, Δ-5 desaturase; Δ8D, Δ-8 desaturase; SCD, stearoyl-CoA desaturase.

Chapter 3 Intraspecific variation and plasticity in mitochondrial oxygen binding affinity as a response to environmental temperature

3.1 Summary

Mitochondrial function has been suggested to underlie constraints on whole-organism aerobic performance and associated hypoxia and thermal tolerance limits, but most studies have focused on measures of maximum mitochondrial capacity. Here we investigated whether variation in mitochondrial oxygen binding kinetics could contribute to local adaptation and plasticity in response to temperature using two subspecies of the Atlantic killifish (*Fundulus heteroclitus*) acclimated to a range of temperatures (5, 15, and 33 °C). The southern subspecies of *F. heteroclitus*, which has superior thermal and hypoxia tolerances compared to the northern subspecies, exhibited lower mitochondrial O_2 P_{50} (higher O_2 affinity). Acclimation to thermal extremes (5 or 33 °C) altered mitochondrial O_2 P_{50} in both subspecies consistent with the effects of thermal acclimation on whole-organism thermal tolerance limits. We also examined differences between subspecies and thermal acclimation effects on whole-blood Hb O_2-P_{50} to assess whether variation in oxygen delivery is involved in these responses. In contrast to the clear differences between subspecies in mitochondrial O_2 P_{50}, there were no differences in whole-blood Hb-O_2 P_{50} between subspecies. Taken together these findings support a general role for mitochondrial oxygen kinetics in differentiating whole-organism aerobic performance and thus in influencing species responses to environmental change.

3.2 Introduction

Both ambient temperature and O_2 availability vary widely across the biosphere, and this has profound implications for the geographic distributions of aquatic organisms (Deutsch et al., 2015; Sunday et al., 2011). The physiological constraints imposed by hypoxia and temperature are thought to be a consequence of their effects on aerobic metabolism and, by extension, mitochondrial function (Deutsch et al., 2015; Fry and Hart, 1948; Iftikar and Hickey, 2013; Pörtner, 2001; Pörtner and Farrell, 2008). Attempts to link whole organism thermal and hypoxia performance and mitochondrial function have typically examined maximum mitochondrial

capacity (Chapter 2). Studies of this nature have had mixed success in identifying mitochondrial processes that putatively constrain whole-organism performance or that are altered following environmental stress (Chapters 4 and 5; Baris et al., 2016a; Baris et al., 2016b; Baris et al., 2017; Costa et al., 1997; Dos Santos et al., 2013; Du et al., 2016; Galli et al., 2013; Gnaiger, 2001; Guderley, 2004). In addition, *in vitro* studies of maximum mitochondrial capacity can be difficult to link back to *in vivo* function because mitochondria are unlikely to operate at maximum flux *in vivo* under most circumstances (Gnaiger, 2001).

One factor that can constrain mitochondrial flux is low O_2 supply. Indeed, mitochondrial O_2 consumption rate exhibits a hyperbolic relationship with O_2 partial pressure (PO_2) and the kinetics of mitochondrial O_2 binding can be altered through modifications such as competitive inhibition of cytochrome *c* oxidase by NO (Gnaiger, 2003).The effects of O_2 supply on mitochondrial function can be described using mitochondrial O_2 P_{50} (Mito-P_{50}), the PO_2 at which mitochondrial O_2 consumption rate is 50% of maximum flux (Gnaiger et al., 1998). Because Mito-P_{50} is measured during the aerobic to anoxic transition, it provides information on mitochondrial function over a PO_2 range that is relevant to *in vivo* performance. In theory, a low Mito-P_{50} results in a greater capacity to extract O_2 from the cytosol. Consequently, there has been interest in this property as a predictor of whole-organism performance. Indeed, intraspecific variation in Mito-P_{50} is a predictor of basal metabolic rate in humans (Larsen et al. 2011). Moreover, Lau et al. (2017) provide evidence for putative adaptation of Mito-P_{50} as a mechanism underlying variation in hypoxia tolerance among intertidal sculpin species (family: Cottidae). Links between Mito-P_{50} and hypoxia tolerance are not universal, however, as Du et al. (2016) did not observe altered Mito-P_{50} following hypoxic acclimation in *Fundulus heteroclitus*. By comparison, nothing is known about variation in Mito-P_{50} in the context of putative local thermal adaptation or thermal acclimation. It has been suggested that there may be a link between whole-organism thermal performance and systemic hypoxemia, although there is some debate about the role of systemic O_2 limitation as a general mechanism underlying thermal tolerance limits in fishes (Brijs et al., 2015; Ern et al., 2015). However, given the relationship between ambient temperature and aerobic metabolism, prolonged thermal stress likely alters mitochondrial function, and thus an investigation of temperature effects on Mito-P_{50} is necessary (Fry and Hart, 1948; Pörtner, 2001; Pörtner and Farrell, 2008).

To address this question, here we utilize *F. heteroclitus*, a eurythermal teleost found in estuarine salt marshes along a large latitudinal range that spans a steep thermal gradient [(Northern Florida, USA (mean monthly southern temperature range Sapelo Island, GA, USA: 11 – 30 °C; NOAA National Estuarine Research Reserve System, 2012) to Nova Scotia, Canada (mean monthly northern temperature range 3 – 11 °C Wells Inlet, ME, USA NOAA National Estuarine Research Reserve System, 2012)]. This species is highly tolerant of both thermal and hypoxic stress, experiencing considerable variation in these abiotic factors over diel as well as seasonal cycles (Borowiec et al., 2015; Fangue et al., 2006; McBryan et al., 2016). Furthermore, northern and southern *F. heteroclitus* subspecies exhibit variation in thermal and hypoxia tolerance that is consistent with apparent adaptation to their local environments (Fangue et al., 2006; McBryan et al., 2016). This species recruits a wide array of physiological responses to thermal stress, including altered mitochondrial function (Chapter 4; Baris et al., 2016b; Dhillon and Schulte, 2011; Fangue et al., 2009; McBryan et al., 2016). Thus, this species is an ideal model in which to investigate the potential roles of mitochondrial kinetic properties in thermal acclimation and adaptation.

The objectives of this study were three-fold, (1) determine if intraspecific variation in Mito-P_{50} exists between putatively thermally adapted northern (*Fundulus heteroclitus heteroclitus*) and southern (*Fundulus heteroclitus macrolepidotus*) Atlantic killifish subspecies, (2) investigate the effects of thermal acclimation (5, 15, and 33 °C) on Mito-P_{50} and, (3) characterize the acute thermal response of Mito-P_{50} between *F. heteroclitus* subspecies acclimated to different temperatures. We also assessed intraspecific variation and thermal acclimation effects on hemoglobin (Hb) O_2-P_{50}, as there is some evidence of intraspecific variation in this parameter in *F. heteroclitus* (Dimichele and Powers, 1982b) and any variation in this parameter could result in changes in PO_2 gradients between the circulatory system and the mitochondrion.

3.3 Methods

3.3.1 Animals

All procedures were carried out at the University of British Columbia according to the University of British Columbia Animal Care Committee approved protocol # A11-0372. Northern (*Fundulus heteroclitus* macrolepidotus; Ogden's Pond Estuary, NS, 45º71'N; 61º90'W) and southern (*Fundulus heteroclitus* heteroclitus; Jekyll Island, GA, 31º02'N; 81º25'W) Atlantic killifish were collected in summer, 2014, and were transported to UBC's Aquatics Facility where they were kept in 190 L tanks with biological filtration. Fish were held at 15 ± 2 °C, and 20 ppt salinity, with a 12:12 L:D photoperiod. Animals were fed once daily to satiation (Nutrafin Max). In June 2015, fish were transferred to 114 L tanks with biological filtration. Temperature was held at 5, 15 or 33 ± 2 °C and all other conditions were maintained. After a minimum of four weeks of thermal acclimation, fish were fasted for 24 h and sampled as described below.

3.3.2 Loss of equilibrium in hypoxia assay

Brackish water (T_a = 15 °C, 20 ppt salinity) was circulated in a 50 l plexiglass arena with bubblewrap at the water's surface to prevent O_2 diffusion. Fish were placed in individual containers in the arena (10 fish per trial, one fish container), where the former allowed for full mixing of water while preventing access to the water's surface. PO_2 was monitored continuously using a fiber-optic oxygen probe (NEO-Fox, Ocean Optics, Dunedin, FL). Following 10 min of acclimation to the container, PO_2 was decreased over 30 min by bubbling N_2 gas to one of four PO_2 values (0.84, 0.44, 0.24, or 0.13 ± 0.02 kPa). When the desired PO_2 was reached, the trial began and time to LOE_{hyp} was recorded. LOE_{hyp} was determined as the time at which fish no longer responded to gentle movement of their containers following which fish were removed and placed in a recovery tank.

3.3.3 Hemoglobin O_2 P_{50} and hematocrit content

Fundulus heteroclitus were removed from the 5, 15, or 33 °C thermal acclimation tanks at 8:00 AM PST, euthanized by cervical dislocation and weighed. The caudal peduncle was severed, and blood was collected from the incision using micro-hematocrit tubes. Micro-

hematocrit tubes were centrifuged (10 min, 12,700 *g*, 25 °C) and hematocrit was measured as the volume percentage of packed RBCs within the total blood sample.

Micro-hematocrit tubes were separated at the boundary between RBCs and plasma. RBCs were re-suspended to approximately the same measured hematocrit content with buffered saline (50 mM HEPES with 100 mM NaCl, final osmolality = 390 Osm kg^{-1}, pH = 7.8 at 25 °C) for O_2 equilibria experiments (Wells et al., 2005). The osmolality of the buffered saline solution was set based on plasma osmolality measurements (10 μL of whole blood measured using standard protocols with an osmometer, Vapro 5520, Wescor, Logan, UT) from five randomly selected 15 °C acclimated *F. heteroclitus* (396 ± 14 Osm·kg^{-1} mean ± sd).

Oxygen equilibrium curves were generated using protocols described by Lilly et al. (2013). Re-suspended RBCs (3 μL) were sandwiched between two sheets of low-density polyethylene that were secured on an aluminum ring with two plastic O-rings. Blood samples were placed in a gas-tight tonometry cell modified to fit into a SpectraMax 190 microplate reader (Molecular Devices, Sunnyvale, USA). Assay temperature was maintained at 15 or 33 °C, and blood from the three acclimation temperatures was assayed at both assay temperatures. Samples were equilibrated with pure N_2 for 30 min to achieve full Hb deoxygenation (deoxyHb). The O_2 tension was increased by 6 to 12 increments of air (21% O_2) balanced with N_2 using a Wösthoff DIGAMIX gas mixing pump (H. Wösthoff Messtechnik, Bochum, Germany). Optical density (OD) was measured every 10 s at 390nm, and 430nm, which correspond to the isosbestic point (i.e., OD is independent of Hb-O_2 saturation), and maxima for deoxygenated Hb, respectively. Hb was assumed to be fully saturated (oxyHb) with O_2 (100% air) when no change in OD at 430nm was detected after three equilibration steps.

Hb-O_2 saturation for each equilibration step was calculated using Eqn. 1.

$$Hb - O_2\ saturation = \frac{[(OD_{430\ nm} - OD_{390\ nm})_i - (OD_{430\ nm} - OD_{390\ nm})_{deoxy\ Hb}]}{[(OD_{430\ nm} - OD_{390\ nm})_{oxy\ Hb} - (OD_{430\ nm} - OD_{390\ nm})_{deoxy\ Hb}]} \quad \text{(Equation 1)}$$

Oxygen equilibrium curves (OECs) were constructed for each sample by non-linear least squares curve fitting to fit the Hb-O_2 saturation data to the Hill equation (Eqn. 2).

$$y = \frac{PO_2^n}{PO_2^n + P_{50}^n} \quad \text{(Equation 2)}$$

Where P_{50} is the PO_2 at which Hb is 50% saturated and is a measure of Hb-O_2 affinity, and *n* is the cooperativity (Hill) coefficient (Lilly et al., 2013). All curves used in the final analyses fit well to the data ($r^2 > 0.99$).

We estimated the effects of acute thermal shifts (T_{assay} = 15 to 33 °C) on Hb-O_2 affinity by calculating the apparent heat of oxygenation using the van't Hoff isochore (ΔH, Eqn. 3; Wyman, 1964).

$$\Delta H = 2.303 \cdot R \cdot \frac{\Delta \log(P_{50})}{(\frac{1}{T_1 - T_2})} \qquad \text{(Equation 3)}$$

Where R is the gas constant and T_1 and T_2 are the absolute temperatures 306 and 288 K respectively.

3.3.4 Liver mitochondrial isolation

Seven *F. heteroclitus* were removed from the 5, 15, or 33 °C thermal acclimation tanks and euthanized for liver mitochondrial isolation as described previously (Chapter 4). Liver tissue was excised and pooled into one aliquot of ice-cold homogenization buffer (250 mM sucrose, 50 mM KCl, 0.5 mM EGTA, 25 mM KH_2PO_4, 10 mM HEPES, 1.5% BSA, pH = 7.4 at 20 °C). Liver tissue was cut into approximately 1 mm^3 pieces and homogenized with 5 passes of a loose-fitting Teflon pestle followed by filtration through 1-ply cheesecloth. Crude liver homogenate was centrifuged at 4 °C for 10 min at 600 *g*. The fat layer was removed with aspiration, and the remaining supernatant was filtered through 4-ply cheesecloth. Filtered supernatant was centrifuged at 4 °C for 10 min at 6000 *g*. The resulting pellet was washed twice and suspended in 800 µL of homogenization buffer and stored on ice until experimentation. Protein content was determined using a Bradford assay with BSA as a standard (Bradford, 1976).

3.3.5 Mitochondrial assays

Mitochondrial O_2 binding affinity (Mito-P_{50}) was measured using a high-resolution respirometry system (O2k MiPNetAnalyzer; Oroboros Instruments, Innsbruck, Austria). Air-

saturated and O_2-depleted (achieved with a yeast suspension) calibrations of respiration buffer (MiRO5; 110 mM sucrose, 0.5 mM EGTA, 3 mM $MgCl_2$, 60 mM K-lactobionate, 20 mM taurine, 10 mM KH_2PO_4, 20 mM HEPES, 0.1% BSA, pH=7.1 at 30 °C; Gnaiger and Kuznetsov, 2002) were taken at each assay temperature (15, 33 and 37 °C) using published O_2 solubilities. Mito-P_{50} was determined using DatLab 2 software (Oroboros Instruments). Mitochondrial respiration rate during the transition into anoxia was fit against Eqn. 4.

$$\dot{M}_{O_2} = \frac{J_{max} \times P_{O_2}}{P_{50} + P_{O_2}} \qquad \text{(Equation 4)}$$

Where $\dot{M}_{O_2}$ is the mitochondrial respiration rate, J_{max} is maximal respiration rate and P_{50} is the P_{O_2} at which respiration rate is half of J_{max}. We accounted for the time delay of the O_2 sensor, background O_2 consumption and internal zero drift at each assay temperature (Grainger et al., 1998).

Two ml of MiRO5 was air-equilibrated at each assay temperature (15, 33 and 37 °C) followed by the addition of liver mitochondria (0.5 mg protein). A saturating mixture of substrates (glutamate 10 mM, pyruvate 10 mM, malate 2 mM, succinate 10 mM, palmitoyl-carnitine 20 mM) was added to the chamber followed by ADP (2.5 mM) to fuel mitochondrial respiration. Mitochondrial respiration was allowed to proceed until all O_2 was consumed (i.e., anoxia). Anoxic conditions were maintained for 15 min, followed by the termination of the experiment.

The effects of acute temperature shifts on Mito-P_{50} were estimated by calculating the difference in Mito-P_{50} between T_{assay} = 15 and 33 °C for each treatment.

3.3.6 Statistics and calculations

Statistical tests were completed using R software (v3.3.3). Data are presented as mean ± SEM and α was set at .05. Sample size is indicated (*n*) in the respective figure captions.

We compared the effects of subspecies, thermal acclimation, assay temperature using three-separate linear mixed effect models (individual as the random effect) to compare Hb and Mito-P_{50} and Hill coefficients.

We used separate t-tests to compare subspecies effects on Hb and mitochondrial O_2 binding affinity. Comparisons were made between subspecies assayed at their acclimation temperature (e.g., 33 °C acclimated northern and southern fish assayed at 33 °C). We accounted for an increased false discovery rate by adjusting α using a Benjamini-Hochberg correction for our specific test of subspecies effects.

Thermal acclimation effects (5, 15, and 33 °C) were assessed between subspecies at T_{assay} = 15 °C using a two-way ANOVA. The effects of acute thermal shifts (T_{assay} = 15 to 33 °C) on mitochondrial (Δ Mito-P_{50}) and Hb-P_{50} (ΔH) were assessed between subspecies and among thermal acclimation treatments using a two-way ANOVA.

Thermal acclimation and subspecies effects on hematocrit content were assessed using a two-way ANOVA. The effects of subspecies and decreasing PO_2 on time to LOE_{hyp} were assessed using a two-way ANOVA.

3.4 Results

3.4.1 Whole-organism hypoxia tolerance (LOE_{hyp})

We measured time to loss of equilibrium in hypoxia (LOE_{hyp}) at 15 °C in fish acclimated to 15 °C to confirm subspecies differences in whole organism hypoxia tolerance (McBryan et al., 2016). The northern and southern subspecies of killifish acclimated to 15 °C differed in LOE_{hyp} at T_{assay} = 15 °C across a range of PO_2 (Fig. 3.1). Southern killifish exhibited greater hypoxia tolerance, as indicated by time to LOE_{hyp} when compared to northern killifish ($p_{subspecies} < .001$). PO_2 also affected $LOE_{hyp,}$ which decreased with decreasing PO_2 ($p_{partial\ pressure} < .001$), as did the difference between the subspecies ($p_{partial\ pressure*subspecies} < .05$).

3.4.2 Hb and Mito-P_{50}

In this study, we examined mitochondrial O_2 binding affinity using isolated mitochondria from the liver because high-quality mitochondria can be isolated from this tissue in this species (Chapter 4; Fangue et al., 2009). These assays were conducted using a mixture of substrates at saturating levels to be representative of working or stressed states. For Mito-P_{50}, there were significant effects of subspecies ($p_{subspecies} < .05$), assay temperature ($p_{assay} < .0001$), thermal acclimation ($p_{acclimation} < .0005$), and the interaction between thermal acclimation and assay temperature ($p_{acclimation*assay} < .0001$) on Mito-$P_{50}$. No additional significant interaction effects

were detected ($p_{subspecies*acclimation}$ = .181, $p_{subspecies*assay}$ = .144, $p_{population*acclimation*assay}$ = .273). (Fig. 3.2)

In contrast, there was no significant effect of subspecies ($p_{subspecies}$ = .230) on Hb-P_{50}, but we detected significant effects of thermal acclimation ($p_{acclimation}$ < .05), assay temperature (p_{assay} < .0001), the interaction between subspecies and assay temperature ($p_{subspecies*assay}$ < .001), and the interaction between subspecies, acclimation and assay temperature ($p_{subspecies*acclimation*assay}$ < .05) but no other significant interaction effects ($p_{subspecies*acclimation}$ = .146, $p_{acclimation*assay}$ = .071). (Fig. 3.3). Hill coefficients derived from Hb-O_2 equilibrium curves did not differ between subspecies (Fig. 3.4; $p_{subspecies}$ = .196) or with acclimation ($p_{acclimation}$ < .181), but were significantly affected by assay temperature (p_{assay} < .05), and there were no significant interactions ($p_{subspecies*acclimation}$ = .070, $p_{subspecies*assay}$ = .634, $p_{acclimation*assay}$ = .637, $p_{subspecies*acclimation*assay}$ = .714). Hematocrit did not differ following thermal acclimation (Fig. 3.5; $p_{acclimation}$ = .080), or between subspecies ($p_{subspecies}$ = .992), and there were no significant interactions ($p_{acclimation*subspecies}$ = .350).

Because of the complex interactive effects of subspecies, acclimation temperature, and assay temperature on both Mito-P_{50} and Hb-P_{50}, we tested a series of specific hypotheses regarding the effects of individual factors on both of these parameters.

3.4.3 Subspecies effects on mitochondrial and Hb-O_2 affinity

We compared mitochondrial and Hb-P_{50} between subspecies when assayed at their acclimation temperature to test our prediction that southern killifish maintain lower O_2 P_{50} when compared to northern killifish (Fig. 3.6). Mito-P_{50} was lower in southern killifish compared to northern killifish when acclimated to 15 °C and assayed at 15 °C (Fig. 3.6A; $p_{subspecies}$ < .005), but not in 33 °C acclimated killifish assayed at 33 °C (Fig. 3.6B; $p_{subspecies}$ = .301). Hb-O_2 binding affinity did not differ between subspecies at either acclimation temperature (Fig. 3.6C, 3.6D; 15 °C: $p_{subspecies}$ = .446, 33 °C: $p_{subspecies}$ = .817).

3.4.4 Thermal acclimation effects on mitochondrial and Hb-O_2 affinity

We compared thermal acclimation effects (5, 15, and 33 °C) on mitochondrial (Fig. 3.7A) and Hb-P_{50} (Fig. 3.7B) between subspecies at a common assay temperature of 15 °C. We predicted that acclimation to higher temperatures would result in lower O_2 P_{50} for both parameters.

We detected a significant effect of acclimation on Mito-P_{50} (Fig. 3.7A; $p_{acclimation} < .001$). This effect was driven by higher Mito-P_{50} in 5 °C acclimated killifish and lower Mito-P_{50} in 33 °C acclimated northern killifish. We also detected a significant effect of subspecies that was driven by greater Mito-P_{50} in northern killifish ($p_{subspecies} < .05$). Significant interactions between subspecies and thermal acclimation effects were a result of subspecies differences being removed as $T_{acclimation}$ increased to 33 °C ($p_{subspecies*acclimation} < .05$).

We did not detect a significant effect of acclimation on Hb-P_{50} (Fig. 3.7B; $p_{acclimation} = .087$) or an effect of subspecies ($p_{subspecies} = .599$) or an interaction between subspecies and acclimation temperature ($p_{subspecies*acclimation} = .140$).

3.4.5 Acute thermal effects on mitochondrial and Hb-O_2 affinity

We assessed the effects of thermal acclimation and local adaptation on Δ Mito-P_{50} (i.e., the difference in Mito-P_{50} between T_{assay} = 15 and 33 °C) and the heat of oxygenation of Hb, ΔH (Fig. 3.8). We predicted that thermal acclimation and putative local adaptation would alter the acute thermal response for both parameters. Acute changes in temperature alter buffer pH, and this has the potential to affect both Mito-P_{50} and Hb-P_{50}. But this variation in pH does not affect the interpretation of our specific predictions as most comparisons were made at the same assay temperature. The only exception is our assessment of acute thermal effects on O_2 binding affinity (Fig. 3.8), which might be subject to an interaction between intraspecific variation or thermal acclimation effects and pH variation induced by the acute temperature shift between 15 and 33 °C.

Acclimation temperature affected Δ Mito-P_{50} (Fig. 3.8A; $p_{acclimation} < .001$). Northern *F. heteroclitus* exhibited a greater Δ Mito-P_{50} when compared to the southern subspecies ($p_{subspecies} < .005$). No significant interaction effects were detected ($p_{acclimation*subspecies} = .907$).

Thermal acclimation did not significantly change ΔH (Fig. 3.8B; $p_{acclimation} = .583$). Northern *F. heteroclitus* maintained more negative ΔH when compared to southern *F. heteroclitus* ($p_{subspecies} < .005$). No significant interaction effects were detected ($p_{acclimation*subspecies} = .371$).

3.5 Discussion

Here we demonstrate that Mito-P_{50} differs between putatively thermally adapted subspecies of killifish and is sensitive to thermal acclimation. These effects on Mito-P_{50} are consistent with intraspecific variation and the effects of thermal acclimation on whole-organism thermal and hypoxia tolerance (McBryan et al., 2016). These data provide evidence for altered mitochondrial oxygen affinity as a potential mechanism for maintaining whole-organism performance under environmental stress, which may ultimately contribute to subspecies-specific differences in thermal tolerance.

There were clear intraspecific differences in Mito-P_{50} between northern and southern *F. heteroclitus* subspecies, with southern fish maintaining lower O_2-P_{50} (Fig. 3.2, 3.6A). We propose that variation in Mito-P_{50} partially underlies intraspecific variation in hypoxia tolerance (Fig 3.1, McBryan et al., 2016). Intraspecific variation in Mito-P_{50} may be a consequence of variation in genes encoding cytochrome *c* oxidase (CCO) subunits. CCO is the terminal acceptor of the electron transport chain and the primary site of O_2 consumption in the mitochondrion. In addition, CCO subunits are encoded by both nuclear and mitochondrial genomes, the latter being subject to high mutation rates. Consequently, CCO function has been demonstrated to be a target of selection (Larsen et al., 2011; Scott et al., 2010; Zhang et al., 2013). Genome sequencing efforts in *F. heteroclitus* (Baris et al., 2017) have revealed mixed evidence for the presence of functionally significant variation in CCO among *F. heteroclitus* populations, but at present, there have been no comprehensive examinations of sequence variation between populations from the extremes of the species distribution. In addition, differences in CCO function could be a consequence of variation in mitochondrial membrane composition or post-translational modifications of the enzyme (Kraffe et al., 2007).

In contrast to the variation between subspecies in Mito-P_{50}, we did not observe significant differences in Hb-P_{50} between *F. heteroclitus* subspecies (Fig. 3.6C, D), consistent with previous observations in a hybrid *F. heteroclitus* population (Dimichele and Powers, 1982b). However, in this population individuals with differing LDH-B genotypes differed in Hb-P_{50} following exhaustive swimming, implicating a genotype-specific Bohr shift (i.e., low pH decreasing O_2 affinity) due to allosteric modification of Hb by ATP (Dimichele and Powers, 1982b). These differences are thought to result from differences in glycolytic metabolism due to variation in LDH-B (Dimichele et al., 1991). Both subspecies maintain equivalent hematocrit (Fig. 3.5),

indicating that if Hb characteristics differentiate aerobic performance between subspecies it likely occurs through allosteric mechanisms.

Hb-P_{50} in killifish (approximately 0.4 kPa) is low relative to other fish species (e.g., Hb-P_{50} = 3.6 kPa in *Oncorhynchus mykiss*, (Perry and Reid, 1994); 2.6 kPa in *Kryptolebias marmoratus*, (Turko et al., 2014); and ranges between 3 – 8 kPa among intertidal sculpins, (Mandic et al., 2009) suggesting that selection may have acted on *F. heteroclitus* to maximize O_2 extraction from the environment. However, for Hb, there is a trade-off between the ability to load O_2 at the gills and unload at the tissues. The fact that we do not observe much variation between subspecies in Hb-P_{50} may reflect this trade-off. Thus, variation in Mito-P_{50} could represent an adaptation to maximize tissue O_2 diffusion in the hypoxia-tolerant southern subspecies. The hypothesis of a tissue O_2 diffusion limitation in this species is supported by electron microscope observations of the location of the mitochondrion in this species, which at least in muscle are localized immediately below the plasma membrane (Dhillon and Schulte, 2011). However, both Hb-P_{50} and Mito-P_{50} are subject to considerable regulation *in vivo*, and this is an effect that we are unable to account for in our assays. Nevertheless, the difference in O_2 binding affinity between Hb and the mitochondrion likely contributes to the shape of O_2 diffusion gradients at the tissue (Jones, 1986).

Alternatively, in humans, there is an inverse relationship between basal metabolic rate (BMR) and Mito-P_{50} (Larsen et al. 2011). If a similar relationship occurs in *F. heteroclitus* we might predict that northern *F. heteroclitus* would have lower Mito-P_{50} than southern fish because northern populations maintain higher routine metabolic rates than do their southern counterparts (Healy and Schulte, 2012). In contrast, we found that the southern subspecies has a lower Mito-P_{50}, suggesting that the relationship between metabolic rate and Mito-P_{50} does not represent a functional constraint in *F. heteroclitus*. These results thus support a tighter functional link between Mito-P_{50} and hypoxia tolerance when compared to Mito-P_{50} and routine metabolism in *F. heteroclitus*. Alternatively, the inconsistent relationship between Mito-P_{50} and estimates of basal metabolism in humans and *F. heteroclitus* may be a consequence of the energetic demands imposed by endothermy when compared with ectothermy. The combination of low routine metabolic rate and Mito-P_{50} exhibited by the southern subspecies may represent a beneficial strategy in high-temperature hypoxic environments, allowing for greater tissue O_2 extraction while also decreasing overall demand in the face of environmental hypoxia.

Organisms' thermal tolerance limits are thought to be shaped by temperature effects on aerobic metabolism that may, at least in part, be due to effects at the level of the mitochondrion (Dos Santos et al., 2013; Fry and Hart, 1948; Pörtner, 2001). However, these effects have mostly been examined in the context of mitochondrial respiratory capacity. Here we show that northern and southern *F. heteroclitus* subspecies that differ in thermal tolerance (Fangue et al., 2006) also exhibit differences in Mito-P_{50}. The lower Mito-P_{50} in the southern subspecies, which reflects a greater mitochondrial oxygen affinity, could aid in the maintenance of mitochondrial O_2 diffusion gradients, particularly at high temperatures, which could help to sustain aerobic metabolism at high temperatures. Similarly, low Mito-P_{50} has the potential to aid O_2 delivery during environmental hypoxia. Thus, in southern habitats where temperatures are higher and hypoxic events are more likely, low Mito-P_{50} could be favored. Alternatively, the relatively low temperatures and higher oxygen levels in northern habitats might result in relaxed selection on these traits, reducing the constraints on Mito-P_{50} in this subspecies. Taken together, our demonstration of intraspecific variation in Mito-P_{50} thus provides a candidate trait accounting for potential covariation of both whole-organism hypoxia and thermal tolerance.

Acclimation to both 5 and 33 °C resulted in clear changes in Mito-P_{50} that were subspecies-dependent (Fig. 3.2, 3.7). In contrast, Hb-P_{50} did not exhibit a clear response to thermal acclimation (Fig. 3.3, 3.8). This previously undescribed phenomenon identifies potential targets and mechanisms of thermal acclimation and provides support for a role for mitochondrial function in maintaining performance following prolonged thermal stress.

We predicted that acclimation to 33 °C would decrease Mito-P_{50} thereby compensating for the aerobic challenges associated with high temperature (Chapters 4 and 5; Guderley and Johnston, 1996; Pörtner, 2001). When compared at a common assay temperature of 15 °C, acclimation to 33 °C decreased Mito-P_{50} in northern but not southern *F. heteroclitus* (Fig. 3.7A). Decreases in Mito-P_{50} under these conditions may alleviate limitations on total O_2 flux suggested to occur with elevated temperatures (Pörtner, 2001) and is consistent with the maintenance of a PO_2 gradient to the mitochondrion. In contrast, southern *F. heteroclitus* exhibit low Mito-P_{50} (high oxygen affinity) at both intermediate and high temperatures, indicating a difference in strategy between the subspecies. However, when compared at a higher assay temperature of 33 °C, acclimation to 33 °C increased Mito-P_{50} in both subspecies (Fig. 3.2). This paradoxical response could represent maladaptive acclimation as this would presumably decrease O_2

diffusion gradients to the tissues. Thus, it is possible that this response may instead be a consequence of sub-lethal effects associated with 33 °C acclimation. 33 °C is a non-lethal temperature to which *F. heteroclitus* can acclimate for prolonged periods (Fangue et al., 2006). However, acclimation to 33 °C is associated with decreases in whole body mass and routine O_2 consumption, perhaps indicative of trade-offs necessary to mitigate the effects of extremely high acclimation temperatures on energetic balance (Chapter 5; Healy and Schulte, 2012). Thus, our observed change in Mito-P_{50} may be a consequence of other mitochondrial responses associated with high temperature acclimation (e.g., altered mitochondrial morphology and membrane composition; Grim et al., 2010; Wodtke, 1981a). This raises interesting questions as to the mitochondrial responses of organisms under conditions of sub-lethal stress, which are likely to have a profound influence on species' fitness (Iles, 2014; Lemoine and Burkepile, 2012; Salin et al., 2016).

In both subspecies, we observed higher Mito-P_{50} in fish acclimated to low temperature when assayed at 15 °C (Fig. 3.7A). Indeed, cold acclimation is associated with increases in mitochondrial respiratory capacity, mitochondrial volume density and lipid content in aquatic ectotherms (Chapter 4; Dhillon and Schulte, 2011; Grim et al., 2010; Guderley, 2004). Increases in lipid content increase O_2 solubility (Widomska et al., 2007) which may alleviate potential mitochondrial O_2 limitations in systemic tissues at low temperatures that are brought on by decreased O_2 diffusion rates (Sidell, 1998). This 5 °C acclimation response may reveal a mechanism for life at low temperatures as it is consistent with the greater Mito-P_{50} exhibited by northern *F. heteroclitus* (Fig. 3.6).

Similar to our demonstration of thermal acclimation effects on Mito-P_{50} (Fig 3.7A), prolonged exposure to hypoxia might be predicted to decrease Mito-P_{50} (Costa et al., 1997; Du et al., 2016), if reductions in Mito-P_{50} are important for maintaining O_2 diffusion gradients. However, hypoxia acclimated northern *F. heteroclitus* exhibit no modification of Mito-P_{50} (Du et al., 2016). This suggests that declines in Mito-P_{50} at high temperatures are not directly mediated by the associated environmental hypoxia or resulting hypoxemia. Thus, the effects of thermal acclimation that we observe may play a role other than maintaining oxygen diffusion gradients. Alternatively, during hypoxic acclimation this species could recruit other mechanisms for maintaining O_2 supply and demand balance, such reductions in demand (Borowiec et al., 2015) would reduce the necessity for decreased Mito–P_{50} following acclimation.

Although we detected intraspecific variation and thermal acclimation effects on liver Mito-P_{50}, this effect might not be present in mitochondria from other tissues (Benard et al., 2006). Indeed, thermal acclimation and intraspecific variation effects on *F. heteroclitus* mitochondrial respiratory capacity vary among the heart, liver, and brain (Chapters 2 and 5; Fangue et al., 2009), suggesting that mitochondria from different tissues may respond differently. The role of liver mitochondria in constraining whole-organism hypoxia and thermal tolerance is not clear, whereas other tissues such as the heart and brain may be more important (Ern et al., 2015; Iftikar and Hickey, 2013; Pörtner, 2001). Consistent with this idea, variation in Mito-P_{50} from brain mitochondria has been shown to be associated with evolutionary variation in hypoxia tolerance (Lau et al., 2017) whereas Mito-P_{50} from liver mitochondria does not change in response to hypoxic acclimation in *F. heteroclitus* despite changes in whole-organism hypoxia tolerance (Du et al., 2016). Thus, the role of the differences in liver Mito-P_{50} that we observe in setting whole organism thermal or hypoxia tolerance requires further investigation.

As assay temperature increased (assay temperature: 15 – 33 °C), both Hb and Mito-P_{50} increased (Fig. 3.2, 3.3). The loss of Hb-O_2 affinity associated with increasing assay temperature is often observed and is primarily a consequence of the exothermic nature of Hb oxygenation (Weber and Jensen, 1988). Decreased Hb-O_2 binding affinity with acute increases in temperature might aid in unloading O_2 to the tissues but might also compromise O_2 loading at the gills. However, these effects are likely subject to considerable regulation *in vivo*. In contrast, decreased mitochondrial O_2 affinity with increased assay temperature has not been previously characterized and is presumably a result of temperature effects on enzyme stability. This decrease in mitochondrial O_2 binding affinity at high assay temperatures might cause a decline in mitochondrial ATP synthesis, perhaps revealing an aspect of declining mitochondrial function associated with acute increases in temperature.

We detected clear subspecies effects on the acute thermal sensitivity of O_2 binding affinity at all acclimation temperatures (Fig. 3.7). Northern *F. heteroclitus* exhibited greater Δ Mito-P_{50} and a more exothermic Hb ΔH (i.e., greater thermal sensitivity) when compared to the southern subspecies (T_{assay} = 15 to 33 °C). These data indicate that northern *F. heteroclitus* exhibit a greater relative loss of O_2 binding affinity than the southern subspecies following acute increases in temperature. This loss of O_2 binding affinity at high acute temperatures may result in

greater constraints on aerobic metabolism in this subspecies, which could be associated with the differences between subspecies in acute thermal tolerance limits (Fangue et al., 2006).

Thermal acclimation also altered the acute thermal sensitivity of Mito-P_{50} (Fig. 3.2). This is reflected by increased Δ Mito-P_{50} following 33 °C acclimation in both *F. heteroclitus* subspecies (Fig. 3.8A). This increase in sensitivity may be a consequence of sub-lethal effects associated with 33 °C acclimation and changes in mitochondrial morphology as discussed previously. In contrast, we did not detect significant thermal acclimation effects on hemoglobin thermal sensitivity ($\Delta H°$, Fig. 3.8B), although such effects have been detected in other fish species. (e.g., *Oncorhynchus mykiss*; Weber et al., 1976).

In this study, we demonstrate greater mitochondrial O_2 binding affinity in southern *F. heteroclitus* and as a result of increasing acclimation temperature. This variation in mitochondrial O_2 kinetic properties likely aids in the maintenance of O_2 diffusion gradients, and is consistent with the greater whole-organism hypoxia tolerance in the southern subspecies. The greater mitochondrial O_2 binding affinity exhibited by the southern subspecies also potentially accounts for the greater upper thermal tolerance limits in this subspecies, acting as a mechanism to offset systemic hypoxemia suggested to occur at high acute temperatures. Finally, subspecies variation in Mito-P_{50} is inversely correlated with subspecies differences in routine metabolism, suggesting that variation in Mito-P_{50} may have a closer functional association with whole organism hypoxia and thermal tolerance in this species. We thus propose that altered Mito-P_{50} is involved in differentiating organism-level aerobic and thermal performance between putatively adapted *F. heteroclitus* subspecies and in response to thermal acclimation and could represent a novel target for thermal adaptation.

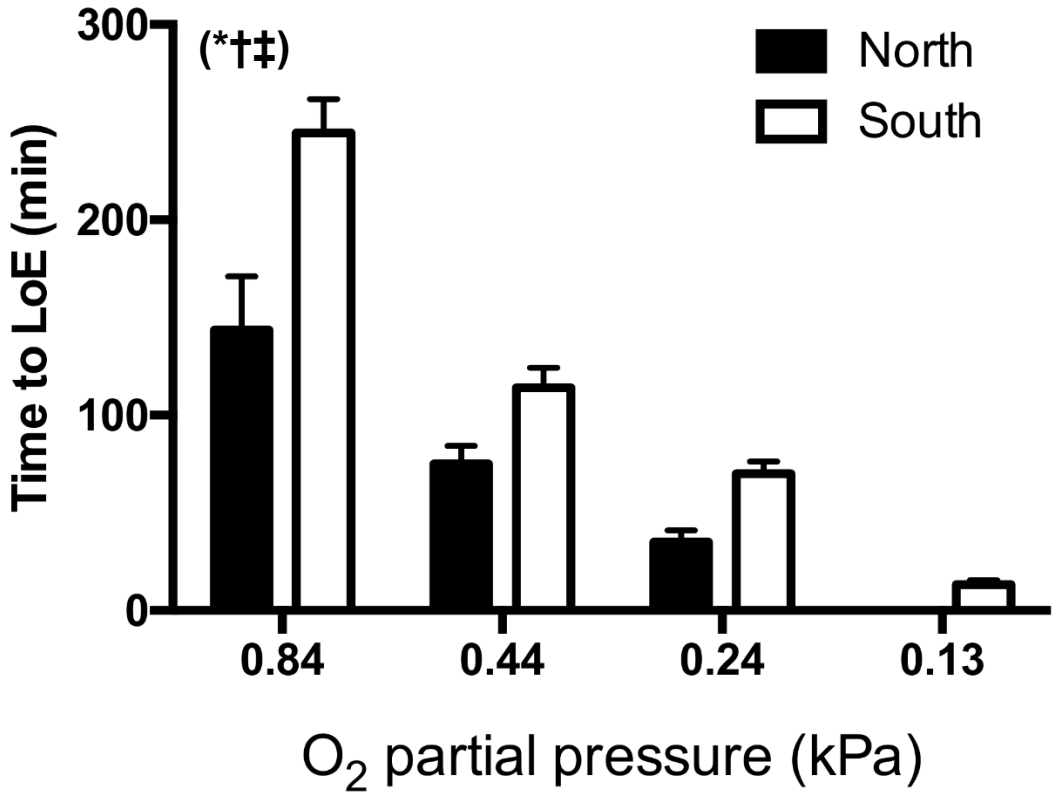

Figure 3.1 Intraspecific differences in whole-organism hypoxia tolerance. Northern and southern *F. heteroclitus* were acclimated to and assayed at 15 °C. Hypoxia tolerance was estimated using a time to loss of equilibrium assay across a range of low O_2 partial pressures. Data are mean ± SEM, n = 9-10. Symbols indicate significant effects of O_2 partial pressure (*), subspecies (†), and the interaction between acclimation and subspecies (‡).

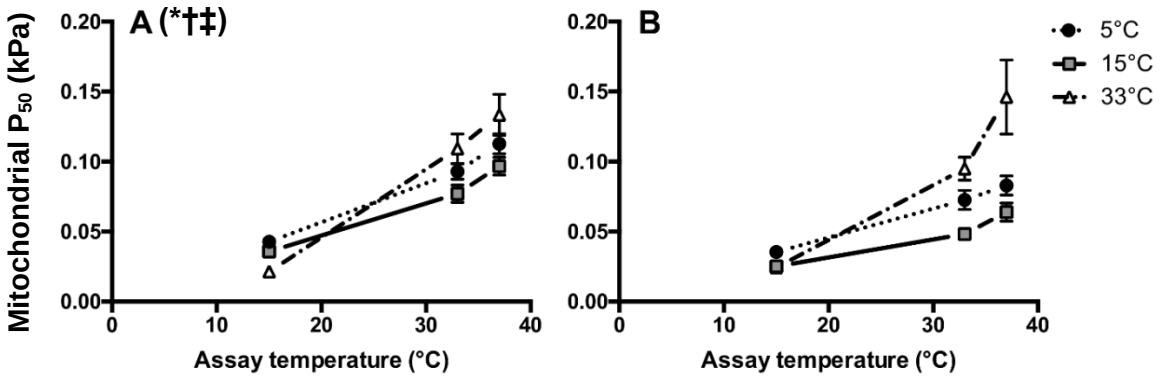

Figure 3.2 Full-model of thermal acclimation and intraspecific variation effects on mitochondrial O_2 binding affinity from *Fundulus heteroclitus*. Northern (A) and southern (B) *F. heteroclitus* were acclimated to 5 (black circle), 15 (grey square), or 33 °C (white triangle) for four weeks. Data are mean ± SEM, n = 7-8. Symbols indicate significant main effects of assay temperature (*), acclimation (†), and subspecies (‡).

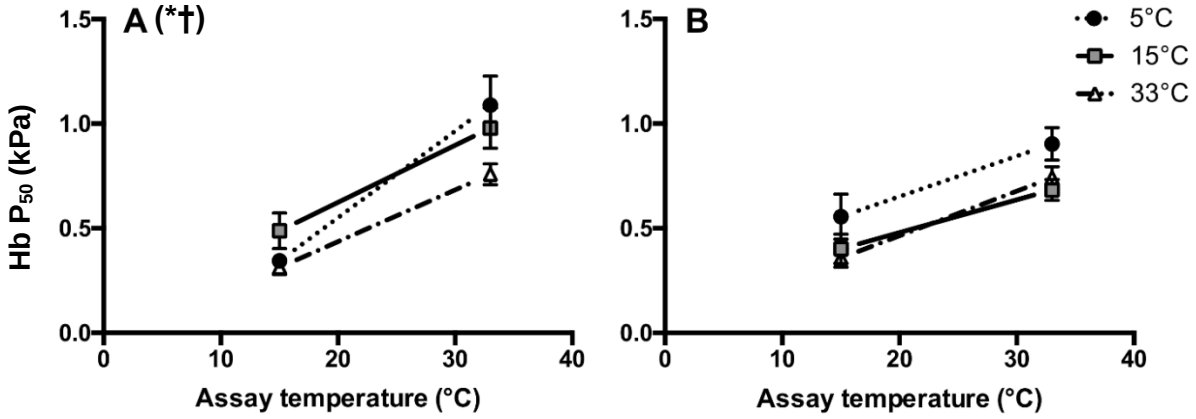

Figure 3.3 Full-model of thermal acclimation and intraspecific variation effects on whole blood hemoglobin O_2 binding affinity from *Fundulus heteroclitus*. Northern (A) and southern (B) *F. heteroclitus* were acclimated to 5 (black circle), 15 (grey square), or 33 °C (white triangle) for four weeks. Data are mean ± SEM, n = 7-20. Symbols indicate significant main effects of assay temperature (*), and acclimation (†).

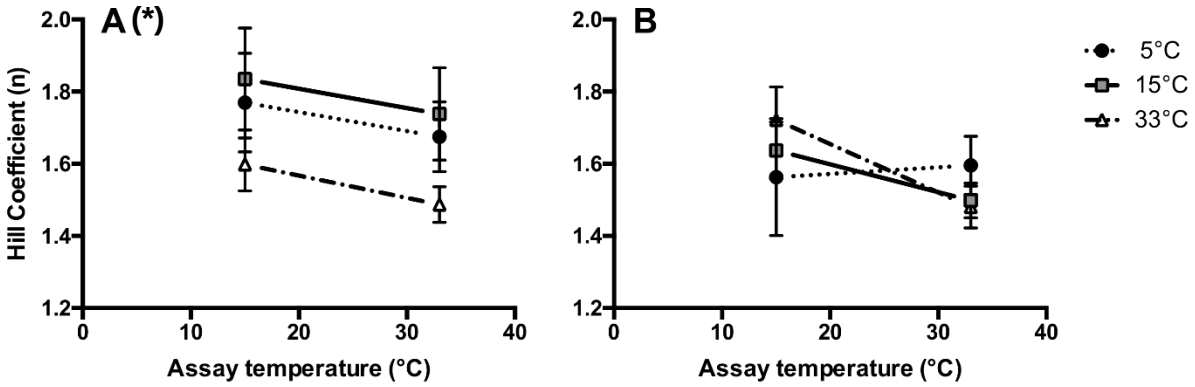

Figure 3.4 Full-model of thermal acclimation and intraspecific variation effects on Hill coefficients derived from hemoglobin O_2 equilibrium curves from *Fundulus heteroclitus*. Northern (A) and southern (B) *F. heteroclitus* were acclimated to 5 (black circle), 15 (grey square), or 33 °C (white triangle) for four weeks. Data are mean ± SEM, n = 7-20. Symbols indicate a significant main effect of assay temperature (*).

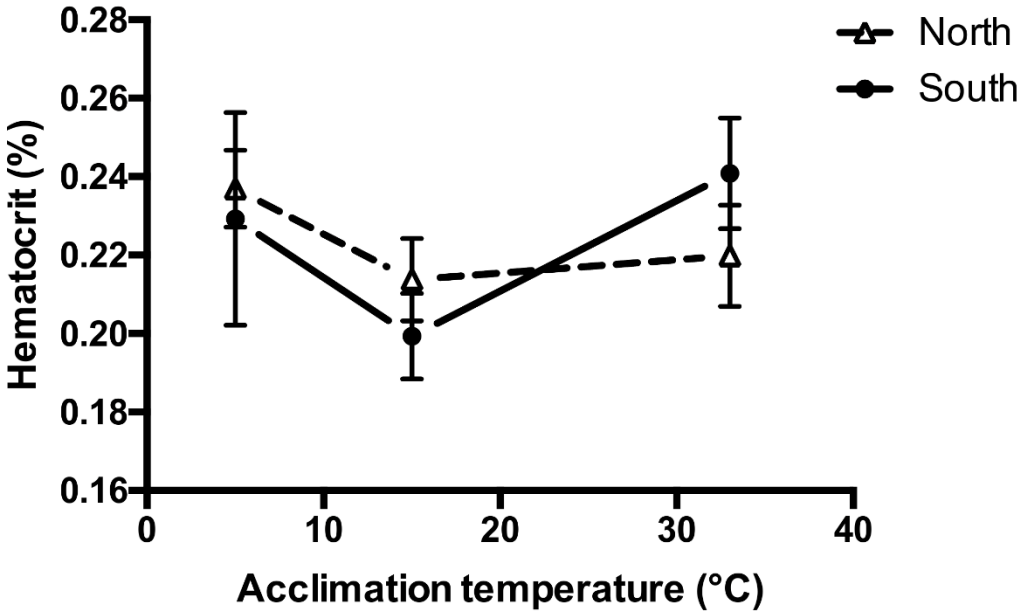

Figure 3.5 Thermal acclimation and intraspecific variation effects on hematocrit in *Fundulus heteroclitus*. Northern (white triangle) and southern (black circle) *F. heteroclitus* were acclimated to 5, 15, or 33 °C for four weeks. Data are mean ± SEM, n = 7-20. No significant main effects were detected.

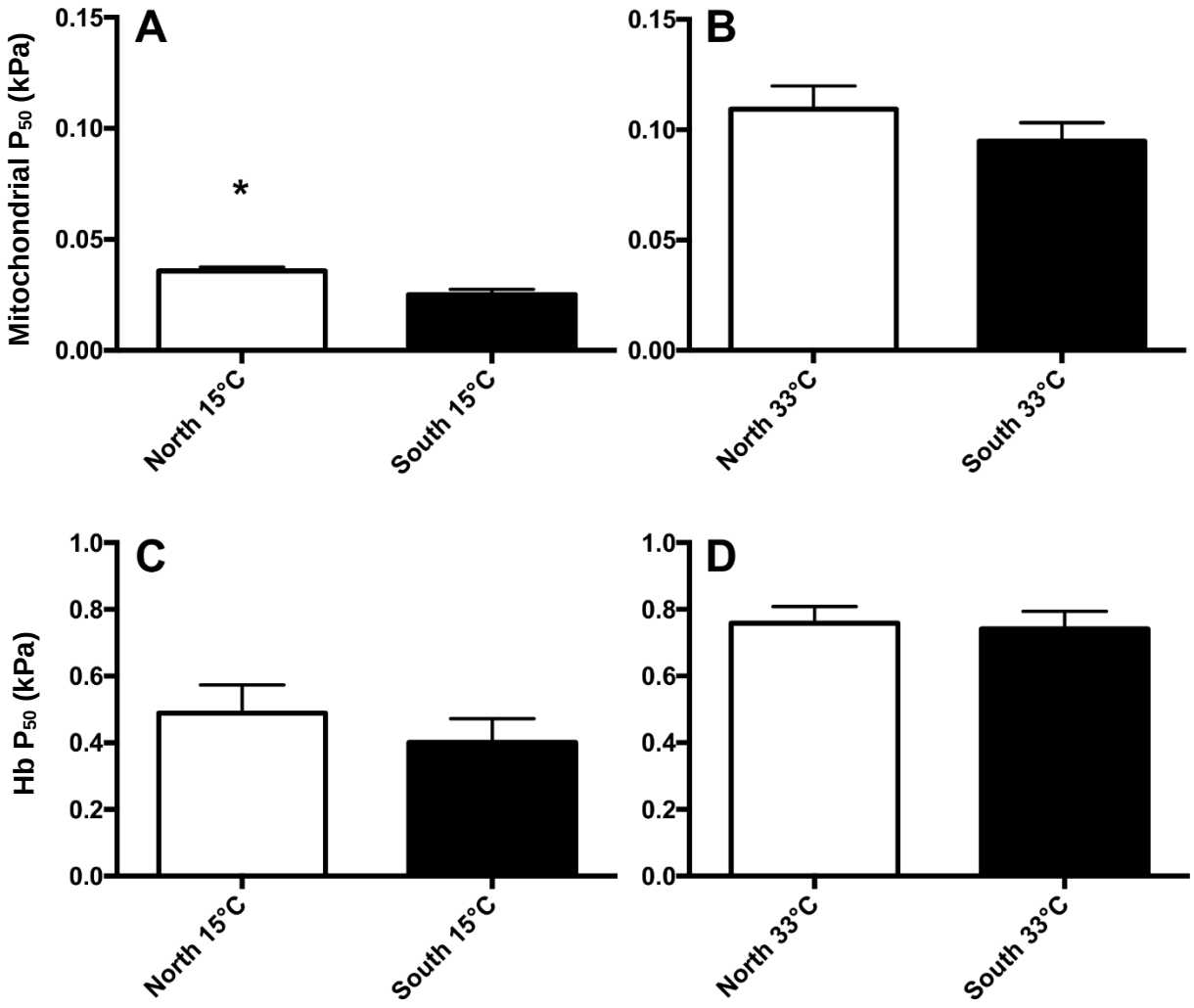

Figure 3.6 Intraspecific differences in mitochondrial (A, B; *n* = 7-8) and hemoglobin (C, D; *n* = 7-20) O_2 binding affinity. Northern and southern *Fundulus heteroclitus* were acclimated to 15 (A, C) or 33 °C (B, D). The assay temperature for subspecies comparisons was the same as acclimation temperature (e.g., 33 °C acclimated fish were compared at T_{assay} = 33 °C). Asterisks indicate a significant subspecies effect within an acclimation treatment (T-test, $p < .05$). Data are mean ± SEM.

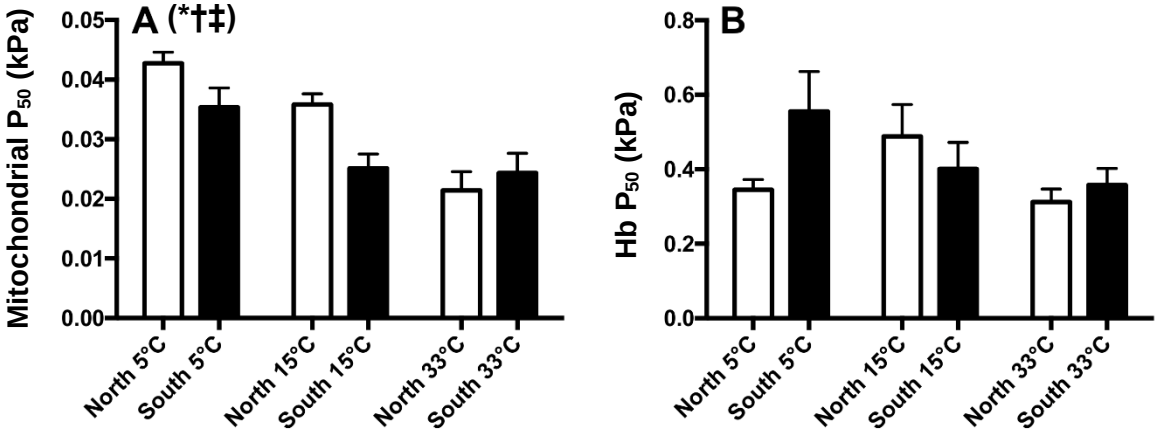

Figure 3.7 Thermal acclimation effects on mitochondrial (A; *n* = 7-8) and hemoglobin (B; *n* = 7-20) O_2 binding affinity. Northern and southern *Fundulus heteroclitus* were acclimated to 5, 15 or 33 °C (T_{assay} = 15 °C). Data are mean ± SEM. Symbols indicate significant effects of acclimation (*), subspecies (†), and the interaction between acclimation and subspecies (‡) within a measurement.

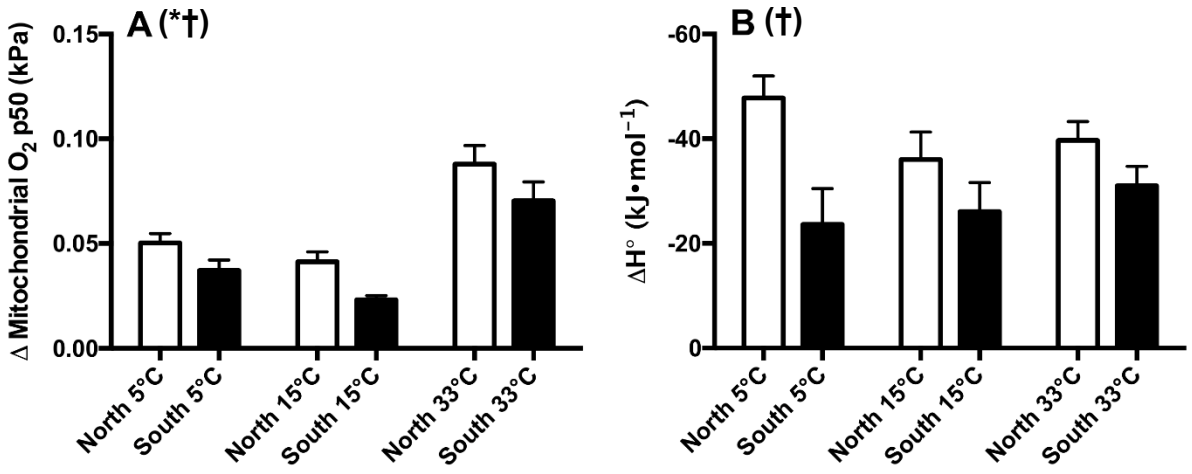

Figure 3.8 Acute thermal sensitivity (T_{assay} = 15 to 33 °C) of mitochondrial (A, Δ mitochondrial O_2 P_{50}; *n* = 7-8) and hemoglobin (B, ΔH°; *n* = 7-20) O_2 P_{50}. Northern and southern *Fundulus heteroclitus* were acclimated to 5, 15, or 33 °C. A more negative ΔH° is indicative of favorable Hb-O_2 binding at lower temperatures. Data are mean ± SEM. Symbols indicate significant effects of acclimation (*), and subspecies (†).

Chapter 4 Mechanisms and costs of mitochondrial thermal acclimation in a eurythermal killifish (*Fundulus heteroclitus*)

4.1 Summary

Processes acting at the level of the mitochondria have been suggested to affect the thermal limits of organisms. To determine whether changes in mitochondrial properties could underlie shifts in thermal limits, we have examined how mitochondrial properties are affected by thermal acclimation in the eurythermal killifish, *Fundulus heteroclitus*—a species with substantial plasticity in whole-organism thermal limits. We hypothesized that thermal acclimation would result in functional changes in the mitochondria that could result in trade-offs in function during acute thermal shifts. We measured mitochondrial respiration rates through multiple complexes of the ETS following thermal acclimation (5, 15, 33 °C), and assessed maintenance of mitochondrial membrane potential (Δp), and rates of reactive oxygen species (ROS) production as an estimate of costs. Acclimation to 5 °C resulted in a modest compensation of mitochondrial respiration at low temperatures, but these mitochondria were able to maintain Δp with acute exposure to high temperatures, and ROS production did not differ between acclimation groups, suggesting that these increases in mitochondrial capacity do not alter mitochondrial thermal sensitivity. Acclimation to 33 °C caused suppression of mitochondrial respiration due to effects on NADH-dehydrogenase (complex I). These high-temperature acclimated fish nonetheless maintained Δp and ROS production similar to that of the other acclimation groups. This work demonstrates that killifish mitochondria can successfully acclimate to a wide range of temperatures without incurring major functional trade-offs during acute thermal shifts and that high temperature acclimation results in a suppression of metabolism, consistent with patterns observed at the organismal level.

4.2 Introduction

Environmental temperature imposes clear limitations on the geographic distribution of ectotherms due to the effects of temperature on the rates of biochemical reactions (Hochachka and Somero, 2002), which constrains whole-animal aerobic performance at thermal extremes. Indeed, aerobic scope (the difference between maximum and resting metabolic rate) has been

demonstrated to decrease at the edge of species' thermal ranges (Eliason et al., 2011; Healy and Schulte, 2012; Pörtner and Farrell, 2008) implicating aerobic metabolism in establishing thermal limits. Improving understanding of the physiological and biochemical mechanisms that link temperature changes, aerobic scope, and organismal thermal performance is thus critical to providing predictive power over species' responses to global climate change.

Thermal performance curves of aerobic metabolism, a temperature-sensitive process critical to maintaining eukaryotic energetic balance, can shift following thermal acclimation (Angilletta, 2009; Schulte et al., 2011). Although thermal acclimation may improve performance at the acclimation temperature, it can also cause a decrease in performance at temperatures that were not stressful prior to acclimation (e.g., a decrease in aerobic capacity at high temperatures following low-temperature acclimation). Changes such as these represent a 'cost of acclimation.' Identifying mechanisms that underlie these costs may provide insights into the factors that influence whole-animal thermal tolerance.

Due to its role in aerobic metabolism and energy balance, mitochondria are a likely site of processes influencing whole-organism thermal limits (Iftikar and Hickey, 2013; Pörtner, 2001), and thermal acclimation has been shown to alter mitochondrial properties in ways that may help to maintain aerobic scope. For example, previous studies have demonstrated low-temperature acclimation effects on mitochondrial enzyme function (Fangue et al., 2009; Kraffe et al., 2007), inner mitochondrial membrane (IMM) composition (for review see: Guderley, 2004; Grim et al., 2010; Kraffe et al., 2007), and mitochondrial volume density (Dhillon and Schulte, 2011; Egginton and Johnston, 1984; for review see: O'Brien, 2011). Although beneficial at the acclimation temperature, changes in mitochondrial physiology associated with thermal acclimation may result in dysfunction during acute thermal shifts (to previously unstressful temperatures), which may be a potential mechanism underlying shifts in thermal limits. For example, increased inner mitochondrial membrane fluidity during low temperature acclimation is thought to help maintain mitochondrial output at low temperatures by increasing the frequency of enzyme interactions and substrate diffusion rates (Hazel, 1995). An acute increase in temperature under these conditions, however, may result in membrane destabilization and a loss of the driving force to synthesize ATP (proton motive force, Δp; comprised of a mitochondrial membrane potential, Ψ_m and $[H^+]$ gradient, pH). These effects represent a cost of low-temperature acclimation.

Acute high-temperature shifts, in contrast, are thought to increase mitochondrial function, resulting in deleterious consequences such as unsustainable O_2 consumption, and increased reactive oxygen species (ROS) production (Abele et al., 2002). Acclimation to high-temperatures, therefore, ought to result in a suppression of mitochondrial function to limit these effects. Thus, suppression of metabolism with acclimation to high temperature could be interpreted as a benefit of acclimation. Although there are relatively few studies examining this phenomenon, some groups have demonstrated that high-temperature acclimation results in a decrease in mitochondrial membrane fatty acid saturation, and a decrease in respiration rate (Guderley and Johnston, 1996; Khan et al., 2014; Strobel et al., 2013).

Eurythermal ectotherms are ideal models in which to test the role of the mitochondria in thermal acclimation, as their broad thermal tolerance likely occurs through recruitment of detectable changes in physiology (Guderley and St-Pierre, 2002). Indeed, studies of mitochondrial thermal acclimation that focus on climate change often employ stenothermal species, making eurythermal responses a critical point of comparison. The Atlantic killifish (*Fundulus heteroclitus*) typifies this eurythermal physiology. These fish can be acclimated to temperatures from ~2 °C up to ~35 °C, and can tolerate an even wider thermal range in acute challenges (CT_{min} = -1 °C and CT_{max} = 41 °C). Their acute thermal limits are also highly plastic, shifting by more than 10 °C when these fish are acclimated to different temperatures (Fangue et al., 2006). There is some data to suggest that warm-acclimation (25 °C) of *F. heteroclitus* may be associated with a trade-off in mitochondrial function, as liver mitochondrial respiration from warm-acclimated groups is sustained at high T_{assay} (up to 37 °C) but is significantly depressed compared to lower $T_{acclimation}$ groups (5, and 15 °C) when assayed at low temperatures (5 °C; Fangue et al., 2009). Similarly, low-temperature (5 °C) acclimation also causes an apparent trade-off, as respiratory control ratios (RCR, an approximation of mitochondrial coupling) in low-temperature acclimated fish decline at high T_{assay} (37 °C) precluding assessment of mitochondrial respiration (Fangue et al., 2009). What remains unclear from these data is the specificity of these changes, because in these previous studies mitochondria were only provided with an electron transport system (ETS) complex I-linked substrate (pyruvate), whereas work in goldfish (*Carrassius auratus* L.), indicates that thermal acclimation responses may be recruited through other ETS components such as complex II (Dos Santos et al., 2013). In addition, the effects of acclimation on mitochondrial membrane potential and ROS production have not been

assessed in *F. heteroclitus*, and thus the mechanisms underlying this apparent trade-off remain unknown.

In this study, we assessed thermal acclimation effects on the respiration of *F. heteroclitus* liver mitochondria, the maintenance of Ψ_m, the kinetics of proton leak, and the amount of ROS production when respiration is fueled with different substrates. We addressed the following objectives (1) assess the degree to which thermal acclimation (four weeks at 5, 15, and 33 °C) alters mitochondrial capacity, (2) determine if these modifications are specific to individual components of the mitochondrial apparatus (i.e., pyruvate dehydrogenase, ETS complex I, and complex II), and (3) determine if these changes in capacity incur a trade-off that causes costs to function during acute thermal shifts (i.e., loss of Δp, and increased ROS production rate). In so doing, we provide an assessment of the role of, mitochondria in the maintenance of whole-animal thermal performance, and shifts in thermal tolerance following acclimation.

4.3 Materials and methods

4.3.1 Reagents

All reagents can be obtained from Sigma-Aldrich (Oakville, ON)

4.3.2 Animals

Treatment of animals was completed in accordance with the University of British Columbia animal care protocol # A11-0372. Adult northern killifish (*Fundulus heteroclitus macrolepidotus*) were collected in Odgen's Pond estuary, Jimtown, N.S. (45°71'N; -61°90'W) during September of 2013. Fish were housed at the University of British Columbia Aquatics Facility in 190 L tanks with biological filtration at T_a = 20 ± 2 °C, 20 ppt salinity, and 12:12 L:D photoperiod for four weeks prior to experimental acclimation. Food (Tetrafin Max; Rolf C. Hagen Inc., Montreal, QC) was provided once daily to satiation. Following the holding period, fish were randomly distributed into 114 L acclimation tanks with T_a = 5, 15, or 33 °C, and 12:12 L:D photoperiod for four weeks prior to sampling. We chose a high acclimation temperature of 33 °C as opposed to 30 °C due to the induction of breeding physiology at 30 °C. Trends of increased gonadosomatic index and spermatogenesis have been noted in the killifish following

acclimation to temperatures ranging from 20-25 °C (Healy and Schulte, 2012; Matthews, 1939). Acclimation to 33 °C induces a warm-acclimation response while avoiding these artifacts.

4.3.3 Liver mitochondrial isolation

Seven randomly selected killifish were pooled for each mitochondrial sample. Killifish were euthanized (8:00AM PST) by cervical dislocation; liver tissue (approximately 1 g total tissue) was excised and finely minced (1 mm^3 pieces) in ice-cold homogenization buffer (250 mM sucrose, 50 mM KCl, 0.5 mM EGTA, 25 mM KH_2PO_4, 10 mM HEPES, 1.5% BSA, pH = 7.4 at 20 °C). Liver pieces were homogenized using five passes of a loose-fitting Teflon pestle and filtered through 1-ply cheesecloth. Homogenate was centrifuged at 600 *g* at 4 °C for 10 min. The fat layer was aspirated from the supernatant, and filtered through 4-ply cheesecloth. The defatted supernatant was centrifuged at 6000 *g* for 10 min at 4 °C. The pellet was isolated and washed twice in homogenization buffer, and resuspended in 800 μL of homogenization buffer (approximately 11 $mg \cdot ml^{-1}$ protein). Mitochondria were kept on ice and used to measure respiration, membrane potential, proton leak kinetics, and ROS production. Protein content was determined by the Bradford (1976) method with BSA standards.

4.3.4 Mitochondrial respiration rate and proton motive force

Mitochondrial respiration rate and proton motive force (Δp, estimated as mitochondrial membrane potential; $\Delta\Psi_m$) measurements were completed using a high-resolution respirometry system (O2k MiPNetAnalyzer), and tetraphenylphosphonium (TPP^+) selective electrodes (Oroboros Instruments; Innsbruck, Austria). Oxygen electrodes were calibrated at each assay temperature (T_{assay} = 5, 15, 33, 35, and 37 °C) with air-saturated, and oxygen-depleted (achieved with a yeast suspension) MiRO5 assay buffer (110 mM sucrose, 0.5 mM EGTA, 3 mM $MgCl_2$, 60 mM K-lactobionate, 20 mM taurine, 10 mM KH_2PO_4, 20 mM HEPES, 1% BSA, pH = 7.1 at 30 °C; Gnaiger and Kuznetsov, 2002) using O_2 solubilities published by Gnaiger and Forstner (1983).

Measurement of $\Delta\Psi_m$ and mitochondrial respiration rates through ETS complex I, and complex II were completed using methodologies modified from Brand (Brand, 1995). Through preliminary experiments, we determined that incubation of mitochondrial preparations with nigericin (80 $ng \cdot mL^{-1}$; which eliminates the ΔpH component of Δp, leaving only $\Delta\Psi_m$) had a

large inhibitory effect on mitochondrial respiration. Given that $\Delta\Psi_m$ is the major contributor to mitochondrial Δp (discussed by Brown et al., 2007; Nicholls and Ferguson, 2013) we decided not to use nigericin and approximated Δp using $\Delta\Psi_m$. Following air-equilibration of 2 mL MiRO5 assay buffer to T_{assay} = 5, 15, 33, 35, or 37 °C, TPP^+-selective electrodes were introduced to the chamber and calibrated with five additions of TPP^+ (the first 1 μM TPP^+ addition was followed by four additions of 0.5 μM TPP^+, 3 μM TPP^+ total). Liver mitochondrial protein (0.5 mg) was added to the chamber followed by ADP (1 mM). Flux through complex I was obtained through introduction of glutamate (10 mM) and malate (2 mM). Once state 3 (ADP-phosphorylating) and membrane potential measurements were obtained, flux through complex I was inhibited with rotenone (0.5 μM in ethanol). Complex II was activated with the addition of succinate (10 mM). State 4 (ADP non-phosphorylating) respiration rates and membrane potential were approximated through inhibition of the ATP synthase with oligomycin (2 $\mu g \cdot ml^{-1}$ dissolved in ethanol). Carbonyl cyanide-*p*-trifluoro-methoxyphenylhydrazone (FCCP 1 μM, dissolved in ethanol) was added to uncouple the mitochondria and assess electrode drift. TPP^+ dilution and substrate-inhibitor effects on TPP^+ measurements were corrected by measuring TPP^+ concentration during a substrate-inhibitor protocol in the absence of mitochondria. Respiratory control ratios (RCR, the ratio of state 3 and state 4 respiration rates) were calculated as a means of estimating mitochondrial coupling.

External TPP^+ concentrations were used to calculate Ψ_m using a modified Nernst equation (Rottenberg, 1984).

$$\Delta\Psi_m = a \cdot log\left(\frac{\frac{[TPP^+]_{total}}{[TPP^+]_{free}} - V_{external} - K'_o \cdot mg\ protein}{v_{mt} \cdot mg\ protein + K'_i \cdot mg\ protein}\right) \quad \text{(Equation 1)}$$

In Equation 1, a is the temperature-dependent coefficient ($a = RT/zF$, where R is the universal gas constant, T is the absolute temperature, z is the ion's valence, and F is the Faraday constant), $V_{external}$ is the volume outside the mitochondria, K'_i, and K'_o are partition coefficients used to correct for nonspecific internal, and external binding of TPP^+ respectively, and v_{mt} is the mitochondrial matrix volume. Values for K' (Rottenberg, 1984) and v_{mt} (Halestrap, 1989) were set according to literature values from rat liver mitochondria.

Although matrix volume has the potential to vary with temperature, changes in this parameter result in negligible changes in membrane potential in the presence of TPP^+ (Rottenberg, 1984). We calculate that a 50% increase in v_{mt} results in a 1% change in the estimated membrane potential of killifish mitochondria. Non-specific TPP^+ binding to dipalmitoylphosphatidylcholine liposomes has been shown to be temperature sensitive (Demura et al., 1987). The effect this has on isolated mitochondria is unknown, and while changes in *K'* have a larger effect on calculated values of membrane potential when compared to an equivalent change of v_{mt} (5% versus 1% respectively), this is within our accepted range of error. We, therefore, assumed that nonspecific binding of TPP^+ and matrix volume remained constant across our manipulations. This assumption does not affect the analysis of differences in $\Delta\Psi_m$ following thermal acclimation because mitochondria from all acclimation groups were assayed across the same range of temperatures.

4.3.5 Glutamate + malate and pyruvate + malate fueled state 3 and 4 respiration rate

We assessed the effect of thermal acclimation on mitochondrial respiration rate (state 3, and state 4), in the absence of TPP^+ when fueled by pyruvate + malate, and glutamate + malate. Liver mitochondrial protein (0.3 mg) was added to 2 mL of air-saturated (T_{assay} = 5, 15, 33, 35, or 37 °C) MiRO5. This was followed by an addition of saturating ADP (1 mM). State 3 respiration rates were obtained through the addition of glutamate (10 mM), and malate (2 mM) allowing for electron flux through complex I. State 4 respiration rates were approximated through the addition of oligomycin (2 $\mu g \cdot ml^{-1}$ dissolved in ethanol). Pyruvate-fueled state 3 and 4 respiration rates were obtained using the protocol previously described with pyruvate (5 mM) used in place of glutamate.

4.3.6 Proton leak kinetics

Proton leak kinetics were assessed using methods similar to those described above. Following air-equilibration of 2 mL MiRO5 to T_{assay} = 5, 15, 33, 35, or 37 °C, and calibration of the TPP^+ electrodes, isolated liver mitochondria (0.5 mg) were added to the chamber. Rotenone (0.5 μM in ethanol) and oligomycin (2 $\mu g \cdot ml^{-1}$ dissolved in ethanol) were added to the chamber to inhibit flux through ETS complex I and the ATP synthase respectively. State 4 respiration was

approximated by measuring state 2 respiration in the presence of succinate (10 mM). State 2 respiration was subsequently titrated with seven additions of malonate (0.5 mM each). After the final titration step, mitochondria were uncoupled with FCCP (1 μM, dissolved in ethanol). Proton leak kinetic curves for each mitochondrial preparation were fit to a two-parameter exponential growth equation using GraphPad Prism 6 software (La Jolla, CA) and the kinetic parameter: k (the rate constant) was used for statistical analysis.

4.3.7 ROS production rates

We estimated mitochondrial ROS production rates by measuring extra-mitochondrial H_2O_2 concentrations using a modified Amplex UltraRed (Invitrogen; Burlington, ON) assay. Liver mitochondria (total of 0.3 mg of mitochondrial protein) were incubated in 2 mL MiRO5 held at T_{assay} = 5, 15, or 33 °C. Mitochondrial ROS production was measured under state 4 conditions (i.e., in the absence of ADP) with saturating substrate. Basal (succinate and rotenone, concentrations as described above), and maximum (basal treatment in the presence of antimycin A; 2.5 μM, dissolved in ethanol) ROS production rates were corrected against background rates (no substrates or inhibitors). Reactions were completed on a 96-well plate using a one-to-one ratio of mitochondrial sample and Amplex UltraRed working solution (horseradish peroxidase, 1U activity per well; Amplex UltraRed 100 μM, in DMSO; and sodium citrate 50 mM, pH = 6.0 at 20 °C). Standards were composed of diluted H_2O_2. Absorbance (λ = 565 nm) was measured using a spectrophotometer (Spectramax 190; Molecular Devices; Sunnyvale, CA). Linear regions of ROS production rate curves (0 – 45 min, sampled every 5 min) were used for analyses. Free radical leak (FRL, H_2O_2 production rate corrected for mitochondrial oxygen consumption) was calculated using the equation described by Barja et al. (1994).

4.3.8 Statistical analyses

All data are presented as mean ± SEM, with α = 0.05. The sample size for each acclimation group is presented in relevant figures (where *n* = the number of pooled mitochondrial preparations from 7 fish each). Statistical analyses were completed using R software (version 3.0.2). We tested the effect of assay and acclimation temperature on mitochondrial respiration rates, membrane potential, RCR, FRL, and ROS production rates using linear mixed-effect models. When significant acclimation effects were detected, we performed a

one-way ANOVA within assay temperature. We applied a false discovery rate adjusted *p*-value to one-way ANOVAs using the Benjamini-Hochberg method (Thissen et al., 2002). Measurements of FRL, which are expressed as a percentage, were arcsine transformed prior to statistical analyses to ensure normality. Whole-animal characteristics and the rate constants extracted from proton leak kinetic analyses were compared across acclimation treatments within each assay temperature, using one-way ANOVAs. Post-hoc Tukey's HSD analyses were conducted following the detection of significant major effects.

4.4 Results

4.4.1 Whole-animal characteristics

Acclimation to 33 °C resulted in a reduction of all measured whole-animal characteristics when compared to both 5 and 15 °C acclimations. Whole-animal mass was greater for both the 5 °C (6.29 g ± 0.291) and 15 °C acclimation (6.13 g ± 0.236) groups when compared to the 33 °C (5.04 g ± 0.188) group (one-way ANOVA, $p_{acclimation} < 0.0001$, n = 103-105). A slightly different pattern was observed with wet liver mass (one-way ANOVA, $p_{acclimation} < 0.0001$, n = 103-105) where 15 °C acclimation (0.263 g ± 0.0122) resulted in a marginally greater mass than the 5 °C acclimation (0.223 g ± 0.0096) which was double the mass observed in the 33 °C group (0.138 g ± 0.0093). A similar pattern was observed for pooled liver mitochondrial protein concentration (suspended in 800 μL buffer, one-way ANOVA, $p_{acclimation} < 0.0001$, n = 14 - 15). Again, both the 5 °C (13.07 mg·mL^{-1} ± 1.245) and 15 °C (13.12 mg·mL^{-1} ± 0.975) acclimation groups had greater protein concentration when compared to the 33 °C (7.00 mg·mL^{-1} ± 0.710) acclimation.

4.4.2 Mitochondrial respiration rate and membrane potential (ETS complexes I and II)

We assessed the effect of thermal acclimation and acute changes in assay temperature on liver mitochondrial respiration rate and mitochondrial membrane potential fueled through ETS complex I and complex II. Increased assay temperature resulted in an increase in glutamate + malate fueled (ETS complex I) state 3 (ADP-phosphorylating) respiration (Fig. 4.1A; linear mixed-effect model, $p_{assay} < 0.0001$), and there was a significant effect of acclimation

temperature on respiration (linear mixed-effect model, $p_{acclimation} < 0.0001$); however, there was also a significant interaction between acclimation group and assay temperature (linear mixed-effect model, $p_{interaction} = 0.0231$). Following acclimation to 33 °C, liver mitochondrial respiration in the presence of glutamate + malate decreased up to 75% (T_{assay} = 15-37 °C) when compared to mitochondria from either 5 or 15 °C acclimated fish, and the effects of acute temperature shift were also less pronounced in mitochondria from the 33 °C acclimated group.

As was the case for flux through ETS complex I, increases in assay temperature increased succinate-fueled (complex II) state 3 respiration for all acclimation groups (Fig 4.1B; linear mixed-effect model, $p_{assay} < 0.0001$). Again, significant interaction and acclimation effects were detected (linear mixed-effect model, $p_{interaction} = 0.035$, $p_{acclimation} = < 0.0001$). Acclimation to 33 °C resulted in lower respiration rates at acute temperature shifts from 5 to 37 °C; however, this reduction (up to 40%) was only detected in post-hoc tests when compared to 5 °C acclimated fish.

Acclimation effects on succinate-fueled state 4 (non ADP-phosphorylating) respiration rates differed from those measured under state 3 conditions (Fig. 4.1C). Increasing assay temperature increased succinate-fueled leak respiration (linear mixed-effect model, $p_{assay} < 0.0001$). Similar to succinate-fueled state 3 respiration, both interaction and acclimation effects were statistically significant (linear mixed-effect model, $p_{interaction} = 0.0258$, $p_{acclimation} < 0.0001$). In this case, acclimation to 5 °C resulted in higher leak respiration rates (T_{assay} = 35 and 37 °C) when compared to both 15 and 33 °C acclimation groups.

To determine if thermally acclimated killifish can maintain Δp (measured as Ψ_m see materials and methods for rationale) following acute thermal shifts (potentially representing a cost of acclimation), we measured Ψ_m, in tandem with previously described respiration rates (Fig. 4.1D, E, F). Acute increases in temperature significantly decreased mitochondrial membrane potential when respiring maximally (state 3) fueled either through complex I (Fig. 4.1D; linear mixed-effect model, $p_{assay} = 6.22 \times 10^{-4}$) or complex II (Fig. 4.1E; linear mixed-effect model, $p_{assay} = 0.0305$), but not during leak respiration fueled through complex II (Fig. 4.1F; state 4). There was a significant effect of acclimation on membrane potential, but only for succinate-fueled respiration measured under state 3 and 4 conditions (Fig 4.1E, F; linear mixed-effect model, $p_{acclimation,\ state\ 3} = 0.0092$; $p_{acclimation,\ state\ 4} = 0.0075$). Post-hoc analyses revealed that acclimation to 33 °C decreased membrane potential, but only under maximum leak conditions

(i.e., succinate-fueled state 4) measured at high assay temperatures (T_{assay} = 35 and 37 °C). No additional significant main effects or interactions were detected.

4.4.3 Complex I and PDH-linked state 3 and 4 mitochondrial respiration

It is possible that the observed suppression of ETS complex I mitochondrial respiration following high-temperature acclimation could be dependent on the source of electrons (e.g., flux initiated by substrates entering the tricarboxylic acid cycle at different points). To assess this possibility, we measured state 3 and 4 respiration rates fueled by glutamate and compared them to respiration rates fueled with pyruvate (with malate to support the tricarboxylic acid cycle in each case). Glutamate enters the mitochondrion in exchange for aspartate and is converted by glutamate dehydrogenase into α-ketoglutarate for entry into the tricarboxylic acid cycle, while pyruvate enters the mitochondrion via a monocarboxylate transporter, and is converted by the pyruvate dehydrogenase complex to acetyl CoA prior to tricarboxylic acid cycle entry (Halestrap, 2012).

Increased assay temperature significantly increased state 3 respiration rates fueled with both glutamate + malate (Fig. 4.2A; linear mixed-effect model, $p_{assay} < 0.0001$) and pyruvate + malate (Fig. 4.2C; linear mixed-effect model, $p_{assay} < 0.0001$). Acclimation effects on glutamate + malate (linear mixed-effect model, $p_{acclimation} < 0.0001$) and pyruvate + malate (linear mixed-effect model, $p_{acclimation} < 0.0001$) fueled respiration were identical, such that acclimation to 33 °C resulted in lower respiration rates (for all T_{assay}) compared to both 5 and 15 °C groups. These lower temperature acclimation groups did not differ from each other except at T_{assay} = 5 °C. Significant interaction effects between acclimation and assay temperature on state 3 respiration were detected for both glutamate + malate (linear mixed-effect model, $p_{interaction} < 0.0001$) and pyruvate + malate (linear mixed-effect model, $p_{interaction} < 0.0001$).

State 4 (leak) respiration fueled by glutamate + malate (Fig. 4.2B) and pyruvate + malate (Fig. 4.2D) also behaved similarly. Leak respiration rates fueled by glutamate + malate (linear mixed-effect model, $p_{assay} < 0.0001$) and pyruvate + malate (linear mixed-effect model, $p_{assay} < 0.0001$) increased with increasing T_{assay}. Significant acclimation effects were detected for both glutamate + malate (linear mixed-effect model, $p_{acclimation} < 0.0001$) and pyruvate + malate (linear mixed-effect model, $p_{acclimation} < 0.0001$). No significant interaction effects were detected. Post-hoc analyses revealed that acclimation to 5 °C increased leak respiration compared to 33 °C for

both substrates. Acclimation to 15 °C increased leak respiration compared to 33 °C; however, this only occurred at T_{assay} = 15 °C when fueled with glutamate + malate.

4.4.4 Respiratory control ratio (RCR)

We calculated respiratory control ratios to estimate changes in mitochondrial coupling following thermal acclimation and changes in assay temperature. RCR resulting from flux through ETS complex II (Fig. 4.3A) was significantly affected by assay temperature (linear mixed-effect model, $p_{assay} < 0.0001$), with no significant effect of acclimation temperature. However, there was a significant interaction effect (linear mixed-effect model, $p_{interaction} = 0.0298$), such that RCR was highest in the 5 °C and 33 °C acclimated groups assayed at their respective acclimation temperatures, although these differences were not detected in post-hoc tests.

In contrast, RCR resulting from flux through ETS complex I exhibited an entirely different pattern. We detected a significant assay temperature effect for both glutamate + malate (Fig. 4.3B, linear mixed-effect model, $p_{assay} < 0.0001$) and pyruvate + malate (Fig. 4.3C, linear mixed-effect model, $p_{acute} < 0.0001$). In addition, glutamate + malate (linear mixed-effect model; $p_{acclimation} < 0.0001$, $p_{interaction} = 0.0298$) and pyruvate + malate (linear mixed-effect model, $p_{acclimation} < 0.0001$, $p_{interaction} = 5.97 \times 10^{-3}$) RCRs were subject to significant acclimation and interaction effects. RCRs calculated from fish acclimated to 33 °C was lower compared to other acclimation groups for the majority of assayed temperatures. This effect is driven by the lower state 3 respiration rates in this group. Differences in RCR between the 5 and 15 °C acclimated groups were dependent on T_{assay}, such that 5 °C acclimated fish exhibited higher RCRs at lower T_{assay} and 15 °C acclimated fish surpassed the 5 °C group at higher T_{assay}.

4.4.5 Proton leak kinetics

We measured the kinetics of proton leak over varying membrane potential in order to provide insight into the maintenance of Δp under conditions considered to be more physiologically relevant (as compared to rates at maximum $\Delta\Psi_m$ measured previously). To compare across acclimation temperatures proton leak kinetics were analyzed for each mitochondrial preparation and the kinetic parameter: k (the rate constant) was extracted. Regardless of assay temperature, no significant differences in k across acclimation groups were

detected (Fig. 4.4A, T_{assay} = 5 °C, one-way ANOVA, $p_{acclimation}$ = 0.742, $k_{5\,°C}$ = 0.0044 ± 5.61x 10^{-3}, $k_{15\,°C}$ = 0.0156 ± 8.05x 10^{-3}, $k_{33\,°C}$ = 0.0069 ± 1.36x 10^{-3}; Fig. 4.4B, T_{assay} = 15 °C, one-way ANOVA, $p_{acclimation}$ = 0.723, $k_{5\,°C}$ = 0.0401 ± 1.59x 10^{-2}, $k_{15\,°C}$ = 0.0227 ± 6.15x 10^{-3}, $k_{33\,°C}$ = 0.0375 ± 2.45x 10^{-2}; Fig. 4.4C, T_{assay} = 33 °C, one-way ANOVA, $p_{acclimation}$ = 0.774, $k_{5\,°C}$ = 0.0638 ± 1.41x 10^{-2}, $k_{15\,°C}$ = 0.0570 ± 1.11x 10^{-2}, $k_{33\,°C}$ = 0.0498 ± 1.55x 10^{-2}).

4.4.6 Reactive oxygen species production

We estimated mitochondrial ROS production rate as H_2O_2 production in order to assess deleterious extra-mitochondrial effects resulting from changes in proton leak. Basal and maximum ROS production rates behaved similarly, and increases in assay temperature significantly increased production for all acclimation groups (Fig. 4.5A, B; linear mixed-effect model, $p_{acute,\,basal} < 0.0001$, $p_{acute,\,max} < 0.0001$). No significant interaction or acclimation effects were detected. Free radical leak was also affected by acute assay temperature (Fig. 4.5C, linear mixed-effect model, p_{acute} = 5.97x 10^{-3}, with a trend towards increased FRL at 5 °C, although this was not detected by post-hoc tests. No significant interaction or acclimation effects on FRL were detected.

4.5 Discussion

In this study, we assessed the mechanisms and costs of mitochondrial thermal acclimation in the eurythermal Atlantic killifish, *F. heteroclitus*. Low-temperature acclimation resulted in a modest compensation of respiration that was not specific to any one ETS complex. In contrast, high temperature acclimation induced a large suppression of respiration, which was associated almost exclusively with substrates that supply electrons to ETS complex I. Of particular interest was our finding that these large changes in mitochondrial function occurred without a loss of Ψ_m or increased extra-mitochondrial ROS production, despite the fact that low temperature acclimation resulted in greater declines in RCR at high temperatures and high temperature acclimation resulted in declines in RCR at low temperature relative to the other acclimation groups.

4.5.1 Modest compensation following low-temperature acclimation

Low-temperature compensation of mitochondrial respiration has been demonstrated in several ectothermic species (Dos Santos et al., 2013; Fangue et al., 2009; Kraffe et al., 2007). These increases in functional capacity are thought to play a role in maintaining ATP homeostasis (reviewed by O'Brien, 2011). We observe similar effects, but the magnitude of compensation between 5 and 15 °C acclimated *F. heteroclitus* is small compared to patterns in other species and respiration only differed significantly at low assay temperatures (Fig. 4.1A, B, C, 2). For example, Q_{10} calculated from 5 °C acclimated fish between T_{assay} = 5 and 15 °C was 4.46, for pyruvate-malate fueled state 3 respiration (Fig. 4.2C) but 3.66 when compared between 5 and 15 °C acclimated fish assayed at their respective acclimation temperatures, demonstrating a Precht type III (i.e., partial) compensation of respiration (Precht, 1958). These data are in agreement with previous observations of killifish liver mitochondrial respiration, demonstrating a limited low-temperature acclimation response (Fangue et al., 2009).

The relatively limited cold-compensation of respiration that we observed in *F. heteroclitus* compared to patterns in other species (St-Pierre et al., 1998) suggests that the wide thermal breadth and substantial plasticity in the whole-organism thermal tolerance of *F. heteroclitus* is not associated with exceptional plasticity in mitochondrial function. It is important to note, however, that the apparent discrepancy between our results and previous studies in other eurythermal species such as goldfish (Dos Santos et al., 2013) may be driven by experimental design or tissue type. For example, if we had compared mitochondrial respiration only between our two extreme acclimation groups (i.e., 5 and 33 °C) we would have concluded that there is a large cold-compensation effect, similar to that observed in other studies (e.g., Dos Santos et al., 2013). Indeed, studies of mitochondrial thermal acclimation often utilize a two-point (low versus high temperature) comparison. This design, however, has the potential to confound interpretation of the low-temperature acclimation response, if there is a suppressive effect of warm-acclimation. While we do not discount the compensatory changes observed in previous studies of cold acclimation, caution in interpreting the magnitude of these effects is warranted. Consequently, we recommend including intermediate acclimation treatments to avoid these potentially confounding effects.

Our observation of modest low-temperature acclimation effects on mitochondrial respiration compared to mitochondria from fish acclimated at intermediate temperatures

indicates that if maintenance of ATP balance is to be achieved, mechanisms other than increases in functional capacity (on a per mitochondrion protein basis) must be recruited. Altering mitochondrial structure and quantity can increase capacity in tandem with changes in mitochondrial biochemical function (Guderley and St-Pierre, 2002). Potential mechanisms might include increases in mitochondrial volume density and cristae surface area. Indeed, these changes have been demonstrated in killifish following low-temperature acclimation (Dhillon and Schulte, 2011). Together our results demonstrate that increases in mitochondrial function following low-temperature acclimation do occur; however, the contribution of these changes to maintaining ATP balance may be small in comparison to changes in mitochondrial quantity and structure. Alternatively, at low temperatures, *F. heteroclitus* may exploit a strategy of only partial compensation, taking advantage of the metabolic suppression caused by low temperatures to reduce metabolic demand in the winter when food resources could be limited. This hypothesis is consistent with the observed suppression of whole-organism metabolic rates in response to cold-acclimation in this species (Healy and Schulte, 2012).

4.5.2 Suppression of mitochondrial respiration during warm-acclimation

Although we observed modest low-temperature compensation of mitochondrial respiration, high-temperature acclimation (33 °C) resulted in a clear reduction of mitochondrial function (Fig. 4.1, 4.2). This response was not observed when killifish were acclimated to 25 °C (Fangue et al., 2009). At the whole-animal level, acclimation to 25 and 33 °C induces different responses, and aerobic scope is maintained only at the lower of these temperatures (Healy and Schulte, 2012). This suggests that acclimation to 33 °C is stressful for killifish. Indeed, chronic exposure to a marginally higher temperature (T_a = 36.4 °C) has been shown to induce mortality in killifish, with a significant loss of total muscle lipids and liver glycogen occurring at $T_{acclimation}$ = 29 °C (Fangue et al., 2006; Fangue et al., 2008). Our data demonstrating reductions in whole animal and liver mass following high-temperature acclimation support this conclusion. Given that 33 °C acclimated fish exhibit these changes while still being fed to satiation may be indicative of entrance into a state of negative energy balance or induction of hypometabolism.

The suppression of mitochondrial capacity we observed occurred with substrates that supply electrons to ETS complex I (Fig 4.1, 4.2). Low rates of respiration through complex I were observed with both of the substrates provided (i.e., pyruvate + malate or glutamate +

malate; Fig. 4.2), indicating that transport and decarboxylation of pyruvate (by pyruvate dehydrogenase) are not major points of modification. This observation is similar to the acute low-temperature response in the rainbow trout (Blier and Guderley, 1993). This suggests a possible reduction in total oxidative phosphorylation capacity following high-temperature acclimation. Indeed, complex I and complex II raw oxygen consumption rates and Ψ_m do not differ greatly (Fig. 4.1A, B; T_{assay} = 15 °C), suggesting a fairly equal contribution to total mitochondrial flux. As a large multi-subunit protein complex that contributes heavily to mitochondrial Δp, complex I is a logical candidate for modification during thermal acclimation (Efremov et al., 2010). Indeed, differences in complex I activity have been suggested to play a role in adaptive differences in thermal tolerance among killifish species and sub-populations (Loftus and Crawford, 2013). Alternatively, it is possible that modifications in the activity of one or more tricarboxylic acid cycle enzymes (although not of succinate dehydrogenase) could account for these observations.

Our observation of decreased mitochondrial flux following high-temperature acclimation may be a consequence of entrance into a state of negative energy balance, which may induce hypometabolism. At the whole-animal level, acclimation to high temperatures induces a slight reduction in routine metabolism in killifish, which may be indicative of suppressed metabolism (Healy and Schulte, 2012). Hypometabolism induced by fasting and short-photophase in *Mus musculus* and *Phodopus sungorus* suppresses complex I but not complex II-linked mitochondrial respiration (Brown and Staples, 2011). A similar observation has been made in liver mitochondria from fasted CD1 mice and is thought to occur due to a reduction in supercomplexing between complexes I and III, and increased fatty-acid oxidation (Lapuente-Brun et al., 2013). Similarly, the observed alterations in the contribution of complex I to total ETS flux in killifish may occur due to increased utilization of lipid stores, as demonstrated in fasted *Oncorhynchus mykiss* (Morash and McClelland, 2011). Collectively, our data reveal mitochondrial mechanisms that may be used to alleviate high-temperature induced mismatches between whole-animal metabolic demand and consumption (Iles, 2014; Lemoine and Burkepile, 2012).

4.5.3 Thermal acclimation does not result in a loss of mitochondrial coupling, a loss of Δp or an increase in ROS production

To investigate if acclimation-induced changes in respiration were associated with mitochondrial dysfunction (e.g., uncoupling), we compared RCR (the ratio of mitochondrial ADP-phosphorylating respiration to leak respiration), among acclimation treatments (Fig. 4.3). We observed a decrease in RCR for all acclimation treatments at high assay temperatures (Fig. 4.3). Reductions in mitochondrial function at high temperatures have been proposed to limit whole-animal thermal tolerance. Indeed, declines in cardiac mitochondrial ATP-synthesizing capacity are known to occur at temperatures just below those that induce heart failure in *Notolabrus celidotus* (Iftikar and Hickey, 2013).

When RCR was calculated with respiration fueled through complex II, it declined more sharply when assayed at 5 °C in the 33 °C acclimated fish compared to other acclimation groups (Fig. 4.3A). Conversely, RCR from 5 °C acclimated fish decreased marginally at high T_{assay}. As a result, a higher RCR was observed with 5 and 33 °C acclimated fish at their respective assay temperatures, which may be indicative of beneficial acclimation. However, these differences were small and were not detected in post-hoc analyses.

When fueled through complex I (Fig. 4.3B, C), RCR for 33 °C acclimated fish was lower than that of the other acclimation groups. Although low RCR is often interpreted as increased uncoupling, the lower RCR in 33 °C acclimated fish is driven primarily by suppression of ADP-phosphorylating respiration (state 3; Fig. 4.2A, C) and not increased leak respiration (state 4; Fig. 4.2B, D), emphasizing an important caveat of interpreting RCR discussed by Gnaiger (2014).

Changes in inner-mitochondrial membrane (IMM) lipid composition and mitochondrial enzyme activities during thermal acclimation are thought to cause mitochondrial dysfunction during acute thermal shifts; a mechanism proposed to cause shifts in thermal optima (Guderley, 2004). We assessed state 4 (i.e., leak) respiration and ability to maintain Ψ_m as metrics of these costs. In principle, significant reductions in Ψ_m would reflect a pathological loss of Δp, whereas high Ψ_m would be a consequence of the uncontrolled generation of Δp. We observed a consistent pattern of increased leak respiration in 5 °C acclimated fish at high T_{assay} (Fig. 4.1C, 4.2B, D); however, Ψ_m does not decline under these conditions (Fig. 4.1F). Under maximum state 3 conditions (ETS complex I and complex II-linked, Fig. 4.1D, E), Ψ_m did not differ among acclimation treatments. The observation that Ψ_m is sustained, particularly given the large changes

in complex-I linked ETS flux, may demonstrate that the suppression of respiration is regulated and does not incur a cost in terms of function. In contrast to state 3 flux, Ψ_m fueled under state 4 conditions (complex II-linked) was lower in 33 °C acclimated fish, but only at high assay temperatures (T_{assay} = 35 and 37 °C, Fig. 4.1F). We initially predicted that acute increases in temperature would cause a decline in Ψ_m in low-temperature acclimated fish due to a loss of coupling. Our results are contrary to our initial prediction and are difficult to account for especially given that RCR and state 4 respiration (complex II-linked) in 33 °C acclimated fish do not differ from those at other acclimation temperatures (Fig. 4.1C, 4.3A). This decline in Ψ_m may be indicative of the onset of pathological function, but given that RCR and state 4 respiration are nonetheless sustained at this temperature, we would predict only limited loss of function.

Acute increases to high temperatures decreased maximum Ψ_m under state 3 conditions for all acclimation treatments (Fig. 4.1D, E). This decline in Ψ_m may be a result of increased mitochondrial uncoupling. Given that RCRs also declined at high T_{assay}, some level of mitochondrial uncoupling likely occurs (Fig. 4.3). Although it appears that high T_{assay} does influence mitochondrial coupling, these responses are at best only slightly modulated by thermal acclimation. Furthermore, Ψ_m under maximum state 3 conditions (Fig. 4.1D) did not differ among acclimation groups assessed with complex I-linked fuels, indicating that if our observed declines in RCR were a result of increased uncoupling, they do not cause a dysfunction in maintaining Δp. As a result, killifish appear to be able to maintain coupling across acclimation treatments but are still subject to loss of coupling following acute increases in T_{assay}.

To ensure that our observation of limited thermal acclimation effects on Ψ_m sensitivity was not an artifact of having measured ETS flux under saturating conditions, we measured leak ETS flux over a range of mV (proton leak kinetics; titrated state 4 respiration and Ψ_m measured in tandem) through complex II (Fig. 4.4) and observed no acclimation effect. This contrasts with the warm-acclimation response in lugworms (*Arenicola marina*), which respond with an increase in Ψ_m (Keller et al., 2004). However, the warm-acclimated lugworms were also in spawning, which makes it difficult to disentangle life-history and thermal effects. Altogether, our data are unique in that they are among the few direct assessments of thermal acclimation effects on Ψ_m, and that they demonstrate *F. heteroclitus*' ability to maintain Ψ_m over a wide thermal range despite the profound changes in mitochondrial ETS flux (particularly during warm-acclimation).

We predicted increased ROS production as a consequence of low temperature acclimation, as it is thought to be associated with pathological ETS flux during acute thermal shifts to high temperatures (Guderley, 2004). Similar to our observations of Ψ_m, ROS production rate and free radical leak through ETS complex II did not differ among acclimation treatments (Fig. 4.5A, B). Indeed, increases in assay temperature increased ROS production for all acclimation groups emphasizing the potentially stressful effects of high ambient temperature. Although we did not observe a significant effect of acclimation on ROS production, it is important to acknowledge potential limitations of our methodology. By estimating ROS production as extra-mitochondrial [H_2O_2], we are unable to detect endo-mitochondrial ROS, as these may be scavenged within the mitochondrion prior to detection. Nonetheless, our measurements are informative for estimating the potential for cytosolic damage. Indeed, our observation of no change in ROS production is reflected in the fact that thermal acclimation has little effect on lipid peroxidation rate and anti-oxidant enzyme activities in killifish (Grim et al., 2010). Because we measured ROS production as a result of succinate-fueled state 4 respiration (which drives ROS production primarily through complex III), we largely bypassed complex I, which can be an important contributor to ROS production *in vivo* (Turrens and Boveris, 1980). Given the causative link between increases in state 4 respiration and ROS production, and our observed trends of decreased complex I-linked state 4 respiration in 33 °C acclimated fish (Fig. 4.2B, D), we might predict decreased ROS production in this group. Nonetheless, complex III has been shown to produce greater amounts of ROS compared to complex I under similar assay conditions, and so our observations have physiological importance (Chen et al., 2003).

Similar to our measurements of ROS production, free radical leak (FRL, ROS production adjusted to mitochondrial O_2 consumption) did not differ among acclimation treatments (Fig. 4.5C). Although a trend of increased FRL at low assay temperatures was observed (with a minimal effect size), this is likely driven by low respiration rates, as opposed actual increases in ROS production. These data, therefore, provide additional support to our conclusion that mitochondrial thermal acclimation does not result in large trade-offs in mitochondrial function in killifish.

4.5.4 Conclusions

This study provides a comprehensive assessment of the mechanisms and costs associated with mitochondrial thermal acclimation in a eurythermal teleost. Our data clearly demonstrate the wide range over which killifish can modify mitochondrial activity in response to thermal acclimation. A novel finding is that these changes were largely associated with suppression of ETS flux through complex I following acclimation to high temperatures, and not flux through complex II or PDH. We propose that these shifts in ETS flux may occur in part, due to entrance into a state of negative energy balance at high temperatures. We predicted that changes in mitochondrial function following thermal acclimation would induce a loss of function during acute thermal shifts, perhaps accounting for changes in whole-animal thermal tolerance. Our metrics of dysfunction (loss of Δp, increased ROS production) remained largely unaffected by acute thermal shifts, although we observed modest effects on RCR. Thus, these data provide only limited support for a direct link between mitochondrial plasticity and plasticity in whole-animal thermal tolerance. Instead, our data demonstrate that killifish have a profound ability to maintain mitochondrial function across large acute shifts in temperature, and may suggest a mechanism underlying the eurythermal physiology of this species. Further investigations into the thermal acclimation response of complex I, through studies on pre and post-translational modifications as well as mechanistic responses (e.g., IMM modification, kinetics of ETS flux), especially in the heart, will prove invaluable to improving understanding of physiological responses to changes in environmental temperature.

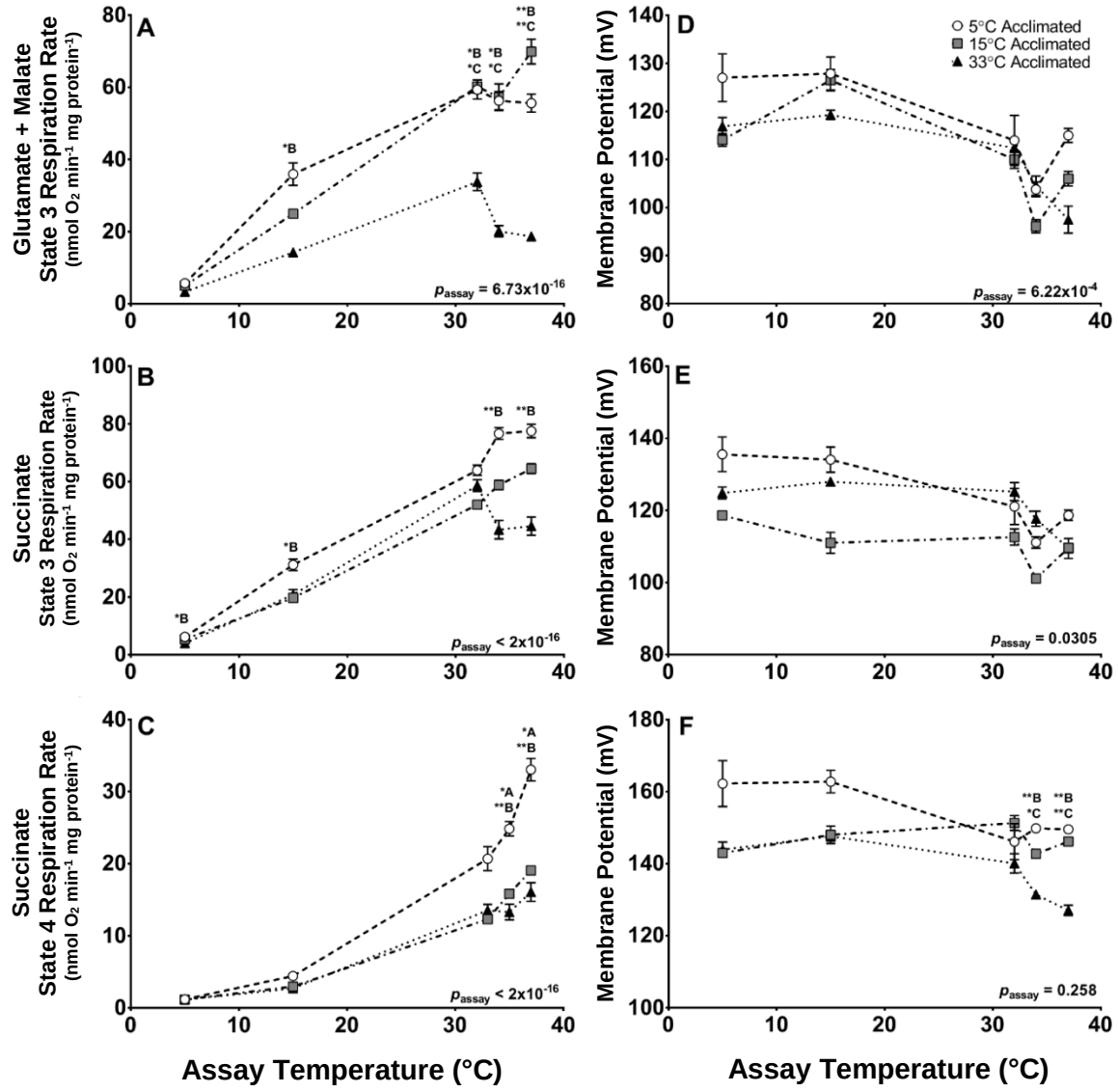

Figure 4.1 Effects of acclimation and assay temperature on respiration rate (A, B, C) and maximum membrane potential (D, E, F) of killifish liver mitochondria. Killifish were acclimated to 5, 15, or 33 °C and mitochondrial parameters were measured in tandem over a range of assay temperatures Mitochondria were provided complex I (A, D; glutamate + malate), or complex II (B, C, E, F; succinate) linked substrates and respiration rate was measured under state 3 (A, B, D, E) or state 4 (C, F) conditions. Assay temperature effects are indicated by *p*-value within each panel. Letters above each assay temperature that differ indicate a significant difference between acclimations within an assay temperature (A: 5 °C ≠ 15 °C, B: 5 °C ≠ 33 °C, C: 15 °C ≠ 33 °C). Asterisks denote the *p*-value of each acclimation effect (*: $p < 0.05$, **: $p < 0.01$). Data are presented as mean ± SEM (n = 8-9). Acclimation treatments indicated by open circles (5 °C), grey squares (15 °C), and black triangles (33 °C).

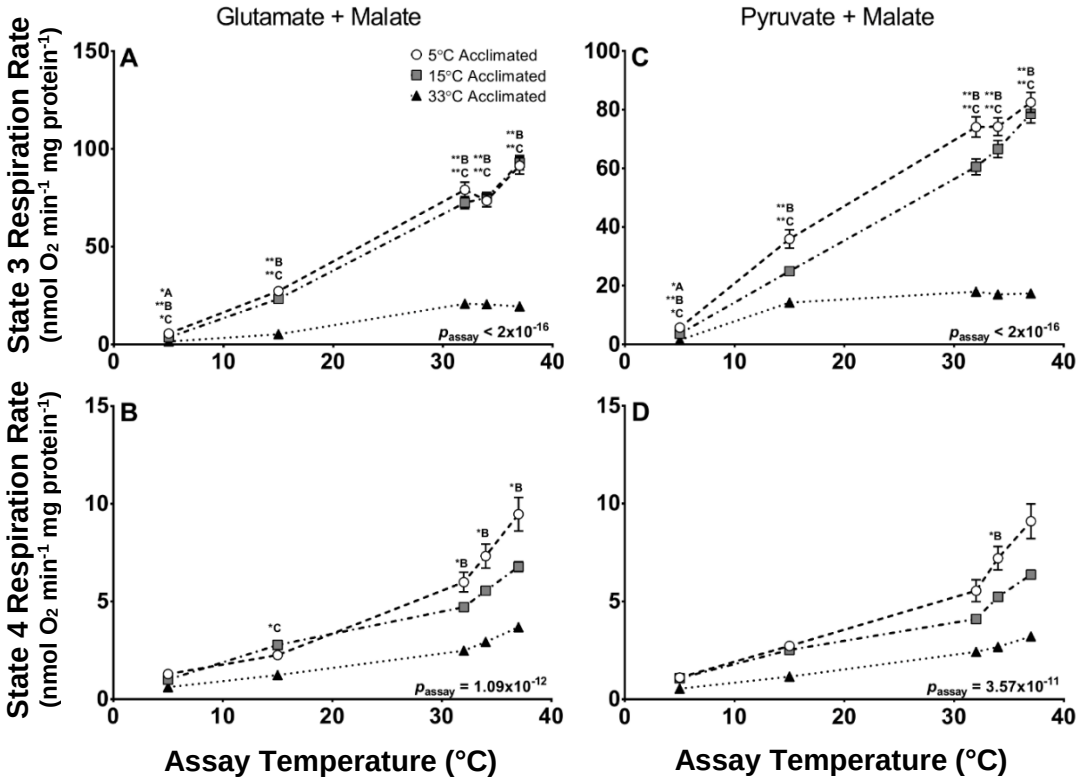

Figure 4.2 Effects of acclimation and assay temperature on respiration rate of killifish mitochondria fueled with different complex I linked substrates. Mitochondria from killifish acclimated to 5, 15, or 33 °C were provided glutamate + malate (A, B), or pyruvate + malate (C, D), which enter the Krebs cycle via different pathways. Respiration rate was measured under state 3 (A, C) or state 4 (B, D) conditions. Assay temperature effects are indicated by *p*-value within each panel. Letters above each assay temperature that differ indicate a significant difference between acclimations within an assay temperature (A: 5 °C ≠ 15 °C, B: 5 °C ≠ 33 °C, C: 15 °C ≠ 33 °C). Asterisks denote the *p*-value of each acclimation effect (*: $p < 0.05$, **: $p < 0.01$). Data are presented as mean ± SEM (n = 5-6). Acclimation treatments indicated by open circles (5 °C), grey squares (15 °C), and black triangles (33 °C).

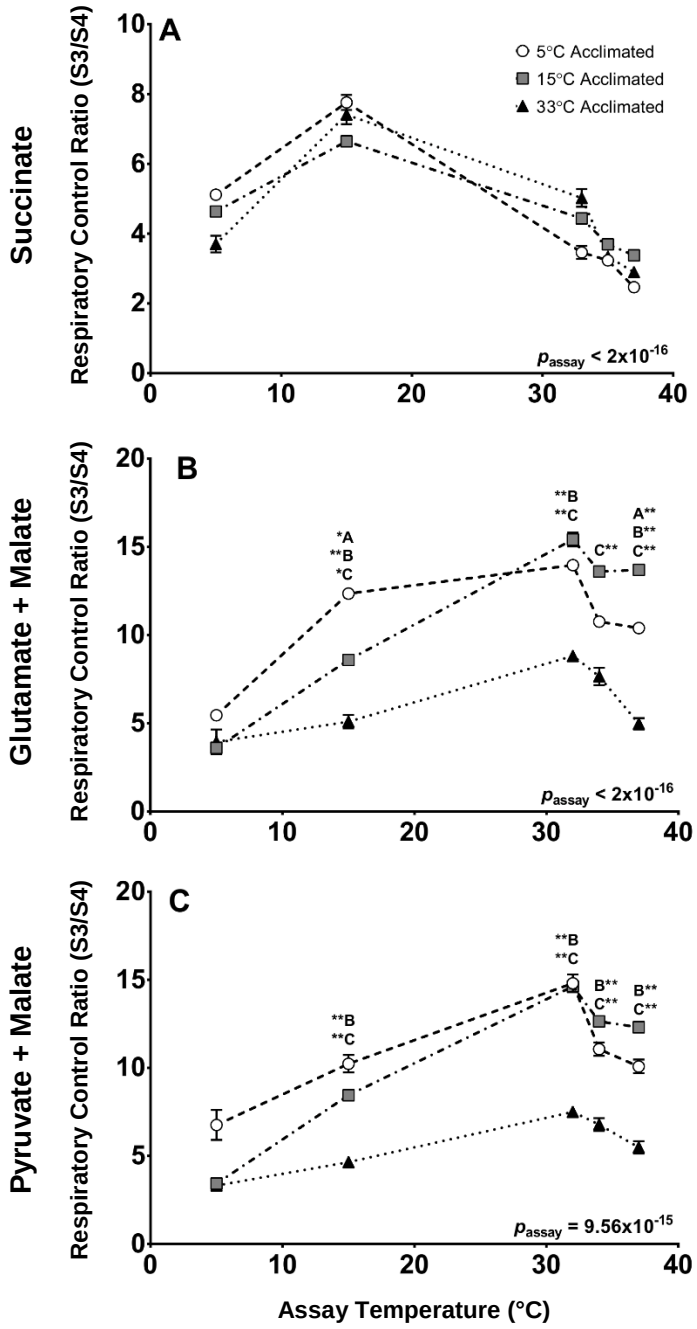

Figure 4.3 Effects of acclimation and assay temperature on the respiratory control ratio (the ratio of state 3 and 4 respiration) of killifish mitochondria. Mitochondria were provided succinate (A), glutamate + malate (B), or pyruvate + malate (C). Assay temperature effects are indicated by *p*-value within each panel. Letters above each assay temperature that differ indicate a significant difference between acclimations within an assay temperature (A: 5 °C ≠ 15 °C, B: 5 °C ≠ 33 °C, C: 15 °C ≠ 33 °C). Asterisks indicate the *p*-value of each acclimation effect (*: $p < 0.05$, **: $p < 0.01$). Data are presented as mean ± SEM (n = 7-9). Acclimation treatments indicated by open circles (5 °C), grey squares (15 °C), and black triangles (33 °C).

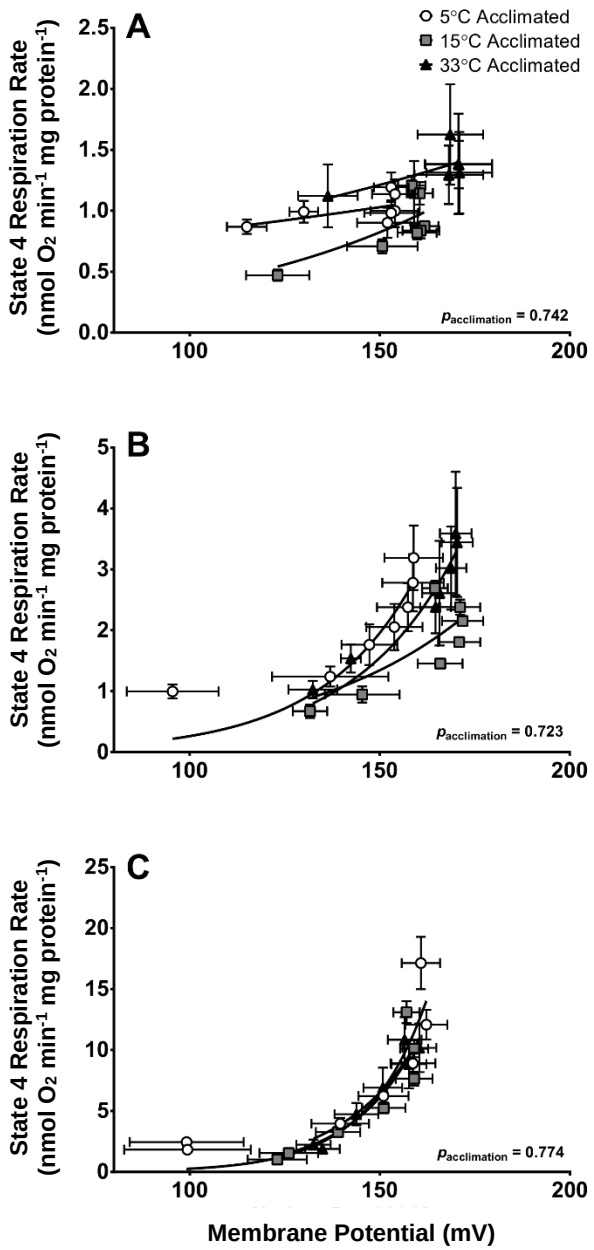

Figure 4.4 Killifish liver mitochondrial proton leak kinetics assayed over a range of temperatures (A: 5 °C, B: 15 °C, C: 33 °C) following acclimation to 5, 15, or 33 °C. Kinetics were measured by titrating saturating state 4 respiration (with succinate as the substrate) with additions of malonate (seven additions). *P*-values for comparisons among acclimation groups of equation parameters (k) are indicated in each panel. Data presented are mean ± SEM (n = 7-9). Acclimation treatments indicated by open circles (5 °C), grey squares (15 °C), and black triangles (33 °C).

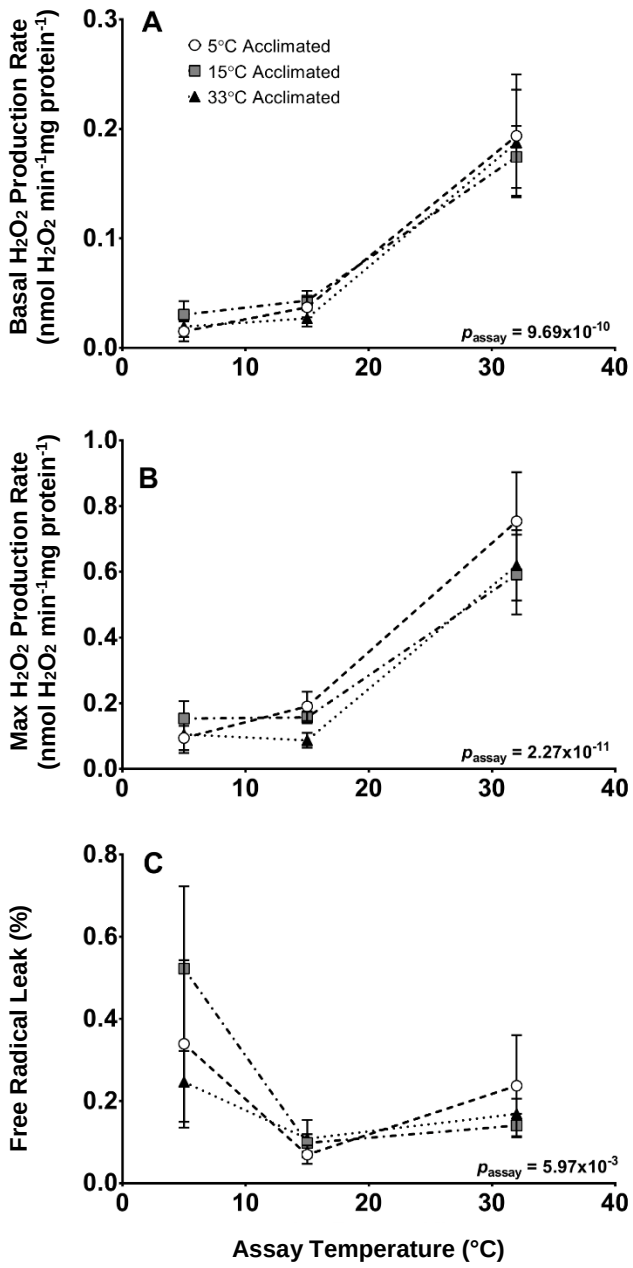

Figure 4.5 Liver mitochondrial H_2O_2 (i.e., reactive oxygen species) production rate (A: basal; B: max) and free radical leak (C, basal ROS production normalized to O_2 consumption rate) of killifish following thermal acclimation (5 °C, 15 °C, 33 °C). Assay temperature effects are indicated by p-value within each panel. Data presented are mean ± SEM (n = 7-9).

Chapter 5 Thermal acclimation and subspecies-specific effects on heart and brain mitochondrial performance in a eurythermal teleost (*Fundulus heteroclitus*)

5.1 Summary

Mitochondrial performance may play a role in setting whole-animal thermal tolerance limits and their plasticity, but the relative roles of adjustments in mitochondrial performance across different highly aerobic tissues remain poorly understood. We compared heart and brain mitochondrial responses to acute thermal challenges and thermal acclimation using high-resolution respirometry in two locally adapted subspecies of Atlantic killifish (*Fundulus heteroclitus*). We predicted that 5 °C acclimation would result in compensatory increases in mitochondrial performance, while 33 °C acclimation would cause suppression of mitochondrial function to minimize the effects of high temperature on mitochondrial metabolism. In contrast, acclimation to both 33 and 5 °C decreased mitochondrial performance compared with fish acclimated to 15 °C. These adjustments could represent an energetic cost-saving mechanism at temperature extremes. Acclimation responses were similar in both heart, and brain; however, this effect was smaller in the heart, which might indicate its importance in maintaining whole-animal thermal performance. Alternatively, larger acclimation effects in the brain could indicate greater acute thermal sensitivity compared to the heart. We detected only modest differences between subspecies and the parameters affected were dependent on the tissue assayed. These data demonstrate extensive plasticity in mitochondrial performance following thermal acclimation in killifish and indicate that the extent of these responses differs between tissues, highlighting the importance and complexity of mitochondrial regulation in thermal acclimation in eurytherms.

5.2 Introduction

Ambient temperature (T_a) constrains whole-organism performance, and this is especially true for ectotherms. These constraints are due, at least in part, to temperature effects on biochemical reaction rates and by extrapolation, aerobic metabolism (Guderley and St-Pierre, 2002; Hochachka and Somero, 2002; Pörtner, 2001; Pörtner and Farrell, 2008; Schulte, 2015). Declines in aerobic performance at thermal extremes are thought to occur because of an inability to deliver O_2 to systemic tissues, possibly owing to effects on cardiac function (Iftikar and

Hickey, 2013; Pörtner, 2001; Somero, 2010). Alternatively, temperature-induced declines in neural function are suggested to constrain thermal performance limits (Cossins, 1977; Ern et al., 2015; Jastroch et al., 2007; Miller and Stillman, 2012; Somero and DeVries, 1967). However, the relative importance of these organ systems in setting an organism's thermal performance limits is still subject to debate (Clark et al., 2013; Ern et al., 2015).

One mechanism that could underlie cardiac and neural failure is mitochondrial dysfunction. For example, the capacity for heart mitochondrial ATP synthesis declines at temperatures preceding heart failure in *Notolabrus celidotus* (Iftikar and Hickey, 2013). However, no studies have examined the possibility of mitochondrial failure being associated with temperature-induced declines in neural performance. Comparisons of mitochondrial function among tissues and within the same organism are thus imperative as differences in thermal sensitivity and plasticity of mitochondrial function may reveal the relative importance of particular tissues in setting thermal tolerance limits.

There is substantial evidence for thermally-induced plasticity in mitochondrial structure and function in ectotherms (Guderley and St-Pierre, 2002; Seebacher et al., 2010). Low-temperature acclimation is associated with increased mitochondrial oxidative phosphorylation (OXPHOS) capacity, mitochondrial volume density, and alterations in mitochondrial membrane composition (Chapter 4; Dhillon and Schulte, 2011; Egginton and Johnston, 1984; Fangue et al., 2009; Grim et al., 2010; Kraffe et al., 2007; Schnell and Seebacher, 2008). In contrast, high-temperature acclimation has been associated with changes in mitochondrial membrane fatty acid saturation and lowered mitochondrial respiratory capacity (Chapter 4; Baris et al., 2016b; Fangue et al., 2009; Guderley and Johnston, 1996; Khan et al., 2014; Strobel et al., 2013). These changes may induce trade-offs causing mitochondrial function to decline at temperatures that were not previously harmful, which may account for shifts in whole-animal thermal tolerance following acclimation (i.e., animals that are acclimated to low temperatures cannot tolerate high temperatures and vice versa; Chapter 4; Fangue et al., 2009).

Natural selection acting on mitochondrial function has the potential to improve performance in subspecies that experience different thermal regimes (Castellana et al., 2011; Guderley, 2011; Pörtner, 2001). Indeed, differences in whole-animal and mitochondrial thermal performance among *Drosophila* species occurs because of divergences in mitochondrial DNA sequence and incompatibilities between mitochondrial and nuclear genomes (Hoekstra et al.,

2013; Pichaud et al., 2012). Although these studies provide support for selection enhancing thermal performance, much remains to be discovered about whether these mechanisms constrain or enhance mitochondrial acclimation capacity and the consequences for whole-animal performance.

Here we utilize Atlantic killifish [*Fundulus heteroclitus* (*Linnaeus 1766*)], a profoundly eurythermal teleost, to examine plasticity and putatively adaptive variation in mitochondrial performance with temperature. These animals reside in intertidal salt marshes along the Atlantic coast of North America. In these estuarine habitats, they experience large diel and seasonal fluctuations in T_a. Their ability to survive (critical thermal [CT] limits = -1 to 41 °C) and acclimate (acclimation limits = 2 to 35 °C) over a large thermal range may be due to a thermally robust mitochondrial physiology (Chapter 4; Fangue et al., 2009), and acclimation capacity (Chapter 4; Baris et al., 2016b; Fangue et al., 2009). In addition, northern and southern subspecies of *F. heteroclitus* have undergone local adaptation to their thermal environments and have diverged for a number of traits such as whole-animal metabolic rates and thermal tolerance (Fangue et al., 2006; Fangue et al., 2009; Schulte, 2001). Despite the existence of genetic polymorphisms in genes encoding mitochondrial proteins that differentiate northern and southern killifish (McKenzie et al., 2016; Whitehead, 2009), few clear differences in mitochondrial function exist between these subspecies (Baris et al., 2016b; Fangue et al., 2009), although differentiation in mitochondrial function has been examined in only heart (Baris et al., 2016b) and liver (Fangue et al., 2009), and nothing is known about the function of brain mitochondria in this species.

In this study, we assessed the relative responses of brain and heart mitochondria to thermal acclimation (5, 15, and 33 °C) in northern and southern *F. heteroclitus*. This design allows us to improve understanding of the mechanisms that underlie the potential failure of these tissues during thermal stress and to identify the relative contribution of each tissue to setting organismal thermal tolerance limits. We measured mitochondrial performance using high-resolution respirometry to quantify changes in function through each component of the mitochondrial electron transport system (ETS). We addressed the following questions: 1) Does acclimation to 5 and 33 °C alter mitochondrial function through compensatory increases and suppression of activity respectively? 2) Do heart and brain mitochondrial performance differ in their acute and acclimation thermal responses, which might reveal a greater contribution of one

tissue to whole-animal thermal intolerance? 3) Do locally adapted killifish subspecies exhibit differences in mitochondrial function that could underlie the previously observed differences in whole-organism metabolic rates and thermal tolerance? In this way, we provide a greater mechanistic understanding of the mitochondrion's role in the setting of whole-animal thermal tolerance limits.

5.3 Methods

5.3.1 Animals

Experiments were conducted following the University of British Columbia approved animal care protocol #A11-0372. Wild-caught adult southern killifish (*Fundulus heteroclitus heteroclitus*) were collected from Jekyll Island, GA (31º02'N; 81º25'W) in June of 2014. Northern killifish *(Fundulus heteroclitus macrolepidotus*) were collected in Ogden's Pond estuary, NS (45º71'N; 61º90'W) in September of 2014. Fish were estimated to be one to two years old based on length at catch (> 5 cm; Valiela et al., 1977). Fish were housed at the UBC Aquatics Facility in 190 L recirculating tanks with biological filtration at T_a = 15 ± 2ºC, 20 ppt salinity and 12:12 L:D photoperiod prior to experimentation. Fish were fed once daily to satiation (Tetrafin Max; Rolf C. Hagen Inc., Montreal, QC). After at least 10 months of laboratory holding (July 2015), fish were distributed into 114 L tanks with T_a = 5, 15, or 33ºC at 20 ppt salinity and 12:12 L:D. We chose 33 °C for our high-temperature acclimation as this is the point at which effects on whole-organism aerobic metabolism are first observed, while also avoiding substantial induction of breeding physiology which occurs at lower temperatures (i.e., 30 °C; Healy and Schulte, 2012; Matthews, 1939). We chose 5 °C as our low acclimation temperature because this is the temperature at which effects on whole-organism aerobic metabolism are first observed (Healy and Schulte, 2012). Fish were acclimated for a minimum of four weeks prior to sampling.

5.3.2 Heart permeabilization

Following thermal acclimation, fish were removed from their holding tanks and euthanized by cervical dislocation and weighed at 09:00 AM PST prior to the daily feeding. Each day, five killifish were sampled. Hearts were excised, weighed and transferred to a single Petri

dish containing ice-cold BIOPS solution (2.77 mM CaK_2EGTA, 7.23 mM K_2EGTA, 5.77 mM Na_2·ATP, 6.56 mM $MgCl_2 \cdot 6H_2O$, 20 mM taurine, 15 mM Na-phosphocreatine, 20 mM imidazole, 0.5 mM dithiothreitol, 50 mM MES hydrate, l $g \cdot L^{-1}$ fatty acid free BSA, pH 7.1 at 0ºC). From this point forward hearts were not individually tracked, making it impossible to associate a specific preparation with a whole-organism mass. For each heart, the bulbus was removed, and the whole ventricle was teased into one fiber bundle (duration 3 min) using sharp forceps. Fibre bundles from different fish were not mixed. Individual fiber bundles were placed into 3 mL of ice-cold BIOPS solution in a 12-well tissue culture plate (one bundle per well). 30 µL of saponin (final concentration 0.05 $mg \cdot mL^{-1}$) was added to each well and ventricle fibers were shaken (80 RPM) on ice for 30 min. Following the saponin treatment, fibers were washed three times for 5 min in ice-cold MiRO5 (0.5mM EGTA, 3 mM $MgCl_2 \cdot 6H_2O$, 60 mM lactobionic acid, 20 mM taurine, 10 mM KH_2PO_4, 20 mM HEPES, 110 mM sucrose, 1 $g \cdot L^{-1}$ fatty acid-free BSA, pH 7.1 at 25 °C). Individual fiber bundles were blotted on filter paper and weighed (5-10 mg) prior to respiration assays.

5.3.3 Brain permeabilization

Brains were also dissected from the killifish, and brain permeabilization was achieved using methods similar to those for heart tissues, with the exception that brains from the five different individuals sampled on a given day were pooled. Brains were weighed, pooled in ice-cold BIOPS solution and cut into approximately 2 mm^3 pieces using a scalpel and sharp forceps. All brain pieces were transferred into one 3 mL aliquot of ice-cold BIOPS solution to which 30 µL of saponin (0.05 $mg \cdot mL^{-1}$) was added. Following saponin treatment and three washes in ice-cold MiRO5, randomly-selected brain pieces were blotted on filter paper and weighed out into 20-35 mg tissue pools immediately prior to respiration assays. Randomization of brain pieces following pooling and mincing of brain pieces prevented the inclusion of fish mass in analyses of respiration data.

5.3.4 Substrate uncoupler inhibitor titration protocol

Flux through the mitochondrial electron transport system (ETS) and oxidative phosphorylation (OXPHOS) apparatus was assessed using a substrate-uncoupler-inhibitor titration (SUIT) protocol modified from (Iftikar and Hickey, 2013). Permeabilized tissue

respiration rates were measured using a high-resolution respirometry system (O2k MiPNet Analyzer; Oroboros Instruments; Innsbruck, Austria). Pre-weighed tissue samples were added to chambers containing 2 mL of air-equilibrated MiRO5. Oxygen electrodes were calibrated across a range of O_2 tensions (350 nmol·mL^{-1} to O_2 depleted) at each assay temperature (T_{assay} = 5, 15, 33, 37 °C) to account for temperature effects and background O_2 consumption by the probes. Zero calibration of the probes at each assay temperature was achieved using a yeast suspension. During the assay, the O_2 tension was maintained between 350 and 200 nmol·mL^{-1} by injecting O_2 into the gas phase above the medium to maintain the partial pressure gradient to the mitochondria. Respiration rates were normalized to tissue wet mass.

State II respiration fueled through ETS complex I (LEAK-I) was achieved through the addition of pyruvate (10 mM) and malate (2 mM). A saturating quantity of ADP (2.5 mM) was introduced to the chamber followed by glutamate (10 mM) to assess complex I-linked state III respiration (oxidative phosphorylation, OXP-I). State III respiration fueled through complexes I and II (OXP-I, II) was measured through the addition of succinate (10 mM). Complex I and II-linked, state IV respiration (LEAK-I, II) was estimated through the introduction of carboxyatractyloside (5 μM). We used carboxyatractyloside as an inhibitor because of oligomycin's suppressive effects on respiration in similar preparations (Baris et al., 2016a). Substrate oxidation capacity (ETS-I, II, fueled through ETS complexes I and II) was achieved by fully uncoupling mitochondria with repeated additions of carbonyl cyanide p-(trifluoro-methoxy) phenyl-hydrazone (FCCP, 0.5 μM). This was followed by inhibition of ETS complexes I, II and III through the sequential addition of rotenone (0.5 μM, dissolved in ethanol; yielding ETS-II), malonate (5 mM) and antimycin A (2.5 μM) respectively. Apparent cytochrome *c*-oxidase (ETS complex IV; CCO) capacity was measured through the addition of N,N,N',N'-tetramethyl-p-phenylenediamine (TMPD, 0.5 mM) and ascorbate (2 mM). We accounted for auto-oxidation of TMPD and ascorbate through chemical background corrections at each assay temperature. Mitochondrial coupling was estimated using the ratio of OXP-I and LEAK-I (respiratory control ratio; RCR-I) and OXP-I, II and LEAK-I, II (RCR-I, II). Limitations on OXPHOS capacity by ETS capacity were assessed using the ratio of OXP-I, II to ETS-I, II.

5.3.5 Citrate synthase assay

We approximated changes in heart and brain mitochondrial quantity following thermal acclimation by measuring changes in citrate synthase (CS) activity (Srere, 1969) in a different subset of fish than those used for mitochondrial assays. Tissues were frozen in liquid N_2 and stored at -80 °C until they were ready to be assayed. Frozen tissues were thawed on ice and homogenized individually in 250 or 350 μL (heart and brain respectively) of homogenization buffer (5 mM EDTA, 50 mM HEPES, 0.1% (v/v) Triton X-100, pH 7.4 at 20 °C) using two 10 s passes of a tissue homogenizer (PowerGen 125; Fisher Scientific, Ottawa, Canada). Homogenized samples were centrifuged (10,000 *g* for 2 min at 4 °C) and the resulting supernatant was used for the assay. Tissue homogenate was diluted (21-fold) in assay buffer (0.30 mM acetyl-CoA, 0.15 mM DTNB, 50 mM Tris-HCl, pH 8.0 at 25 °C) and a background rate of change of absorbance was measured at 412 nm for 10 min using a Molecular Devices Spectramax-190 at 25 °C. This was followed by addition of oxaloacetate (21.5 mM final concentration), and reaction rate was monitored for 10 min at 412 nm. CS activity was corrected to protein concentration as determined by Bradford assay with BSA as a standard (Bradford, 1976).

5.3.6 Statistical analyses

All data are presented as means ± SEM; sample size (*n*) is indicated in the relevant figure and table captions. All statistical tests were completed using R software (version 3.0.2) with $\alpha = 0.05$.

Thermal acclimation effects on whole-animal, heart and brain mass and cardiosomatic and craniosomatic indices were assessed using separate two-way ANOVAs with acclimation temperature and subspecies as factors. The effects of subspecies, assay temperature and acclimation temperature on LEAK-I; OXP-I; OXP-I, II; LEAK-I, II; ETS-I, II; ETS-II; CCO; RCR-I; RCR-I, II; and OXP-I, II/ ETS-I, II were assessed using separate three-way ANOVAs for hearts and brains. Heart and brain CS activity were analyzed using two-way ANOVAs with acclimation temperature and subspecies as factors. We ran Shapiro-Wilk and Bartlett's tests to confirm normal distributions and homogeneity of variance in our data. Our data conformed to the assumption of homogeneity of variance but were not always normally distributed (data were

typically slightly right-skewed). Given that ANOVAs are robust to moderate deviations from normality we proceeded with parametric analysis (Harwell et al., 1992).

5.4 Results

5.4.1 Whole-animal and tissue-specific mass

We measured whole-animal and tissue wet masses following thermal acclimation to estimate the overall energetic status of the animals. Northern and southern killifish acclimated to 5 °C had the highest whole-animal mass, whereas 33 °C acclimated fish had the lowest (Fig. 5.1A; $p_{acclimation} < .001$). Northern killifish had greater whole-animal mass compared with southern killifish ($p_{subspecies} < .05$). This subspecies effect may be influenced by differences in initial mass that we are unable to account for. No interaction effect was detected ($p_{subspecies*acclimation} = .195$).

Acclimation to 5 °C was associated with greater heart mass in both subspecies of killifish compared with 15 °C control fish. In contrast, acclimation to 33 °C was associated with lower heart mass (Fig. 5.1B, $p_{acclimation} < .001$). Northern killifish exhibited greater heart mass at all acclimation temperatures particularly following acclimation to 5 °C ($p_{acclimation*subspecies} < .05$, $p_{subspecies} < .001$). Acclimation to 5 °C was associated with a greater cardiosomatic index compared to 15 °C control fish and a lower index following acclimation to 33 °C (Fig. 5.1D, $p_{acclimation} < .05$). Northern killifish had a greater cardiosomatic index than southern killifish, and there was no significant interaction of subspecies and acclimation effects ($p_{subspecies} < .001$, $p_{subspecies*acclimation} = .469$).

Unlike acclimation effects on the heart, 5 °C acclimation did not result in greater brain mass when compared with 15 °C control fish (Fig. 5.1C). In contrast, acclimation to 33 °C resulted in significantly lower brain mass compared with control fish ($p_{acclimation} < .001$). Northern killifish had greater brain mass than southern killifish ($p_{subspecies} < .001$). No significant interaction effect was detected ($p_{subspecies*acclimation} = .146$). Craniosomatic index was lower in 5 °C acclimated killifish compared with 15 °C control fish, and there was no difference between 15 and 33 °C acclimated killifish. (Fig. 5.1E, $p_{acclimation} < .001$). We did not detect any significant subspecies or interaction effects on craniosomatic index ($p_{subspecies} = .544$, $p_{subspecies*acclimation} = .623$).

5.4.2 Heart OXPHOS and LEAK

We measured OXPHOS (state 3), and LEAK (state 2 or 4) respiration fueled through ETS complex I, and I and II in tandem to estimate changes in mitochondrial respiration resulting from our treatments. Our respiration rates were marginally lower than those measured in hearts from *Notolabrus celidotus* (OXPHOS fueled through complex I = 25 pmol $O_2 \cdot$mg tissue$^{-1} \cdot s^{-1}$, T_{assay} = 15 °C, Iftikar et al., 2015). There was no significant subspecies effect on heart mitochondrial OXPHOS (OXP-I, OXP-I, II) or LEAK (LEAK-I, LEAK-I, II) respiration when fueled through ETS complex I, or I and II (Fig. 5.2; see Table 5.1 for *p*-values). Increases in assay temperature caused an increase of these mitochondrial parameters in both subspecies. In addition, there was a significant interaction between subspecies and assay temperature on OXP-I, II; which was driven by marginally lower acute thermal sensitivity in southern killifish when compared to northern killifish at higher assay temperatures (Fig. 5.2E and 2F; $p_{subspecies*assay} <$ .05).

Unlike the relatively modest differences in respiration rates between the subspecies, there was a large effect of thermal acclimation on OXPHOS and LEAK respiration. Acclimation to 5 and 33 °C resulted in lower OXPHOS and LEAK respiration compared with 15 °C acclimated fish, at most assay temperatures. However, at the highest assay temperatures (i.e., 33 to 37 °C) 5 °C acclimated killifish from both subspecies exhibited an increase in thermal sensitivity that was not present in 15 or 33 °C acclimated fish, such that the respiration in this group became similar to that of the 15 °C acclimated group at the highest assay temperature (Fig. 5.2, see Table 5.1 for *p*-values).

5.4.3 Heart maximum mitochondrial capacity

Killifish heart ETS capacity (i.e., maximum substrate oxidation) through ETS complexes I and II in tandem (ETS-I, II), and ETS complex II (ETS-II), and apparent cytochrome *c* oxidase capacity (CCO) responded similarly to previously described OXPHOS and LEAK parameters (Fig. 5.3). Increases in assay temperature increased respiration rates for both subspecies, acclimation to 5 and 33 °C resulted in lower rates of respiration compared with 15 °C controls, and there were relatively few differences between subspecies (see Table 5.1 for *p*-values).

However, we observed significant interaction effects between subspecies and assay temperature on ETS-I, ETS-I, II, and CCO that are most likely a result of marginally lower respiration rates in southern killifish compared with northern killifish at high assay temperatures (Fig. 5.3, see Table 5.1 for *p*-values). We also detected an interaction effect between acclimation and assay temperature on ETS-I, II which occurred because of acclimation temperature-specific thermal sensitivity changes between T_{assay} = 33 and 37 °C (Fig 5.3A and 3B, $p_{acclimation*assay} <$ .05). CCO was subject to an interaction effect between subspecies, and thermal acclimation which is most likely due to 5 °C acclimated northern fish exhibiting lower respiration compared with 33 °C acclimated individuals and a reversed acclimation effect in southern killifish, nevertheless these effects were modest (Fig. 5.3E and 3F, $p_{subspecies*acclimation} < .05$).

5.4.4 Heart mitochondrial control ratios

Respiratory control ratio (RCR) was calculated to provide insight into the contribution of LEAK to OXPHOS capacity and as a means of estimating changes in mitochondrial coupling among our treatments (Fig. 5.4).

We did not detect any significant subspecies effects on heart RCR-I (Fig 5.4A, B, see Table 5.1 for *p*-values). As assay temperature increased, RCR-I decreased and became indistinguishable among acclimation groups (Table 5.1, $p_{acclimation*assay} < .001$). As assay temperature decreased between 15 and 5 °C we observed a decrease of RCR-I in 33 °C acclimated heart mitochondria. We observed the opposite effect in both 5 and 15 °C acclimated fish.

In both subspecies, heart RCR-I, II was highest at T_{assay} = 15 °C and declined at all other assay temperatures (Fig. 5.4C, D, $p_{assay} < .001$). Thermal acclimation effects were different between subspecies, with 33 and 5 °C acclimation resulting in the greatest RCR-I, II values in northern and southern killifish respectively ($p_{acclimation*subspecies} < .005$).

We calculated OXP-I, II/ ETS-I, II to identify potential limitations on OXPHOS capacity by substrate oxidation capacity (Fig. 5.5, see Table 5.1 for *p*-values). We detected a significant subspecies effect that was driven by a marginally greater ratio in southern killifish compared with their northern counterparts (Fig. 5.5A, B). As assay temperature increased between 33 and 37 °C the ratio of OXP-I, II/ ETS-I, II also increased. No significant acclimation effects or interaction effects were detected.

5.4.5 Brain OXPHOS and LEAK

We assessed the effects of thermal acclimation and local adaptation on brain mitochondrial function as declines in performance might underlie temperature induced failure of the nervous system. We did not detect differences between subspecies when measuring brain OXPHOS (state 3), and LEAK (state 2 or 4) respiration fueled through ETS complex I and ETS complexes I and II in tandem (Fig. 5.6, see Table 5.2 for *p*-values). As T_{assay} increased we observed that respiration increased in all groups and that acclimation to 5 and 33 °C resulted in lower OXPHOS and LEAK respiration compared with 15 °C control fish (Fig. 5.6, $p_{acclimation*assay} < .001$).

5.4.6 Brain maximum mitochondrial capacity

Brain ETS (ETS-I, II; ETS-II) and apparent CCO capacity exhibited responses that were similar to those observed for OXPHOS and LEAK parameters. There were large interaction effects between thermal acclimation and assay temperature that were driven by lower ETS capacity and CCO respiration in 5 and 33 °C acclimated killifish compared with 15 °C acclimated fish, particularly at high assay temperatures (Fig. 5.7, see Table 5.2 for *p*-values).

We detected significant subspecies effects on ETS-II and CCO in the brain. In both cases, southern killifish had marginally greater capacity compared with their northern counterparts (Fig. 5.7C-F; see Table 5.2 for *p*-values). There was a trend toward a similar significant subspecies effect on ETS-I, II (Fig. 5.7A-B; $p_{subspecies} = .087$).

5.4.7 Brain mitochondrial control ratios

Respiratory control ratio fueled through ETS complex I (RCR-I) in brain mitochondria decreased as T_{assay} increased (Fig. 5.8A, B; $p_{subspecies*acclimation*assay} < .01$; see Table 5.2 for *p*-values). At T_{assay} = 5 °C brain RCR-I was greatest in 15 °C acclimated northern killifish whereas 5 °C acclimated southern killifish maintained the highest RCR-I. As T_{assay} increased to 15 °C and higher, differences among acclimation treatments were removed.

Brain RCR-I, II did not differ between subspecies (Fig. 5.8C, D, $p_{subspecies} = .116$, see Table 5.2 for *p*-values). At low T_{assay}, differences among thermal acclimation treatments were apparent, with 5 °C acclimated killifish maintaining the highest RCR-I, II followed by 15 and 33

°C acclimation groups. As T_{assay} increased, RCR-I, II decreased and differences among thermal acclimation treatments were removed ($p_{acclimation*assay} < .05$).

The ratio of brain OXP-I, II/ ETS-I, II increased at T_{assay} extremes of 5 and 37 °C **(**Fig. 5.5C, D; $p_{subspecies*acclimation*assay} < .05$, see Table 5.2 for *p*-values). In general, northern killifish exhibited greater differences among acclimation treatments particularly at T_{assay} = 5 and 15 °C. Overall, 33 °C acclimated killifish maintained the greatest OXP-I, II/ ETS-I, II except when southern killifish were assayed at T_{assay} = 5 °C, and this ratio became indistinguishable among acclimation treatments. In contrast, 5 °C acclimated fish maintained the lowest OXP-I, II/ ETS-I, II ratio except at T_{assay} = 33 and 37 °C in northern killifish when this ratio increased substantially.

5.4.8 Heart and brain citrate synthase activity

We measured whole heart and brain CS activity to estimate changes in mitochondrial content, a mechanism that could account for observed acclimation and subspecies effects on mitochondrial performance.

Heart CS activity was not significantly altered by acclimation (Fig. 5.9A; $p_{acclimation}$ = .190). Southern killifish exhibited greater heart CS activity compared with northern killifish at most acclimation temperatures ($p_{subspecies} < .001$). No significant interaction effects were detected ($p_{subspecies*acclimation}$ = .190).

We detected a significant interaction effect of subspecies and thermal acclimation on brain CS activity (Fig. 5.9B, $p_{acclimation*subspecies} < .05$). In general, northern killifish exhibited greater activity compared with southern killifish ($p_{subspecies} < .05$, n = 7). Northern killifish acclimated to 5 and 33 °C exhibited a decrease in brain CS activity compared with 15 °C controls ($p_{acclimation} < .05$, n = 7). In contrast, southern killifish acclimated to 5 °C exhibited a small increase in brain CS activity, but 33 °C acclimation resulted in a decline. These data indicate that mitochondrial content as estimated by CS activity does not account for our observed acclimation and subspecies effects on mitochondrial performance.

5.5 Discussion

In this study, we compared the effects of thermal acclimation and local adaptation on heart and brain mitochondrial function to assess the relative contributions of these tissues to

setting whole-organism thermal tolerance limits. Tissue comparisons revealed that heart and brain mitochondria responded similarly to thermal acclimation. Acclimation to both 5 and 33 °C decreased heart and brain mitochondrial performance when compared with 15 °C acclimated fish (Figs. 5.2-5.4, 5.6-5.8). These effects were greatest in the brain, suggesting that cardiac mitochondrial performance may be protected and that brain mitochondria are more susceptible to negative effects of acclimation. In contrast, subspecies differences were modest and tissue-specific. Northern killifish exhibited marginally greater maximum ETS capacity (substrate oxidation capacity) and apparent CCO capacity in the heart (Fig. 5.3) whereas southern killifish exhibited slightly greater maximum capacity in the brain (Fig. 5.7). Subspecies effects were not apparent for OXPHOS or LEAK respiration, indicating the potential for subspecies differentiation in parameters associated with maximum enzyme capacity and not coupled respiration (Figs. 5.2, 5.6). These data strongly suggest a role for mitochondrial function in the process of whole-animal thermal acclimation and a modest role for heart or brain mitochondrial capacity in setting subspecies-specific whole-organism thermal tolerance limits.

5.5.1 Does acclimation to 33 °C result in a suppression of mitochondrial activity?

We predicted that acclimation to 33 °C would cause a decline in mitochondrial performance to counteract the unsustainable mitochondrial O_2 consumption and ROS production suggested to occur following acute high-temperature shifts (Abele et al., 2002; Hochachka and Somero, 2002; although see Chapter 4). Our observed decline in heart and brain mitochondrial capacity supports the prediction of decreased mitochondrial capacity at high temperatures (Figs. 5.2-5.4, 5.6-5.8). Similar declines in mitochondrial function have been observed previously in heart and liver mitochondria in *F. heteroclitus* (Chapter 4; Baris et al., 2016b), and in other ectotherms (Guderley and Johnston, 1996; Khan et al., 2014; Strobel et al., 2013). Acclimation to 33 °C results in a decline in routine oxygen consumption in *F. heteroclitus* suggesting that this temperature causes a collapse of aerobic metabolism or that active metabolic suppression is taking place (Healy and Schulte, 2012). Interestingly, these effects may occur at lower temperatures for heart mitochondria than the whole organism, as acclimation to 28 °C causes declines in mitochondrial respiration in killifish (Baris et al., 2016b), whereas whole-organism metabolic rates are maintained (Healy and Schulte, 2012). Declines in whole-animal and tissue mass (Fig. 5.1) following 33 °C acclimation may be indicative of an energetic mismatch induced

by insufficient food supply and high energetic demands (Chapter 4). These data provide support for a mismatch of organism-level energetic supply and demand with increasing temperature and potential sub-lethal costs associated with high-temperature acclimation; this may account for our observed mitochondrial suppression with potential consequences for the fitness of these animals (Iles, 2014; Lemoine and Burkepile, 2012; Salin et al., 2016).

5.5.2 Does acclimation to 5 °C result in compensation of mitochondrial activity?

We predicted that acclimation to 5 °C would cause an increase in mitochondrial capacity to compensate for decreases in enzyme function and mitochondrial membrane fluidity associated with acute low-temperature shifts (Chapter 4; Dos Santos et al., 2013; Fangue et al., 2009; Guderley, 2004; Guderley and Johnston, 1996; Oellermann et al., 2012). In contrast, we observed decreased heart and brain mitochondrial performance following acclimation to low temperatures (Fig. 5.2-5.4, 5.6-5.8). This decrease might be a result of an active suppression of metabolism (Precht, 1958; Richards, 2010). There are few clear demonstrations of low-temperature-associated metabolic suppression in fishes (Campbell et al., 2008; Costa et al., 2013; Crawshaw, 1984). At the whole-animal level, routine metabolism measured at 5 °C is lower in 5 °C acclimated *F. heteroclitus* than in 15 °C acclimated fish, which could point to a role for metabolic suppression (Healy and Schulte, 2012). Alternatively, decreases in metabolic rate following low-temperature acclimation may indicate entrance into quiescent states with reductions in spontaneous activity. Disentangling these metabolic and behavioral effects is difficult because of the challenge of assessing these traits at low temperatures. Nevertheless, our observed decrease in heart and brain mitochondrial performance following acclimation to 5 °C indicates a role for active metabolic suppression in the killifish acclimation response.

5.5.3 Mechanisms of mitochondrial suppression

One mechanism that may account for decreased mitochondrial capacity following thermal acclimation is lower mitochondrial content. However, acclimation to 5 °C is associated with an increase in mitochondrial volume density in *F. heteroclitus* white muscle (Dhillon and Schulte, 2011). We estimated mitochondrial quantity by measuring heart and brain citrate synthase (CS) activity (Fig. 5.9, Larsen et al., 2012). Thermal acclimation exerted limited effects on CS activity when compared with our mitochondrial respiration data, and subspecies effects

were the opposite in the heart (Figs. 5.2-5.4, 5.6-5.8). Although the use of a single mitochondrial marker may be insufficient to assess changes in mitochondrial content (reviewed by Moyes et al., 1998), our data do suggest that limited changes in mitochondrial amount occur in these tissues following thermal acclimation and indicate a larger role for intrinsic changes in mitochondrial properties (e.g., mitochondrial lipid remodeling).

Our observation that declines in mitochondrial performance following acclimation to 5 and 33 °C were not specific to ETS CI is intriguing given that we have previously demonstrated highly specific effects of thermal acclimation on ETS CI in *F. heteroclitus* liver mitochondria (Chapter 4). A lack of ETS-complex specificity in heart mitochondria has also been demonstrated in *F. heteroclitus* acclimated to 28 °C (Baris et al., 2016b). But this phenomenon is not universal as ETS complex-specific responses to thermal acclimation occur in other tissues in *F. heteroclitus* and other species (Chapter 4; Dos Santos et al., 2013). This lack of ETS-complex specificity may be a methodological artifact, as the SUIT protocol used here provides a mixture of substrates simultaneously, whereas traditional mitochondrial respirometry experiments often supply ETS CI and CII substrates in separate assays. Supplying substrates together may decrease the ability to assess the contribution of each ETS complexes' contribution to total mitochondrial flux. Under conditions where mitochondrial respiration is assessed through complex II alone (i.e., ETS-II) we observed identical acclimation effects to those observed when both substrates are presented together (Figs. 5.3C, D; 5.7C, D). We thus conclude that heart and brain mitochondria *in situ* respond to thermal acclimation with a general decrease in ETS function that is not specific to CI.

A potential mechanism for constraining mitochondrial performance is a limitation on OXPHOS capacity by ETS capacity (Fig. 5.5, OXP-I, II/ ETS-I, II). In general, heart OXPHOS capacity was not constrained by ETS capacity (i.e., the ratio was approximately 1) and was insensitive to acute temperature shifts (Fig. 5.5A, B; except at T_{assay} = 37 °C). This relationship contrasts with Baris' et al. (2016a) observation of acute temperature effects on this parameter (direct comparisons between these studies should be made carefully as Baris et al. (2016a) assessed effects on CI and CII separately whereas we make this comparison through CI and CII in tandem). In the brain, OXP-I, II/ ETS-I, II was acclimation-temperature dependent, indicating that these effects may play a role in altering mitochondrial performance (Fig. 5.5C, D). As T_{assay} increased in both tissues OXP-I, II/ ETS-I, II increased, which may be a consequence of

OXPHOS limitations by substrate oxidation capacity or increased LEAK (Fig. 5.2 and 5.6). Subspecies effects were modest and tissue dependent. Although these data point to a potential role of substrate oxidation limiting OXPHOS capacity, the inconsistent direction and tissue specificity mainly serve to highlight the complexity of these processes.

5.5.4 Do heart and brain mitochondrial performance differ?

A novel aspect of this study is our comparison of heart and brain mitochondrial thermal responses, as any differences we observe might reveal a greater contribution of one tissue to setting organismal thermal tolerance limits. Acclimation to 5 and 33 °C lowers both heart and brain mitochondrial capacity (Figs. 5.2-5.4, 5.6-5.8). However, decreases in mitochondrial capacity with acclimation are larger in the brain (Figs. 5.2-5.4, 5.6-5.8). This may reflect a preferential decrease in brain mitochondrial function and at least partially sustained heart mitochondrial performance. This lends support to the idea that cardiac performance is important for maintaining whole-animal thermal performance. Alternatively, these larger decreases in brain mitochondrial function may be a consequence of mitochondrial failure occurring at lower temperatures in the brain when compared to the heart. These scenarios are not mutually exclusive, but they at least indicate differences in the way that these tissues respond to thermal acclimation. However, these effects are not universal as Yan and Xie (2015) detected no difference in the responses of heart and brain mitochondrial function to winter acclimation in *Silurus meridionalis*.

One potential complication of interpreting our brain mitochondrial respiration data is that we are unable to account for differences in brain-region specific mitochondrial performance (Nicholls and Ferguson, 2013). Indeed, Jastroch et al. (2007) demonstrated a brain-region-specific induction of UCP1 mRNA expression in *Cyprinus carpio* following acclimation to 8 °C. Although we are unable to account for these differences, the randomization of brain pieces in our assays would suggest a decrease in overall brain mitochondrial function.

Our data demonstrating similar thermal acclimation responses in heart and brain are intriguing when compared with thermal acclimation responses in liver mitochondria. Northern *F. heteroclitus* exhibit increased liver mitochondrial capacity in the cold and decreased capacity following high-temperature acclimation (Chapter 4). These tissue-specific mitochondrial responses might be a consequence of each tissues' *in vivo* function. Tissues involved with

maintaining aerobic metabolism may be suppressed during cold-acclimation to decrease energetic requirements. In contrast, cold-compensated liver function might allow *F. heteroclitus* to continue processing food and lay down energy stores for use once low-temperatures are removed (Crawshaw, 1984). Indeed, cold-acclimation is associated with greater whole-animal and tissue mass (Fig. 5.1). But an increase in energy stores seems counterintuitive as winter conditions are associated with a reduced abundance of prey items (Chidester, 1920). We thus may be detecting a confounding effect of our photoperiod (12:12 L:D), feeding (once daily ad libitum) and low-temperature treatment. By combining this pseudo-winter condition with excess food, we could be artificially sustaining liver function.

As a general objective, we wanted to determine whether mitochondrial modifications following thermal acclimation were associated with the setting of organism-level thermal tolerance limits. Fangue et al. (2006) previously demonstrated shifts in *F. heteroclitus* whole-animal upper thermal tolerance limits following thermal acclimation (i.e., CT_{max} increases from 31 to 41 °C following acclimation to 5 and 33 °C, respectively). If mitochondrial function sets these thermal tolerance limits, we would expect mitochondrial dysfunction to occur at temperatures approaching CTmax (i.e., between T_{assay} = 33 and 37 °C). In 5 °C acclimated fish (CTmax = ~31 °C), we observed few obvious signs of mitochondrial dysfunction at T_{assay} = 33 °C. However, we observed a steep increase in oxygen consumption between T_{assay} = 33 and 37 °C, indicating mitochondrial failure at temperatures exceeding whole-organism thermal tolerance limits (Fig. 5.2-5.3, 5.5-5.7). In contrast, in 33 °C acclimated fish (CTmax = ~41 °C) most respiratory parameters did not increase between T_{assay} = 33 and 37 °C. This violates the expectation of increases in oxygen consumption with temperature, again suggesting that mitochondrial dysfunction occurs between 33 and 37 °C, which approaches the temperatures of whole-organism thermal failure. Similarly, for 15 °C acclimated fish (CTmax = ~37 °C), we observed level or declining oxygen consumption between T_{assay} = 33 and 37 °C. Although it is difficult to make causal connections between acute temperature effects on mitochondrial performance and declines in tissue or organism function (though see Iftikar and Hickey, 2013), our results are nonetheless suggestive of a role of declining mitochondrial function in the setting of upper thermal tolerance limits in warm-acclimated fish.

5.5.5 Do locally adapted subspecies exhibit differences in mitochondrial respiratory function?

One important objective of this study was to determine the role that mitochondria play in differentiating northern and southern subspecies of killifish. We predicted that northern killifish would exhibit greater mitochondrial respiration compared with their southern counterparts, consistent with the greater whole-animal metabolic rate of northern killifish (Fangue et al., 2009), but that the maximal temperatures at which mitochondrial performance can be sustained would be lower, consistent with the lower whole-organism thermal tolerance of the northern subspecies (Fangue et al., 2006). We demonstrate that differences between subspecies in substrate oxidation and apparent CCO capacity are modest (Figs. 5.3, 5.7) and are absent in coupled respiratory states (Figs. 5.2, 5.6), and that the effects of acute high temperature exposure are similar between the subspecies. We observed subspecies differences in CS activity although the direction of this difference depended on the tissue being assayed (Fig. 5.9). These results indicate that there are subspecies differences in mitochondrial content, which is intriguing given the lack of subspecies differences in mitochondrial respiration. For the heart, where the southern subspecies has greater heart CS activity, this suggests that respiration per unit of mitochondrion may be lower in southern fish. In contrast, in the brain, where the northern subspecies has greater CS activity at the 15 °C acclimation temperature only, this suggests the possibility that respiration per unit mitochondrion may be lower in northern fish. Alternatively, if CS activity is not a strong indicator of mitochondrial amount, these data hint at a potential mismatch between TCA cycle capacity and ETS flux. When considered at the level of the tissue, however, these data indicate that tissue-specific differences in mitochondrial function likely play only modest roles in setting subspecies-specific whole-animal metabolic rate and thermal performance limits.

Intra-specific comparisons of mitochondrial function often reveal modest differences. For example, thermally acclimated (11 and 18 °C) subtropical individuals of *Sepia officinalis* exhibit marginally greater OXPHOS capacity compared with their temperate counterparts (Oellermann et al., 2012). In addition, small subspecies effects on mitochondrial performance are also observed in *F. heteroclitus* hearts and livers (Baris et al., 2016b; Fangue et al., 2009). Our data are consistent with these observations of limited subspecies effects (Figs. 5.2-5.4, 5.6-5.8). Modest subspecies differences are perhaps unsurprising as mitochondrial genes are often subject to neutral and purifying selection and functional differences may only be detected under specific conditions (Melo-Ferreira et al., 2014; Silva et al., 2014), and in general this is true among

species of *Fundulus* as well (Whitehead, 2009). However, mitochondrial respirometry assays often assess function under saturating substrate conditions to ensure a maximum enzyme velocity. This is a distinctly non-physiological condition and may mask nuanced intra-specific differences in performance that could manifest as differences in whole-organism metabolic rate.

Although the sizes of our subspecies effects are not large, it is important to consider their ramifications in the context of the whole organism. Indeed, northern and southern killifish whole-animal critical thermal limits differ by approximately 1.5 °C, while whole-animal acute thermal tolerance extends over a 30 °C range (CT limits of -1 to 34 °C in 12.5 °C acclimated fish, Fangue et al., 2006). Our observation of sustained heart and brain mitochondrial function over a similarly large range of acute temperatures (5 to 37 °C) and small differences between subspecies pairs well with these whole-organism data and suggests that if mitochondrial function does set thermal tolerance limits the size of those differences might be quite small. It is important to note, however, that making clear connections between our mitochondrial data and subspecies differences in whole-animal thermal tolerance is difficult as our subspecies effects were variable between tissues and among our different respiratory states (Figs. 5.2-5.4, 5.6-5.8). It is nevertheless possible that our observed variation in mitochondrial properties contributes to the mechanistic bases for these subspecies differences in whole-organism thermal tolerance and warrants further investigation.

5.5.6 Conclusion

In this study, we provide an assessment of thermal acclimation effects on brain and heart mitochondrial function in genetically distinct northern and southern subspecies of the Atlantic killifish. Our most striking observation was that acclimation to both 5 and 33 °C caused a large decline in mitochondrial performance. These acclimation effects may occur as an energetic cost-saving mechanism following acclimation to low and high temperatures, or as a result of energetic mismatches at both acclimation temperatures. Heart and brain mitochondrial function declined following acclimation to 5 and 33 °C. The size of these effects was larger in the brain, perhaps indicating some level of preserved cardiac mitochondrial function or larger pathological changes in brain mitochondria. We detected small, tissue-specific subspecies effects. These results indicate that the contribution of mitochondrial capacity to differentiating subspecies-specific whole-animal thermal tolerance limits is likely small. Overall, we demonstrate a consistent

decrease in mitochondrial performance following acclimation to thermal extremes with the extent of modification depending on the tissue being assayed. These data highlight the importance and complexity of mitochondrial function in *F. heteroclitus* and improve our understanding of the responses of eurythermal organisms' responses to thermal acclimation in general.

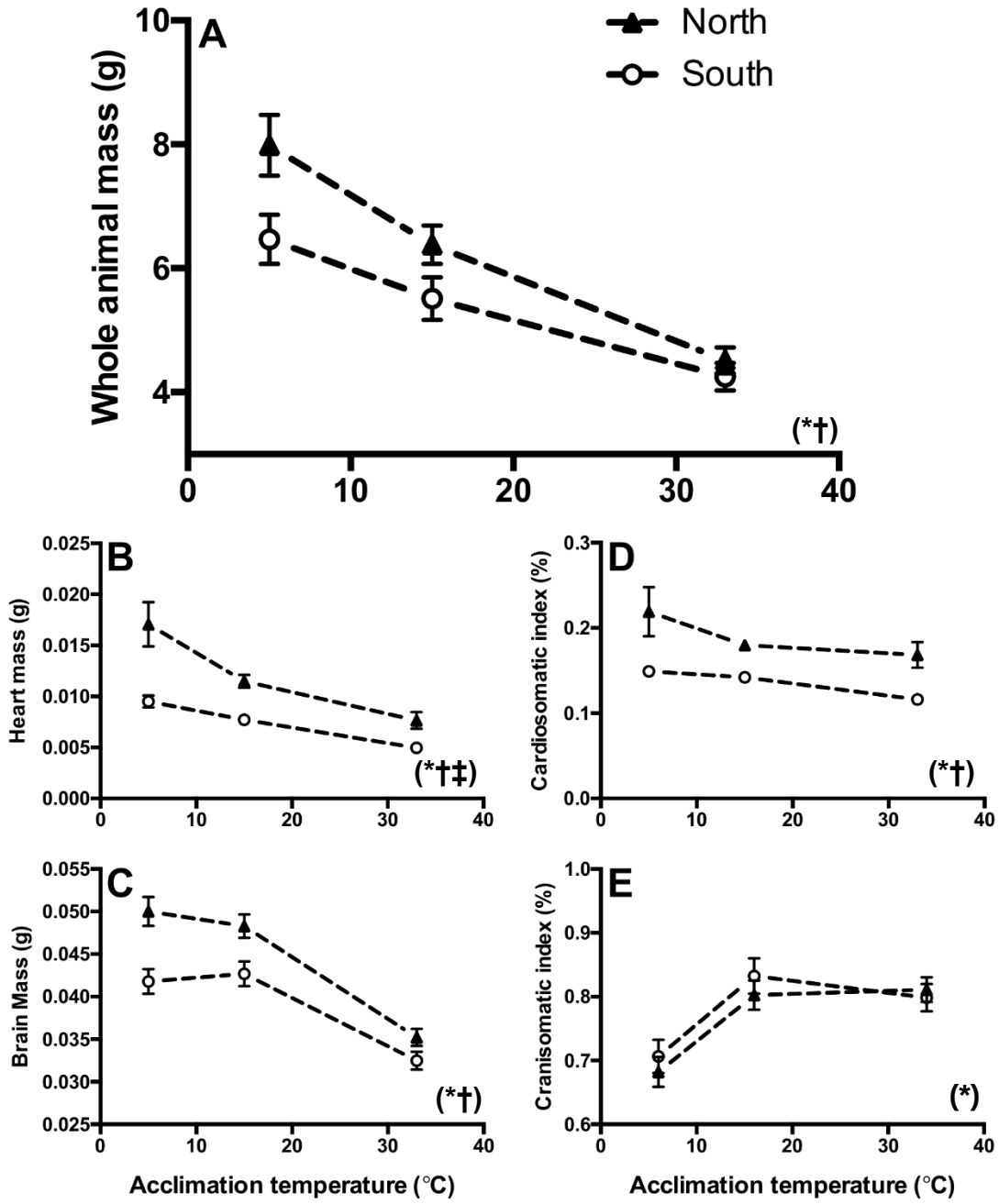

Figure 5.1. Thermal acclimation (5, 15 or 33 °C) effects on whole-animal, heart, and brain wet mass and somatic indices from northern (black triangle) and southern (open circle) subspecies of *Fundulus heteroclitus*. Killifish were thermally acclimated for 4 weeks prior to sampling. Cardiosomatic (D) and craniosomatic (E) indices were calculated as the ratio of tissue mass (B and C, respectively) to whole-animal mass (A). Data are means±SEM; see Results for associated statistics (n=49–56). Symbols indicate significant effects of acclimation (*), subspecies (†), and the interaction between acclimation and subspecies (‡).

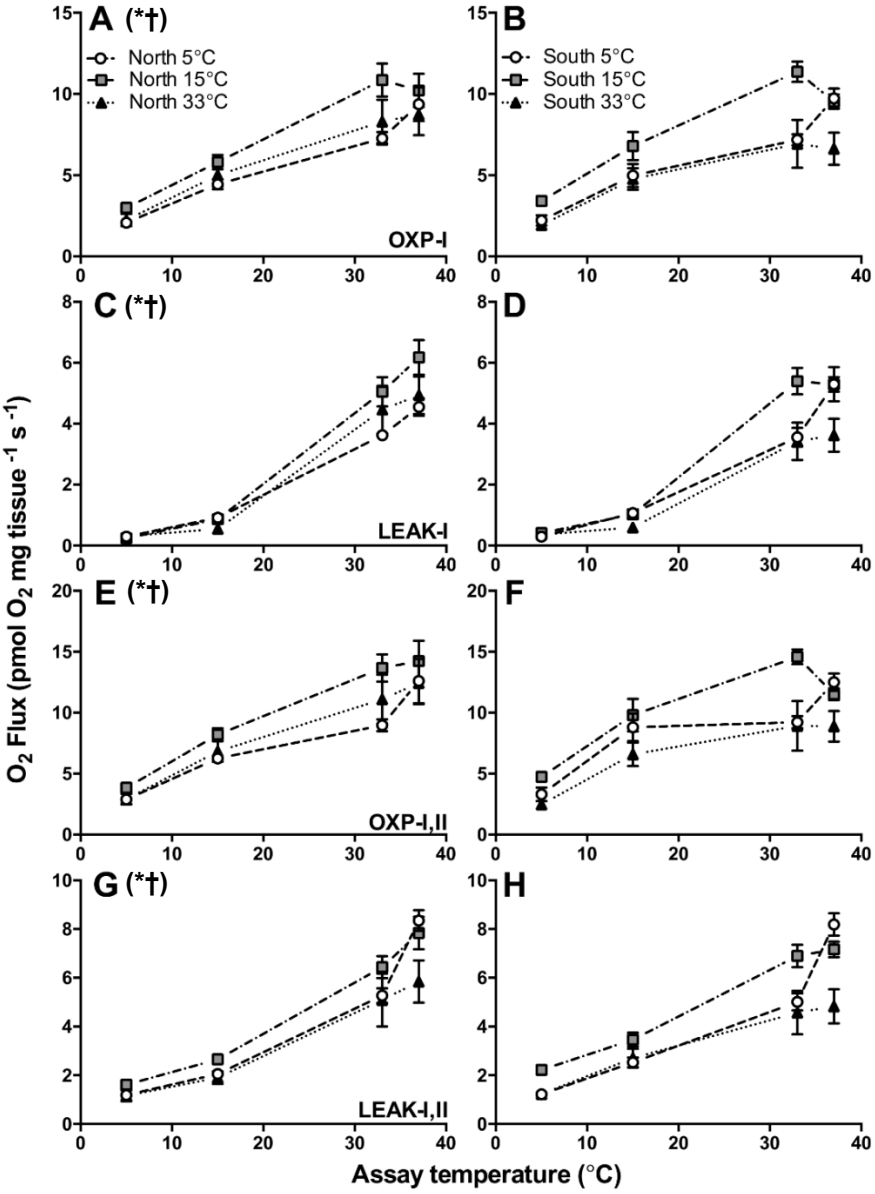

Figure 5.2. Coupled heart mitochondrial respiration from northern and southern killifish acclimated to 5 (open circle), 15 (grey square) or 33 °C (black triangle) for 4 weeks. Permeabilized heart preparations from northern (A, C, E, G) and southern (B, D, F, H) subspecies were subjected to a substrate uncoupler inhibitor titration protocol. Oxidative phosphorylation (OXP; A, B, E, F; state III) and LEAK (C, D, G, H; state II or IV) respiration were measured through electron transport system (ETS) complex I (A–D; pyruvate, malate and glutamate as substrates) and complexes I and II in tandem (E–H; complex I substrates and succinate). Data are means±SEM; see Table 5.1 for associated statistics (n=7–8). Symbols indicate significant main effects of assay temperature (*), and acclimation (†).

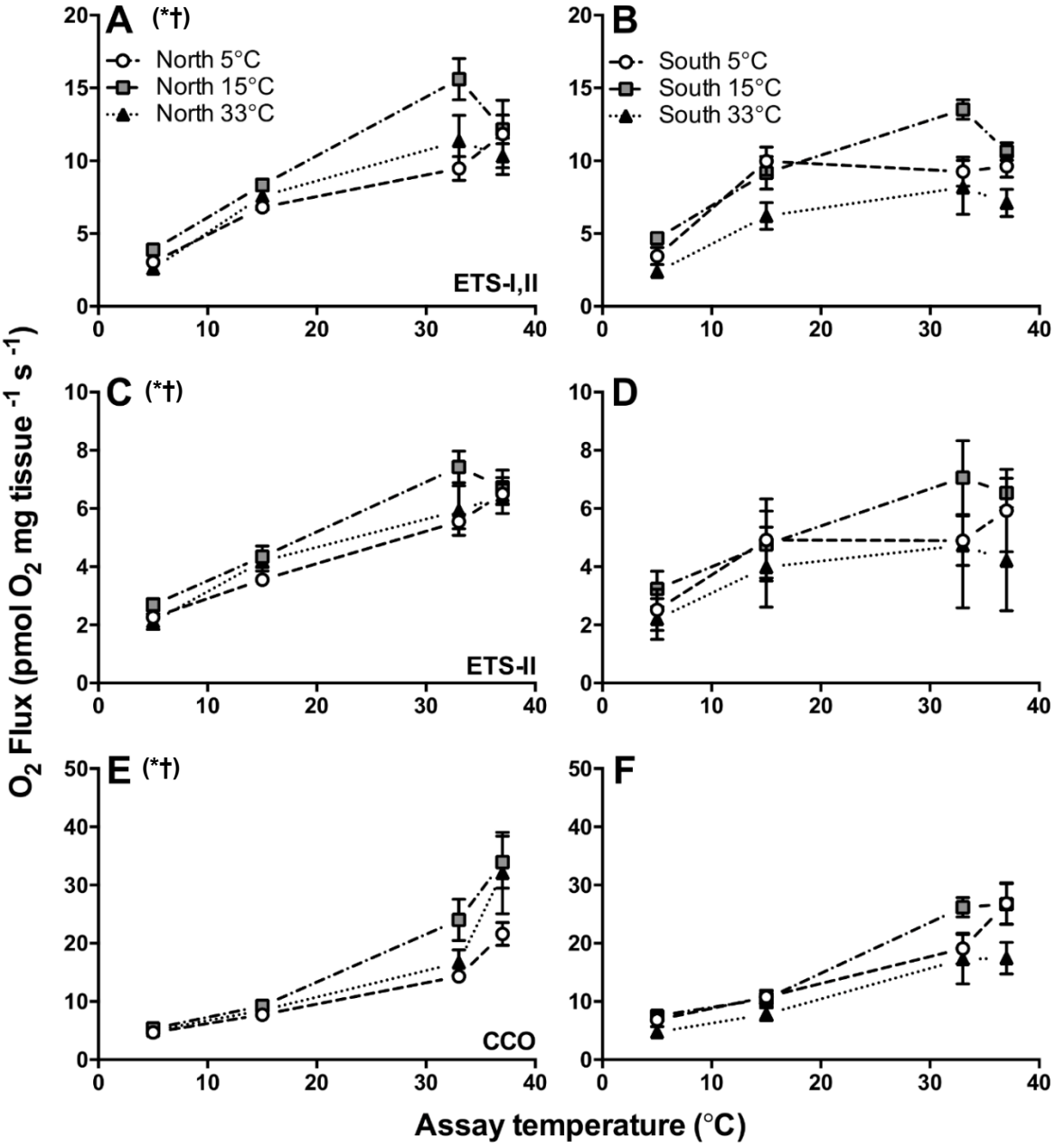

Figure 5.3. Maximum heart mitochondrial substrate oxidation capacity (ETS) and apparent cytochrome c oxidase (CCO) capacity from northern and southern *Fundulus heteroclitus* acclimated to 5 (open circle), 15 (grey square) or 33 °C (black triangle) for 4 weeks. Substrate oxidation capacity was measured in northern (A,C,E) and southern (B,D,F) subspecies through ETS complexes I and II in tandem (A,B; pyruvate, malate, glutamate and succinate as substrates) or complex II alone (C,D; succinate as a substrate, rotenone as a complex I inhibitor). Data are means±SEM; see Table 5.1 for associated statistics (n=7–8). Symbols indicate significant main effects of assay temperature (*), and acclimation (†).

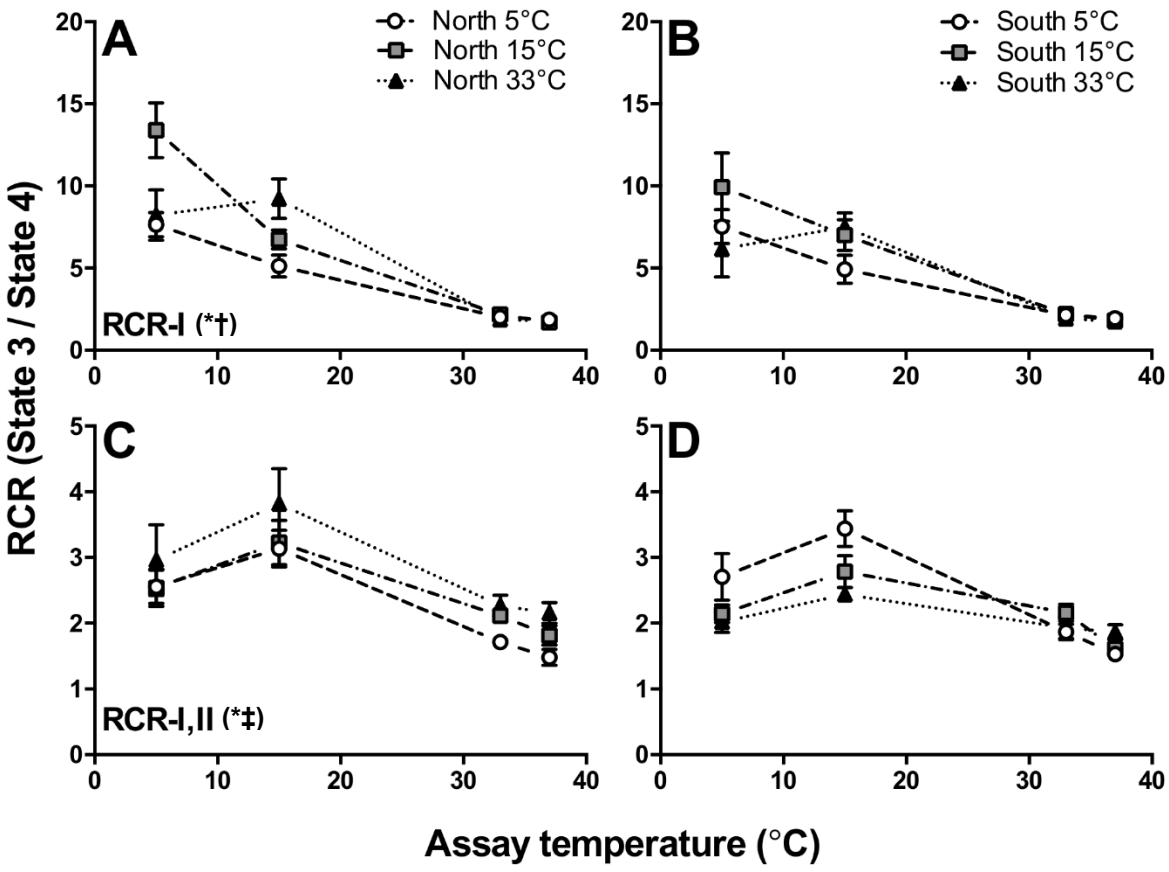

Figure 5.4. Heart respiratory control ratios (RCR; the ratio of state III to state IV respiration) from northern and southern *Fundulus heteroclitus* acclimated to 5 (open circle), 15 (grey square) or 33 °C (black triangle) for 4 weeks. Northern (A, C) and southern (B, D) *F. heteroclitus* RCR were calculated from respiratory states with flux through ETS complex I alone (A, B; pyruvate, malate, and glutamate as substrates) or complexes I and II in tandem (C, D; complex I substrates and succinate). Data are means±SEM; see Table 5.1 for associated statistics (n=7–8). Symbols indicate significant main effects of assay temperature (*), and acclimation (†).

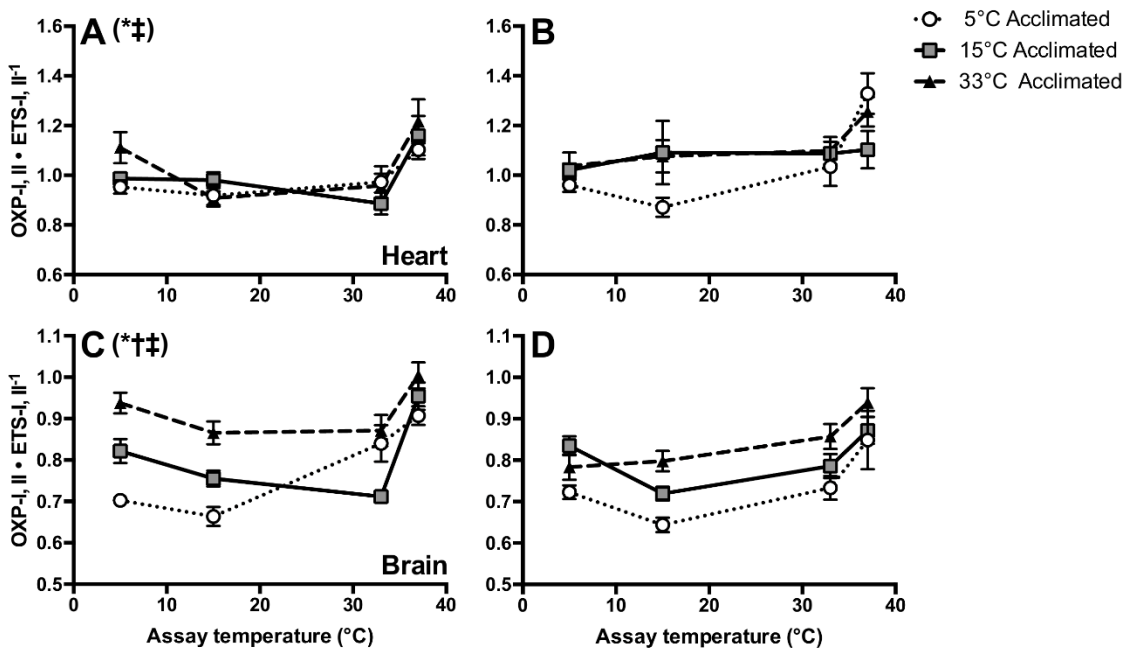

Figure 5.5. Limitations on killifish (*Fundulus heteroclitus*) mitochondrial oxidative phosphorylation capacity (OXP) by substrate oxidation capacity (ETS). Northern (A, C) and southern (B, D) Atlantic killifish were acclimated for four weeks at 5 (open circle), 15 (grey square) and 33 °C (black triangle). Heart (A, B) and brain (C, D) mitochondrial respiration rates were measured through electron transport chain complexes I, and II in tandem (I, II; pyruvate, malate, glutamate and succinate as substrates). Data are mean ± SEM, see Table 5.1 (heart) and Table 5.2 (brain) for associated statistics (n = 7-8). Ratio values greater than one (as observed in the heart) are likely due to the partial inhibition of ETS capacity by FCCP, an effect that has been previously demonstrated (Iftikar and Hickey, 2013). Symbols indicate significant main effects of assay temperature (*), acclimation (†), and subspecies (‡).

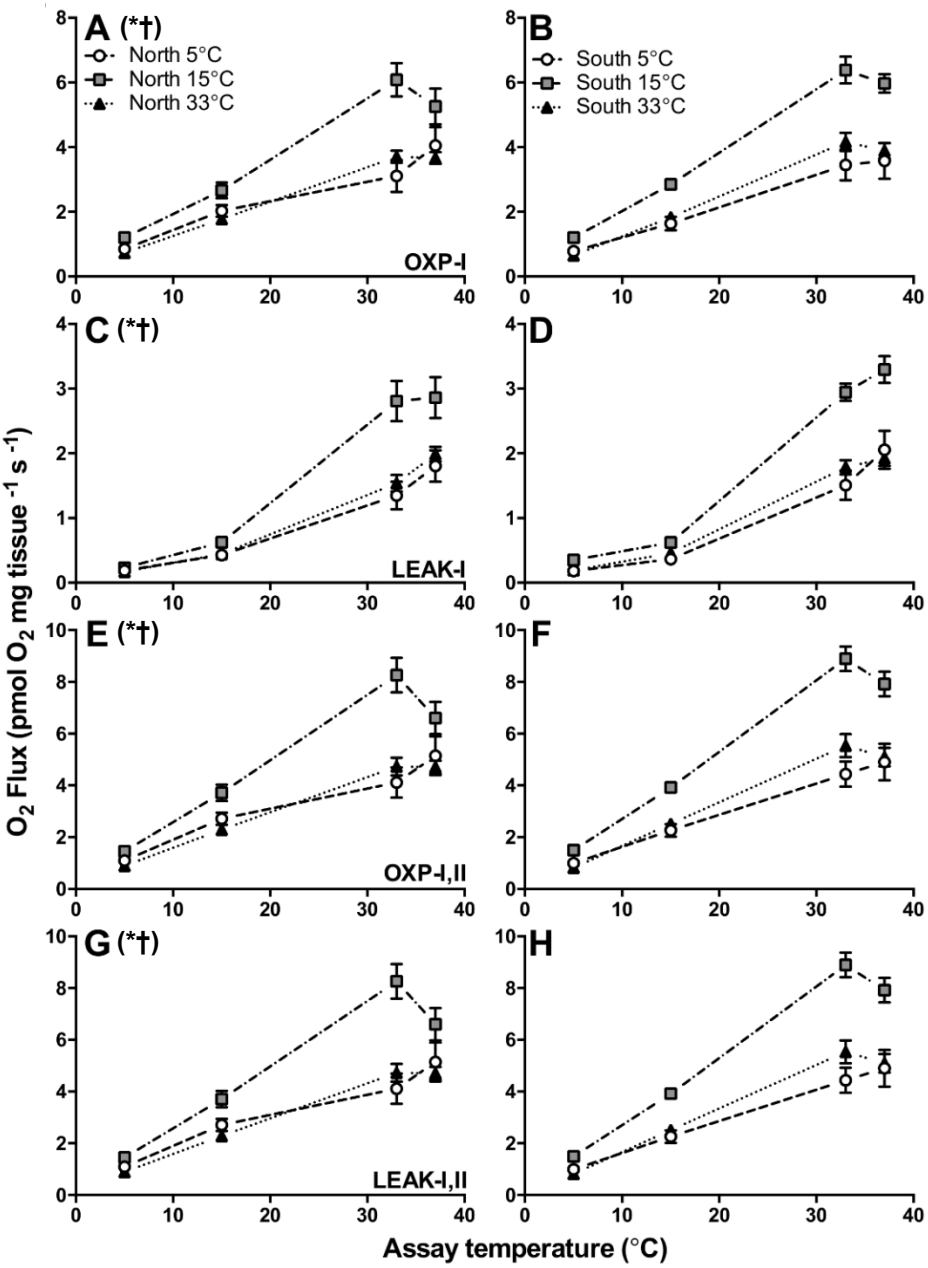

Figure 5.6. Coupled brain mitochondrial respiration from northern and southern killifish acclimated to 5 (open circle), 15 (grey square) or 33 °C (black triangle) for 4 weeks. Permeabilized brain preparations from northern (A, C, E, G) and southern (B, D, F, H) subspecies were subjected to a substrate uncoupler inhibitor titration protocol. Oxidative phosphorylation (OXP; A, B, E, F; state III) and LEAK (C, D, G, H; state II or IV) respiration were measured through ETS complexes I (A–D; pyruvate, malate and glutamate as substrates) and complexes I and II in tandem (E–H; complex I substrates and succinate). Data are means±SEM; see Table 5.2 for associated statistics (n=7–8). Symbols indicate significant main effects of assay temperature (*), and acclimation (†).

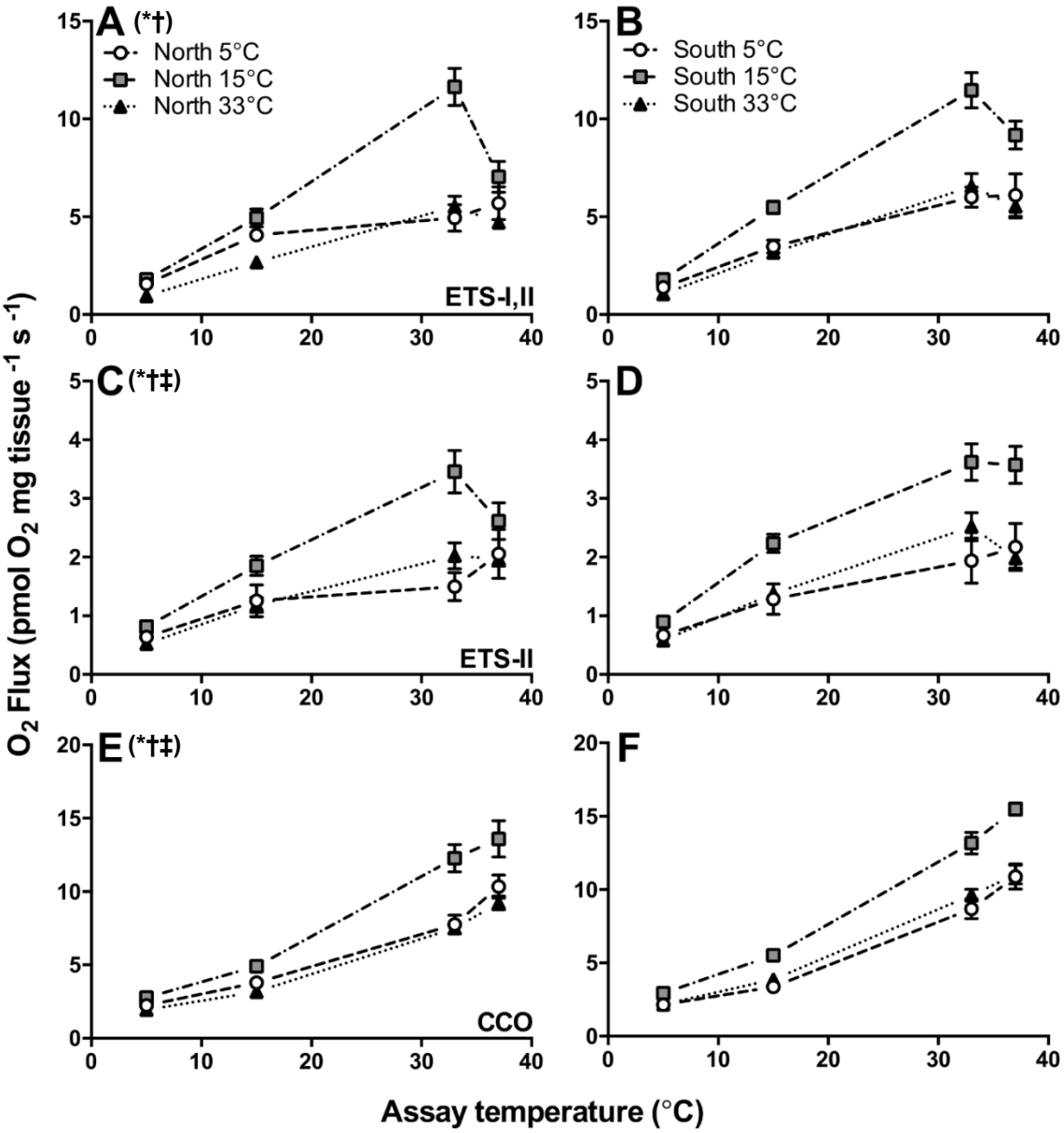

Figure 5.7. Maximum brain mitochondrial substrate oxidation capacity (ETS) and apparent CCO capacity from northern and southern *Fundulus heteroclitus* acclimated to 5 (open circle), 15 (grey square) or 33 °C (black triangle) for 4 weeks. Substrate oxidation capacity was measured in northern (A, C, E) and southern (B, D, F) subspecies through ETS complexes I and II in tandem (A, B; pyruvate, malate, glutamate and succinate as substrates) or complex II alone (C, D; succinate as a substrate, rotenone as a complex I inhibitor). Data are means±SEM; see Table 5.2 for associated statistics (n=7–8). Symbols indicate significant main effects of assay temperature (*), acclimation (†), and subspecies (‡).

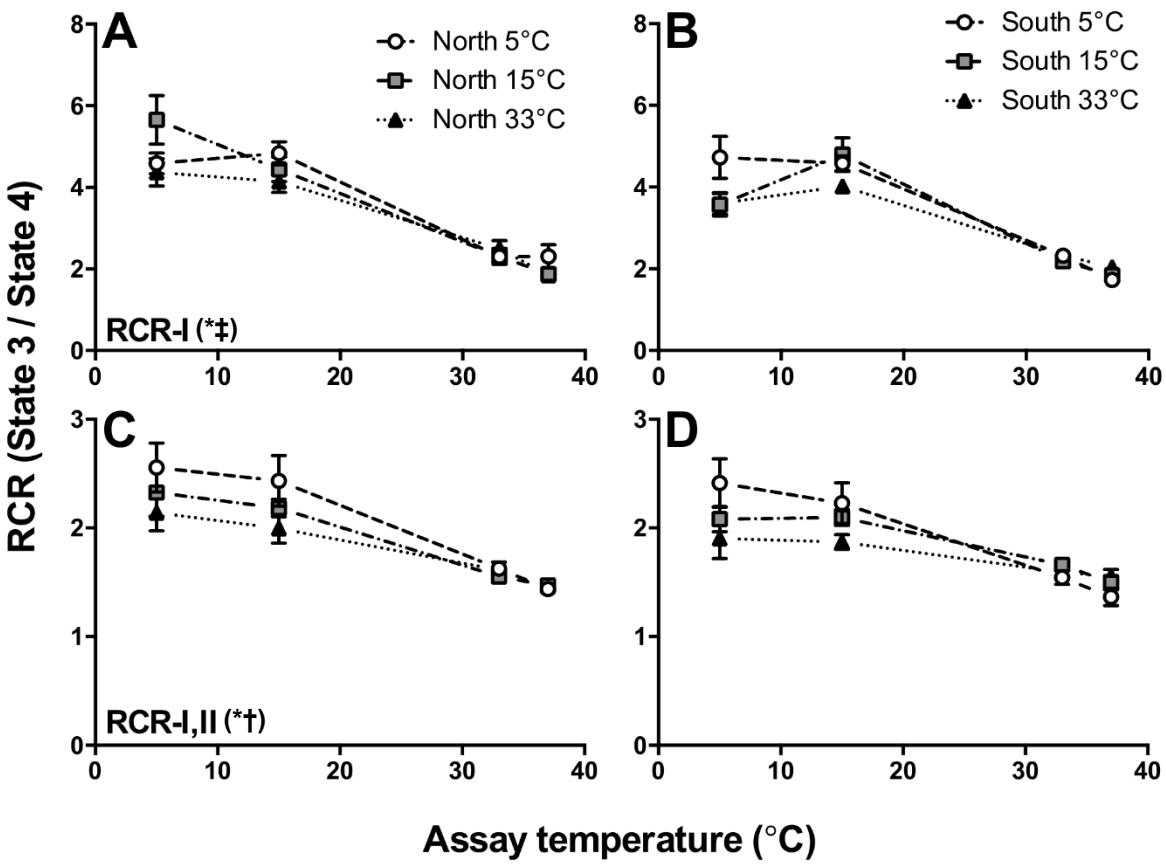

Figure 5.8. Brain RCR (the ratio of state III to state IV respiration) from northern and southern *Fundulus heteroclitus* acclimated to 5 (open circle), 15 (grey square) or 33 °C (black triangle) for 4 weeks. Northern (A, C) and southern (B, D) *F. heteroclitus* RCR were calculated from respiratory states with flux through ETS complex I alone (A, B; pyruvate, malate, and glutamate as substrates) or complex I and II in tandem (C, D; complex I substrates and succinate). Data are means±SEM; see Table 5.2 for associated statistics (n=7–8). Symbols indicate significant main effects of assay temperature (*), acclimation (†), and subspecies (‡).

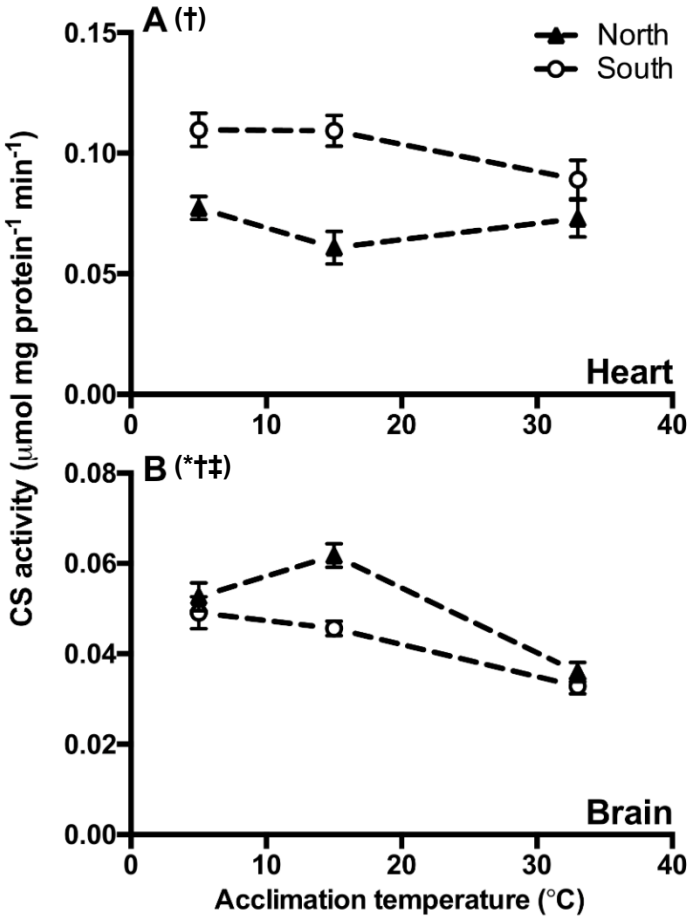

Figure 5.9. Whole heart and brain citrate synthase (CS) activity. Northern (black triangle) and southern (open circle) *Fundulus heteroclitus* were acclimated to 5, 15 and 33 °C for 4 weeks. Data are means±SEM; see Results for associated statistics (n=7). Symbols indicate significant main effects of acclimation (*), subspecies (†), and the interaction between acclimation and subspecies (‡).

Table 5.1. P-values for three-way ANOVAs of *Fundulus heteroclitus* heart mitochondrial parameters

	p-values						
Parameter	Subspecies	Acclimation temperature	Assay temperature	Subspecies* Acclimation	Subspecies* Assay	Acclimation*Assay	Subspecies*Acclimation* Assay
OXP-I	.522	**< .001**	**< .001**	.159	.516	**< .05**	.969
LEAK-I	.362	**< .001**	**< .001**	.103	.329	**< .01**	.234
OXP-I, II	.532	**< .001**	**< .001**	.078	**< .05**	.076	.924
LEAK-I, II	.884	**< .001**	**< .001**	.607	.100	**< .001**	.949
ETS- I, II	.058	**< .001**	**< .001**	.086	**< .05**	**< .05**	.832
ETS-II	.182	**< .001**	**< .001**	.051	**< .01**	.079	.742
CCO	.716	**< .001**	**< .001**	**< .05**	**< .05**	.239	.259
RCR-I	.776	**< .01**	**< .001**	.540	.129	**< .001**	.704
RCR-I, II	**< .01**	.464	**< .001**	**< .005**	.341	.241	.561
OXP-I, II/ ETS-I, II	**< .01**	.065	**< .001**	.912	.155	.213	.103

Significant *p*-values are in bold. OXP: oxidative phosphorylation, ETS: maximum mitochondrial substrate oxidation capacity, CCO: apparent cytochrome *c* oxidase capacity, RCR: respiratory control ratio (OXP/LEAK), I: flux fueled through ETS complex-I, II: flux fueled through ETS complex II; n = 7-8.

Table 5.2. P-values for three-way ANOVAs of *Fundulus heteroclitus* brain mitochondrial parameters

	p-values						
Parameters	Subspecies	Acclimation temperature	Assay temperature	Subspecies* Acclimation	Subspecies* Assay	Acclimation* Assay	Subspecies*Acclimation* Assay
OXP-I	.605	**< .001**	**< .001**	.351	.736	**< .001**	.876
LEAK-I	.200	**< .001**	**< .001**	.741	.685	**< .001**	.889
OXP-I, II	.221	**< .001**	**< .001**	.245	.498	**< .001**	.894
LEAK-I, II	.221	**< .001**	**< .001**	.831	.822	**< .001**	.767
ETS- I, II	.087	**< .001**	**< .001**	.660	.326	**< .001**	.577
ETS-II	**< .05**	**< .001**	**< .001**	.542	.694	**< .001**	.592
CCO	**< .005**	**< .001**	**< .001**	.218	.132	**< .001**	.955
RCR-I	**< .001**	.058	**< .001**	.475	**< .05**	.178	**< .01**
RCR-I, II	.116	**< .05**	**< .001**	.827	.345	**< .05**	.981
OXP-I, II/ ETS-I, II	**< .005**	**< .001**	**< .001**	.079	.411	**< .005**	**< .05**

Significant *p*-values are in bold. OXP: oxidative phosphorylation, ETS: maximum mitochondrial substrate oxidation capacity, CCO: apparent cytochrome *c* oxidase capacity, RCR: respiratory control ratio (OXP/LEAK), I: flux fueled through ETS complex-I, II: flux fueled through ETS complex II; n = 7-8.

Chapter 6 General conclusion

The objective of my doctoral research was to characterize the mitochondrial responses and putative trade-offs associated with thermal variation across multiple timescales, including rapid *in vitro* responses to acute temperature change, longer-term acclimation responses to changes at seasonal scales, and long-term evolutionary responses associated with differentiation between subspecies. I addressed this objective using two subspecies of Atlantic killifish (*Fundulus heteroclitus* Linneaus 1766) acclimated to a range of temperatures representative of the majority of this species' thermal breadth. The results of Chapters 2 and 3 demonstrated that liver mitochondrial respiratory capacity, kinetic properties (i.e., mitochondrial O_2 binding affinity) and mitochondrial membrane composition vary in response to thermal acclimation and between subspecies, putatively due to local adaptation, and are largely consistent with variation in whole-organism thermal performance. Chapters 4 and 5 showed that plasticity of mitochondrial respiratory capacity following thermal acclimation was not associated with a loss of proton motive force or increased ROS production during acute thermal shifts and that thermal acclimation and local adaptation effects on mitochondrial function vary among metabolically active tissues. The results presented in this thesis represent one of the most in-depth investigations of mitochondrial responses to thermal variation across biological timescales and support the importance of mitochondrial function in shaping organisms' responses to thermal variation, which has implications for species' distributions and abundance.

In this chapter, I provide a summary of my major findings and place them within the broader context of what we know about mitochondrial mechanisms associated with thermal stress and where these responses fit into the organisms' integrated response to environmental variation. Where appropriate, I identify areas of future research that I believe are the most promising for advancing our understanding of the role of the mitochondrion in organisms' responses to thermal variation.

6.1 Thermal acclimation effects on mitochondrial function

High temperature acclimation is often predicted to decrease mitochondrial respiratory capacity to offset thermodynamic effects and decrease oxidative damage (Abele et al., 2002; Hochachka and Somero, 2002). My assessments of thermal acclimation effects (33 °C) on

mitochondrial respiratory capacity across tissues and respiratory states were largely consistent with this prediction (Chapters 2, 4 and 5). Indeed, similar thermal acclimation effects following high temperature acclimation are known to occur in other ectotherms (Baris et al., 2016b; Guderley and Johnston, 1996; Khan et al., 2014; Lannig et al., 2005; Strobel et al., 2013), suggesting that decreasing mitochondrial capacity can act to offset high temperature effects on biochemical performance.

In contrast to my findings, in a previous study, *F. heteroclitus* acclimated to a slightly lower temperature (25 °C) did not exhibit a comparable decrease in liver mitochondrial respiratory capacity relative to fish acclimated to lower temperatures (Fangue et al., 2009). There are three potential reasons for the inconsistency between my results and those of Fangue et al. (2009). The first is technical; Fangue et al. (2009) excluded mitochondrial preparations with respiratory control ratios lower than four when assayed at the fish's acclimation temperature (e.g., 25 °C acclimated fish assay at 25 °C). The rationale for setting this cutoff is well-intentioned, as low RCRs are indicative of poorly coupled mitochondria; in this case, presumably due to uncoupling associated with mitochondrial isolation (Brand and Nicholls, 2011). But setting this threshold may have excluded samples that exhibited a lower RCR due to real biological effects. Indeed, I repeatedly demonstrated that acute thermal shifts toward high temperatures (33 °C and higher) decreased RCR across all of my treatments (Chapters 2, 4, and 5) and I argued that this decline was a consequence of decreased state 3 respiration rates (Guderley, 2004). Thus, fish that are acclimated and assayed at high temperatures are more likely to be excluded based on acute temperature effects on mitochondrial performance as opposed to uncoupling induced by isolation technique. The second potential reason for the inconsistency between these studies is the choice of sample populations used to represent northern and southern *F. heteroclitus* subspecies. Indeed, significant genetic variation exists among populations of each *F. heteroclitus* subspecies, raising the possibility that individual populations employ unique modifications of mitochondrial function following thermal acclimation (McKenzie et al., 2016; Reid et al., 2016; Whitehead, 2009). However, Baris et al. (2016b) demonstrate effects that are similar to my own while using different populations of *F. heteroclitus,* lending support to the differences among these studies being a consequence of technical variation. A third possibility is that acclimation to 25 °C is not sufficiently stressful for *F. heteroclitus* to mount a response at the mitochondrial level. There is some evidence for

acclimation to 25 °C not being as stressful as acclimation to 33 °C as *F. heteroclitus* can maintain aerobic scope at the lower of these temperatures (Healy and Schulte, 2012).

Acclimation to low temperatures increased liver mitochondrial respiratory capacity (Chapters 2 and 4), a modification that is consistent with predicted responses to decreasing temperature (Guderley, 2004). But the magnitude of observed low-temperature compensation of mitochondrial respiratory capacity is small relative to low-temperature acclimation effects in other species. For example, *F. heteroclitus*' state 3 respiration increases by approximately 30% (Chapter 2, complex I substrates, assay temperature = 15 °C) following cold-acclimation whereas state 3 respiration increases by as much as 75 and 80% in *Carassius auratus* (Dos Santos et al., 2013, complex II substrates, assay temperature = 25 °C) and *Oncorhynchus mykiss* (Kraffe et al., 2007, complex I substrates, assay temperature = 5 °C) respectively. This seemingly limited compensation of mitochondrial capacity in *F. heteroclitus* might be offset through variation in other mitochondrial properties, such as increased mitochondrial volume density (Dhillon and Schulte, 2011). Alternatively, the inconsistency between my observed low-temperature acclimation effects and those in the literature might be a consequence of experimental design. As discussed in Chapter 4, studies of mitochondrial responses to thermal acclimation often only utilize two acclimation temperatures. These experiments have the potential to misrepresent the magnitude of thermal acclimation effects. Indeed, if I had limited my thermal acclimation treatments to 5 and 33 °C, I might have concluded that my low temperature treatment results in a large compensation of mitochondrial function (over 300%, Chapter 2, complex I substrates, assay temperature = 15 °C). These data highlight the need for carefully designed experiments, especially when using an organism that is as eurythermal as *F. heteroclitus.*

In contrast to liver mitochondrial responses to low-temperature acclimation, both the heart and brain decreased respiratory capacity following 5 °C acclimation (Chapters 2 and 5). It is perhaps unsurprising that mitochondrial responses to thermal stress vary across diverse tissue types given the multiple roles that mitochondria can fill (McBride et al., 2006) and the diverse physiological functions of different tissues. Decreased heart and brain mitochondrial function associated with low temperature acclimation might represent the induction of a partial metabolic suppression (Guderley, 2004; Richards, 2010). Indeed, there is some evidence for these effects as

routine metabolism declines in 5 °C acclimated *F. heteroclitus* when compared to 15 °C acclimated fish (Healy and Schulte, 2012).

It is possible that my observed thermal acclimation effects on mitochondrial function are also associated with shifts in the organisms' metabolic status (Guderley, 2004). Indeed, increasing acclimation temperature decreased whole-organism and tissue mass (Chapters 2, 4, and 5). Increased mass following low temperature acclimation may be a consequence of low metabolic demand and the ability to lay down energy stores. In contrast, decreased mass following high temperature acclimation might represent the onset of sub-lethal temperature stress. I attempted to control for the potential interaction between acclimation temperature and organisms' metabolic status by feeding once daily to satiation. But it is important to acknowledge that thermal acclimation responses do not occur in a vacuum and seasonal changes in temperature are associated with cycles of food availability and reproduction. While attempts should be made to control for these confounding factors, new and potentially ecologically relevant effects of thermal variation might be uncovered. For example, the ability to ingest greater amounts of food during high temperature acclimation is positively correlated with mitochondrial proton leak in *Salmo trutta* (Salin et al., 2016).

In contrast to the considerable remodeling of liver mitochondrial respiratory capacity that I observed (Chapters 2, 4), there was limited plasticity of mitochondrial membrane potential and reactive O_2 species production following thermal acclimation (Chapter 4). These results are consistent with *F. heteroclitus* altering mitochondrial function to offset putative deleterious processes associated with temperature shifts. The maintenance of mitochondrial membrane potential across these thermal acclimation treatments might be achieved through mitochondrial remodeling as described in Chapter 2. Furthermore, these data are consistent with *F. heteroclitus*' maintenance of aerobic metabolism over a similarly large thermal acclimation range (Healy and Schulte, 2012). These patterns were only investigated in the northern subspecies, and it is possible that these metrics differ in the southern subspecies.

Overall, my results are consistent with a role for mitochondrial function in the thermal acclimation response and indicate that mitochondrial remodeling can occur without a significant loss of membrane potential or increased ROS production. These responses likely underlie the eurythermal nature of *F. heteroclitus* and may be a response that is shared among eurythermal ectotherms. The expression of a broad acclimation capacity with limited putative trade-offs

might represent a successful strategy for life in environments that undergo considerable seasonal variation.

6.2 Intraspecific variation of mitochondrial function

One of the most important findings of my thesis was my demonstration of intraspecific variation in *F. heteroclitus* liver mitochondrial function (Chapters 2, 3, and 5). Northern *F. heteroclitus* exhibited greater mitochondrial respiratory capacity when compared to their southern counterparts (Chapter 2). This variation in mitochondrial respiratory capacity is consistent with whole-organism variation in aerobic metabolism (Healy and Schulte, 2012). In addition, southern *F. heteroclitus* exhibited greater mitochondrial O_2 binding affinity when compared with their northern counterparts (Chapter 3), which is consistent with subspecies variation in whole-organism upper-thermal tolerance and hypoxia tolerance. However, intraspecific variation in mitochondrial function was specific to liver mitochondria and was not consistently observed in mitochondria from the heart and brain (Chapter 5). This tissue-specific subspecies variation in mitochondrial function highlights the complexity of mitochondrial regulation within the context of putative local adaptation.

Previous attempts to demonstrate intraspecific variation in *F. heteroclitus* mitochondrial performance have had mixed success (e.g., Baris et al., 2016b; Fangue et al., 2009). The inconsistency among these studies and my data could be due to the choice of the sample population, as there is significant genetic variation within *F. heteroclitus* subspecies (McKenzie et al., 2016; Reid et al., 2016; Whitehead, 2009). The existence of multiple *F. heteroclitus* populations raises an important issue as my demonstration of intraspecific variation in mitochondrial function could be a consequence of using two *F. heteroclitus* populations from the extreme ends of the species distribution, perhaps representing a two-point correlation. Correlations among a limited number of groups can be problematic as they are prone to sampling bias. Due to the design of my experiments, I cannot account for this potential bias. But as a first step, I have been able to identify a signature of a correlation between mitochondrial function and whole-organism aerobic performance. Thus, future experiments should incorporate multiple populations to avoid this issue.

The effects of thermal acclimation on mitochondrial function did not differ between *F. heteroclitus* subspecies (Chapters 2, 3, and 5), indicating that the overall thermal acclimation

response is conserved. Although the direction of thermal acclimation responses is the same between *F. heteroclitus* subspecies, the thermal sensitivity of this response was greater in the northern subspecies, which might reflect the need for additional plasticity or capacity in environments with greater environmental variation (i.e., seasonal variation at higher latitudes). Alternatively, the southern subspecies may exhibit lower mitochondrial acclimation capacity in exchange for greater upper thermal tolerance limits (Somero, 2005; Stillman, 2003). *F. heteroclitus* from northern latitudes are considered to be the derived form of the species (Brown and Chapman, 1991; Crawford et al., 1999). Thus any divergence in thermal acclimation responses between the subspecies is potentially a consequence of the thermal variability associated with life in northern latitudes. Overall, these data agree with predicted evolutionary responses to life in cold environments (Guderley, 2004).

My data support a role for selection acting on mitochondrial function in *F. heteroclitus* and may reflect a general target of selection in response to thermal variation. There is considerable interest in the role of mitochondrial function in evolutionary adaptation (Ballard and Pichaud, 2014; Ballard and Whitlock, 2004; Dowling et al., 2008; James et al., 2016; Wolff et al., 2014) and some of this interest stems from the mitochondrion's position as a hub for metabolic processes (Marden, 2013). Key mitochondrial oxidative phosphorylation enzymes are composed of subunits encoded by both the nuclear and mitochondrial genomes, which exhibit different rates of mutation and mechanisms of inheritance. As a result, interactions between mitochondrial and nuclear genomes are suggested to be a key factor in shaping organisms' performance and ultimately fitness (e.g., Ballard et al., 2007).

6.3 Tissue variation in mitochondrial responses to thermal acclimation and local adaptation

Data from Chapters 2, 4 and 5 demonstrate that mitochondrial responses to thermal acclimation and subspecies variation are tissue dependent. Indeed, modifications to liver mitochondrial respiratory capacity following thermal acclimation were consistent with compensation of thermodynamic effects on biochemical reaction rates. Also, liver mitochondrial capacity was greater in the northern subspecies which is consistent with intraspecific variation in whole-organism aerobic metabolism and perhaps thermal tolerance (Fangue et al., 2006; Healy and Schulte, 2012). In contrast, heart and brain mitochondrial function decreased in response to 5

and 33 °C acclimation and did not differ between *F. heteroclitus* subspecies (Chapter 5), perhaps revealing a suppression of metabolism associated with thermal acclimation as discussed previously.

Tissue-specific mitochondrial responses to temperature variation have been observed in other ectotherms (Trzcionka et al., 2008; Yan and Xie, 2015) and this variation is likely due to each tissue's *in vivo* function. Indeed, the liver regulates whole-organism metabolism and is involved in both catabolic and anabolic processes. Thus, environmental variation that alters the metabolic status of the organism is likely to be reflected in liver mitochondrial performance (e.g., diabetes; Ferreira et al., 2003). Organ systems involved in O_2 delivery (i.e., cardiac system; Iftikar and Hickey, 2013; Pörtner, 2001) or coordinating whole-organism function (i.e., neural system; Ern et al., 2015; Stillman and Somero, 1996) are theorized to constrain whole-organism thermal tolerance limits. Thus, my results appear to support a limited role for heart and brain mitochondrial function in contributing to organism level aerobic metabolism and thermal tolerance.

It is possible that the absence of clear links between heart and brain mitochondrial function and whole-organism performance is a consequence of only comparing mitochondrial respiratory capacity. Although respiratory capacity is a good index of variation in mitochondrial performance (Brand and Nicholls, 2011) other aspects of mitochondrial function might better predict temperature-induced declines in tissue or organism-level performance (e.g., ATP synthesizing capacity; Iftikar and Hickey, 2013). Similarly, limitations on thermal tolerance imposed by the heart and brain might be a consequence of effects on other parts of the cell or tissue-level function (e.g., action potentials and ion balance).

Many biological mechanisms might account for tissue-specific variation in mitochondrial responses to thermal variation. One candidate mechanism is tissue-specific mitochondrial subunit isoforms, which can confer variation in mitochondrial performance among tissues (Arnold, 2012; Benard et al., 2006; Guerrero-Castillo et al., 2017; Rossignol et al., 2000). In addition, tissue-specific mitochondrial membrane composition (Heim et al., 2017), proteomes (Forner et al., 2006) and post-translational modification patterns (e.g., phosphorylation; Bak et al., 2013) all theoretically contribute to this variation. But our understanding of the regulation and plasticity of these mechanisms and their physiological relevance within the context of temperature responses remains limited, and thus represent important avenues for future research.

An alternative explanation for the variable thermal acclimation and intraspecific effects among tissues could be the methodology I employed. Heart and brain mitochondrial performance were assessed using a permeabilized tissue preparation (Kuznetsov et al., 2008), while liver mitochondrial performance was assessed using an isolated mitochondrial preparation (Fangue et al., 2009). The justification for using either of these techniques is largely one of practicality (e.g., permeabilized tissue preparations require small biological samples). But there is some suggestion that the tissue permeabilization technique reverses functionally relevant mitochondrial modifications (Mathers and Staples, 2015). It is possible that similar phenomena influenced my observed tissue-specific variation in thermal acclimation and subspecies mitochondrial responses.

At the broadest level, my data support the existence of tissue variation in mitochondrial performance (Benard et al., 2006). The identity of the organ system responsible for setting thermal tolerance limits is not something that my data can address directly. Nevertheless, the inconsistent thermal acclimation and intraspecific effects on mitochondrial function across tissues might point toward a greater relative importance of some tissue systems in shaping whole-organism thermal tolerance limits (e.g., circulatory and neural; Ern et al., 2015; Pörtner, 2001). The large effects of thermal acclimation and intraspecific variation on liver mitochondrial function might reflect the considerable metabolic adjustments that occur following thermal stress, and that the ability to draw on this capacity is associated with the eurythermal phenotype.

6.4 Mechanisms underlying variation in mitochondrial performance

In Chapter 2 I demonstrated that mitochondrial membrane composition varies in response to thermal acclimation and intraspecific variation. Remodeling of mitochondrial membranes in response to temperature variation is suggested as a mechanism to maintain membrane fluidity (Guderley, 2004; Hazel, 1995; Hochachka and Somero, 2002). In contrast to this prediction, the largest changes in mitochondrial membranes were consistent with a targeted remodeling of the membrane and not with changes in properties that are suggested to alter membrane fluidity (e.g., double-bond index, FA unsaturation index). Admittedly, I did not assess variation in mitochondrial membrane fluidity among my treatments, and it is likely that this property nevertheless varies (e.g., Dahlhoff and Somero, 1993). My observed shifts in mitochondrial

membrane lipids are thus largely consistent with shifts in *F. heteroclitus*' metabolism following thermal stress.

In addition to potentially reflecting shifts in the metabolic status of thermally acclimated *F. heteroclitus* subspecies, the variation in mitochondrial membrane lipids that I observed could reflect changes in lipid-protein interactions (Contreras et al., 2011). Indeed, the presence of nonannular lipids and annular lipid shells (phospholipid species preferentially binding with proteins) are critical for the activity of membrane-bound mitochondrial enzymes (Contreras et al., 2011). But these interactions are enzyme-specific as Wodtke et al. (1981a) concluded that total membrane fluidity and not annular lipid interactions contributes to variation in COX activity following thermal acclimation. In contrast, Lau et al. (2017) suggest that interspecific variation in interactions between cardiolipin binding and COX3 subunits alters mitochondrial O_2 binding affinity. The identity of the specific cardiolipin species specifically bound to *F. heteroclitus* COX is unknown; but Shinzawa-Itoh et al. (2007) suggest that tetra-linoleate (18:2) cardiolipin species are critical to the stability of bovine COX enzymes. My data from Chapter 2 demonstrate that the relative quantity of this cardiolipin species is altered following thermal acclimation, which suggests a role for nonannular phospholipids in altering COX function. The involvement of lipid-protein interactions in altering *F. heteroclitus* mitochondrial function might also extend to the formation of respiratory supercomplexes (Dudkina et al., 2010). These associations of mitochondrial electron transport system complexes are thought to enhance electron flux and decrease reactive O_2 species production. But mitochondrial supercomplexing cannot occur in the absence of cardiolipin (Zhang et al., 2002). Thus, variation in mitochondrial membrane properties likely occurs as a response to thermal variation in *F. heteroclitus* and investigating lipid-protein, and mitochondrial supercomplexing represents a necessary continuation of my research.

Variation in mitochondrial membrane composition could also reflect altered mitochondrial quantity and inner-mitochondrial membrane topology. Indeed, low-temperature acclimation is associated with increased mitochondrial quantity, and this is true for *F. heteroclitus* (Dhillon and Schulte, 2011). But the role of mitochondrial membrane composition in shaping inner-mitochondrial membrane topology is not nearly as well understood (Mannella, 2006). Folding of mitochondrial membranes is suggested to enhance mitochondrial function through increased membrane surface area and the formation of membrane micro-domains. This

membrane folding is thought to be enhanced by protein interactions, such as dimers of the ATP synthase which induce bends in the inner-mitochondrial membrane (Minauro-Sanmiguel et al., 2005). The physiological relevance of altering inner mitochondrial membrane structure as a response to environmental stress is not well understood and could have a profound influence on mitochondrial performance perhaps through effects on mitochondrial reticula (Glancy et al., 2015) which may influence the local distribution of the mitochondrial proton motive force and cellular O_2 diffusion gradients.

The use of specific substrates and inhibitors allowed me to investigate the effects of thermal acclimation and intraspecific variation on individual electron transport system enzymes. Thermal acclimation effects on mitochondrial respiratory capacity were largely associated with upstream electron transport system enzymes (i.e., complex I and II; Chapters 2, and 4). The activity of these mitochondrial enzymes can be altered through several mechanisms. Indeed, my demonstration of mitochondrial membrane remodeling represents one such mechanism (Chapter 2). Within the last decade, post-translational modifications of mitochondrial enzymes (e.g., phosphorylation, acetylation, and methylation) have emerged as a mechanism that likely regulates mitochondrial function (Carroll et al., 2005; Hofer and Wenz, 2014; Kulkarni and Cantó, 2017). But investigating the involvement of these mechanisms in non-model organisms can be difficult due to the transience of these effects and a relative lack of supporting molecular tools (e.g., Chung et al., 2013). As the understanding of these mechanisms and the associated tools improve over time (e.g., mass-spectrometry) I expect that the importance of mitochondrial post-translational modifications as a response to environmental stress will be revealed.

Intraspecific variation of mitochondrial respiratory capacity and O_2 binding affinity was associated with modifications to cytochrome *c* oxidase (Chapters 2 and 3). This variation in COX performance could be due to post-translational modification and mitochondrial membrane composition as described previously. Alternatively, subspecies-specific COX performance could be due to the expression of subspecies-specific isozymes of electron transport system complexes. But the existence of functionally relevant variation in these enzymes among *F. heteroclitus* populations remains equivocal (Baris et al., 2017; Reid et al., 2016). There is, however, evidence of fixed amino acid polymorphisms for mitochondrially encoded electron transport system enzymes among *F. heteroclitus* populations (Whitehead, 2009). Thus, a comprehensive

investigation of sequence variation in nuclear-encoded mitochondrial genes among *F. heteroclitus* populations is warranted.

6.5 Do killifish get to have their temperature cake and eat it?

Maintaining a broad thermal performance window is thought to be energetically costly, resulting in constraints on maximum thermal performance (i.e., an allocation trade-off; Angilletta, 2009; Huey and Hertz, 1984). This specialist-generalist trade-off is suggested to occur due to thermodynamic effects on enzyme function (Hochachka and Somero, 2002). But investigations of these effects at the whole animal level have shown that some species can maintain wide thermal performance windows and acclimation capacity while also exhibiting relatively high maximum thermal performance (Huey and Hertz, 1984; Tepolt and Somero, 2014). My data demonstrate that a similar "jack-of-all-temperatures is a master of all" effect occurs at the level of the mitochondrion (Chapters 2, 3, 4 and 5). Indeed, mitochondrial respiratory capacity is maintained at greater levels and over a wide range of assay temperatures in northern *F. heteroclitus* and fish acclimated to low temperatures (Chapter 2). At the whole-animal level, acute thermal performance curves for aerobic scope are not clearly different between *F. heteroclitus* subspecies, suggesting that this 'master of all' phenomenon may extend across multiple levels of biological organization (Healy and Schulte, 2012).

The absence of clear allocation trade-offs on mitochondrial function might underlie the broad eurythermal physiology of *F. heteroclitus*. Alternatively, this apparent phenomenon might be due to the difficulty of detecting allocation trade-offs. Indeed, the fish used in my experiments were all sampled from wild populations, making it difficult to account for developmental and epigenetic effects. The role that these mechanisms play in shaping mitochondrial function is not something that I can account for and could mask predicted allocation trade-offs. Furthermore, allocation trade-offs might not be present in the mitochondrial properties that I assessed and may manifest in other aspects of mitochondrial physiology (e.g., ATP synthesis; Iftikar and Hickey, 2013). Taking an integrated view, it is possible that allocation trade-offs occur at other levels of biological organization (e.g., tissue-level performance) and the broad thermal performance at the mitochondrial level acts to compensate for these trade-offs allowing for sustained function at the whole-organism level (e.g., aerobic scope; Healy and Schulte, 2012).

6.6 Mitochondrial function as a constraint on acute thermal tolerance limits

One of the primary goals of my research was to identify the role that mitochondria play in shaping acute whole-organism thermal tolerance limits. I addressed this goal with the prediction that mitochondrial function declines at assay temperatures approaching whole-organism thermal tolerance limits (Pörtner, 2001). *F. heteroclitus*' upper thermal tolerance limits vary as a result of thermal acclimation and intraspecific variation (Fangue et al., 2009). Thus *F. heteroclitus* mitochondrial function was predicted to decline at assay temperatures ranging from 30 to 32 °C (northern and southern *F. heteroclitus* respectively acclimated to 5 °C) and up to 41 and 42 °C (northern and southern *F. heteroclitus* respectively acclimated to 33 °C). In contrast to this prediction, declines or plateaus in mitochondrial respiratory capacity did not consistently occur at assay temperatures that aligned with upper critical thermal tolerance limits (Chapters 2, 4 and 5). Indeed, declines in respiratory capacity occurred between 33 and 37 °C and did not demonstrate consistent variation in response to acclimation or between subspecies, an effect that has been noted previously (Fangue et al., 2009). It has been suggested that *in vitro*, mitochondria maintain function at temperatures that exceed whole-organism thermal tolerance limits (Hochachka and Somero, 2002). In contrast to this suggestion, 33 °C acclimated *F. heteroclitus* from both subspecies exhibited declining mitochondrial function at assay temperatures preceding upper thermal tolerance limits. This inconsistent relationship might indicate that mitochondrial function does not directly influence acute upper thermal tolerance in *F. heteroclitus*. Alternatively, whole-organism acute thermal tolerance limits might only be limited by mitochondrial function following acclimation to high temperatures.

It is unlikely that the previously described declines in mitochondrial respiratory capacity at high assay temperatures represent an experimental artifact, as this phenomenon occurred across a suite of respiratory states and tissues (Chapters 2, 4, 5; Fangue et al., 2009). Instead, these results point toward a general property of mitochondrial function in *F. heteroclitus*. Decreased mitochondrial function at high assay temperatures occurred under oxidative phosphorylation (OXP or state 3) and maximum substrate oxidation (ETS) capacity and not under leak respiration (LEAK or state 2 and 4) or for measurements of apparent cytochrome *c* oxidase capacity (CCO). This difference between the maximal temperatures for state 3 respiration and other respiratory states occurs in other aquatic ectotherms (Fangue et al., 2009; Hardewig et al., 1999; Heise, 2003; Pörtner et al., 1999). The absence of declining state 4

respiration at high assay temperatures in the face of declines in state 3 respiration indicates an increase in mitochondrial uncoupling, an effect that is reflected in my demonstration of decreased respiratory control ratios at high assay temperatures (33 to 37 °C). Increased mitochondrial uncoupling at high assay temperatures has been proposed as a mechanism constraining upper thermal tolerance limits (Guderley, 2004). But respiratory control ratios did not consistently differ among my thermal acclimation treatments or between *F. heteroclitus* subspecies. The functional relevance of respiratory control ratios as a true estimate of mitochondrial coupling is not settled (Brand and Nicholls, 2011; Gnaiger, 2014), with direct measures of mitochondrial proton motive force (often estimated as mitochondrial membrane potential) suggested as a more appropriate measure of proton conductance.

Given that I did not observe a clear link between mitochondrial respiratory capacity and acute upper thermal tolerance limits, I next investigated the effects of acute high temperature on *F. heteroclitus* mitochondrial proton motive force. The proton motive force is the source of potential energy for the ATP synthase and may thus better reflect energetic constraints imposed by high temperatures. I predicted that changes in proton motive force could account for the substantial plasticity of *F. heteroclitus* whole-organism thermal tolerance limits following thermal acclimation (Fangue et al., 2006). In contrast to this prediction, maximum mitochondrial membrane potential under ADP-phosphorylating conditions did not differ among acclimation treatments at high assay temperatures (Chapter 4) and thus does not appear to constrain upper thermal tolerance limits (i.e., between 33 and 37 °C; Chapter 4).

It is interesting to note that at high assay temperatures maximum membrane potential decreased (33 to 35 °C) and appeared to recover (35 to 37 °C) in fish acclimated to 5 and 15 °C. In contrast, fish acclimated to 33 °C exhibited a decline in maximum membrane potential with increasing assay temperature. The apparent recovery of mitochondrial membrane potential in 5 and 15 °C acclimated fish might reflect the regulation of mitochondrial membrane potential above a lower critical threshold. Indeed, mitochondrial depolarization results in the opening of the mitochondrial permeability transition pore leading to apoptosis *in vivo* (Crompton, 1999). Under conditions of environmental stress (e.g., anoxia or ischemia), mitochondrial membrane potential can be sustained through ATP consuming H^+ pumping via the ATP synthase (e.g., cellular treason in anoxia; St-Pierre et al., 2000a; Takeda et al., 2004). Although beneficial in the short term, this H^+ pumping cannot be sustained indefinitely due to the associated energetic cost.

Thus, the putative involvement of this response in 5 and 15 °C but not 33 °C acclimated fish might reflect a large ATP consuming process at high temperatures, resulting in an energetic imbalance and perhaps a constraint on aerobic metabolism. To my knowledge, the involvement of this mechanism has not been investigated within the context of thermal stress and represents a worthwhile line of future research.

Like maximum mitochondrial membrane potential, mitochondrial proton leak kinetics and ROS production did not differ among thermally acclimated Atlantic killifish at a high assay temperature (i.e., 33 °C; Chapter 4). Analysis of proton leak kinetic curves is thought to better reflect *in vivo* proton conductance when compared to leak respiration (i.e., state IV) and maximum membrane potential (Brand et al., 1999; Divakaruni and Brand, 2011). Thus, the absence of thermal acclimation effects on proton leak kinetic curves is consistent with mitochondrial performance not constraining acute thermal tolerance limits. It is possible that proton leak kinetics differ among thermal acclimation treatments at assay temperatures higher than 33 °C (e.g., 35 and 37 °C). I did not measure proton leak kinetics at these temperatures, and so I cannot account for the potential contribution of variation in sub-maximal proton conductance to acute thermal tolerance limits. But maximum mitochondrial membrane potential (under leak conditions) was lower in 33 °C acclimated fish when compared to 5 and 15 °C acclimated fish at 35 and 37 °C, indicating that proton leak kinetics might differ among thermal acclimation treatments at high assay temperatures. Although I did not detect thermal acclimation effects on proton leak kinetics or maximum mitochondrial membrane potential in northern *F. heteroclitus*, it is possible that thermal acclimation alters these parameters in southern *F. heteroclitus*, perhaps contributing to the setting of acute thermal tolerance limits in this subspecies.

Another property that might account for thermal acclimation effects and intraspecific variation in acute thermal tolerance is mitochondrial O_2 binding affinity, as this property is thought to alter mitochondrial O_2 extraction from the cellular environment (Gnaiger et al., 1998; Larsen et al., 2011). As assay temperature increased, mitochondrial O_2 binding affinity decreased (Chapter 3), perhaps representing a constraint on aerobic performance and thermal tolerance. But this does not necessarily account for thermal acclimation and intraspecific variation effects on acute thermal tolerance limits. Indeed, at high assay temperatures (33 to 37 °C) mitochondrial O_2 binding affinity was greatest in 15 °C acclimated fish, followed by 5 and 33 °C acclimated fish.

This inconsistency is largely due to the response of 33 °C acclimated fish, and I have discussed the potential confounding factors associated with this acclimation temperature (Chapters 2, 3, 4, and 5). Indeed, when thermally acclimated fish are compared at their respective acclimation temperatures, I observed an increase in affinity with increasing acclimation temperature. This increase in mitochondrial O_2 binding affinity associated with increased acclimation temperature might represent a response to systemic hypoxemia that is suggested to occur with increased environmental temperatures.

In general, increases in mitochondrial O_2 P_{50} associated with increased environmental temperature are likely a consequence of temperature effects on the stability of mitochondrial enzyme structure. Another factor that might account for *in vivo* variation in mitochondrial O_2 binding affinity is allosteric modification of cytochrome *c* oxidase by ATP, with increasing ATP levels resulting in decreased mitochondrial O_2 binding affinity (e.g., Porplycia et al., 2017). I assessed mitochondrial O_2 binding affinity with saturating quantities of ADP (i.e., state 3 conditions) which presumably results in high, but variable, ATP levels. It is possible that variation in ATP levels allows for the rapid modification of mitochondrial O_2 binding affinity and contributes to the maintenance of aerobic performance under acute thermal stress.

Subspecies variation in mitochondrial O_2 binding affinity was largely consistent with subspecies variation in acute upper thermal tolerance limits (Chapter 3). These results are the first demonstration of intraspecific variation in this mitochondrial property as a putative evolutionary response to thermal variation. Intraspecific variation in mitochondrial O_2 binding affinity potentially occurs through the expression of isoforms of mitochondrial enzymes, specifically cytochrome *c* oxidase (Lau et al., 2017; Pierron et al., 2012; Porplycia et al., 2017). But there is insufficient molecular evidence to confirm the presence of such isoforms between *F. heteroclitus* subspecies (Baris et al., 2017; Reid et al., 2016). Thus, identifying intraspecific variation in nuclear genes encoding mitochondrial enzymes, perhaps through genome sequencing, and potential effects on mitochondrial O_2 binding affinity will illuminate the involvement of these mechanisms.

Next, I asked the question of whether *F. heteroclitus*' mitochondrial responses to acute low temperature shifts may partly account for whole-organism low thermal tolerance limits (Chapters 2, 4 and 5). Thermal acclimation and intraspecific variation have been shown to alter lower thermal tolerance limits in this species (Fangue et al., 2006). Thus, at low assay

temperatures (i.e., 5 °C), mitochondrial function was predicted to be lowest in 33 °C acclimated killifish (CT_{min} = 5 and 7 °C for northern and southern *F. heteroclitus* respectively, Fangue et al., 2006) followed by fish acclimated to 15 (CT_{min} = approximately -0.5 °C) and 5 °C (CT_{min} = approximately -1 °C). Also, I predicted that northern *F. heteroclitus* would maintain greater mitochondrial performance relative to their southern counterparts at these low assay temperatures. In general, my results are consistent with these predictions. However, these effects are difficult to discern in the figures presented in Chapters 2, 4, and 5 because activities are very low at low assay temperatures compared to activities at high assay temperatures due to Q_{10} effects.

Overall, it is difficult to conclude that mitochondrial function is a mechanism that consistently shapes thermal acclimation and intraspecific variation in acute whole-organism thermal tolerance limits based on my data from *F. heteroclitus*. It is possible that I was unable to detect these relationships because my data lacked resolution on the acute thermal scale. Given that upper thermal tolerance limits differ by 10 °C among thermally acclimated *F. heteroclitus* (CT_{max} 30 to 42 °C between 5 and 33 °C acclimated *F. heteroclitus*; Fangue et al., 2006), and there was no clear variation associated with declining in mitochondrial function across this range, it is unlikely that this is the case. Thus, other biological properties (e.g., neural signaling) may place greater control on acute thermal tolerance measured as CT_{Max} and CT_{Min} (Ern et al., 2015; Miller and Stillman, 2012; Somero, 2002; Stillman, 2003).

It is possible that *F. heteroclitus*' acute mitochondrial performance does not decline at temperatures that align with whole organism critical thermal maxima (CT_{max}) because mitochondrial function underlies other aspects of thermal tolerance. Indeed, investigations of the OCLTT often employ CT_{max} (Lutterschmidt and Hutchison, 1997) as an estimate of acute thermal tolerance and by extension the critical temperature at which thermal-tolerance is time-limited (i.e., T_{crit}; Pörtner and Knust, 2007). However, there is a debate about the equivalence of CT_{max} and T_{crit} (Verberk et al., 2016), and the ecological relevance of CT_{max} as estimated under laboratory conditions (Terblanche et al., 2011). Although *F. heteroclitus* mitochondrial respiratory capacity does not decline at temperatures that match CT_{max}, it is probable that mitochondrial performance influences whole-organism thermal performance. For example, declines in mitochondrial respiratory capacity at high temperatures might underlie decrements in performance and aerobic scope associated with the pejus temperature (T_p; Pörtner and Knust,

2007). While these declines in performance might not manifest as an acute thermal limit, they can impact other performance metrics associated with fitness such as growth and reproduction over longer timescales (e.g., acclimation and evolution).

6.7 Consequences for *Fundulus heteroclitus* in natural environments

Overall my data support a role for altered mitochondrial function as a response to thermal variation. The direction of these responses was consistent over thermal acclimation and putative evolutionary timeframes which supports a role for countergradient variation of mitochondrial thermal performance (Conover and Schultz, 1995). Although I demonstrate considerable plasticity of mitochondrial function in response to prolonged thermal stress these effects might be influenced by the nature of the stress that I imposed. Indeed, I acclimated my fish to constant high and low ambient temperatures, and it is unlikely that natural *F. heteroclitus* populations will experience this kind of environmental stress. Thus, the physiological responses I demonstrate may reflect the limits of mitochondrial capacity that *F. heteroclitus* can recruit in response to temperature stress.

In estuarine environments, ambient temperature varies over a wide range of timescales. Perhaps one of the most overlooked timescales in thermal acclimation studies is diel cycling. This cycling is critical, as it represents a period over which organisms can recover from thermal stress and mount a physiological response. In some cases, the response recruited following a cyclic environmental stress may be larger than the response recruited following constant thermal exposure (Drake et al., 2017; Sørensen et al., 2016). The use of ecologically relevant acclimation treatments to investigate temperature effects on mitochondrial function is relatively uncommon (although see: Guderley et al., 1997; St-Pierre et al., 1998). But these types of experiments will be necessary if we are to understand organisms' capacity to respond to natural environmental variation.

One of the most striking findings in my thesis was the demonstration of decreases in mitochondrial function associated with high-temperature acclimation. This treatment involved prolonged constant temperatures of 33 °C, an intensity of exposure that natural *F. heteroclitus* populations are unlikely to experience under present-day conditions, as mean monthly temperatures during the summer at the southern end of the species range do not exceed 30 °C

(mean monthly southern temperature range = 11 – 30 °C; Sapelo Island, GA, USA, NOAA National Estuarine Research Reserve System, 2012). Acclimation to the constant 33 °C treatment decreased whole-body and tissue mass, which might reflect the onset of sublethal stress in *F. heteroclitus*. It should be noted that acclimation to slightly lower temperatures (25 to 30 °C) induces a breeding physiology, making it difficult to isolate temperature acclimation responses. Although 33 °C acclimation is potentially associated with sublethal effects, these results do highlight an understudied aspect of the metabolic consequences of prolonged high-temperature exposure, a condition in which natural populations of fish might find themselves in shortly.

It is important to acknowledge that in many cases I used measurements of mitochondrial functional capacity to compare the effects of thermal acclimation and intraspecific variation. It is unlikely that *in vivo* performance consistently occurs at these saturating levels, and it could be argued that comparing mitochondrial kinetic properties (e.g., proton leak kinetics, and mitochondrial O_2 binding affinity) might better reflect variation in performance in natural environments. In general, my investigations of mitochondrial performance at more physiologically relevant levels were consistent with responses observed under saturating conditions. Thus, my demonstration of variation in maximum mitochondrial capacity provides putative targets of modification that likely underlie natural variation in performance (Dalziel et al., 2009).

Overall, my data provide evidence of the mechanisms that eurythermal species might employ to survive in highly variable thermal habitats. Although the treatments that I utilized likely do not fully reflect the complex thermal nature of natural environments, they allowed me to demonstrate the considerable plasticity available to a eurythermal teleost. Whether this plasticity is available to other species that share this environment will likely dictate their success in a progressively warming world.

6.8 Future directions

My thesis lays the groundwork for future investigations of the role of mitochondrial function in shaping organisms' responses to temperature. My demonstration of altered mitochondrial respiratory capacity and mitochondrial O_2 binding affinity between *F. heteroclitus*

subspecies provides evidence for local adaptation at the level of the mitochondrion. Identifying intraspecific variation in these mitochondrial properties among multiple *F. heteroclitus* populations (spanning this species' latitudinal distribution) would provide greater evidence for selection acting on mitochondrial function in this species.

Thermal acclimation and intraspecific variation of mitochondrial function support the existence of isoforms of electron transport system enzymes in *F. heteroclitus*. Identifying these isozymes would provide support for a mechanism that differentiates whole-organism aerobic and thermal performance. Alternatively, this altered mitochondrial function might be a result of post-translational modifications (e.g., acetylation, phosphorylation, methylation), altered enzyme-enzyme interactions (e.g., mitochondrial supercomplexing), or altered lipid-enzyme interaction (e.g., annular and non-annular lipids). The involvement of these mechanisms and their regulation in ectotherms' responses to thermal acclimation and intraspecific variation remains poorly understood, making these worthwhile lines of inquiry.

My demonstration of mitochondrial membrane remodeling following thermal acclimation and between *F. heteroclitus* subspecies is likely due to variation in the regulation of lipid remodeling between subspecies. The potential association between this remodeling and altered mitochondrial function make *F. heteroclitus* an ideal model in which to investigate the functional consequences of variation in the plasticity of mitochondrial membrane remodeling. Furthermore, intraspecific variation in mitochondrial membrane composition indicates the potential for variation in mitochondrial morphology and mitochondrial localization. Intraspecific variation in mitochondrial structure and location likely contributes to variation in mitochondrial performance (e.g., Dhillon and Schulte, 2011) at both the tissue and whole-organism level and should be investigated more thoroughly.

At a broader level, investigating the effects of epigenetic modifications and developmental conditions on mitochondrial function will improve our understanding of organisms' responses to thermal variation in complex natural environments. Indeed, these are two mechanisms that I was unable to account for given my use of natural populations. Finally, future experiments should aim to investigate the effects of more ecologically relevant stressors (e.g., cyclic thermal stress) on mitochondrial function and their consequences for whole-organism performance.

6.9 Conclusions and implications

My thesis provides evidence that mitochondrial function is associated with responses to thermal stress across a range of biological timescales in a eurythermal ectotherm. Thermal acclimation to low temperatures and local adaptation to northern latitudes were both associated with greater liver mitochondrial respiratory capacity, and a lower mitochondrial O_2 binding affinity. Low-temperature acclimation was also associated with an increase in specific mitochondrial membrane fatty acids (e.g., 18:1n7 and 20:4n6) and the northern subspecies exhibited a lower ratio of PC/PE when compared to the southern subspecies. The alteration of mitochondrial properties following thermal acclimation was not associated with increased ROS production or a loss of membrane potential during acute thermal shifts away from the acclimation temperature. In contrast to liver mitochondrial function, heart and brain mitochondrial respiratory capacity did not consistently differ between subspecies and decreased following acclimation to thermal extremes. These data provide support for mitochondrial function as a mechanism that underlies the broad eurythermal physiology of *F. heteroclitus* and perhaps eurythermal physiology of ectotherms more generally.

Overall, my data provide limited support for declines in mitochondrial function as a mechanism that constrains acute whole-organism thermal tolerance limits, as suggested by the OCLTT. These results do not imply that mitochondrial function is not involved in whole-organism thermal responses. Indeed, my demonstration of thermal acclimation and local adaptation effects on mitochondrial properties points toward a role for mitochondrial function as a mechanism that shapes thermal performance at longer timescales. This putative relationship may in turn influence species' fitness. From the mechanistic insights that I have generated through my studies, I have been able to identify new targets that likely contribute to organisms' responses to thermal variation. Investigating the involvement of these mechanisms will ultimately improve our understanding of organisms' responses to thermal variation in complex natural environments.

References

Abdi, H. and Williams, L. J. (2010). Principal component analysis. *WIREs Comp Stat* **2**, 433–459.

Abele, D., Heise, K., Pörtner, H. O. and Puntarulo, S. (2002). Temperature-dependence of mitochondrial function and production of reactive oxygen species in the intertidal mud clam *Mya arenaria*. *J. Exp. Biol.* **205**, 1831–1841.

Angilletta, M. J. (2009). *Thermal Adaptation*. Oxford: Oxford University Press.

Arnold, S. (2012). The power of life--cytochrome *c* oxidase takes center stage in metabolic control, cell signalling and survival. *Mitochondrion* **12**, 46–56.

Arthur, H. and Watson, K. (1976). Thermal adaptation in yeast: growth temperatures, membrane lipid, and cytochrome composition of psychrophilic, mesophilic, and thermophilic yeasts. *J. Bacteriol.* **128**, 56–68.

Bak, S., León, I. R., Jensen, O. N. and Højlund, K. (2013). Tissue specific phosphorylation of mitochondrial proteins isolated from rat liver, heart muscle, and skeletal muscle. *J. Proteome Res.* **12**, 4327–4339.

Ballard, J. W. O. and Pichaud, N. (2014). Mitochondrial DNA: more than an evolutionary bystander. *Funct. Ecol.* **28**, 218–231.

Ballard, J. W. O. and Whitlock, M. C. (2004). The incomplete natural history of mitochondria. *Mol. Ecol.* **13**, 729–744.

Ballard, J. W. O., Katewa, S. D., Melvin, R. G. and Chan, G. (2007). Comparative analysis of mitochondrial genotype and aging. *Ann. N.Y. Acad. Sci.* **1114**, 93–106.

Balloux, F., Handley, L.-J. L., Jombart, T., Liu, H. and Manica, A. (2009). Climate shaped the worldwide distribution of human mitochondrial DNA sequence variation. *P. Roy. Soc. B-Biol. Sci.* **276**, 3447–3455.

Baris, T. Z., Blier, P. U., Pichaud, N., Crawford, D. L. and Oleksiak, M. F. (2016a). Gene by environmental interactions affecting oxidative phosphorylation and thermal sensitivity. *Am. J. Physiol.-Reg. I.* **311**, R157–65.

Baris, T. Z., Crawford, D. L. and Oleksiak, M. F. (2016b). Acclimation and acute temperature effects on population differences in oxidative phosphorylation. *Am. J. Physiol.-Reg. I.* **310**, R185–96.

Baris, T. Z., Wagner, D. N., Dayan, D. I., Du, X., Blier, P. U., Pichaud, N., Oleksiak, M. F. and Crawford, D. L. (2017). Evolved genetic and phenotypic differences due to mitochondrial-nuclear interactions. *PLOS Genet.* **13**, e1006517.

Barja, G., Cadenas, S., Rojas, C., Pérez-Campo, R. and López-Torres, M. (1994). Low

mitochondrial free radical production per unit O_2 consumption can explain the simultaneous presence of high longevity and high aerobic metabolic rate in birds. *Free Radical Res.* **21**, 317–327.

Barrientos, A., Kenyon, L. and Moraes, C. T. (1998). Human xenomitochondrial cybrids. Cellular models of mitochondrial complex I deficiency. *J. Biol. Chem.* **273**, 14210–14217.

Bazin, E., Glémin, S. and Galtier, N. (2006). Population size does not influence mitochondrial genetic diversity in animals. *Science* **312**, 570–572.

Benard, G., Faustin, B., Passerieux, E., Galinier, A., Rocher, C., Bellance, N., Delage, J.-P., Casteilla, L., Letellier, T. and Rossignol, R. (2006). Physiological diversity of mitochondrial oxidative phosphorylation. *Am. J. Physiol.-Cell Ph.* **291**, C1172–82.

Blier, P. U. and Guderley, H. (1993). Effects of pH and Temperature on the Kinetics of Pyruvate Oxidation by Muscle Mitochondria from Rainbow Trout (*Oncorhynchus mykiss*). *Physiol. zool.* **66**, 474–489.

Blier, P. U., Lemieux, H. and Pichaud, N. (2014). Holding our breath in our modern world: will mitochondria keep the pace with climate changes? *Can. J. Zool.* **92**, 591–601.

Bogdanov, M., Mileykovskaya, E. and Dowhan, W. (2008). Lipids in the Assembly of membrane proteins and organization of protein supercomplexes: Implications for lipid-linked disorders. In *Lipids in Health and Disease* (eds. Quinn, P. J. and Wang, X.), pp. 197–239. Dordrecht: Springer Netherlands.

Borowiec, B. G., Darcy, K. L., Gillette, D. M. and Scott, G. R. (2015). Distinct physiological strategies are used to cope with constant hypoxia and intermittent hypoxia in killifish (*Fundulus heteroclitus*). *J. Exp. Biol.* **218**, 1198–1211.

Bradford, M. M. (1976). A rapid and sensitive method for the quantitation of microgram quantities of protein utilizing the principle of protein-dye binding. *Anal. Biochem.* **72**, 248–254.

Brand, M. D. (1995). Measurement of mitochondrial proton motive force. In *Reductive stress* (eds. Brown, G. C. and Cooper, C. E.), pp. 39–62. Oxford: Oxford University Press.

Brand, M. D. (1997). Regulation analysis of energy metabolism. *J. Exp. Biol.* **200**, 193–202.

Brand, M. D. (2010). The sites and topology of mitochondrial superoxide production. *Exp. Gerontol.* **45**, 466–472.

Brand, M. D. and Nicholls, D. G. (2011). Assessing mitochondrial dysfunction in cells. *Biochem. J.* **435**, 297–312.

Brand, M. D., Brindle, K. M., Buckingham, J. A., Harper, J. A., Rolfe, D. and Stuart, J. A. (1999). The significance and mechanism of mitochondrial proton conductance. *Int. J. Obesity* **23**, S4–S11.

Brand, M. D., Chien, L. F., Ainscow, E. K., Rolfe, D. F. and Porter, R. K. (1994). The causes and functions of mitochondrial proton leak. *Biochim. Biophys. Acta* **1187**, 132–139.

Brijs, J., Jutfelt, F., Clark, T. D., Gräns, A., Ekström, A. and Sandblom, E. (2015). Experimental manipulations of tissue oxygen supply do not affect warming tolerance of European perch. *J. Exp. Biol.* **218**, 2448–2454.

Brown, B. L. and Chapman, R. W. (1991). Gene flow and mitochondrial DNA variation in the killifish, *Fundulus heteroclitus*. *Evolution* **45**, 1147.

Brown, J. C. L. and Staples, J. F. (2011). Mitochondrial metabolic suppression in fasting and daily torpor: Consequences for reactive oxygen species production. *Physiol. Biochem. Zool.* **84**, 467–480.

Brown, J. C. L., Chung, D. J., Belgrave, K. R. and Staples, J. F. (2011). Mitochondrial metabolic suppression and reactive oxygen species production in liver and skeletal muscle of hibernating thirteen-lined ground squirrels. *Am. J. Physiol.-Reg. I.* **302**, R15–R28.

Brown, J. C. L., Gerson, A. R. and Staples, J. F. (2007). Mitochondrial metabolism during daily torpor in the dwarf Siberian hamster: role of active regulated changes and passive thermal effects. *Am. J. Physiol.-Reg. I.* **293**, R1833–R1845.

Brown, J. H., Gillooly, J. F., Allen, A. P., Savage, V. M. and West, G. B. (2004). Toward a metabolic theory of ecology. *Ecology* **85**, 1771–1789.

Caldwell, R. S. and Vernberg, F. J. (1970). The influence of acclimation temperature on the lipid composition of fish gill mitochondria. *Comp. Biochem. Physiol.* **34**, 179–191.

Campbell, H. A., Fraser, K. P. P., Bishop, C. M., Peck, L. S. and Egginton, S. (2008). Hibernation in an antarctic fish: on ice for winter. *PLoS ONE* **3**, e1743–.

Carroll, J., Fearnley, I. M., Skehel, J. M., Runswick, M. J., Shannon, R. J., Hirst, J. and Walker, J. E. (2005). The post-translational modifications of the nuclear encoded subunits of complex I from bovine heart mitochondria. *Mol. Cell. Proteomics* **4**, 693–699.

Castellana, S., Vicario, S. and Saccone, C. (2011). Evolutionary patterns of the mitochondrial genome in Metazoa: exploring the role of mutation and selection in mitochondrial protein coding genes. *Genome Biol. Evol.* **3**, 1067–1079.

IPCC. (2014). *Climate Change 2014 – Impacts, Adaptation and Vulnerability: Part A: Global and Sectoral Aspects: Volume 1, Global and Sectoral Aspects*. (eds. Field, C.B., V.R. Barros, D.J. Dokken, K.J. Mach, M.D. Mastrandrea, T.E. Bilir, M. Chatterjee, K.L. Ebi, Y.O. Estrada, R.C. Genova, B. Girma, E.S. Kissel, A.N. Levy, S. MacCracken, P.R. Mastrandrea, and L.L.White) New York: Cambridge University Press.

Chen, Q., Vazquez, E. J., Moghaddas, S., Hoppel, C. L. and Lesnefsky, E. J. (2003). Production of reactive oxygen species by mitochondria: central role of complex III. *J. Biol. Chem.* **278**, 36027–36031.

Chicco, A. J. and Sparagna, G. C. (2007). Role of cardiolipin alterations in mitochondrial dysfunction and disease. *Am. J. Physiol.-Cell Ph.* **292**, C33–44.

Chidester, F. E. (1920). The behavior of *Fundulus heteroclitus* on the salt marshes New Jersey. *Am. Nat.* **54**, 551–557.

Chung, D. J. and Schulte, P. M. (2015). Mechanisms and costs of mitochondrial thermal acclimation in a eurythermal killifish (*Fundulus heteroclitus*). *J. Exp. Biol.* **218**, 1621–1631.

Chung, D. J., Bryant, H. J. and Schulte, P. M. (2017). Thermal acclimation and subspecies-specific effects on heart and brain mitochondrial performance in a eurythermal teleost (*Fundulus heteroclitus*). *J. Exp. Biol.* **220**, 1459–1471.

Chung, D. J., Szyszka, B., Brown, J. C. L., Huner, N. P. A. and Staples, J. F. (2013). Changes in the mitochondrial phosphoproteome during mammalian hibernation. *Physiol. Genomics* **45**, 389–399.

Clark, T. D., Jeffries, K. M., Hinch, S. G. and Farrell, A. P. (2011). Exceptional aerobic scope and cardiovascular performance of pink salmon (*Oncorhynchus gorbuscha*) may underlie resilience in a warming climate. *J. Exp. Biol.* **214**, 3074–3081.

Clark, T. D., Sandblom, E. and Jutfelt, F. (2013). Aerobic scope measurements of fishes in an era of climate change: respirometry, relevance and recommendations. *J. Exp. Biol.* **216**, 2771–2782.

Conover, D. O. and Schultz, E. T. (1995). Phenotypic similarity and the evolutionary significance of countergradient variation. *Trends Ecol. Evol.* **10**, 248–252.

Contreras, F.-X., Ernst, A. M., Wieland, F. and Brügger, B. (2011). Specificity of intramembrane protein-lipid interactions. *CSH Perspect. Biol.* **3**, a004705.

Cossins, A. R. (1977). Adaptation of biological membranes to temperature. The effect of temperature acclimation of goldfish upon the viscosity of synaptosomal membranes. *Biochim. Biophys. Acta.* **470**, 395–411.

Costa, I. A. S. F., Driedzic, W. R. and Gamperl, A. K. (2013). Metabolic and cardiac responses of cunner *Tautogolabrus adspersus* to seasonal and acute changes in temperature. *Physiol. Biochem. Zool.* **86**, 233–244.

Costa, L. E., Mendez, G. and Boveris, A. (1997). Oxygen dependence of mitochondrial function measured by high-resolution respirometry in long-term hypoxic rats. *Am. J. Physiol.* **273**, C852–8.

Crawford, D. L. and Powers, D. A. (1989). Molecular basis of evolutionary adaptation at the lactate dehydrogenase-B locus in the fish *Fundulus heteroclitus*. *P Natl Acad Sci USA* **86**, 9365–9369.

Crawford, D. L., Pierce, V. A. and Segal, J. A. (1999). Evolutionary physiology of closely

related taxa: Analyses of enzyme expression. *Integr. Comp. Biol.* **39**, 389–400.

Crawshaw, L. I. (1984). Low-temperature dormancy in fish. *Am. J. Physiol.* **246**, R479–86.

Crockett, E. and Hazel, J. (1995). Cholesterol levels explain inverse compensation of membrane order in brush border but not homeoviscous adaptation in basolateral membranes from the intestinal epithelia of rainbow trout. *J. Exp. Biol.* **198**, 1105–1113.

Crockett, E. L., Dougherty, B. E. and McNamer, A. N. (2001). Effects of acclimation temperature on enzymatic capacities and mitochondrial membranes from the body wall of the earthworm *Lumbricus terrestris*. *Comp. Biochem. Phys. B* **130**, 419–426.

Crompton, M. (1999). The mitochondrial permeability transition pore and its role in cell death. *Biochem. J.* **341**, 233–249.

Dahlhoff, E. A. and Somero, G. N. (1993). Effects of temperature on mitochondria from abalone (genus *Haliotis*): adaptive plasticity and its limits. *J. Exp. Biol.* **185**, 151–168.

Dalziel, A. C., Rogers, S. M. and Schulte, P. M. (2009). Linking genotypes to phenotypes and fitness: how mechanistic biology can inform molecular ecology. *Mol. Ecol.* **18**, 4997–5017.

Darveau, C.-A., Suarez, R. K., Andrews, R. D. and Hochachka, P. W. (2002). Allometric cascade as a unifying principle of body mass effects on metabolism. *Nature* **417**, 166–170.

Dell, A. I., Pawar, S. and Savage, V. M. (2013). The thermal dependence of biological traits. *Ecology* **94**, 1205–1206.

Demura, M., Kamo, N. and Kobatake, Y. (1987). Mitochondrial membrane potential estimated with the correction of probe binding. *BBA - Bioenergetics* **894**, 355–364.

Deuticke, B. and Haest, C. W. (1987). Lipid modulation of transport proteins in vertebrate cell membranes. *Annu. Rev. Physiol.* **49**, 221–235.

Deutsch, C., Ferrel, A., Seibel, B., Pörtner, H. O. and Huey, R. B. (2015). Climate change tightens a metabolic constraint on marine habitats. *Science* **348**, 1132–1135.

Dhillon, R. S. and Schulte, P. M. (2011). Intraspecific variation in the thermal plasticity of mitochondria in killifish. *J. Exp. Biol.* **214**, 3639–3648.

Dillon, M. E., Wang, G. and Huey, R. B. (2010). Global metabolic impacts of recent climate warming. *Nature* **467**, 704–706.

Dimichele, L. and Powers, D. A. (1982a). LDH-B genotype-specific hatching times of *Fundulus heteroclitus* embryos. *Nature* **296**, 563–564.

Dimichele, L. and Powers, D. A. (1982b). Physiological basis for swimming endurance differences between LDH-B genotypes of *Fundulus heteroclitus*. *Science* **216**, 1014–1016.

Dimichele, L. and Westerman, M. E. (1997). Geographic variation in development rate

between populations of the teleost *Fundulus heteroclitus*. *Mar. Biol.* **128**, 1–7.

Dimichele, L., Paynter, K. and Powers, D. A. (1991). Evidence of lactate dehydrogenase-B allozyme effects in the teleost, *Fundulus heteroclitus*. *Science* **253**, 898–900.

Divakaruni, A. S. and Brand, M. D. (2011). The regulation and physiology of mitochondrial proton leak. *Physiology* **26**, 192–205.

Dos Santos, R. S., Galina, A. and Da-Silva, W. S. (2013). Cold acclimation increases mitochondrial oxidative capacity without inducing mitochondrial uncoupling in goldfish white skeletal muscle. *Biol. Open* **2**, 82–87.

Dowling, D. K., Friberg, U. and Lindell, J. (2008). Evolutionary implications of non-neutral mitochondrial genetic variation. *Trends Ecol. Evol.* **23**, 546–554.

Drake, M. J., Miller, N. A. and Todgham, A. E. (2017). The role of stochastic thermal environments in modulating the thermal physiology of an intertidal limpet, *Lottia digitalis*. *J. Exp. Biol.* **220**, 3072–3083.

Du, S. N. N., Mahalingam, S., Borowiec, B. G. and Scott, G. R. (2016). Mitochondrial physiology and reactive oxygen species production are altered by hypoxia acclimation in killifish (*Fundulus heteroclitus*). *J. Exp. Biol.* **219**, 1130–1138.

Dudkina, N. V., Kouril, R., Bultema, J. B. and Boekema, E. J. (2010). Imaging of organelles by electron microscopy reveals protein-protein interactions in mitochondria and chloroplasts. *FEBS Lett.* **584**, 2510–2515.

Efremov, R. G., Baradaran, R. and Sazanov, L. A. (2010). The architecture of respiratory complex I. *Nature* **465**, 441–445.

Egginton, S. and Johnston, I. A. (1984). Effects of acclimation temperature on routine metabolism muscle mitochondrial volume density and capillary supply in the elver (*Anguilla anguilla* L.). *J. Therm. Biol.* **9**, 165–170.

Eliason, E. J., Clark, T. D., Hague, M. J., Hanson, L. M., Gallagher, Z. S., Jeffries, K. M., Gale, M. K., Patterson, D. A., Hinch, S. G. and Farrell, A. P. (2011). Differences in thermal tolerance among sockeye salmon populations. *Science* **332**, 109–112.

Ern, R., Do Thi Thanh Huong, Phuong, N. T., Madsen, P. T., Wang, T. and Bayley, M. (2015). Some like it hot: Thermal tolerance and oxygen supply capacity in two eurythermal crustaceans. *Sci. Rep.* **5**, 10743.

Ern, R., Huong, D. T. T., Phuong, N. T., Wang, T. and Bayley, M. (2014). Oxygen delivery does not limit thermal tolerance in a tropical eurythermal crustacean. *J. Exp. Biol.* **217**, 809–814.

Fangue, N. A., Hofmeister, M. and Schulte, P. M. (2006). Intraspecific variation in thermal tolerance and heat shock protein gene expression in common killifish, *Fundulus heteroclitus*.

J. Exp. Biol. **209**, 2859–2872.

Fangue, N. A., Mandic, M., Richards, J. G. and Schulte, P. M. (2008). Swimming performance and energetics as a function of temperature in killifish *Fundulus heteroclitus*. *Physiol. Biochem. Zool.* **81**, 389–401.

Fangue, N. A., Richards, J. G. and Schulte, P. M. (2009). Do mitochondrial properties explain intraspecific variation in thermal tolerance? *J. Exp. Biol.* **212**, 514–522.

Ferreira, F. M., Seiça, R., Oliveira, P. J., Coxito, P. M., Moreno, A. J., Palmeira, C. M. and Santos, M. S. (2003). Diabetes induces metabolic adaptations in rat liver mitochondria: role of coenzyme Q and cardiolipin contents. *Biochim. Biophys. Acta* **1639**, 113–120.

Finkel, E. (2001). The mitochondrion: is it central to apoptosis? *Science* **292**, 624–626.

Fobian, D., Overgaard, J. and Wang, T. (2014). Oxygen transport is not compromised at high temperature in pythons. *J. Exp. Biol.* **217**, 3958–3961.

Forner, F., Foster, L. J., Campanaro, S., Valle, G. and Mann, M. (2006). Quantitative proteomic comparison of rat mitochondria from muscle, heart, and liver. *Mol. Cell. Proteomics* **5**, 608–619.

Fry, F. E. J. and Hart, J. S. (1948). The relation of temperature to oxygen consumption in the goldfish. *Biol. Bull.* **94**, 66–77.

Galli, G. L. J., Lau, G. Y. and Richards, J. G. (2013). Beating oxygen: chronic anoxia exposure reduces mitochondrial F_1F_O-ATPase activity in turtle (*Trachemys scripta*) heart. *J. Exp. Biol.* **216**, 3283–3293.

Glancy, B., Hartnell, L. M., Malide, D., Yu, Z.-X., Combs, C. A., Connelly, P. S., Subramaniam, S. and Balaban, R. S. (2015). Mitochondrial reticulum for cellular energy distribution in muscle. *Nature* **523**, 617–620.

Gnaiger, E. (2001). Bioenergetics at low oxygen: dependence of respiration and phosphorylation on oxygen and adenosine diphosphate supply. *Resp. Physiol.* **128**, 277–297.

Gnaiger, E. (2003). Oxygen conformance of cellular respiration. In *Hypoxia: Through the lifecycle*, pp. 39-55. New York: Springer Science.

Gnaiger, E. (2014). *Mitochondrial pathways and respiratory control.* 4 ed. Innsbruck: Oroboros MiPNet.

Gnaiger, E. and Forstner, H. (1983). Calculation of equilibrium oxygen concentration. In *Polarographic Oxygen Sensors*, pp. 321–333. Berlin, Heidelberg: Springer Berlin Heidelberg.

Gnaiger, E. and Kuznetsov, A. V. (2002). Mitochondrial respiration at low levels of oxygen and cytochrome *c*. *Biochem. Soc. T.* **30**, 252–258.

Gnaiger, E., Lassnig, B., Kuznetsov, A., Rieger, G. and Margreiter, R. (1998). Mitochondrial oxygen affinity, respiratory flux control and excess capacity of cytochrome *c* oxidase. *J. Exp. Biol.* **201**, 1129–1139.

Grigg, G. C. (1969). Temperature-induced changes in the oxygen equilibrium curve of the blood of the brown bullhead, *Ictalurus nebulosus*. *Comp. Biochem. and Physiol.* **28**, 1203–1223.

Grim, J. M., Miles, D. R. B. and Crockett, E. L. (2010). Temperature acclimation alters oxidative capacities and composition of membrane lipids without influencing activities of enzymatic antioxidants or susceptibility to lipid peroxidation in fish muscle. *J. Exp. Biol.* **213**, 445–452.

Guderley, H. (2004). Metabolic responses to low temperature in fish muscle. *Biol. Rev.* **79**, 409–427.

Guderley, H. (2011). Mitochondria and Temperature. In *Encyclopedia of Fish Physiology*, pp. 1709–1716. Elsevier Inc.

Guderley, H. and Johnston, I. (1996). Plasticity of fish muscle mitochondria with thermal acclimation. *J. Exp. Biol.* **199**, 1311–1317.

Guderley, H. and St-Pierre, J. (2002). Going with the flow or life in the fast lane: contrasting mitochondrial responses to thermal change. *J. Exp. Biol.* **205**, 2237–2249.

Guderley, H., St-Pierre, J., Couture, P. and Hulbert, A. J. (1997). Plasticity of the properties of mitochondria from rainbow trout red muscle with seasonal acclimatization. *Fish Physiol. Biochem.* **16**, 531–541.

Guerrero-Castillo, S., Cabrera-Orefice, A., Huynen, M. A. and Arnold, S. (2017). Identification and evolutionary analysis of tissue-specific isoforms of mitochondrial complex I subunit NDUFV3. *Biochim. Biophys. Acta* **1858**, 208–217.

Hagve, T.-A., Woldseth, B., Brox, J., Narce, M. and Poisson, J.-P. (2009). Membrane fluidity and fatty acid metabolism in kidney cells from rats fed purified eicosapentaenoic acid or purified docosahexaenoic acid. *Scand. J. Clin. Lab. Inv.* **58**, 187–194.

Halestrap, A. P. (1989). The regulation of the matrix volume of mammalian mitochondria in vivo and in vitro and its role in the control of mitochondrial metabolism. *BBA - Bioenergetics* **973**, 355–382.

Halestrap, A. P. (2012). The mitochondrial pyruvate carrier: Has it been unearthed at last? *Cell Metab.* **16**, 141–143.

Hardewig, I., Peck, L. S. and Pörtner, H. O. (1999). Thermal sensitivity of mitochondrial function in the Antarctic Notothenioid *Lepidonotothen nudifrons*. *J. Comp. Physiol. B* **169**, 597–604.

Harman, D. (1956). Aging: a theory based on free radical and radiation chemistry. *J. Gerontol.*

11, 298–300.

Harwell, M. R., Rubinstein, E. N., Hayes, W. S. and Olds, C. C. (1992). Summarizing Monte Carlo results in methodological research: The one- and two-factor fixed effects ANOVA cases. *J. Educ. Stat.* **17**, 315.

Hazel, J. (1984). Effects of temperature on the structure and metabolism of cell membranes in fish. *Am. J. Physiol.* **246**, R460–R470.

Hazel, J. (1995). Thermal adaptation in biological membranes: is homeoviscous adaptation the explanation? *Annu. Rev. Physiol.* **57**, 19–42.

Hazel, J. and Landrey, S. R. (1988). Time course of thermal adaptation in plasma membranes of trout kidney. II. Molecular species composition. *Am. J. Physiol.* **255**, R628–34.

Hazel, J. and Williams, E. E. (1990). The role of alterations in membrane lipid composition in enabling physiological adaptation of organisms to their physical environment. *Prog. Lipid Res.* **29**, 167–227.

Healy, T. M. and Schulte, P. M. (2012). Thermal acclimation is not necessary to maintain a wide thermal breadth of aerobic scope in the common killifish (*Fundulus heteroclitus*). *Physiol. Biochem. Zool.* **85**, 107–119.

Heard, E. and Martienssen, R. A. (2014). Transgenerational Epigenetic Inheritance: Myths and Mechanisms. *Cell* **157**, 95–109.

Heim, A. B., Chung, D. J., Florant, G. L. and Chicco, A. J. (2017). Tissue-specific seasonal changes in mitochondrial function of a mammalian hibernator. *Am. J. Physiol.-Reg. I.* **313**, R180–R190.

Heise, K. (2003). Production of reactive oxygen species by isolated mitochondria of the Antarctic bivalve *Laternula elliptica* (King and Broderip) under heat stress. *Comp. Biochem. Phys. C* **134**, 79–90.

Hochachka, P. W. and Somero, G. N. (2002). *Biochemical Adaptation*. 2nd ed. Oxford: Oxford University Press.

Hoekstra, L. A., Siddiq, M. A. and Montooth, K. L. (2013). Pleiotropic effects of a mitochondrial-nuclear incompatibility depend upon the accelerating effect of temperature in Drosophila. *Genetics* **195**, 1129–1139.

Hofer, A. and Wenz, T. (2014). Post-translational modification of mitochondria as a novel mode of regulation. *Exp. Gerontol.* **56**, 202–220.

Hosler, J., Burns, J. and Esch, H. (2000). Flight muscle resting potential and species-specific differences in chill-coma. *J. Insect Physiol.* **46**, 621–627.

Houten, S. M. and Wanders, R. J. A. (2010). A general introduction to the biochemistry of

mitochondrial fatty acid β-oxidation. *J. Inherit. Metab. Dis.* **33**, 469–477.

Huey, R. B. and Hertz, P. E. (1984). Is a jack-of-all-temperatures a master of none? *Evolution* **38**, 441–444.

Hulbert, A. J. (2003). Life, death and membrane bilayers. *J. Exp. Biol.* **206**, 2303–2311.

Iftikar, F. I. and Hickey, A. J. R. (2013). Do mitochondria limit hot fish hearts? Understanding the role of mitochondrial function with heat stress in *Notolabrus celidotus*. *PLoS ONE* **8**, e64120.

Iftikar, F. I., Morash, A. J., Cook, D. G., Herbert, N. A. and Hickey, A. J. R. (2015). Temperature acclimation of mitochondria function from the hearts of a temperate wrasse (*Notolabrus celidotus*). *Comp. Biochem. Physiol. A* **184**, 46–55.

Iles, A. C. (2014). Towards predicting community level effects of climate: Relative temperature scaling of metabolic and ingestion rates. *Ecology* **95**, 2657–2668.

Itoi, S., Kinoshita, S., Kikuchi, K. and Watabe, S. (2003). Changes of carp F_oF_1-ATPase in association with temperature acclimation. *Am. J. Physiol.-Reg. I.* **284**, R153–R163.

James, J. E., Piganeau, G. and Eyre-Walker, A. (2016). The rate of adaptive evolution in animal mitochondria. *Mol. Ecol.* **25**, 67–78.

Jastroch, M., Buckingham, J. A., Helwig, M., Klingenspor, M. and Brand, M. D. (2007). Functional characterisation of UCP1 in the common carp: uncoupling activity in liver mitochondria and cold-induced expression in the brain. *J. Comp. Physiol. B* **177**, 743–752.

Jastroch, M., Divakaruni, A. S., Mookerjee, S., Treberg, J. R. and Brand, M. D. (2010). Mitochondrial proton and electron leaks. *Essays Biochem.* **47**, 53–67.

Jensen, F. B. (2004). Red blood cell pH, the Bohr effect, and other oxygenation-linked phenomena in blood O_2 and CO_2 transport. *Acta. Physiol. Scand.* **182**, 215–227.

Johnston, I., Guderley, H., Franklin, C., Crockford, T. and Kamunde, C. (1994). Are mitochondria subject to evolutionary temperature adaptation? *J. Exp. Biol.* **195**, 293–306.

Jones, D. P. (1986). Intracellular diffusion gradients of O_2 and ATP. *Am. J. Physiol.* **250**, C663–75.

Keller, M., Sommer, A. M., Pörtner, H. O. and Abiko, Y. (2004). Seasonality of energetic functioning and production of reactive oxygen species by lugworm (*Arenicola marina*) mitochondria exposed to acute temperature changes. *J. Exp. Biol.* **207**, 2529–2538.

Khan, J. R., Iftikar, F. I., Herbert, N. A., Gnaiger, E. and Hickey, A. J. R. (2014). Thermal plasticity of skeletal muscle mitochondrial activity and whole animal respiration in a common intertidal triplefin fish, *Forsterygion lapillum* (Family: Tripterygiidae). *J. Comp. Physiol. B* **184**, 991–1001.

Kleiber, M. (1932). Body size and metabolism. *Hilgardia* **6**, 315–353.

Kleiber, M. (1947). Body size and metabolic rate. *Physiol. Rev.* **27**, 511–541.

Klok, C. J., Sinclair, B. J. and Chown, S. L. (2004). Upper thermal tolerance and oxygen limitation in terrestrial arthropods. *J. Exp. Biol.* **207**, 2361–2370.

Kraffe, E., Marty, Y. and Guderley, H. (2007). Changes in mitochondrial oxidative capacities during thermal acclimation of rainbow trout *Oncorhynchus mykiss*: roles of membrane proteins, phospholipids and their fatty acid compositions. *J. Exp. Biol.* **210**, 149–165.

Kulkarni, S. S. and Cantó, C. (2017). Mitochondrial post-translational modifications and metabolic control: sirtuins and beyond. *Curr. Diabetes Rev.* **13**, 338–351.

Kuznetsov, A. V., Veksler, V., Gellerich, F. N., Saks, V., Margreiter, R. and Kunz, W. S. (2008). Analysis of mitochondrial function in situ in permeabilized muscle fibers, tissues and cells. *Nature Protocols* **3**, 965–976.

Lannig, G., Storch, D. and Pörtner, H. O. (2005). Aerobic mitochondrial capacities in Antarctic and temperate eelpout (*Zoarcidae*) subjected to warm versus cold acclimation. *Polar Biol.* **28**, 575–584.

Lapuente-Brun, E., Moreno-Loshuertos, R., Acin-Perez, R., Latorre-Pellicer, A., Colás, C., Balsa, E., Perales-Clemente, E., Quirós, P. M., Calvo, E., Rodriguez-Hernandez, M. A., et al. (2013). Supercomplex assembly determines electron flux in the mitochondrial electron transport chain. *Science* **340**, 1567–1570.

Larsen, F. J., Schiffer, T. A., Sahlin, K., Ekblom, B., Weitzberg, E. and Lundberg, J. O. (2011). Mitochondrial oxygen affinity predicts basal metabolic rate in humans. *FASEB J.* **25**, 2843–2852.

Larsen, S., Nielsen, J., Hansen, C. N., Nielsen, L. B., Wibrand, F., Stride, N., Schroder, H. D., Boushel, R., Helge, J. W., Dela, F., et al. (2012). Biomarkers of mitochondrial content in skeletal muscle of healthy young human subjects. *J. Physiol.* **590**, 3349–3360.

Lau, G. Y., Lau, G. Y., Mandic, M., Mandic, M., Richards, J. G. and Richards, J. G. (2017). Evolution of cytochrome *c* oxidase in hypoxia tolerant sculpins (*Cottidae, Actinopterygii*). **34**, 2153–2162.

Laursen, J. S., Andersen, N. A. and Lykkeboe, G. (1985). Temperature acclimation and oxygen binding properties of blood of the European eel, *Anguilla anguilla*. *Comp. Biochem. Physiol. A* **81**, 79–86.

Lemoine, N. P. and Burkepile, D. E. (2012). Temperature-induced mismatches between consumption and metabolism reduce consumer fitness. *Ecology* **93**, 2483–2489.

Leray, C., Chapelle, S., Duportail, G. and Florentz, A. (1984). Changes in fluidity and 22:6(n − 3) content in phospholipids of trout intestinal brush-border membrane as related to

environmental salinity. *BBA - Biomembranes* **778**, 233–238.

Li, Z., Agellon, L. B., Allen, T. M., Umeda, M., Jewell, L., Mason, A. and Vance, D. E. (2006). The ratio of phosphatidylcholine to phosphatidylethanolamine influences membrane integrity and steatohepatitis. *Cell Metab.* **3**, 321–331.

Lilly, L. E., Blinebry, S. K., Viscardi, C. M., Perez, L., Bonaventura, J. and McMahon, T. J. (2013). Parallel assay of oxygen equilibria of hemoglobin. *Anal. Biochem.* **441**, 63–68.

Liu, X., Strable, M. S. and Ntambi, J. M. (2011). Stearoyl CoA desaturase 1: role in cellular inflammation and stress. *Adv. Nutr.* **2**, 15–22.

Loftus, S. J. and Crawford, D. L. (2013). Interindividual variation in complex I activity in *Fundulus heteroclitus* along a steep thermocline. *Physiol. Biochem. Zool.* **86**, 82–91.

Lotrich, V. A. (1975). Summer home range and movements of *Fundulus heteroclitus* (Pisces: cyprinodontidae) in a tidal creek. *Ecology* **56**, 191–198.

Lutterschmidt, W. I. and Hutchison, V. H. (1997). The critical thermal maximum: data to support the onset of spasms as the definitive end point. *Can. J. Zool.* **75**, 1553–1560.

Mandic, M., Todgham, A. E. and Richards, J. G. (2009). Mechanisms and evolution of hypoxia tolerance in fish. *Proc. Roy. Soc. B* **276**, 735–744.

Mannella, C. A. (2006). Structure and dynamics of the mitochondrial inner membrane cristae. *Biochim. Biophys. Acta* **1763**, 542–548.

Marden, J. H. (2013). Nature's inordinate fondness for metabolic enzymes: why metabolic enzyme loci are so frequently targets of selection. *Mol. Ecol.* **22**, 5743–5764.

Mark, F. C., Lucassen, M., Strobel, A., Barrera-Oro, E., Koschnick, N., Zane, L., Patarnello, T., Pörtner, H. O. and Papetti, C. (2012). Mitochondrial function in antarctic nototheniids with ND6 translocation. *PLoS ONE* **7**, e31860.

Marsh, D. (2010). Structural and thermodynamic determinants of chain-melting transition temperatures for phospholipid and glycolipids membranes. *BBA - Biomembranes* **1798**, 40–51.

Mathers, K. E. and Staples, J. F. (2015). Saponin-permeabilization is not a viable alternative to isolated mitochondria for assessing oxidative metabolism in hibernation. *Biol. Open* **4**, 858–864.

Matthews, S. A. (1939). The effects of light and temperature on the male sexual cycle in *Fundulus*. *Biol. Bull.* **77**, 92–95.

McBride, H. M., Neuspiel, M. and Wasiak, S. (2006). Mitochondria: more than just a powerhouse. *Curr. Biol.* **16**, R551–60.

McBryan, T. L., Healy, T. M., Haakons, K. L. and Schulte, P. M. (2016). Warm acclimation improves hypoxia tolerance in *Fundulus heteroclitus*. *J. Exp. Biol.* **219**, 474–484.

McKenzie, J. L., Dhillon, R. S. and Schulte, P. M. (2016). Steep, coincident, and concordant clines in mitochondrial and nuclear-encoded genes in a hybrid zone between subspecies of Atlantic killifish, *Fundulus heteroclitus*. *Ecol. Evol.* **6**, 5771–5787.

Melo-Ferreira, J., Vilela, J., Fonseca, M. M., da Fonseca, R. R., Boursot, P. and Alves, P. C. (2014). The elusive nature of adaptive mitochondrial DNA evolution of an arctic lineage prone to frequent introgression. *Genome Biol. Evol.* **6**, 886–896.

Mileykovskaya, E. and Dowhan, W. (2014). Cardiolipin-dependent formation of mitochondrial respiratory supercomplexes. *Chem Phys Lipids* **179**, 42–48.

Miller, N. A. and Stillman, J. H. (2012). Neural thermal performance in porcelain crabs, genus *Petrolisthes*. *Physiol. Biochem. Zool.* **85**, 29–39.

Minauro-Sanmiguel, F., Wilkens, S. and García, J. J. (2005). Structure of dimeric mitochondrial ATP synthase: novel F_0 bridging features and the structural basis of mitochondrial cristae biogenesis. ***P. Natl. Acad. Sci. USA* 102**, 12356–12358.

Mitchell, P. (1961). Coupling of phosphorylation to electron and hydrogen transfer by a chemiosmotic type of mechanism. *Nature* **191**, 144–148.

Morash, A. J. and McClelland, G. B. (2011). Regulation of carnitine palmitoyltransferase (CPT) I during fasting in rainbow trout (*Oncorhynchus mykiss*) promotes increased mitochondrial fatty acid oxidation. *Physiol. Biochem. Zool.* **84**, 625–633.

Morin, R. P. and Able, K. W. (1983). Patterns of geographic variation in the egg morphology of the Fundulid fish, *Fundulus heteroclitus*. *Copeia* **1983**, 726.

Moyes, C., Battersby, B. and Leary, S. C. (1998). Regulation of muscle mitochondrial design. *J. Exp. Biol.* **201**, 299–307.

Mulligan, C. M., Le, C. H., deMooy, A. B., Nelson, C. B. and Chicco, A. J. (2014). Inhibition of delta-6 desaturase reverses cardiolipin remodeling and prevents contractile dysfunction in the aged mouse heart without altering mitochondrial respiratory function. *J. Gerontol. A-Biol.* **69**, 799–809.

Muriana, F. J. G., Vazquez, C. M. and Ruiz-Gutierrez, V. (1992). Fatty acid composition and properties of the liver microsomal membrane of rats fed diets enriched with cholesterol. *J. Biochem.* **112**, 562–567.

Nettle, D. and Bateson, M. (2015). Adaptive developmental plasticity: what is it, how can we recognize it and when can it evolve? *Proc. Roy. Soc. B* **282**, 20151005.

Nicholls, D. G. (2006). The physiological regulation of uncoupling proteins. *Biochim. Biophys. Acta* **1757**, 459–466.

Nicholls, D. G. and Ferguson, S. J. (2013). *Bioenergetics 4*. 4 ed. Elsevier.

NOAA National Estuarine Research Reserve System (NERRS) (2012).

O'Brien, J., Dahlhoff, E. and Somero, G. N. (1991). Thermal-resistance of mitochondrial respiration - hydrophobic interactions of membrane-proteins may limit thermal-resistance. *Physiol. Zool.* **64**, 1509–1526.

O'Brien, K. M. (2011). Mitochondrial biogenesis in cold-bodied fishes. *J. Exp. Biol.* **214**, 275–285.

Oellermann, M., Pörtner, H. O. and Mark, F. C. (2012). Mitochondrial dynamics underlying thermal plasticity of cuttlefish (*Sepia officinalis*) hearts. *J. Exp. Biol.* **215**, 2992–3000.

Paradies, G., Paradies, V., De Benedictis, V., Ruggiero, F., & Petrosillo, G. (2014). Functional role of cardiolipin in mitochondrial bioenergetics. *Biochim. Biophys. Acta - Bioenergetics*, **1837**, 408-417.

Paton, C. M. and Ntambi, J. M. (2009). Biochemical and physiological function of stearoyl-CoA desaturase. *Am. J. Physiol.-Endoc. M.* **297**, E28–E37.

Pernet, F., Tremblay, R., Comeau, L. and Guderley, H. (2007). Temperature adaptation in two bivalve species from different thermal habitats: energetics and remodelling of membrane lipids. *J. Exp. Biol.* **210**, 2999–3014.

Perry, S. and Reid, S. (1994). The effects of acclimation temperature on the dynamics of catecholamine release during acute hypoxia in the rainbow trout *Oncorhynchus mykiss*. *J. Exp. Biol.* **186**, 289–307.

Pichaud, N., Ballard, J. W. O., Tanguay, R. M. and Blier, P. U. (2012). Mitochondrial haplotype divergences affect specific temperature sensitivity of mitochondrial respiration. *J. Bioenerg. Biomembr.* **45**, 25–35.

Pierron, D., Wildman, D. E., Hüttemann, M., Markondapatnaikuni, G. C., Aras, S. and Grossman, L. I. (2012). Cytochrome *c* oxidase: evolution of control via nuclear subunit addition. *Biochim. Biophys. Acta* **1817**, 590–597.

Place, A. R. and Powers, D. A. (1979). Genetic variation and relative catalytic efficiencies: lactate dehydrogenase B allozymes of *Fundulus heteroclitus*. *Proc. Nat. Acad. Sci. USA* **76**, 2354–2358.

Place, A. R. and Powers, D. A. (1984). Purification and characterization of the lactate dehydrogenase (LDH-B4) allozymes of *Fundulus heteroclitus*. *J. Biol. Chem.* **259**, 1299–1308.

Porplycia, D., Lau, G. Y., McDonald, J., Chen, Z., Richards, J. G. and Moyes, C. D. (2017). Subfunctionalization of COX4 paralogs in fish. *Am. J. Physiol.-Reg. I.* **312**, R671–R680.

Powers, D. A. and Schulte, P. M. (1998). Evolutionary adaptations of gene structure and expression in natural populations in relation to a changing environment: a multidisciplinary approach to address the million-year saga of a small fish. *J. Exp. Zool.* **282**, 71–94.

Powers, D. A., Greaney, G. S. and Place, A. R. (1979). Physiological correlation between lactate dehydrogenase genotype and haemoglobin function in killifish. *Nature* **277**, 240–241.

Powers, D. A., Lauerman, T., Crawford, D. and Dimichele, L. (1991). Genetic mechanisms for adapting to a changing environment. *Annu. Rev. Genet.* **25**, 629–659.

Powers, D. A., Ropson, I., Brown, D. C., van Beneden, R., Cashon, R., Gonzalez-Villaseñor, L. I. and Dimichele, J. A. (1986). Genetic Variation in *Fundulus heteroclitus*: Geographic Distribution. *Integr. Comp. Biol.* **26**, 131–144.

Pörtner, H. (2001). Climate change and temperature-dependent biogeography: oxygen limitation of thermal tolerance in animals. *Naturwissenschaften* **88**, 137–146.

Pörtner, H. O. and Farrell, A. P. (2008). Physiology and climate change. *Science* **322**, 690–692.

Pörtner, H. O. and Knust, R. (2007). Climate change affects marine fishes through the oxygen limitation of thermal tolerance. *Science* **315**, 95–97.

Pörtner, H. O., Bennett, A. F., Bozinovic, F., Clarke, A., Lardies, M. A., Lucassen, M., Pelster, B., Schiemer, F. and Stillman, J. H. (2006). Trade-offs in thermal adaptation: the need for a molecular to ecological integration. *Physiol. Biochem. Zool.* **79**, 295–313.

Pörtner, H. O., Hardewig, I. and Peck, L. S. (1999). Mitochondrial function and critical temperature in the Antarctic bivalve, *Laternula elliptica*. *Comp. Biochem. Physiol. A* **124**, 179–189.

Precht, H. (1958). Concepts of temperature adaptation of changing reaction systems of cold-blooded animals. In *Physiological Adaptation* (ed. Prosser, C. L.), pp. 51–78. Washington, DC.

Reid, N. M., Proestou, D. A., Clark, B. W., Warren, W. C., Colbourne, J. K., Shaw, J. R., Karchner, S. I., Hahn, M. E., Nacci, D., Oleksiak, M. F., et al. (2016). The genomic landscape of rapid repeated evolutionary adaptation to toxic pollution in wild fish. *Science* **354**, 1305–1308.

Richards, J. G. (2010). Metabolic rate suppression as a mechanism for surviving environmental challenge in fish. In *Aestivation*, pp. 113–139. Springer Berlin Heidelberg.

Rossignol, R., Letellier, T., Malgat, M., Rocher, C. and Mazat, J. P. (2000). Tissue variation in the control of oxidative phosphorylation: implication for mitochondrial diseases. *Biochem. J.* **347**, 45–53.

Rottenberg, H. (1984). Membrane potential and surface potential in mitochondria: uptake and

binding of lipophilic cations. *J. Membr. Biol.* **81**, 127–138.

Sagan, L. (1967). On the origin of mitosing cells. *J. Theor. Biol.* **14**, 225–IN6.

Salin, K., Auer, S. K., Anderson, G. J., Selman, C. and Metcalfe, N. B. (2016). Inadequate food intake at high temperatures is related to depressed mitochondrial respiratory capacity. *J. Exp. Biol.* **219**, 1356–1362.

Samartsev, V. N., Mokhova, E. N. and Skulachev, V. P. (1997). The pH-dependent reciprocal changes in contributions of ADP/ATP antiporter and aspartate/glutamate antiporter to the fatty acid-induced uncoupling. *FEBS Lett.* **412**, 179–182.

Santigosa, E. and Vagner, M. (2011). Characterization and modulation of gene expression and enzymatic activity of delta-6 desaturase in teleosts: A review. *Aquaculture* **315**, 131.

Schlame, M. (2007). Assays of Cardiolipin Levels. In *Mitochondria, 2nd Edition*, pp. 223–240. Elsevier.

Schlame, M. (2013). Cardiolipin remodeling and the function of tafazzin. *Biochim. Biophys. Acta* **1831**, 582–588.

Schnell, A. K. and Seebacher, F. (2008). Can phenotypic plasticity facilitate the geographic expansion of the tilapia *Oreochromis mossambicus*? *Physiol. Biochem. Zool.* **81**, 733–742.

Schulte, P. M. (2001). Environmental adaptations as windows on molecular evolution. *Comp. Biochem. Physiol. B* **128**, 597–611.

Schulte, P. M. (2015). The effects of temperature on aerobic metabolism: towards a mechanistic understanding of the responses of ectotherms to a changing environment. *J. Exp. Biol.* **218**, 1856–1866.

Schulte, P. M., Gómez-Chiarri, M. and Powers, D. A. (1997). Structural and functional differences in the promoter and 5' flanking region of LDH-B within and between populations of the teleost *Fundulus heteroclitus*. *Genetics* **145**, 759–769.

Schulte, P. M., Healy, T. M. and Fangue, N. A. (2011). Thermal performance curves, phenotypic plasticity, and the time scales of temperature exposure. *Integr. Comp. Biol.* **51**, 691–702.

Scott, G. R., Scott, G. R., Egginton, S., Schulte, P. M., Scott, A. L. M., Egginton, S., Scott, A. L. M., Richards, J. G., Richards, J. G., Milsom, W. K., et al. (2010). Molecular evolution of cytochrome c oxidase underlies high-altitude adaptation in the bar-headed Goose. *Mol. Biol. Evol.* **28**, 351–363.

Seebacher, F., Brand, M. D., Else, P. L., Guderley, H., Hulbert, A. J. and Moyes, C. D. (2010). Plasticity of oxidative metabolism in variable climates: molecular mechanisms. *Physiol. Biochem. Zool.* **83**, 721–732.

Shinzawa-Itoh, K., Aoyama, H., Muramoto, K., Terada, H., Kurauchi, T., Tadehara, Y., Yamasaki, A., Sugimura, T., Kurono, S., Tsujimoto, K., et al. (2007). Structures and physiological roles of 13 integral lipids of bovine heart cytochrome c oxidase. *EMBO J.* **26**, 1713–1725.

Sidell, B. D. (1998). Intracellular oxygen diffusion: the roles of myoglobin and lipid at cold body temperature. *J. Exp. Biol.* **201**, 1119–1128.

Sidell, B. D., Johnston, I. A., Moerland, T. S. and Goldspink, G. (1983). The eurythermal myofibrillar protein complex of the mummichog (*Fundulus heteroclitus*): adaptation to a fluctuating thermal enviroment. *J. Comp. Physiol. B* **153**, 167–173.

Silva, G., Lima, F. P., Martel, P. and Castilho, R. (2014). Thermal adaptation and clinal mitochondrial DNA variation of European anchovy. *Proc. Roy. Soc. B* **281**, 20141093.

Sinensky, M. (1974). Homeoviscous adaptation—A homeostatic process that regulates the viscosity of membrane lipids in *Escherichia coli*. *Proc. Natl. Acad. Sci. USA* **71**, 522–525.

Singer, S. J. and Nicolson, G. L. (1972). The fluid mosaic model of the structure of cell membranes. *Science* **175**, 720–731.

Somero, G. N. (2002). Thermal physiology and vertical zonation of intertidal animals: optima, limits, and costs of living. *Integr. Comp. Biol.* **42**, 780–789.

Somero, G. N. (2010). The physiology of climate change: how potentials for acclimatization and genetic adaptation will determine 'winners' and 'losers'. *J. Exp. Biol.* **213**, 912–920.

Somero, G. N. (2005). Linking biogeography to physiology: Evolutionary and acclimatory adjustments of thermal limits. *Front. Zool.* **2**, 1.

Somero, G. N. and DeVries, A. L. (1967). Temperature Tolerance of Some Antarctic Fishes. *Science* **156**, 257–258.

Sparagna, G. C., Johnson, C. A., McCune, S. A., Moore, R. L. and Murphy, R. C. (2005). Quantitation of cardiolipin molecular species in spontaneously hypertensive heart failure rats using electrospray ionization mass spectrometry. *J. Lipid Res.* **46**, 1196–1204.

Srere, P. A. (1969). [1] Citrate synthase. In *Citric Acid Cycle*, pp. 3–11. Elsevier.

St-Pierre, J., Brand, M. D. and Boutilier, R. G. (2000a). Mitochondria as ATP consumers: Cellular treason in anoxia. *Proc. Natl. Acad. Sci. USA.* **97**, 8670–8674.

St-Pierre, J., Tattersall, G. J. and Boutilier, R. G. (2000b). Metabolic depression and enhanced O_2 affinity of mitochondria in hypoxic hypometabolism. *Am. J. Physiol. - Reg. I.* **279**, R1205-R1214.

St-Pierre, J., Charest, P. M. and Guderley, H. (1998). Relative contribution of quantitative and qualitative changes in mitochondria to metabolic compensation during seasonal

acclimatisation of rainbow trout *Oncorhynchus mykiss*. *J. Exp. Biol.* **201**, 2961–2970.

Stillman, J. and Somero, G. (1996). Adaptation to temperature stress and aerial exposure in congeneric species of intertidal porcelain crabs (genus *Petrolisthes*): correlation of physiology, biochemistry and morphology with vertical distribution. *J. Exp. Biol.* **199**, 1845–1855.

Stillman, J. H. (2003). Acclimation capacity underlies susceptibility to climate change. *Science* **301**, 65–65.

Stillwell, W. and Wassall, S. R. (2003). Docosahexaenoic acid: membrane properties of a unique fatty acid. *Chem. Phys. Lipids* **126**, 1–27.

Strobel, A., Graeve, M., Pörtner, H. O. and Mark, F. C. (2013). Mitochondrial acclimation capacities to ocean warming and acidification are limited in the Antarctic nototheniid fish, *Notothenia rossii* and *Lepidonotothen squamifrons*. *PLoS ONE* **8**, e68865.

Sunday, J. M., Bates, A. E. and Dulvy, N. K. (2011). Global analysis of thermal tolerance and latitude in ectotherms. *Proc. Roy. Soc. B* **278**, 1823–1830.

Sørensen, J. G., Schou, M. F., Kristensen, T. N. and Loeschcke, V. (2016). Thermal fluctuations affect the transcriptome through mechanisms independent of average temperature. *Sci. Rep.* **6**, 2068.

Taanman, J. W. (1999). The mitochondrial genome: structure, transcription, translation and replication. *Biochim. Biophys. Acta* **1410**, 103–123.

Takeda, Y., Pérez-Pinzón, M. A., Ginsberg, M. D. and Sick, T. J. (2004). Mitochondria consume energy and compromise cellular membrane potential by reversing ATP synthetase activity during focal ischemia in rats. *J. Cerebr. Blood F Met.* **24**, 986–992.

Tasseva, G., Bai, H. D., Davidescu, M., Haromy, A., Michelakis, E. and Vance, J. E. (2013). Phosphatidylethanolamine deficiency in mammalian mitochondria impairs oxidative phosphorylation and alters mitochondrial morphology. *J. Biol. Chem.* **288**, 4158–4173.

Taylor, W. A., Dolinsky, V. W., Hatch, G. M. and Ma, B. J. (1999). Acylation of monolysocardiolipin in rat heart. *J. Lipid Res.* **40**, 1837–1845.

Tepolt, C. K. and Somero, G. N. (2014). Master of all trades: thermal acclimation and adaptation of cardiac function in a broadly distributed marine invasive species, the European green crab, *Carcinus maenas*. *J. Exp. Biol.* **217**, 1129–1138.

Terblanche, J. S., Hoffmann, A. A., Mitchell, K. A., Rako, L., le Roux, P. C. and Chown, S. L. (2011). Ecologically relevant measures of tolerance to potentially lethal temperatures. *J. Exp. Biol.* **214**, 3713–3725.

Thissen, D., Steinberg, L. and Kuang, D. (2002). Quick and easy implementation of the benjamini-hochberg procedure for controlling the false positive rate in multiple comparisons.

J. Educ. Behav. Stat. **27**, 77–83.

Tosi, F., Sartori, F., Guarini, P., Olivieri, O. and Martinelli, N. (2014). Delta-5 and delta-6 desaturases: crucial enzymes in polyunsaturated fatty acid-related pathways with pleiotropic influences in health and disease. In *Oxygen Transport to Tissue XXXI* (eds. Takahashi, E. and Bruley, D. F., pp. 61–81. Cham: Springer International Publishing.

Trzcionka, M., Withers, K. W., Klingenspor, M. and Jastroch, M. (2008). The effects of fasting and cold exposure on metabolic rate and mitochondrial proton leak in liver and skeletal muscle of an amphibian, the cane toad *Bufo marinus*. *J. Exp. Biol.* **211**, 1911–1918.

Turko, A. J., Robertson, C. E., Bianchini, K., Freeman, M. and Wright, P. A. (2014). The amphibious fish *Kryptolebias marmoratus* uses different strategies to maintain oxygen delivery during aquatic hypoxia and air exposure. *J. Exp. Biol.* **217**, 3988–3995.

Turrens, J. F. and Boveris, A. (1980). Generation of superoxide anion by the NADH dehydrogenase of bovine heart mitochondria. *Biochem. J.* **191**, 421–427.

Valiela, I., Wright, J. E., Teal, J. M. and Volkmann, S. B. (1977). Growth, production and energy transformations in the salt-marsh killifish *Fundulus heteroclitus*. *Mar. Biol.* **40**, 135–144.

Van 't Hoff, J. H. (1899). *Lectures on theoretical and physical chemistry*. University of Michigan Library.

van den Thillart, G. and Modderkolk, J. (1978). The effect of acclimation temperature on the activation energies of state III respiration and on the unsaturation of membrane lipids of goldfish mitochondria. *BBA - Biomembranes* **510**, 38–51.

van der Veen, J. N., Lingrell, S., da Silva, R. P., Jacobs, R. L. and Vance, D. E. (2014). The concentration of phosphatidylethanolamine in mitochondria can modulate ATP production and glucose metabolism in mice. *Diabetes* **63**, 2620–2630.

Vance, D. E., Li, Z. and Jacobs, R. L. (2007). Hepatic phosphatidylethanolamine N-methyltransferase, unexpected roles in animal biochemistry and physiology. *J. Biol. Chem.* **282**, 33237–33241.

Verberk, W. C. E. P., Overgaard, J., Ern, R., Bayley, M., Wang, T., Boardman, L. and Terblanche, J. S. (2016). Does oxygen limit thermal tolerance in arthropods? A critical review of current evidence. *Comp. Biochem. Physiol. A* **192**, 64–78.

Virtue, S., Dale, M., Tan, C. Y., Bidault, G., Hagen, R., Griffin, J. L. and Vidal-Puig, A. (2015). Brown adipose tissue thermogenic capacity is regulated by Elovl6. *Cell Rep.* **13**, 2039–2047.

Wahjudi, P. N., K Yee, J., Martinez, S. R., Zhang, J., Teitell, M., Nikolaenko, L., Swerdloff, R., Wang, C. and Lee, W. N. P. (2011). Turnover of nonessential fatty acids in cardiolipin from the rat heart. *J. Lipid Res.* **52**, 2226–2233.

Weber, R. E. and Jensen, F. B. (1988). Functional adaptations in hemoglobins from ectothermic vertebrates. *Annu. Rev. Physiol.* **50**, 161–179.

Weber, R. E., Wood, S. C. and Lomholt, J. P. (1976). Temperature acclimation and oxygen-binding properties of blood and multiple haemoglobins of rainbow trout. *J. Exp. Biol.* **65**, 333–345.

Wells, R. M. G., Baldwin, J., Seymour, R. S., Christian, K. and Brittain, T. (2005). Red blood cell function and haematology in two tropical freshwater fishes from Australia. *Comp. Biochem. Physiol. A* **141**, 87–93.

West, G. B., Brown, G. C. and Enquist, B. J. (1997). A general model for the origin of allometric scaling laws in biology. *Science* **276**, 122–126.

White, C. R., Alton, L. A. and Frappell, P. B. (2012). Metabolic cold adaptation in fishes occurs at the level of whole animal, mitochondria and enzyme. *Proc. Biol. Sci.* **279**, 1740–1747.

Whitehead, A. (2009). Comparative mitochondrial genomics within and among species of killifish. *BMC Evol. Biol.* **9**, 11.

Widomska, J., Raguz, M. and Subczynski, W. K. (2007). Oxygen permeability of the lipid bilayer membrane made of calf lens lipids. *Biochim. Biophys. Acta*. **1768**, 2635-2645.

Wodtke, E. (1981a). Temperature adaptation of biological membranes. Compensation of the molar activity of cytochrome *c* oxidase in the mitochondrial energy-transducing membrane during thermal acclimation of the carp (*Cyprinus carpio* L.). *BBA - Biomembranes* **640**, 710–720.

Wodtke, E. (1981b). Temperature adaptation of biological membranes. The effects of acclimation temperature on the unsaturation of the main neutral and charged phospholipids in mitochondrial membranes of the carp (*Cyprinus carpio* L.). *Biochim. Biophys. Acta* **640**, 698–709.

Wolff, J. N., Ladoukakis, E. D., Enriquez, J. A. and Dowling, D. K. (2014). Mitonuclear interactions: evolutionary consequences over multiple biological scales. *Philos. T. Roy. Soc. B* **369**, 20130443–20130443.

Wyman, J., Jr. (1964). Linked functions and reciprocal effects in hemoglobin: a second look. *Adv. in Prot. Chem.* **19**, 223–286.

Yan, Y. and Xie, X. (2015). Metabolic compensations in mitochondria isolated from the heart, liver, kidney, brain and white muscle in the southern catfish (*Silurus meridionalis*) by seasonal acclimation. *Comp Biochem Physiol. A* **183**, 64–71.

Zhang, M., Mileykovskaya, E. and Dowhan, W. (2002). Gluing the respiratory chain together. Cardiolipin is required for supercomplex formation in the inner mitochondrial membrane. *J. Biol. Chem.* **277**, 43553–43556.

Zhang, Z.-Y., Chen, B., Zhao, D.-J. and Kang, L. (2013). Functional modulation of mitochondrial cytochrome c oxidase underlies adaptation to high-altitude hypoxia in a Tibetan migratory locust. *Proc. Roy. Soc. B* **280**, 20122758–20122758.